Regulation of Inflammatory Signalling in Adipocytes by AMPK

Sarah Mancini (MSci)

Thesis submitted in fulfilment of the requirements for the Degree of Doctor of Philosophy

March 2014

School of Medical, Veterinary and Life Sciences
Institute of Cardiovascular and Medical Sciences
University of Glasgow

Abstract

AMP-activated protein kinase (AMPK) has been proposed to be a potential therapeutic target for patients with Type 2 diabetes and the metabolic syndrome. While the role of AMPK in muscle and liver is relatively well-characterised, less is known about the role of AMPK in the other principal metabolic tissue, adipose. Obesity is associated with the chronic, sub-clinical inflammation of adipose tissue. Characteristic hypertrophic adipocytes and the elevated infiltration and activation of macrophages stimulate production of cytokines and chemokines, including tumour necrosis factor-α (TNF-α), interleukin-1β (IL-1β), interleukin-6 (IL-6) and monocyte chemoattractant protein-1 (MCP-1). These have autocrine, paracrine and endocrine effects which have been suggested to play a key role in the development of peripheral insulin resistance. Increasing evidence suggests that AMPK has anti-inflammatory actions, independent of its effect on carbohydrate and lipid metabolism. Previous work in our laboratory has demonstrated that AMPK inhibits TNF-α-stimulated MCP-1 secretion and monocyte adhesion in endothelial cells. The role of AMPK in the regulation of inflammatory signalling in adipocytes is currently poorly characterised.

To address this, the effect of AMPK activation on the phosphorylation of TNF-α/IL-1β and IL-6 signalling pathway intermediates was initially assessed in cultured 3T3-L1 adipocytes. Furthermore, the molecular mechanism by which AMPK elicits these effects was investigated. In addition, the effect of AMPK activation on downstream functional consequences of proinflammatory signalling in 3T3-L1 adipocytes and RAW 264.7 macrophages were examined. Finally, the effect of macrophage AMPK activation on inflammation-induced insulin resistance in 3T3-L1 adipocytes was also investigated.

A769662 and infection with adenovirus expressing a constitutively active AMPK mutant suppressed IL-1β-stimulated NFκB nuclear translocation in 3T3-L1 adipocytes. Conversely, this was abrogated upon adenoviral expression of a dominant negative AMPK mutant. In line with this, phosphorylation of upstream IκBα and IKK were also ameliorated upon AMPK activation. In parallel, A769662-mediated AMPK activation inhibited TNF-α/IL-1β-stimulated phosphorylation of JNK, ERK1/2 and p38 MAPKs in 3T3-L1 adipocytes. Furthermore, A769662-

mediated inhibition of TNF-α/IL-1β proinflammatory signalling was likely to be independent of endothelial nitric oxide synthase (eNOS) activation and subsequent nitric oxide production. The target of AMPK may be downstream of TAK1, as IKK, JNK and p38 are inhibited in response to both TNF-α and IL-1β; however the mechanism by which AMPK elicits these effects remains to be elucidated. A769662-mediated AMPK activation inhibited phosphorylation of IL-6-stimulated STAT3 (signal transducer and activator of transcription 3) in 3T3-L1 adipocytes independently of phosphatase action, yet A769662 was unable to inhibit constitutive Janus kinase (JAK)-mediated phosphorylation of STAT3, suggesting AMPK may inhibit JAK activity. Inhibition of mTOR was found to suppress STAT3 phosphorylation in a manner mutually exclusive with A769662 stimulation, potentially via activation of T cell protein tyrosine phosphatase (TC-PTP). Adipose tissue from *AMPKα1*$^{-/-}$ mice demonstrated increased basal JNK and STAT3 phosphorylation, further providing evidence for an anti-inflammatory role for AMPK in adipose tissue. In 3T3-L1 adipocytes, A769662 abrogated cytokine-stimulated MCP-1 gene expression, and secretion of chemokines IP-10 (CXCL10), KC (CXCL1) and MCP-1. Furthermore, AMPK activation reduced secretion of IL-5, MCP-1 and MIP-1α, but not TNF-α, from proinflammatory RAW 264.7 macrophages. Preliminary results indicated that chronic IL-6 and acute TNF-α or IL-1β exposure suppressed insulin-stimulated glucose transport in 3T3-L1 adipocytes. Conditioned medium from activated RAW 264.7 macrophages also inhibited 3T3-L1 adipocyte insulin sensitivity; however, prior AMPK activation failed to attenuate this, potentially as a result of the presence of TNF-α.

Overall these results suggest that activation of AMPK inhibits activation of multiple distinct proinflammatory signalling pathways in adipocytes and macrophages. AMPK activation may suppress IL-6 signalling via regulation of JAK, while the AMPK-mediated inhibition of IKK and concomitant suppression of MAPKs in response to TNF-α/IL-1β suggests TAK1 as a potential AMPK target. Finally, proinflammatory stimuli induce insulin resistance in adipocytes, however whether this can be rescued by AMPK activation remains to be fully elucidated.

Table of Contents

List of Tables

List of Figures

Acknowledgements

I wish to express my deepest gratitude to my supervisor Dr. Ian Salt for his endless support, guidance and enthusiasm. I couldn't have wished for a better, more encouraging supervisor.

I would like to thank Dr. Tim Palmer, whose advice and comments have been of great help throughout this project, and Dr. Jim Reilly for his technical assistance with the Luminex assay. I am grateful to members of Lab 241 past and present, for their advice and for making my time in the lab so enjoyable, in particular Dr. Silvia Bijland and Dr. Kim Boney for their friendship, stimulating discussions and for all the fun we have had over the last 3 years.

Finally and most importantly, I am truly thankful to my husband Daniel for his love, support and patience, and that of both our families.

Funding for this project was provided by Diabetes UK.

Per tagliare una lunga storia breve…

Declaration

I declare that the work presented in this thesis has been carried out by myself, unless otherwise stated. It is entirely of my own composition and has not, in whole or in part, been submitted for any other degree.

Sarah Mancini

March 2014

Abbreviations

β-AR	Beta-adrenoreceptor
α-MSH	α-Melanocyte stimulating hormone
4E-BP1	Elongation factor-4E binding protein 1
ACC	Acetyl CoA carboxylase
AgRP	Agouti-related protein
AICAR	5'-aminoimidazole-4-carboxamide ribonucleoside
AMPK	AMP-activated protein kinase
aP2	Adipocyte-specific FA-binding protein
APP	Amyloid precursor protein
APS	Ammonium peroxidisulphate
ARG1	Arginase 1
AS160	Akt substrate of 160 kDa
ASK1/2	Apoptosis signal-regulating kinase 1/2
ATF-2	Activating transcription factor-2
basic-FGF	basic-fibroblast growth factor
BAT	Brown adipose tissue
BSA	Bovine serum albumin
C/EBP	CCAAT/enhancer-binding protein
CaMKK	Ca^{2+}/calmodulin-dependent protein kinase kinase
CAR	Coxackie virus and adenovirus receptor
CBM	Carbohydrate-binding module
CBS	Cystathione-β-synthase
CCR	C-C chemokine receptor
CHI313	Chitinase like lectin
CPT1	Carnitine palmitoyl transferase 1
CRP	C-Reactive Protein
CXCL	C-X-C motif ligand
DAB	Diaminobenzidine
DAG	Diacylglycerol
DG	Diglyceride
DGAT	Diacylglycerol acetyltransferase
DHAP	Dihydroxyacetone phosphate
DIO	Diet-induced obesity

DMEM	Dulbecco's modified Eagle's medium
DMSO	Dimethyl sulphoxide
D-NAME	N_ω-Nitro-D-arginine methyl ester hydrochloride
dNTP	Deoxyribonucleotide triphosphate
ECL	Enhanced chemiluminescence
eNOS	Endothelial nitric oxide synthase
ERK	Extracellular signal-regulated kinase
FA	Fatty acid
FAS	Fatty acid synthase
FCS	Foetal calf serum
G3P	Glycerol-3-phosphate
G6P	Glucose-6-phosphate
G6Pase	Glucose-6-phosphatase
GAPDH	Glyceraldehyde 3-phosphate dehydrogenase
GLUT	Glucose transporter
GM-CSF	Granulocyte macrophage colony stimulating factor
gp130	Glycoprotein 130
GPAT	Glycerol phosphate acyltransferase
Grb2	Growth factor receptor-bound protein 2
GS	Glycogen synthase
GSK	Glycogen synthase kinase
GSV	GLUT4 storage vesicle
HEK	Human embryonic kidney
HFD	High-fat diet
HMGR	HMG-CoA reductase
HSL	Hormone-sensitive lipase
HUVEC	Human umbilical vein endothelial cell
IκBα	Inhibitor of κB
IBMX	Isobutylxanthine
IFN-γ	Interferon gamma
IKK	IκB kinase
IL-	Interleukin-
IL-1RAcP	Interleukin-1 coreceptor
IL-1RI	Interleukin-1 receptor
IP	Immunoprecipitation

IP-10 (CXCL10)	Interferon-γ-induced protein 10 kDa
IR	Insulin receptor
IRAK4	Interleukin-1 receptor-activated protein kinase 4
IRS	Insulin receptor substrate
JAK	Janus kinase
JNK	c-Jun N-terminal kinase
KC (CXCL1)	Keratinocyte chemoattractant
KRH	Krebs-Ringer HEPES
KRP	Krebs-Ringer phosphate
LCACoA	Long-chain fatty-acyl CoA
LKB1	Liver kinase B1
L-NAME	N_{ω}-Nitro-L-arginine methyl ester hydrochloride
LPL	Lipoprotein lipase
LPS	Lipopolysaccharide
MAP2K/MEK	Mitogen activated protein kinase kinase
MAP3K/MEKK	Mitogen activated protein kinase kinase kinase
MAPK	Mitogen activated protein kinase
MC4R	Melanocortin 4 receptor
MCE	Mitotic clonal expansion
MCP-1 (CCL2)	Monocyte chemoattractant protein-1
MEF	Mouse embryonic fibroblast
MG	Monoglyceride
MGL	Monoglyceride lipase
MIG (CXCL9)	Monokine induced by gamma interferon
MIP-1α (CCL3)	Macrophage inflammatory protein
MLK2/3	Mixed-lineage kinase
mTORC2	Mammalian target of rapamycin complex
MyD88	Myeloid differentiation response gene 88
NCS	Newborn calf serum
NEFA	Non-esterified fatty acid
NFκB	Nuclear factor κB
NLRP3	Nucleotide-binding and oligomerisation domain-like receptor family pyrin domain-containing 3
NOS2	Nitric oxide synthase 2
NPY	Neuropeptide Y

NPYR	Neuropeptide Y receptor
OBB	Odyssey® blocking buffer
p70 S6K	p70 S6 kinase
PBS	Phosphate buffered saline
PBST	PBS + Tween 20
PCR	Polymerase chain reaction
PDE3B	Phosphodiesterase 3B
PDK1	3-phosphoinositide-dependent protein kinase-1
PEPCK	Phosphoenolpyruvate carboxykinase
PFK-2	Phosphofrucokinase-2
PGC1α	Peroxisome proliferator-activated receptor-γ co-activator 1α
PH	Pleckstrin homology
PI(3,4,5)P_3	Phosphatidylinositol 3,4,5 trisphosphate
PI(4,5)P_2	Phosphatidylinositol-4,5 bisphosphate
PI3K	Phosphatidylinositol-3'-kinase
PKA	Protein kinase A
PKB	Protein kinase B
PKC	Protein kinase C
POMC	Proopiomelanocortin
PP2C	Protein phosphatase 2C
PPARγ	Peroxisome proliferator-activated receptor γ
PTB	Phosphotyrosine binding
PTP	Protein tyrosine phosphatase
RabGAP	Rab GTPase-activating protein
RELM-α	Resistin like-alpha
RTK	Receptor tyrosine kinase
S6K1	Ribosomal protein S6 kinase
SCAT	Subcutaneous adipose tissue
SDS	Sodium dodecyl sulphate
SDS-PAGE	SDS-polyacrylamide gel electrophoresis
SGK1	Serum/glucocorticoid regulated kinase 1
SH2	Src homology 2
SHP-2	Src homology domain-containing protein tyrosine phosphatase-2
sIL-6Rα	Soluble IL-6 receptor alpha
siRNA	Small interfering RNA

SIRT1	Sirtuin 1
SOCS3	Suppressor of cytokine signalling 3
SOS	Son of sevenless
SREBP-1c	Sterol regulatory element-binding protein
STAT	Signal transducer and activator of transcription
TAK1	Transforming growth factor-β activated kinase 1
TAO1/2	Thousand and one amino acid protein kinase
TBK1	TRAF family member-associated-binding kinase 1
TBS	Tris buffered saline
TBST	TBS + Tween 20
TCA	Trichloroacetic acid
TC-PTP	T cell protein tyrosine phosphatase
TEMED	N, N, N', N'-tetramethylenediamine
TG	Triacylglycerol (trigyceride)
TIF-IA	RNA polymerase I-associated transcription factor
TLR	Toll-like receptor
TNF-α	Tumour necrosis factor-α
Tpl2	Tumour progression locus 2
TSC1/2	Tuberous sclerosis complex 1/2
TZD	Thiazolidinedione
UCP1	Uncoupling protein 1
ULK1/2	Unc-51-like kinase
VAT	Visceral adipose tissue
vLDL	Very low density lipoprotein
WAT	White adipose tissue
ZMP	5'-aminoimidazole-4-carboxamide ribonucleoside monophosphate

Chapter 1 - Introduction

1.1 Adipose Tissue

1.1.1 Adipose tissue composition and function

Adipose tissue is composed of several cell types, including adipocytes, pre-adipocytes, fibroblasts, and cells from the vascular, immune and nervous systems. At the whole-body level, it can be divided into SCAT (subcutaneous adipose tissue) and VAT (visceral adipose tissue) depots, and is further classified as being white (WAT) or brown (BAT). VAT tends to be located around abdominal viscera and is more metabolically active than SCAT, exhibiting increased lipolysis (Arner 2005) as well as an increase in inflammatory cells (Bruun et al. 2005). Indeed, increased VAT accumulation is associated with an elevated risk of Type 2 diabetes (Fox et al. 2007). WAT and BAT have distinct functions; adipocytes within WAT are the primary site for energy storage, while adipocytes within BAT allow energy dissipation by thermogenesis.

1.1.1.1 White adipose tissue

A physiological role of WAT is to function as an energy storage organ: energy is stored during periods of caloric excess as TG [triacylglycerol (trigyceride)] within white adipocytes, forming the core lipid droplet. This energy reserve can then be broken down to liberate fatty acids which can be utilised as fuel for muscle and other tissues when energy expenditure exceeds intake. The amount of energy stored in adipose tissue is regulated via the anabolic and catabolic processes, lipogenesis and lipolysis, respectively. Furthermore, WAT functions as an endocrine organ, secreting proteins which produce autocrine, paracrine and endocrine effects.

1.1.1.2 Brown adipose tissue

BAT contains high numbers of mitochondria which express UCP1 (uncoupling protein 1) which physiologically uncouples ATP synthesis from substrate oxidation.

Interestingly, clusters of adipocytes expressing UCP1 with thermogenic capabilities have recently been identified within WAT in response to various stimuli (Vitali et al. 2012). These adipocytes have been termed 'beige' or 'brite' and are similar to classical brown adipocytes insofar as they exhibit multilocular lipid droplet morphology, contain high numbers of mitochondria and express UCP1. Key differences distinguishing beige from classical brown adipocytes are that they are not derived from the same embryonic precursors (Seale et al. 2008), and importantly, that classical brown adipocytes express UCP1 and other thermogenic genes under basal conditions, while beige adipocytes only express these genes in response to activation by cold exposure, β-adrenergic receptor agonists or PPARγ (peroxisome proliferator-activated receptor γ) (Rosenwald et al. 2013, Petrovic et al. 2010, Wu, Cohen, and Spiegelman 2013). It is not clear whether beige adipocytes arise from white adipocytes through transdifferentiation in response to stimuli, as suggested by Vitali and coworkers (Vitali et al. 2012) or from the *de novo* differentiation and maturation of preadipocytes (Wang et al. 2013). Intriguingly, it has been suggested that the thermogenic profile of beige adipocytes is fully reversible. Cold-exposure induced beige adipocytes lose UCP1 expression when mice are transferred to warmer conditions; however UCP1 expression is induced again within the same cells upon re-exposure to cold, indicating beige adipocytes are retained and may function similarly to white adipocytes until induced to function as brown adipocytes (Rosenwald et al. 2013). There is increasing interest in the capacity of beige and brown adipocytes to counteract obesity-related disorders, such as Type 2 diabetes; indeed increased brown and beige adipocytes are associated with obesity resistance in many mouse models (Cederberg et al. 2001, Seale et al. 2011).

1.1.2 Lipogenesis

Lipogenesis is the *de novo* synthesis of fatty acids (FAs) from non-lipid substrates such as glucose, and is stimulated by insulin during the fed state in adipocytes as shown in Figure 1.1. Insulin secretion stimulates glucose uptake by initiating a signalling pathway which culminates in the translocation of the glucose transporter GLUT4 to the plasma membrane (Saltiel and Kahn 2001), thereby facillitating glucose uptake. Glucose is then metabolised by glycolysis in the

cytosol, where it is broken down via a series of steps first to an intermediate dihydroxyacetone phosphate (DHAP), which is then converted to glycerol-3-phosphate (G3P) by glycerol-3-phosphate dehydrogenase. DHAP is also metabolised to pyruvate which is converted to acetyl CoA in the mitochondrion. Acetyl CoA can be shunted back to the cytoplasm to act as a substrate for the formation of FA via the action of ACC (acetyl CoA carboxylase) and FAS (fatty acid synthase) (Wakil 1989, Wakil, Stoops, and Joshi 1983). The action of insulin on target tissues activates ACC, which catalyses the carboxylation of acetyl CoA to form the intermediate malonyl CoA (Tong 2005). FAS is a multienzyme complex which is arranged around a central acyl carrier protein and functions to synthesise FA from both acetyl CoA and malonyl CoA in an NADPH-dependent manner. FAs can also be obtained from the hydrolysis of circulating vLDL (very low density lipoproteins) or chylomicrons by LPL (lipoprotein lipase)-mediated lipolysis and are transported into the adipocyte (Figure 1.1).

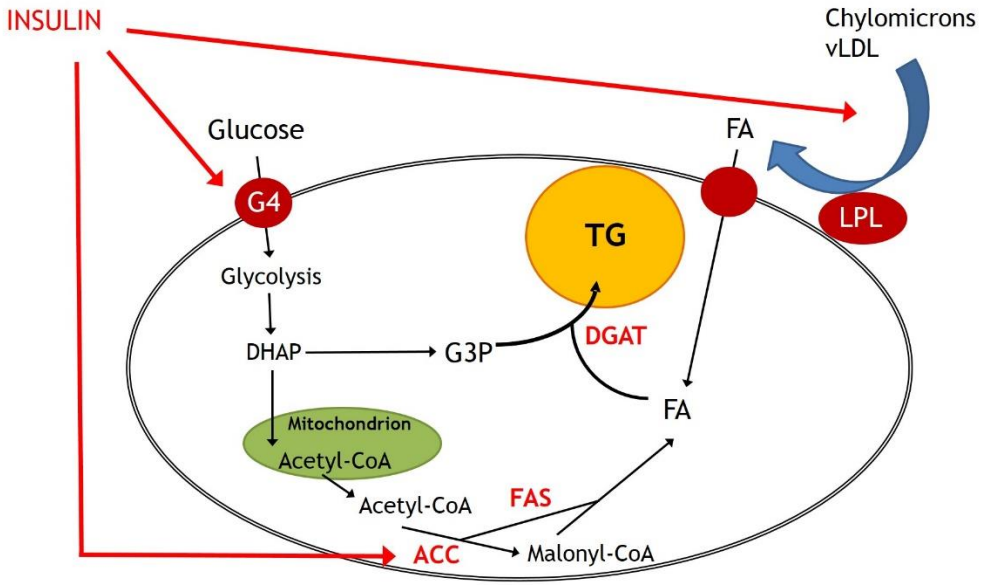

Figure 1-1: Regulation of lipogenesis in adipocytes

G3P and FA are esterified to form TGs in response to insulin. Glucose is metabolised to G3P and acetyl CoA which is converted to FA via the enzymes ACC and FAS. FAs are also obtained from the LPL-mediated hydrolysis of circulating lipoproteins. Abbreviations: G4, GLUT4; DHAP, dihydroxyacetone phosphate; G3P, glycerol-3-phosphate; DGAT, diacylglycerol acetyltransferase.

TG is formed from G3P and FA via a series of steps. In order for FA to be utilised in TG synthesis they must first be activated via esterification to Coenzyme A by

fatty acyl CoA synthetase (Watkins 1997). Phosphatidate is formed via the addition of two FA to G3P, catalysed by glycerol phosphate acyltransferase. Finally, phosphatidate is hydroysed by a phosphatase to yield diacylglyceride, which is then acylated to a TG by diacylglycerol acetyltransferase (DGAT) (Coleman and Lee 2004).

1.1.3 Lipolysis

In the fasted state, or during prolonged physical activity, the catabolic process of lipolysis occurs in order to yield FAs and glycerol, for use by other tissues such as muscle and liver for generation of ATP or hepatic gluconeogenesis, respectively. Binding of lipolytic hormones and neurotransmitters such as noradrenaline to adipocyte β-adrenergic receptors triggers an increase in cAMP via adenylyl cyclase, as demonstrated in Figure 1.2. This increase in cAMP within the cell then activates PKA (protein kinase A) (Collins, Cao, and Robidoux 2004, Holm et al. 2000), which subsequently phosphorylates perilipin and HSL (hormone-sensitive lipase). PKA phosphorylates HSL at Ser563, increasing its intrinsic activity, and Ser659 and Ser660, which are involved in the translocation of HSL to the lipid droplet. Perilipins are proteins found in mature adipocytes which cover the lipid droplet and thereby block HSL activity (Londos et al. 1999); phosphorylation of perilipins by PKA relieves their inhibition of HSL. Interestingly, it has been demonstrated that an absence of perilipin in adipocytes results in failure of HSL translocation, and thus failure of lipolysis (Sztalryd et al. 2003).

Activation of HSL via PKA phosphorylation is the rate-limiting step in hydrolysis of TG and induces its translocation from the cytosol to the surface of the lipid droplet (Anthonsen et al. 1998) where it hydrolyses TG to form diacylglycerides, and diacylglycerides into monoacylglycerides. A second enzyme, known as monoglyceride lipase, is necessary for complete hydrolysis of monoacylglycerides into non-esterified fatty acids (NEFAs) and glycerol, thus completing the process of lipolysis in adipocytes (Fredrikson, Tornqvist, and Belfrage 1986). Conversely, insulin negatively regulates lipolysis by initiating a signalling cascade which leads to the activation of phosphodiesterase 3B (PDE3B), triggering the hydrolysis of cAMP, thus suppressing PKA activation and subsequent HSL action (Shakur et al. 2001).

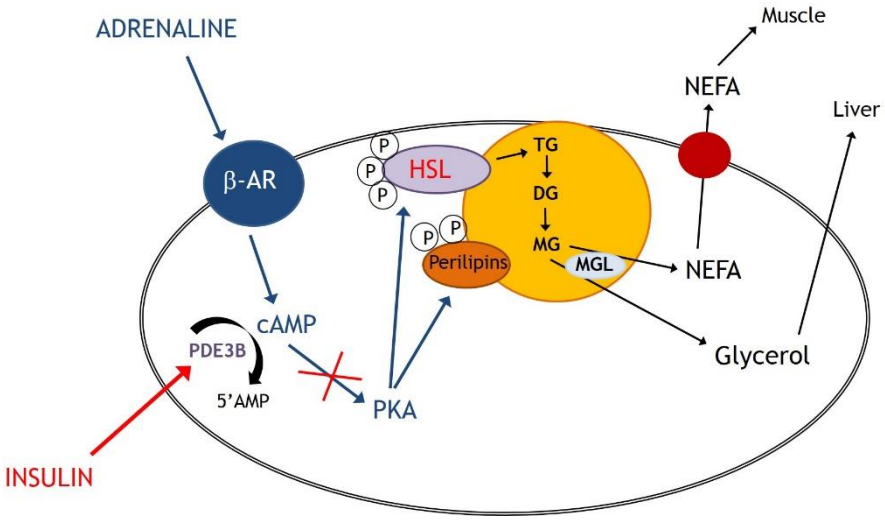

Figure 1-2: Hormonal control of adipocyte lipolysis

Lipolysis is stimulated by β-AR-mediated stimulation of cAMP production, resulting in PKA activation. PKA phosphorylates HSL and perilipins, stimulating hydrolysis of TG to MG. MGL further hydrolyses MG to NEFA and glycerol. Insulin suppresses lipolysis via stimulation of PDE3B and subsequent hydrolysis of cAMP, suppressing PKA activation. Abbreviations: β-AR, β-adrenergic receptor; PKA, protein kinase A; HSL, hormone-sensitive lipase; MGL, monoglyceride lipase; NEFA, non-esterified fatty acid; PDE3B, phosphodiesterase 3B.

1.1.4 Insulin-stimulated glucose transport

Insulin secretion is stimulated in response to glucose by pancreatic β-cells. In healthy, insulin sensitive individuals, insulin acts on skeletal muscle and adipocytes to stimulate glucose uptake via the regulated translocation of vesicles containing the glucose transporter GLUT4 to the plasma membrane as shown in Figure 1.3. The insulin receptor (IR) is a transmembrane receptor of the RTK (receptor tyrosine kinase) family and is composed of two extracellular α-subunits containing the insulin-binding domains and two transmembrane β-subunits linked by disulphide bonds (Lee and Pilch 1994). Insulin binding to the extracellular α-subunits induces a conformational change in the β-subunits, activating the tyrosine kinase activity of the receptor. The kinase activity of each β subunit initially phosphorylates tyrosine residues near the catalytic site in the adjacent β subunit, leading to the subsequent autophosphorylation of tyrosine residues in other parts of the cytosolic domain. Specific phosphotyrosine modifications stabilise an active conformation of the kinase domain and provide docking sites

for downstream signalling molecules, such as proteins containing src homology 2 (SH2) and phosphotyrosine binding (PTB) domains (Czech and Corvera 1999, Ullrich and Schlessinger 1990, Ward and Lawrence 2009).

IRS (insulin receptor substrate) adaptor proteins contain a PTB domain which recognises phosphotyrosines on the IR of the NPXpY motif. The IRS also has an N-terminal Pleckstrin homology (PH) domain which recognises and associates with polar lipids in the plasma membrane, and is also thought to interact with the IR kinase (Burks et al. 1997). The bound IRS is then tyrosine-phosphorylated by the IR (Ward and Lawrence 2009). IRS-1 and IRS-2 are essential for the insulin-stimulated transport of glucose into skeletal muscle and adipocytes; indeed both *IRS1*$^{-/-}$ and *IRS2*$^{-/-}$ mice have been reported to be insulin resistant (Araki et al. 1994), (Withers et al. 1998); with IRS2 deficiency also causing impaired pancreatic β-cell function and secretion of insulin (Withers et al. 1998).

Certain phosphotyrosines of IRS provide docking sites for the Class 1A lipid kinase PI3K (phosphatidylinositol-3'-kinase), which is a heterodimer composed of a p85 regulatory subunit and a catalytic p110 subunit. PI3K binds certain phosphotyrosines of IRS via its SH2 domain on p85, which leads to a conformational change of the p110 catalytic subunit and activation of the protein. Activated PI3K can then phosphorylate the plasma membrane lipid $PI(4,5)P_2$ (phosphatidylinositol-4,5 bisphosphate) on the 3' position of the inositol ring, thus forming the second messenger $PI(3,4,5)P_3$ (phosphatidylinositol 3,4,5 trisphosphate) (Vanhaesebroeck et al. 1997). $PI(3,4,5)P_3$ stimulates recruitment of two substrates to the plasma membrane: PDK1 (3-phosphoinositide-dependent protein kinase-1) and PKB (protein kinase B) (also known as Akt), which both contain PH domains that mediate their recruitment to the membrane from the cytosol. These two proteins are involved in the translocation of vesicles containing GLUT4 to the membrane (Brazil, Yang, and Hemmings 2004, Calleja et al. 2007, Currie et al. 1999). The close proximity of PDK1 allows it to phosphorylate PKB at Thr308, a residue situated within its kinase domain activation loop (Alessi et al. 1997). PKB is also phosphorylated by mTORC2 (mammalian target of rapamycin complex 2) at Ser473, further stimulating an increase in PKB kinase activity (Sarbassov et al. 2005, Hresko and Mueckler 2005). Activation of PKB causes it to dissociate from the membrane and go on to phosphorylate various downstream

effectors in both the cytoplasm and the nucleus which are involved in mediating the cellular effects of insulin, including GSK (glycogen synthase kinase) and AS160 (Akt substrate of 160kDa). PKB phosphorylates and inhibits AS160, permitting GLUT4 to translocate from GLUT4 storage vesicles to the plasma membrane (Sano et al. 2003). AS160 is a Rab GTPase-activating protein (RabGAP); when AS160 becomes phosphorylated its RabGap activity is inhibited, leading to increased active Rab-GTP which stimulates trafficking of GLUT4 vesicles from the cytoplasm to the plasma membrane (Sakamoto and Holman 2008).

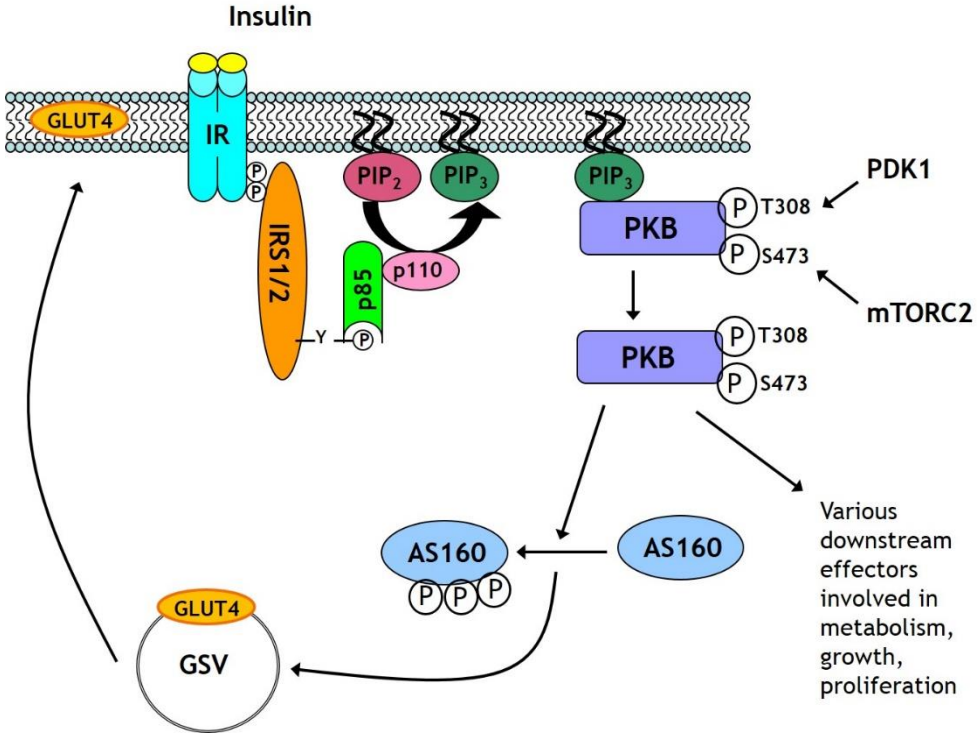

Figure 1-3: Insulin receptor signalling

Insulin binding stimulates receptor autophosphorylation and tyrosine phosphorylation of IRS, facilitating association of IRS with the regulatory p85 subunit of PI3K, inducing activation. Activated PI3K phosphorylates PIP_2, forming PIP_3, which in turn stimulates recruitment of PDK1 and PKB to the plasma membrane. PKB is activated upon phosphorylation by PDK1 at T308 and mTORC2 at S473, leading to the phosphorylation and inactivation of AS160 and the subsequent translocation of GLUT4 to the plasma membrane and glucose uptake. Abbreviations: PI3K, phosphatidylinositol 3-kinase; PIP_2, phosphatidylinositol 4,5 bisphosphate; PIP_3, (phosphatidylinositol 3,4,5-trisphosphate); PDK1, 3-phosphoinositide-dependent protein kinase-1; PKB, protein kinase B; mTORC2, mammalian target of rapamycin complex 2; AS160, Akt substrate of 160 kDa; GSV, GLUT4 storage vesicle.

1.2 Obesity and Inflammation

1.2.1 Adipocytokines

It is well accepted that WAT is not simply a site for energy storage during periods of caloric excess; it secretes fatty acids and proteins which function in an autocrine, paracrine and endocrine fashion to influence metabolism and inflammation. These factors are collectively termed 'adipocytokines', and include leptin, adiponectin, and inflammatory mediators such as MCP-1 (monocyte chemoattractant protein-1), TNF-α (tumour necrosis factor-α), IL-1β (interleukin-1β) and IL-6 (interleukin-6).

Leptin is primarily secreted from adipocytes during the fed state (Green et al. 1995), and plasma leptin levels are positively correlated with body fat mass as more leptin is released from large hypertrophic adipocytes relative to smaller adipocytes (Lönnqvist et al. 1997). Leptin functions at neurons within the hypothalamus to regulate satiety. Following a meal, leptin binds to Ob-Rb receptors on orexigenic (appetite-stimulating) and anorexigenic (appetite-suppressing) neurones in the arcuate nucleus of the hypothalamus. Orexigenic neurones co-express the peptides neuropeptide Y (NPY) and agouti-related protein (AgRP), which, when stimulated, mediate an increase in feeding and decrease in energy expenditure by signalling to their receptors on the ventromedial hypothalamus (NPY receptor (NPYR) and melanocortin 4 receptor (MC4R), respectively) (Zigman and Elmquist 2003). Leptin binding its receptor in orexigenic neurones suppresses this signalling. Concommitantly, in anorexigenic neurones, leptin binding its receptor stimulates proopiomelanocortin (POMC) which produces α-melanocyte stimulating hormone (α-MSH) (Rouillé et al. 1995), which then binds MC4R on the ventromedial hypothalamus. Thus, leptin is a negative-feedback signal which results in an overall decrease in feeding and increase in energy expenditure following satiety. Ob-Rb is a class I cytokine receptor which activates the JAK2-STAT3 (Janus kinase-Signal transducer and activator of transcription) signalling pathway in target cells (Frühbeck 2006). STAT proteins dimerise in the cytoplasm once phosphorylated and activated by JAKs, and from here translocate to the nucleus to initiate transcription of target genes (Figure 1.5), as described in more detail in 1.2.2.2. Furthermore, leptin has also been reported to increase

FA oxidation in skeletal muscle directly, indicating anti-diabetic actions independent of effects on body fat mass (Minokoshi et al. 2002, Muoio et al. 1997, Coppari and Bjørbæk 2012).

Adiponectin is an adipose-specific secreted protein, and plasma levels are paradoxically reduced with increasing adiposity (Arita et al. 1999). Adiponectin functions to promote peripheral insulin sensitivity; indeed a reduction in circulating adiponectin concentrations is associated with insulin resistance and hyperinsulineamia (Arita et al. 1999, Hotta et al. 2001). Furthermore, adiponectin has been reported to elicit systemic anti-inflammatory effects (Ouchi and Walsh 2007). Proinflammatory cytokines and chemokines such as TNF-α, IL-1β, IL-6 and MCP-1 are also secreted by WAT, with elevated concentrations associated with obesity (Gustafson 2010). Indeed, obesity is associated with dysfunctional metabolism and a chronic, sub-clinical proinflammatory environment within WAT which plays an important role in the development of systemic insulin resistance and Type 2 diabetes (Glass and Olefsky 2012).

1.2.2 Proinflammatory cytokines and obesity

1.2.2.1 TNF-α and IL-1β signalling to NFκB and MAP kinases

TNF-α and IL-1β are proinflammatory cytokines which are secreted primarily by macrophages and monocytes, but also by WAT adipocytes in obese states. Plasma concentrations of these proinflammatory cytokines have been reported to be elevated in obese individuals (Kern et al. 1995, Dandona et al. 1998, Moschen et al. 2011). These cytokines trigger proinflammatory effects via simultaneous activation of the NFκB (nuclear factor kappa B) and MAPK (mitogen activated protein kinase) intracellular signalling pathways. Soluble TNF-α mediates its effects via binding to the ubiquitously expressed receptor TNF-RI, stimulating recruitment of specific adaptor molecules TRADD and TRAF2 which are essential for the subsequent binding of RIP1 and the E3 ubiquitin ligases cIAP1 or cIAP2 (Karin and Gallagher 2009, Meloni et al. 1988). Polyubiquitination of downstream molecules are necessary for recruitment and activation of TGF-β-activated kinase 1 (TAK1) and IKK complexes and subsequent stimulation of MAPK and NFκB signalling pathways (Bianchi and Meier 2009, Walczak 2011). IL-1β initiates

proinflammatory signalling via a similar mechanism. Upon binding of IL-1 to its cognate receptor (IL-1RI), IL-1 coreceptor (IL-1RAcP) is recruited. This is followed by binding of two intracellular adaptor proteins myeloid differentiation response gene 88 (MyD88) and interleukin-1 receptor-activated protein kinase 4 (IRAK4) to conserved cytosolic Toll/IL-1 receptor domains, thus forming a stable signalling module (O'Neill 2008, Weber, Wasiliew, and Kracht 2010, Brikos et al. 2007). IRAK4 undergoes autophosphorylation before phosphorylating IRAK1 and 2, prior to recruitment and oligomerisation of TRAF6 which serves as an E3 ubiquitin ligase (Cao, Henzel, and Gao 1996, Cao et al. 1996). Ubiquitination of signalling intermediates triggers the recruitment of TAK1 and IKK complexes; it is here that the TNF-α and IL-1β signalling pathways can converge to stimulate downstream MAPK and NFκB signalling pathways (Yamazaki et al. 2009).

MAPK signalling pathways are protein kinase cascades in which MAPK kinase kinases (MAP3Ks) phosphorylate and activate MAPK kinases (MAP2Ks) which subsequently activate MAPK by dual phosphorylation of a TxY motif (Figure 1.4) (Kyriakis and Avruch 2012, Rose, Force, and Wang 2010, Muslin 2008). ERK1/2 are phosphorylated and activated by MEK1/2 which are, in turn, activated by a variety of MAP3Ks including Raf (in response to mitogens), MEKK2/3 and Tlp2 (in response to TNF-α) (Muslin 2008, Kyriakis and Avruch 2012, Rose, Force, and Wang 2010). JNK is phosphorylated and activated by MKK4 and MKK7, which are activated by the MAP3Ks MEKK1-4, MLK2/3, TAO1/2, ASK1/2 and TAK1 in response to mitogens, cellular stress and proinflammatory cytokines. p38 MAPKs are phosphorylated and activated by MKK3 and MKK6 which are substrates for the MAP3Ks MEKK4, MLK2/3, ASK1/2 and TAK1, also in response to mitogens, cell stress and proinflammatory cytokines (Rose, Force, and Wang 2010, Kyriakis and Avruch 2012, Muslin 2008). Upon stimulation, active MAPKs can translocate to the nucleus, thereby influencing transcription by phosphorylation of transcription factors such as c-Jun, c-fos and ATF-2 (Plotnikov et al. 2011). Activated TAK1 simultaneously stimulates the NFκB signalling pathway (Figure 1.4) as it activates the IKK complex, which is composed of IKKα, IKKβ and NFκB essential modulator (NEMO) (DiDonato et al. 1997, Yamaoka et al. 1998), via phosphorylation of key serine residues (Ser177 and Ser181) within the activation loop of IKKβ (Mercurio et al. 1997). Activation of IKKβ results in the phosphorylation of IκB family of proteins, most notably IκBα. IκBα is phosphorylated on Ser32 and Ser36 which facilitates its K48-linked

polyubiquitination by a βTrCP E3 ubiquitin ligase complex and subsequent degradation by the proteasome (Israël 2010). In the absence of stimulation, NFκB (most commonly the p50-p65 heterodimer) is sequestered in the cytoplasm as it is bound to IκBα; however it is released upon IκBα degradation and translocates to the nucleus where it initiates transcription of target genes including proinflammatory cytokines, chemokines, anti-apoptotic proteins and adhesion molecules. Full transcriptional activation of NFκB is achieved by phosphorylation of p65 at Ser536, which has been proposed to be mediated by multiple kinases, including IKKα, IKKβ, IKKε and TBK1 (TRAF family member-associated (TANK)-binding kinase 1) (Sakurai et al. 1999, Sakurai et al. 2003, Buss et al. 2004). Importantly, NFκB induces *de novo* synthesis of IκBα, which enters the nucleus and effectively strips NFκB from the target gene promotors. This IκBα-NFκB complex is then exported to the cytoplasm where it remains inactive until further stimulation, thereby acting as a rapid negative feedback loop (Zabel and Baeuerle 1990).

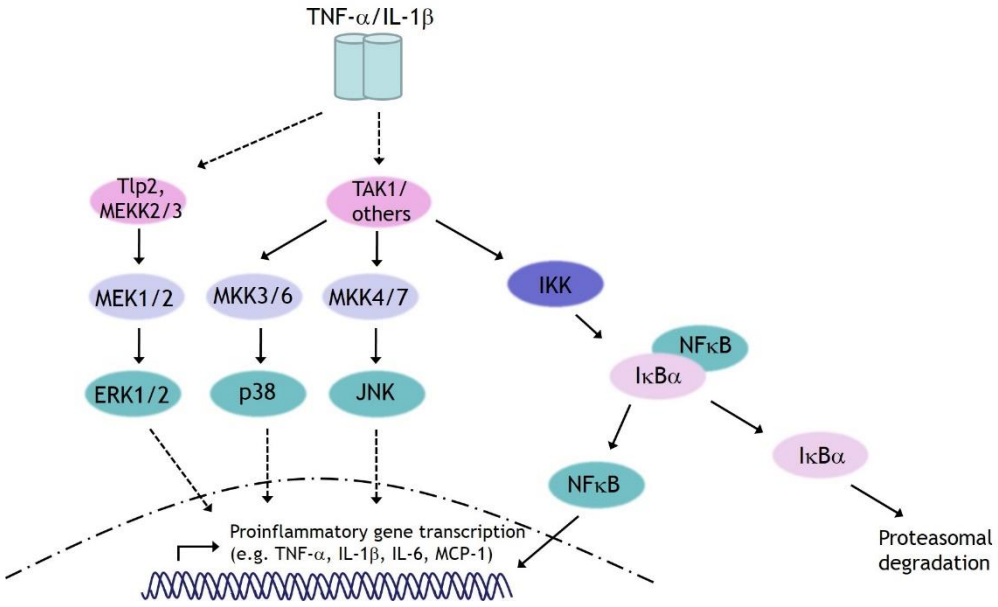

Figure 1-4: MAPK/NFκB signalling

TNF-α and IL-1β simultaneously activate the MAPK cascade and the NFκB pathway, stimulating transcription of proinflammatory genes. Abbreviations: MAPK, mitogen activated protein kinase; ERK1/2, extracellular signal regulated protein kinase 1/2; p38, p38 MAPK; JNK, c-Jun N-terminal kinase; MEK1/2, ERK1/2 kinase; MKK3/6/4/7, MAPK kinase 3/6/4/7; IKK, IκB kinase; IκB, NFκB inhibitor; NFκB, nuclear factor κB; MCP-1, monocyte chemoattractant protein-1.

1.2.2.2 IL-6 signalling to JAK/STAT

IL-6 is a proinflammatory cytokine secreted predominantly by macrophages and hypertrophic adipocytes, as found in obese adipose tissue. Plasma IL-6 concentrations are positively correlated with body mass (Lee et al. 2009); interestingly, it has been found that expression of IL-6 is much higher in visceral, rather than subcutaneous, adipose tissue (Fried, Bunkin, and Greenberg 1998). Elevated levels of IL-6 are associated with an increase in the production of C-Reactive Protein (CRP) which is a marker for inflammation and is linked to cardiovascular disease, hypertension and type 2 diabetes; therefore increased plasma IL-6 is a predictor for the development of these conditions (Pradhan et al. 2001, Ridker, Rifai, et al. 2000, Ridker, Hennekens, et al. 2000).

In most cell types, IL-6 initially forms a complex with a soluble receptor (sIL-6Rα) before binding the signal-transducing gp130 (glycoprotein 130) receptor homodimer. IL-6 signal transduction utilises the tyrosine kinases of the JAK (Janus kinase) family and transcription factors of the STAT (Signal transducers and activators of transcription) family, as demonstrated in Figure 1.5. JAKs are gp130-associated kinases which become activated following IL-6/sIL-6Rα binding the gp130 receptor. Activated JAKs then phosphorylate tyrosine residues on the cytoplasmic tails of gp130, which in turn function as docking sites for STAT factors. STAT1 and STAT3 bind these phosphotyrosines via their SH2 domains (Stahl et al. 1995, Gerhartz et al. 1996), and are subsequently tyrosine-phosphorylated by the JAKs (STAT1 on Tyr701 and STAT3 on Tyr705) (Kaptein, Paillard, and Saunders 1996, Shuai et al. 1993). STAT3 is more strongly activated by IL-6 than STAT1 and binds pYxxQ motifs (Stahl et al. 1995, Gerhartz et al. 1996), while the STAT1 recruitment site is more restricted (pYxPQ) (Gerhartz et al. 1996). Phosphorylated STATs form dimers and translocate to the nucleus, where they regulate transcription of target genes, including APP (amyloid precursor protein) genes such as CRP (C-reactive protein) (Zhang et al. 1996), transcription factors such as AP-1 (activator protein-1) (Coffer et al. 1995), and chemokines such as MCP-1 (Fasshauer, Klein, et al. 2004); all of which are involved in the inflammatory response. Interestingly, although dimerisation of STATs is essential for translocation to the nucleus, tyrosine phosphorylation itself is not specifically required as artificially dimerised STATs have been shown to have the ability to

enter the nucleus (Bromberg et al. 1999, Milocco et al. 1999). SHP-2 (src homology domain-containing protein tyrosine phosphatase-2) can also be recruited to phosphorylated tyrosine residues of gp130 via SH2 domains, before being phosphorylated by JAKs, leading to the activation of the ERK MAPK cascade (Fig. 1.5) (Fukada et al. 1996).

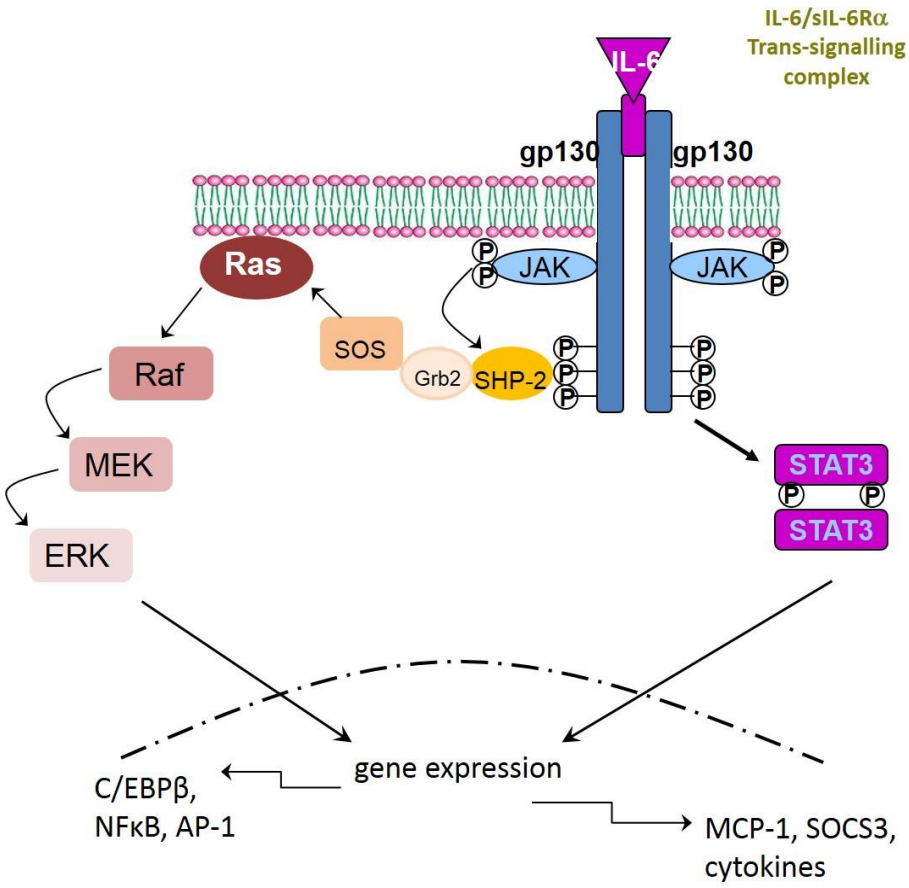

Figure 1-5: IL-6 signalling

IL-6 activates the gp130 receptor subunits, initiating their dimerization and recruitment and activation of JAK proteins. Activated JAKs phosphorylate gp130 subunits which function as docking sites for SH2-containing proteins. STAT3 binds, is phosphorylated by JAK which induces dimer formation. SHP-2 is also phosphorylated by JAKs and initiates the Ras/Raf/MEK signalling pathway, activating ERK1/2. STAT3 dimers and ERK1/2 translocate to the nucleus where they stimulate the transcription of genes. Abbreviations: SHP-2, src homology domain-containing protein tyrosine phosphatase-2; Grb2, growth factor receptor-bound protein 2; SOS, son of sevenless; MEK, ERK kinase; AP-1, activator protein-1; SOCS3, suppressor of cytokine signalling 3.

1.2.3 Macrophage recruitment and activation in adipose tissue

Obesity is associated with a low-grade inflammation of WAT as a result of the chronic activation of the innate immune system. The cytokine-stimulated NFκB, MAPK and JAK/STAT pathways described above culminate in the secretion of chemokines, including MCP-1, which stimulate the recruitment of macrophages to the site of inflammation. The migration of macrophages into WAT is central to the development of obesity-associated inflammation of WAT, as demonstrated by several *in vivo* studies (Arkan et al. 2005, Solinas et al. 2007, Odegaard et al. 2007). Indeed, as many as 50% of cells within obese adipose tissue have been proposed to be macrophages, while the macrophage content of lean adipose tissue is just 5-10% (Weisberg et al. 2003).

The initial events which lead to the recruitment of macrophages and the development of inflammation in WAT are currently not well understood, however it is believed that the increased adipose tissue mass and the characteristic hypertrophic adipocytes exhausts the local oxygen supply to the tissue, leading to hypoxia within the individual cells, which then in turn activates cellular stress pathways resulting in the release of proinflammatory mediators from adipocytes (de Luca and Olefsky 2008). Hypoxia may also contribute towards the increased adipocyte necrosis observed in obese WAT; indeed obesity-associated adipocyte death has been reported to occur primarily via necrosis, rather than apoptosis (Cinti et al. 2005). Necrosis is characterised as inflammatory, as the contents of the dying cell are released into the extracellular space where they provoke proinflammatory responses (Fink and Cookson 2005); moreover, 90% of macrophages recruited to WAT of obese mice are reported to be localised to necrotic adipocytes, where they scavenge for lipid droplets and aggregate to form giant multinucleate cells which are a hallmark of chronic inflammation (Cinti et al. 2005). Obesity is often associated with an increase in saturated FA which can activate the TLR (Toll-like receptor) family, and can also play a role in the recruitment of macrophages to WAT. Indeed, mice with a hematopoietic cell-specific deletion of TLR4 are protected from HFD (high-fat diet)-induced inflammation (Saberi et al. 2009). Taken together, macrophages may be recruited to WAT in response to proinflammatory signals secreted by hypertrophic,

dysfunctional adipocytes, necrosis of these adipocytes and the increased presence of saturated FA.

Upon migration into adipose tissue, macrophages undergo a shift in polarisation from an anti-inflammatory 'alternatively activated' M2 state, to a 'classically activated' proinflammatory M1 state (Olefsky and Glass 2010). Adipose tissue macrophages are differentially activated depending on the level of adiposity; *in vivo* macrophage pulse-labelling studies have demonstrated that macrophages within obese adipose tissue are highly proinflammatory and show increased expression of genes associated with adhesion, migration and inflammation (Lumeng et al. 2007, Lumeng, Bodzin, and Saltiel 2007). In contrast, macrophages within lean adipose tissue tend to be anti-inflammatory (Lumeng, Bodzin, and Saltiel 2007). It is important to note that the existence of these M1/M2 polarisation states has largely been defined *in vitro*, and tissue macrophages *in vivo* are most likely to be activated along a continuum between these states, rather than existing in a completely homogenous M1 or M2 state (Lumeng, Bodzin, and Saltiel 2007). Regulation of these activation states in response to various stimuli is shown in Figure 1.6.

Whether adipose tissue macrophages are classically or alternatively activated can depend on the secretory products of the adipocytes. As previously described, dysfunctional hypertrophic adipocytes of obese adipose tissue secrete proinflammatory cytokines and chemokines. This, in addition to the increased presence of proinflammatory saturated FA, induces the classical activation of macrophages, which in turn also secrete proinflammatory cytokines and chemokines (Figure 1.6). Furthermore, macrophages can also induce inflammatory responses through activation of the inflammasome, the best-characterised being the NLRP3 (nucleotide-binding and oligomerisation domain-like receptor family pyrin domain-containing 3) inflammasome. This stimulates maturation and secretion of proinflammatory cytokines IL-1β and IL-18; thus activation of the inflammasome has been associated with obesity-related inflammation, insulin resistance and Type 2 diabetes (Vandanmagsar et al. 2011). This positive feedback loop therefore further exacerbates the inflammatory state of the tissue. In contrast, adipocytes in lean adipose tissue secrete anti-inflammatory factors, including IL-4, IL-10 and IL-13, and anti-inflammatory FA (Olefsky and Glass 2010,

Solinas et al. 2007, Fujisaka et al. 2009), which promote the alternative activation of macrophages (Figure 1.6). These M2-activated macrophages secrete IL-10, which not only acts on adipocytes to maintain an insulin-sensitive state, but also elicits a protective effect by inhibiting secretion of proinflammatory mediators (Lumeng, Bodzin, and Saltiel 2007).

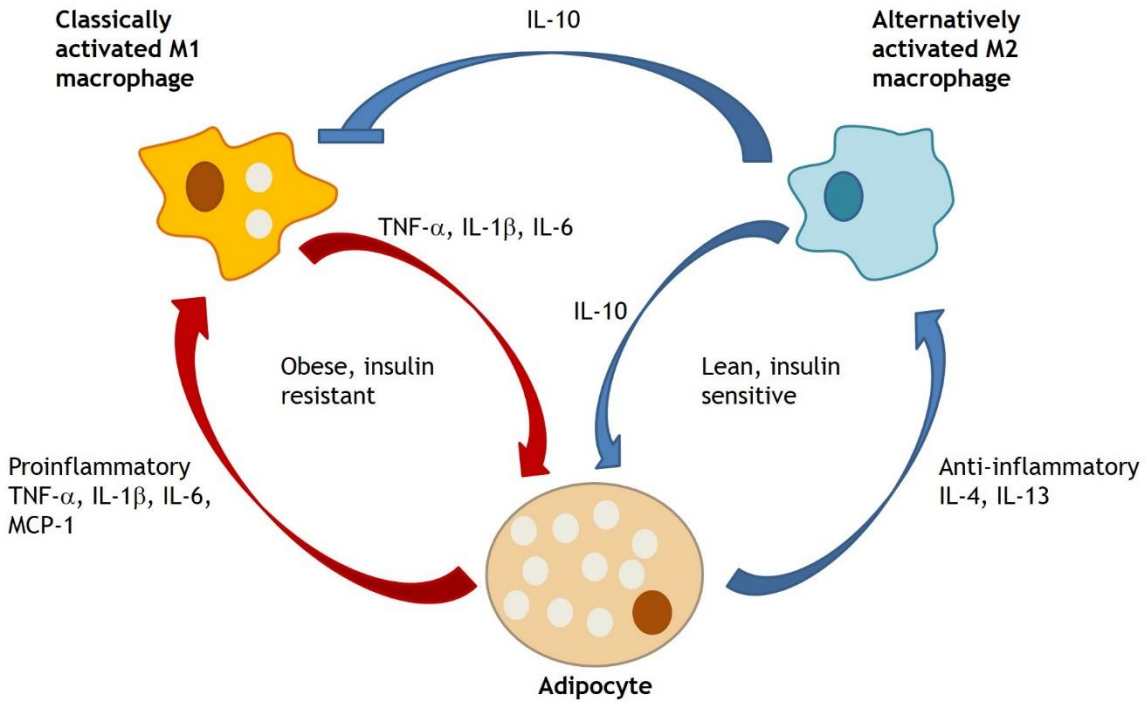

Figure 1-6: Regulation of macrophage activation states

Obesity is associated with hypertrophic adipocytes which secrete proinflammatory cytokines and chemokines, stimulating macrophage recruitment and M1 activation, leading to further production of proinflammatory mediators and insulin resistance in metabolic tissues. Lean adipocytes secrete anti-inflammatory cytokines such as IL-4 and IL-13 which induces macrophage M2 polarisation; M2 macrophages secrete anti-inflammatory cytokines such as IL-10 and contribute toward an insulin sensitive phenotype.

Proinflammatory T-cells have been reported to be present in VAT of mice with HFD-induced obesity, and their accumulation has been proposed to stimulate macrophage infiltration and M1 activation (Nishimura et al. 2009, Kintscher et al. 2008, Wu et al. 2007). Indeed, adipocyte production of the chemokine IP-10 (interferon-γ-induced protein 10 kDa) has been reported to induce T-cell

migration, which was ablated following NFκB blockade in adipocytes (Krinninger et al. 2011). Furthermore, levels of protective, anti-inflammatory regulatory T-cells have been found to be diminished in adipose tissue of mice with HFD-induced obesity (Nishimura et al. 2009, Feuerer et al. 2009), further enhancing the proinflammatory environment.

1.2.4 Role of inflammation in the development of insulin resistance

Inflammation is a key factor in the development of obesity-related insulin resistance, with a plethora of evidence suggesting that inhibition of proinflammatory signalling either via genetic or pharmacological means ablates diet-induced insulin resistance and subsequent Type 2 diabetes. Insulin sensitivity is reduced in response to elevated serum FA and increased production of proinflammatory cytokines by adipocytes and M1 activated macrophages in obese WAT (Figure 1.7). Macrophages contribute the most significant proportion of inflammatory mediators within obese WAT; consistent with this, genetic ablation of the MCP-1 receptor CCR2 is associated with a reduction in adipose tissue macrophage infiltration and an improvement in insulin sensitivity in HFD-fed mice (Weisberg et al. 2006). Furthermore, mice with macrophage-specific deletion of JNK or IKK were reported to exhibit a reduction in proinflammatory gene expression and adipose tissue macrophage infiltration, with a concomitant increase in insulin sensitivity (Arkan et al. 2005, Solinas et al. 2007). The molecular mechanism by which proinflammatory cytokines such as TNF-α, IL-1β and IL-6 have been reported to negatively regulate the insulin signalling pathway in target tissues is outlined in Figure 1.7.

1.2.4.1 TNF-α/IL-1β signalling induces insulin resistance

TNF-α was the first cytokine to be linked to obesity-related insulin resistance, with studies carried out by Hotamisligil and co-workers using animal models of obesity and diabetes demonstrating that neutralisation of TNF-α could improve glucose metabolism (Hotamisligil, Shargill, and Spiegelman 1993). An abundance of studies followed, all supporting a key role for TNF-α in obesity-related insulin resistance.

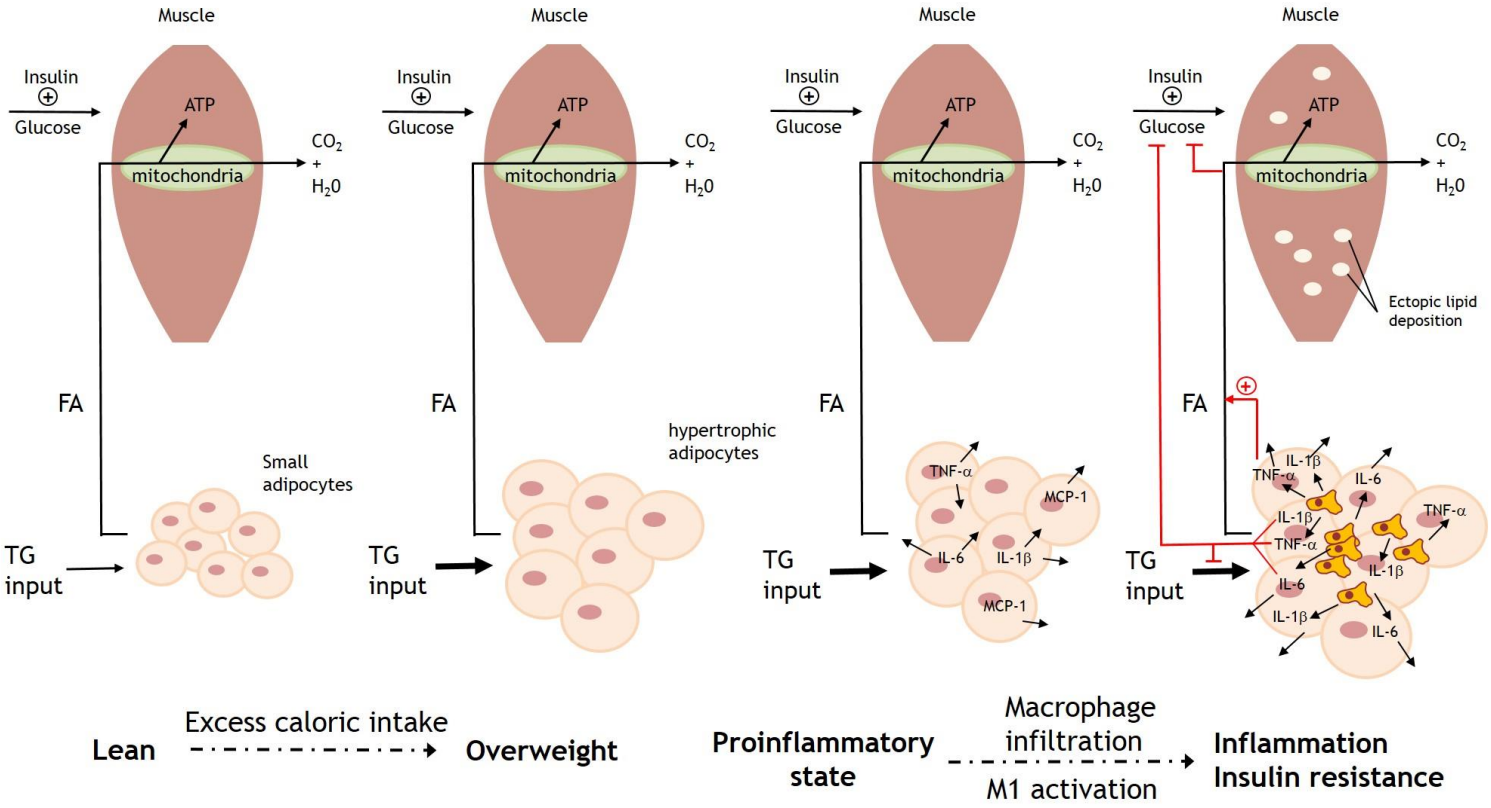

Figure 1-7: Inflammation-mediated inhibition of insulin signalling

A positive energy balance causes an increase in adipocyte size due to increased TG storage. Dysfunctional hypertrophic adipocytes secrete proinflammatory cytokines and chemokines, which stimulate the recruitment and M1 activation of macrophages, further exacerbating the inflammatory environment within the tissue. Proinflammatory cytokines can stimulate an increase serum FA, promote ectopic lipid deposition and induce insulin resistance in the metabolic tissues.

Dietary and genetic (*ob*/*ob*) mouse models of obesity deficient in either TNF-α or TNF-RI displayed improved insulin sensitivity (Uysal et al. 1997), while there was found to be elevated expression of TNF-α in adipose tissue of obese humans which was reduced upon weight loss (Kern et al. 1995, Dandona et al. 1998). Several studies sought to determine the mechanism by which TNF-α signalling induced insulin resistance, with early studies suggesting the JNK1–mediated inhibitory phosphorylation of Ser307 (equivalent to Ser312 in human) of IRS-1 (Aguirre et al. 2000, Hotamisligil et al. 1996) (Figure 1.8). Increased insulin resistance was reported following activation or overexpression of IKKβ in Zucker *fa*/*fa* and *ob*/*ob* mice, while conversely, a reduction in IKKβ activity or expression led to an improvement in insulin sensitivity (Yuan et al. 2001). IRS-1 Ser307 was later proposed to also be a substrate for IKKβ as interactions were observed using a co-immunoprecipitation approach and the TNF-α-induced Ser307 phosphorylation of IRS-1 was diminished following IKKβ inhibition (Figure 1.8). Cells derived from IKK-deficient mice supported this finding (Gao et al. 2002).

Following the plethora of *in vitro* and animal studies conducted on the importance of TNF-α in obesity-related insulin resistance, further studies were carried out to assess the clinical relevance of TNF-α in humans. Infliximab (a TNF-α neutralising monoclonal antibody) is widely used in the treatment of chronic inflammatory conditions, such as rheumatoid arthritis (RA). A small study conducted in patients with RA taking Infliximab demonstrated a significant reduction in insulin resistance (Gonzalez-Gay et al. 2006). Other studies, however, showed no improvement in insulin sensitivity with TNF-α-neutralising antibodies or inhibitors, despite improvements in inflammatory status (Ofei et al. 1996, Wascher et al. 2011, Ferraz-Amaro et al. 2011). Taken together, these studies indicate that while chronic low-grade inflammation plays a key role in the development of obesity-related insulin resistance, it is likely that proinflammatory cytokines other than TNF-α alone may play a more prominent role.

Recent evidence suggests IL-1β may be important in the development of insulin resistance, with IL-1β expression found to be elevated in serum and WAT of obese patients and positively correlated with body mass index and insulin resistance. Conversely, IL-1β levels are reduced upon weight loss (Moschen et al. 2011, Meier et al. 2002). IL-1β expression was found to be upregulated in adipose tissue of

obese and insulin resistant mouse models (diet-induced and *ob*/*ob*), while phosphorylation of insulin signalling pathway components including IRS-1 and PKB were inhibited in 3T3-L1 and human adipocytes treated with IL-1β (Lagathu et al. 2006) (Figure 1.8). It has also been proposed that prolonged treatment of IL-1β in 3T3-L1 adipocytes downregulates mRNA expression of IRS-1 in an ERK-dependent manner (Jager et al. 2007).

An interesting study conducted by Larsen and co-workers found that neutralisation of IL-1β with anakinra (a recombinant IL-1R antagonist) over 13 weeks improved hyperglycaemia and reduced markers of systemic inflammation in human subjects. Furthermore, these effects were maintained 39 weeks following withdrawal of treatment (Larsen et al. 2007, Larsen et al. 2009).

Taken together, NFκB and MAPK signalling plays a key role in the development of chronic inflammatory disorders, particularly obesity-related insulin resistance (Figure 1.8). Clinical studies indicate IL-1β may be a more important activator of these pathways than TNF-α in terms of insulin resistance in humans.

1.2.4.2 IL-6 signalling induces insulin resistance

There is conflicting evidence regarding the role of IL-6 in the development of insulin resistance in different tissues. IL-6 has been reported to induce insulin resistance in both adipose and liver (Rotter, Nagaev, and Smith 2003, Senn et al. 2002, Klover et al. 2003), while locally stimulating glucose uptake in muscle (Carey et al. 2006). While it would seem paradoxical that exercise, which has been well established to enhance insulin action, would stimulate the release of a factor from muscle that inhibits insulin signalling, there are a number of *in vitro* and *in vivo* studies demonstrating the proinflammatory nature of IL-6 in liver and adipose. It is thought that these pro- and anti-inflammatory effects of IL-6 are context-dependent, with many different cells producing IL-6 under varying physiological conditions. Adipose tissue has been proposed to release 10-35 % of circulating IL-6 levels in healthy individuals (Mohamed-Ali et al. 1997), with macrophages within the adipose being the primary site of production. The number of macrophages present in adipose tissue is positively correlated with obesity (Weisberg et al. 2003); therefore an increase in macrophages is associated with an increase in

production of proinflammatory mediators. Furthermore, hypertrophic adipocytes in obese adipose tissue have also been found to produce IL-6 (Gustafson 2010, Sopasakis et al. 2004). As previously described, obesity is characterised as a state of sustained, low-grade inflammation, with a 2-3 fold increase in secretion of proinflammatory mediators from adipose tissue (Weisberg et al. 2003, Kern et al. 2001) (Figure 1.7). In direct contrast, exercise has been suggested to induce an acute, but transient, increase in IL-6 (but not other inflammatory markers such as TNF-α) production in skeletal muscle (Brandt and Pedersen 2010, Jonsdottir et al. 2000), found to be approximately 100 fold, depending on the duration and intensity of the exercise (Jonsdottir et al. 2000). Moreover, the acute increase in IL-6 levels in muscle in response to exercise has been proposed to be independent of macrophage activation (Moldoveanu, Shephard, and Shek 2000). Therefore the source and duration of IL-6 production is likely to determine whether IL-6 has beneficial anti-inflammatory effects, or whether it is a key player in the development of a chronic, proinflammatory, insulin resistant phenotype in obesity.

While the effect of TNF-α on inhibition of insulin signalling has been thoroughly examined, comparatively fewer studies have been undertaken concerning the mechanism by which IL-6 may inhibit insulin signalling (Figure 1.8). Mooney and co-workers found that IL-6 inhibited insulin signalling and action *in vitro* in isolated hepatocytes and hepatoma cell lines (Senn et al. 2002), and *in vivo* in livers of mice chronically administered IL-6 at levels physiologically similar to those found in obesity (Klover et al. 2003). Conversely, neutralisation with an anti-IL-6 antibody was found to improve hepatic insulin sensitivity in DIO (diet-induced obesity) and *ob/ob* mouse models of obesity (Klover, Clementi, and Mooney 2005). It was found that IL-6 transiently increased expression of the negative regulator of IL-6 signalling, SOCS3 (suppressor of cytokine signalling 3), in HepG2 and rat liver cells which was associated with an inhibition of insulin-stimulated IRS-1 tyrosine phosphorylation, p85 binding, and subsequent PKB phosphorylation (Senn et al. 2003). Similarly in adipocytes, Rotter and co-workers found that chronic exposure of 3T3-L1 adipocytes with IL-6 induced insulin resistance via inhibition of IRS-1 and GLUT4 protein expression, while short term incubation with IL-6 had no effect on insulin sensitivity (Rotter, Nagaev, and Smith 2003). Importantly, this

was not found to be due to an increase in TNF-α, as IL-6 was not found to stimulate TNF-α expression in this study (Rotter, Nagaev, and Smith 2003).

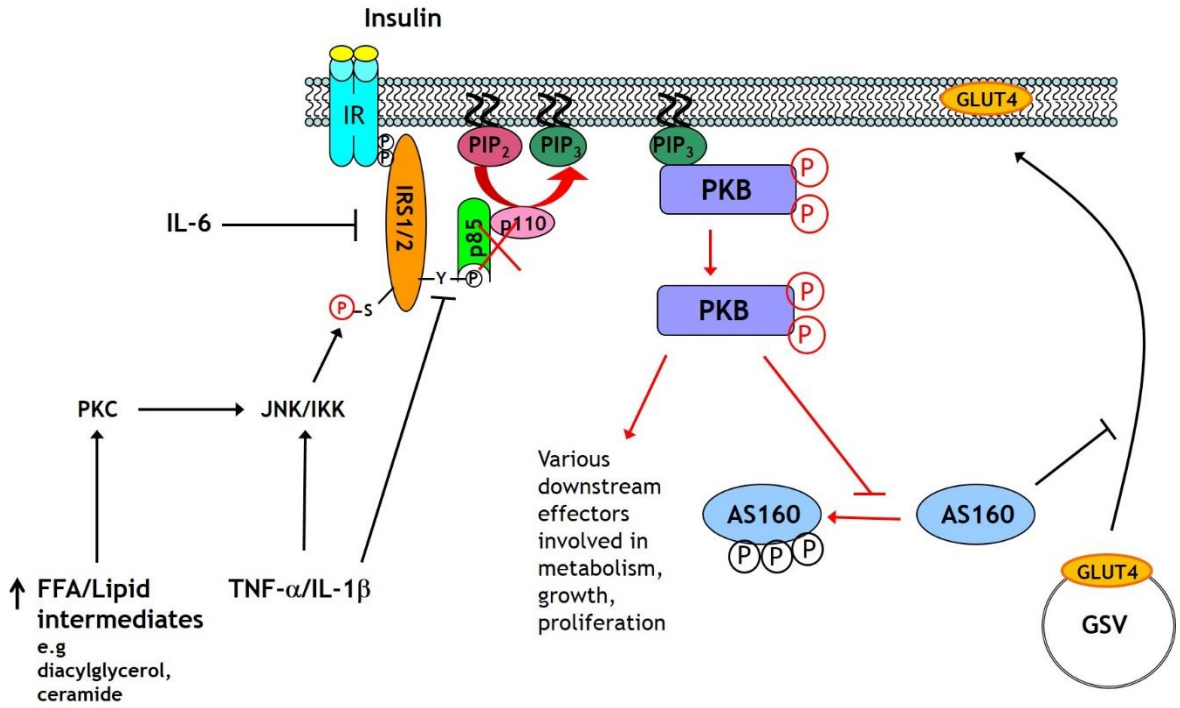

Figure 1-8: Inflammation-mediated inhibition of insulin signalling

Insulin signalling has been reported to be inhibited at the level of IRS, via downregulation, IKK/JNK-mediated serine phosphorylation or inhibition of tyrosine phosphorylation by proinflammatory cytokines and FFA/activated lipid intermediates. Inhibition of insulin signalling results in a reduction in GLUT4-mediated glucose uptake in adipose tissue and skeletal muscle. Abbreviations: IRS, insulin receptor substrate; PI3K, phosphatidylinositol 3-kinase; PIP_2, phosphatidylinositol 4,5 bisphosphate; PIP_3, (phosphatidylinositol 3,4,5-trisphosphate); PKB, protein kinase B; AS160, Akt substrate of 160 kDa; GSV, GLUT4 storage vesicle; PKC, protein kinase C.

Consistent with a role for IL-6 in reducing insulin sensitivity, it has been reported that adipose tissue IL-6 content correlated with insulin resistance both *in vitro* and *in vivo* (Bastard et al. 2002). Moreover, neutralisation with an anti-IL-6 antibody improved hepatic insulin sensitivity in DIO and *ob/ob* mouse models of obesity (Klover, Clementi, and Mooney 2005). Furthermore, clinical trials for tocilizumab (a monoclonal antibody against the IL-6 receptor) demonstrated an improvement in insulin sensitivity in RA patients upon inhibition of IL-6 signalling (Schultz et al. 2010). Taken together, these studies indicate that while chronic

low-grade inflammation plays a key role in the development of obesity-related insulin resistance, further studies are required to delineate the pro- and anti-inflammatory effects of IL-6 in different tissues.

1.2.4.3 Serum FA induces insulin resistance

Cytokines such as TNF-α cause an increase in circulating FA by stimulating lipolysis and impairing storage of FA as TG in adipocytes (Figure 1.7). Elevated circulating FA can contribute to the development of obesity-related insulin resistance; FAs can stimulate TLR4 on adipocytes and macrophages, activating proinflammatory signalling pathways and further enhancing the inflammatory environment (Shi, Kokoeva, et al. 2006). Moreover, TLR4 is reported to be essential for FA-induced insulin resistance in myotubes and adipocytes (Senn 2006, Suganami et al. 2007), while *TLR4*$^{-/-}$ mice have been reported to be protected from obesity-induced inflammation and insulin resistance (Shi, Kokoeva, et al. 2006). Furthermore, an increase in circulating FA leads to an accumulation of TG and activated lipids in the form of long-chain fatty-acyl CoA (LCACoA) esters in tissues other than adipose, namely liver and skeletal muscle (Figure 1.7), as well as pancreatic β-cells (Guilherme et al. 2008). This ectopic deposition of FA and their derivatives has been shown to induce insulin resistance via disruption of the insulin signalling pathway (Kraegen et al. 2001). FA and their derivatives can directly activate PKC (protein kinase C), which in turn activates JNK and IKK leading to the subsequent serine phosphorylation of IRS-1 (Gao et al. 2004, Yu et al. 2002). Interestingly, while it is the TG content of the liver and skeletal muscle that is used as a marker for abnormal lipid accumulation, it has been suggested that it is in fact the lipid intermediates, primarily diacylglycerol (DAG), ceramide and LCACoA that have a negative impact upon insulin sensitivity (Kraegen and Cooney 2008, Timmers, Schrauwen, and de Vogel 2008).

1.3 AMPK

1.3.1 Overview of AMPK

In the 1970's two separate groups discovered that incubating acetyl CoA carboxylase (ACC) or HMG-CoA reductase (HMGR) (Timmers, Schrauwen, and de

Vogel 2008, Beg, Stonik, and Brewer 1978), with ATP resulted in their inactivation, however it was not until later that a third group provided evidence suggesting it was the same protein kinase which was responsible for the phosphorylation and inactivation of both these enzymes (Carling, Zammit, and Hardie 1987). This group subsequently named this kinase AMP-activated protein kinase (AMPK) after its allosteric activator 5'-AMP (Munday et al. 1988).

AMPK is the downstream component of a protein kinase cascade that plays a key role in the regulation of energy balance at both the cellular and whole-body level. AMPK is sensitive to cellular energy levels and is activated in response to a decrease in cellular energy, and functions to stimulate catabolic ATP-producing pathways while suppressing anabolic ATP-consuming pathways in order to restore the energy balance.

1.3.2 AMPK structure and regulation

AMPK exists as a heterotrimeric complex consisting of a catalytic α subunit and regulatory β and γ subunits, as shown in Figure 1.9. Isoforms of each AMPK subunit ($\alpha1$, $\alpha2$, $\beta1$, $\beta2$, $\gamma1$, $\gamma2$, $\gamma3$) are encoded by seven genes in mammals, thus 12 heterotrimeric complexes are theoretically possible (Kahn et al. 2005). Expression levels of the different subunit isoforms vary between tissues and may dictate the subcellular localisation of the AMPK complex; the $\alpha1$, $\beta1$ and $\gamma1$ isoforms are ubiquitously expressed, while the $\alpha2$ and $\beta2$ isoforms are predominantly expressed in striated muscle (Thornton, Snowden, and Carling 1998, Verhoeven et al. 1995). The $\gamma2$ and $\gamma3$ isoforms are expressed in several different tissues (Cheung et al. 2000). These can also be subject to alternative splicing, thereby further increasing the diversity of the complexes. Homologues have been found to be highly conserved in a wide range of species, from mammals to yeast to primitive protozoa, indicating the importance of the system in various species (Hardie et al. 2003).

Figure 1.9 outlines the domain structures of the AMPK subunits. The catalytic α subunit consists of a serine/threonine kinase domain at the N-terminus which contains a conserved threonine residue at position 172, phosphorylation of which is essential for AMPK activity (Woods et al. 1994). The last 150 amino acids of the

C-terminus are responsible for interaction with β and γ subunits and subsequent complex formation (Crute et al. 1998). The β subunit stabilises the interaction between the α and γ subunits via its C-terminus (Hudson et al. 2003). The β subunit also contains a carbohydrate-binding module (CBM) (Hudson et al. 2003, Polekhina et al. 2003) to which oligosaccharide components of glycogen can bind and inhibit AMPK (McBride et al. 2009). The γ subunits are characterised by the presence of four CBS (cystathione-β-synthase) motifs, which occur as tandem pairs, known as Bateman domains (Bateman 1997, Kemp 2004), with a deep binding cleft separating them and are found in a small number of proteins which tend to bind adenosine-containing ligands (Scott et al. 2004). The Bateman domains of the AMPK γ subunit bind adenine nucleotides; crystallisation of the regulatory core of mammalian AMPK revealed that three of the four CBS motifs contained nucleotide binding sites (Xiao et al. 2007). Two of these sites can bind AMP, ADP or ATP with approximately equal affinity in a competitive manner, while the remaining site contains a tightly-bound, non-exchangable molecule of AMP (Xiao et al. 2007).

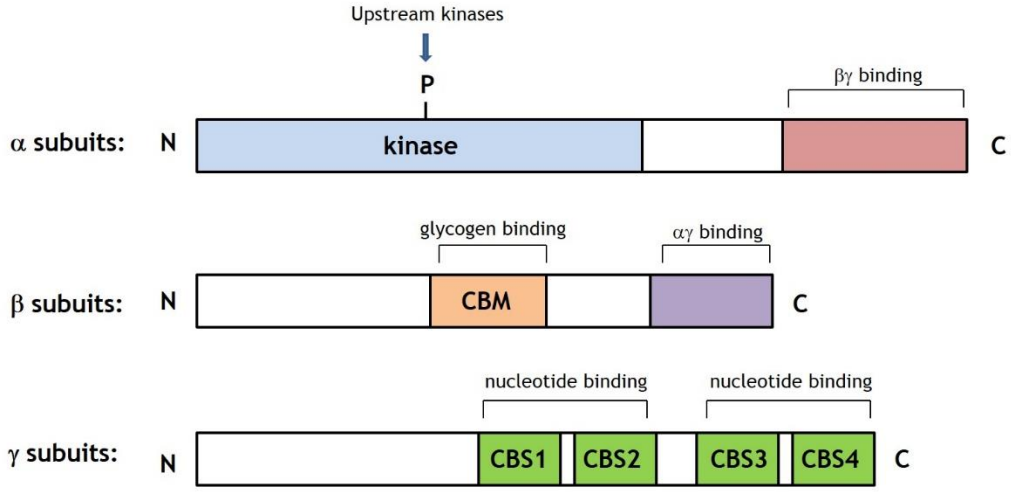

Figure 1-9: Domain structure of AMPK subunit isoforms

Binding of AMP or ADP to the γ subunit regulates AMPK activity, as it promotes allosteric activation of the enzyme and phosphorylation of the catalytic α subunit at Thr172 by upstream kinases. In contrast, binding of ATP to the γ subunit competitively antagonises the AMP or ADP-mediated allosteric activation and Thr172 phosphorylation (Carling et al. 2012, Hardie, Ross, and Hawley 2012b); therefore an increase in the AMP/ATP or ADP/ATP ratio allosterically activates AMPK and further promotes activity as a result of increased Thr172

phosphorylation (Figure 1.10). Furthermore, AMP/ADP binding to the γ subunit renders AMPK a poor substrate for protein phosphatases such as PP2C; therefore Thr172 phosphorylation is maintained (Davies et al. 1995). Interestingly, the different γ subunit isoforms exhibit differential adenine nucleotide sensitivity, therefore potentially allowing for tissue-specific regulation of AMPK (Hardie, Ross, and Hawley 2012b, Carling et al. 2012, Cheung et al. 2000). It has recently been suggested that ADP may be the principal nucleotide to allosterically activate AMPK, not AMP as previously thought. While the exchangable nucleotide binding sites on the γ subunit exhibit similar binding affinity for AMP, ADP and ATP, the cellular concentrations of ADP and ATP far exceed that of AMP; thus the ADP/ATP ratio has been proposed to be a more physiologically relevant stimulus for AMPK and the extent to which AMPK is activated allosterically *in vivo* may be modest compared to the effect of phosphorylation at Thr172 (Carling et al. 2012). On the contrary, a recent study suggests that the allosteric regulation of AMPK by AMP may be at least as important as the effect of Thr172 phosphorylation in the activation of AMPK in intact cells, if not more so. Gowans and co-workers reported that AMP is a more potent inhibitor of Thr172 dephosphorylation than ADP; furthermore, AMP stimulated an increase in downstream substrate ACC phosphorylation without Thr172 phosphorylation; thus entirely by allosteric activation of AMPK (Gowans et al. 2013).

The AMPK phosphorylation site Thr172 lies within the activation loop of the catalytic α subunit (Hawley et al. 1996). Two upstream kinases have been identified which mediate this phosphorylation: LKB1 (liver kinase B1) and CaMKKβ (Ca^{2+}/calmodulin-dependent protein kinase kinase β) (Figure 1.10). While LKB1 is ubiquitously expressed, CaMKKβ expression appears to be restricted to primarily neuronal cells (Anderson et al. 1998).

LKB1 was originally identified as a tumour suppressor which is mutated in Peutz-Jeghers Syndrome (PJS) (Anderson et al. 1998). LKB1 exists in complex with two accessory subunits, STRAD and MO25 (Woods et al. 2003, Hawley et al. 2003). MO25 is thought to stabilise the LKB1-STRAD complex (Milburn et al. 2004), while STRAD is essential for the phosphorylation of AMPK on Thr172 by the complex (Hawley et al. 2003). Indeed, cells deficient in LKB1 were demonstrated to exhibit reduced AMPK activity, and AMPK was found not to be activated in response to

stimuli which would normally activate it (Shaw et al. 2004, Hawley et al. 2003, Woods et al. 2003); thereby highlighting LKB1 as an AMPK kinase. Furthermore, LKB1 itself was not found to be regulated by AMP (Hawley et al. 2003, Woods et al. 2003), or other stimuli which activate AMPK in cells (Woods et al. 2003, Lizcano et al. 2004), or skeletal muscle (Sakamoto et al. 2004). These findings suggested LKB1 was constitutively active, and that AMPK activation was regulated directly by binding of AMP to γ subunits.

Hawley and co-workers first reported that CaMKK could phosphorylate and activate AMPK in cell-free assays (Hawley et al. 1995); however the major AMPK kinase purified from rat liver was not found to be calmodulin dependent (Hawley et al. 1996), and was later identified as LKB1 (Hawley et al. 2003, Shaw et al. 2004). Interestingly, Hawley and co-workers found there to be significant basal AMPK activity in LKB1-deficient cells, indicating the existence of an alternative AMPK kinase which was demonstrated to be CaMKKβ (Hawley et al. 2005).

Although the LKB1 complex is the predominant upstream kinase of AMPK in most cells, this alternative pathway for AMPK activation is AMP-independent and is triggered by an increase in cytoplasmic Ca^{2+}, which activates CaMKKβ (Hawley et al. 2005, Woods et al. 2005, Hurley et al. 2005). AMPK was demonstrated to be rapidly phosphorylated in HeLa cells (which lack LKB1) in response to the Ca^{2+} ionophore A23187 (Hawley et al. 2005). Furthermore, AMPK activation was ablated by addition of the CaMKK inhibitor STO-609 or siRNA-mediated knockdown of the CaMKK gene (Hawley et al. 2005).

1.3.3 AMPK activation and physiological role

AMPK is activated under conditions upon which the energy demands within the cell are increased and thus ATP consumption rises, or fuel availability is reduced, such that ATP synthesis falls; i.e. there is a reduction in the ATP/AMP ratio. As a consequence, activated AMPK phosphorylates key target proteins in order to stimulate FA oxidation, muscle glucose transport, mitochondrial biogenesis and caloric intake; thereby increasing ATP production. Concurrently, AMPK activation suppresses ATP-consuming anabolic pathways, including FA synthesis, cholesterol and isoprenoid synthesis, hepatic gluconeogenesis and mTOR (mammalian target

of rapamycin)-mediated protein translation. Thus, AMPK activation regulates the energy balance at a cellular and whole-body level. Physiological stimuli which activate AMPK include metabolic stresses such as hypoxia, ischaemia, glucose deprivation and heat shock; all of which inhibit ATP production, while exercise stimulates AMPK activation in muscle as it increases ATP consumption.

1.3.3.1 AMPK activation by adipocytokines

Leptin can activate AMPK in skeletal muscle, leading to an increase in glucose uptake and FA oxidation (Minokoshi et al. 2002). Minokoshi and co-workers observed that leptin acts directly on muscle to activate AMPK by acutely triggering an increase in the cellular AMP/ATP ratio, while prolonged treatment with leptin activates AMPK indirectly via the hypothalamic-sympathetic nervous system axis and is independent of nucleotides (Minokoshi et al. 2002). Furthermore, chronic leptin treatment in skeletal muscle is associated with increased expression of the $\alpha 2$ and $\beta 2$ subunits and sustained AMPK activation in the tissue, with subsequent increased rates of fatty acid oxidation being observed (Steinberg, Rush, and Dyck 2003). In addition to skeletal muscle, leptin has also been found to activate AMPK in adipocytes, stimulating fatty acid oxidation and mitochondrial biosynthesis (Wang et al. 2005). In contrast, the anorexigenic action of leptin previously mentioned is mediated by inhibition of AMPK activity in the arcuate and paraventricular hypothalamus (Minokoshi et al. 2004). The mechanism by which AMPK is inhibited by leptin in the hypothalamus has not been characterised. Reduced AMPK activity in the arcuate nucleus suppresses the actions of orexigenic peptides NPY/AgRP, while the anorexigenic MC4Rs appear to be required for regulation of AMPK in the hypothalamus, as a MC4R agonist was found to suppress AMPK activity in the paraventricular nucleus. Moreover, MC4R-deficient mice have a hyperphagic and obese phenotype, and are unable to suppress AMPK activity in response to feeding or leptin (Minokoshi et al. 2004).

Adiponectin has been reported to acutely stimulate AMPK in muscle and liver, with a concomitant increase in FA oxidation and glucose uptake in myocytes, reduction in gluconeogenic enzymes in the liver, and a reduction in overall glucose levels *in vivo* (Yamauchi et al. 2002). These effects of adiponectin were abolished with the use of a dominant-negative AMPK mutant, indicating the AMPK-dependence of

these effects by adiponectin (Yamauchi et al. 2002). Furthermore, adiponectin has been demonstrated to activate AMPK in adipocytes (Wu et al. 2003, Liu et al. 2010), pancreatic β-cells (Huypens, Moens, et al. 2005) and endothelial cells, resulting in increased eNOS (endothelial nitric oxide (NO) synthase) phosphorylation and subsequent NO production (Hattori et al. 2008). The mechanism by which adiponectin stimulates AMPK activation is unclear. One hypothesis is that the interaction of an adaptor protein APPL1 with the adiponectin receptor induces LKB1 translocation from the nucleus to the cytosol in muscle, thus enhancing AMPK Thr172 phosphorylation (Zhou, Deepa, et al. 2009, Dadson et al. 2014). A separate study suggested that activation of the adiponectin receptor is coupled to acyl-CoA synthetase activity, and the 5'AMP released during the attachment of FA to CoA activates AMPK in adipocytes (Liu et al. 2010).

There is conflicting evidence surrounding whether or not levels of proinflammatory cytokines such as IL-6 and TNF-α have any effect on activation of AMPK. TNF-α has been reported to rapidly activate AMPK in endothelial and kidney cell lines (Tang et al. 2010), while in contrast, chronic exposure to TNF-α has been reported to attenuate AMPK activity in myotubes and muscle, thought to be the result of dephosphorylation of Thr172 via upregulation of PP2C transcription (Steinberg et al. 2006). Similarly, LPS treatment was found to inhibit AMPK activation in macrophages *in vitro* (Sag et al. 2008), and attenuate AMPK expression in leukocytes and liver *in vivo* (Zhang et al. 2010). Exercise induced an increase in plasma IL-6, which was associated with an increase in AMPKα2 activity in rat muscle and epididymal adipose tissue (Ruderman et al. 2006). IL-6 treatment was reported to acutely stimulate AMPK activation in L6 myotubes (Carey et al. 2006) and cultured F422A adipocytes (Kelly et al. 2004). Furthermore, Kelly and co-workers found AMPK activation to be diminished in skeletal muscle and adipose of *IL-6*$^{-/-}$ mice compared to control mice (Kelly et al. 2004). In contrast, Nerstedt and co-workers found that IL-6 did not have any significant effect on AMPK activation in hepatocytes (Nerstedt et al. 2010), suggesting that activation of AMPK by IL-6 could be cell type-specific.

1.3.3.2 Pharmacological AMPK activation

AMPK is a central regulator of energy balance not only at a cellular level, but also at the level of the whole organism; AMPK activation results in many changes including regulation of glucose uptake and metabolism by muscle and other tissues, reduced glucose production in the liver and reduced synthesis and increased oxidation of FA. These are all effects which would be beneficial to individuals with Type 2 diabetes and the metabolic syndrome, thus making activation of AMPK in the metabolic tissues an attractive therapeutic target. In support of this, two widely used classes of insulin-sensitising drugs, the thiazolidinediones (TZDs) and the biguanide metformin have been reported to stimulate AMPK (Figure 1.10); however the extent to which AMPK activation mediates their clinical effects is still unclear. TZDs such as rosiglitazone are adipocyte PPARγ agonists (Lehmann et al. 1995); while the insulin-sensitising effects of TZDs are largely due to regulation of gene transcription by PPARγ, it has been suggested that the more acute effects of TZDs may be mediated by their ability to stimulate adiponectin production in adipocytes, which in turn activates AMPK, thereby reducing gluconeogenesis and stimulating FA oxidation (Kubota et al. 2006). Metformin is an antihyperglycaemic agent, with its main function being to suppress hepatic glucose production. It was discovered that metformin activates AMPK in hepatocytes (Zhou et al. 2001) in an AMP-dependent manner (Shaw et al. 2005) via inhibition of NADH dehydrogenase (Complex I) of the mitochondrial respiratory chain, which blocks ATP production and therefore increases the cellular AMP/ATP ratio (Brunmair et al. 2004), thus activating AMPK. Metformin has also been demonstrated to activate AMPK in WAT from mice and individuals with Type 2 diabetes in addition to cultured 3T3-L1 adipocytes (Boyle et al. 2011, Caton et al. 2011). Several plant-derived compounds including berberine, resveratrol and galgeine have also been reported to activate AMPK by altering adenine nucleotide ratios (Hawley et al. 2010) (Figure 1.10).

Several other compounds have been used experimentally activate AMPK. A widely used compound is AICAR (5'-aminoimidazole-4-carboxamide ribonucleoside), an adenosine analogue which enters cells via adenosine transporters. It is phosphorylated to the AMP mimetic ZMP by adenosine kinase (Vincent et al. 1991), thereby activating AMPK without altering adenine nucleotide ratios (Figure 1.10). AICAR has been widely used to activate AMPK in intact cells, tissues and animals. Actions of AICAR are not completely specific to AMPK, however, as ZMP has the

ability to regulate any enzyme which is sensitive to cellular AMP; though it is not known to activate any other kinases, AICAR has been demonstrated to inhibit fructose-1,6-bisphosphate in isolated rat hepatocytes (Vincent et al. 1991) and stimulate glycogen phosphorylase in rat muscle preparations *in vitro* (Longnus et al. 2003).

A769662 is a member of the thienopyridine family and can directly activate AMPK (Cool et al. 2006) in a similar manner to AMP, in that it triggers allosteric activation of the enzyme and inhibits dephosphorylation of Thr172 by protein phosphatases; however A769662 activates AMPK independently of AMP (Figure 1.10). Scott and co-workers reported that A769662 selectively activates AMPK complexes containing the β1, but not β2, regulatory subunit, and activation involves the CBM of the β1 subunit interacting with γ subunit residues distinct from those involved in AMP binding (Scott et al. 2008). Mutation of Ser108 within the CBM was reported to reduce A769662-mediated AMPK activation (Sanders et al. 2007), suggesting this site is critical for the action of A769662. Furthermore, mutagenesis studies revealed a cluster of hydrophobic amino acids proximal to the carbohydrate-binding loop of the CBM of β1 were important for the allosteric activation and phosphorylation of Thr172, and therefore activation of the enzyme (Scott et al. 2008). The development of this compound demonstrates that selective manipulation of AMPK complexes containing specific subunit isoforms is possible. A recent study by Ducommum and co-workers proposed that simultaneous administration of AICAR and A769662 in primary hepatocytes resulted in a synergistic effect of AMPK activation and subsequent downstream events, compared to treatment with a single compound (Ducommun et al. 2014). As AICAR and A769662 act on different sites of the AMPK protein, co-treatment is attractive from a therapeutic point of view as it would mean lower doses by promoting sensitivity via dual treatment.

Salicylate, a derivative of aspirin, has recently been demonstrated to stimulate AMPK activation (Hawley et al. 2012) (Figure 1.10). It was found to bind at the same AMPK site as A769662 and, similarly to A769662, salicylate caused allosteric activation and inhibition of Thr172 dephosphorylation independently of alterations in adenine nucleotide concentrations (Hawley et al. 2012). Moreover, salicylate-stimulated FA oxidation was ameliorated in *AMPKβ1*$^{-/-}$ mice, thus indicating the

effects of salicylate on lipid metabolism *in vivo* are mediated by AMPK (Hawley et al. 2012).

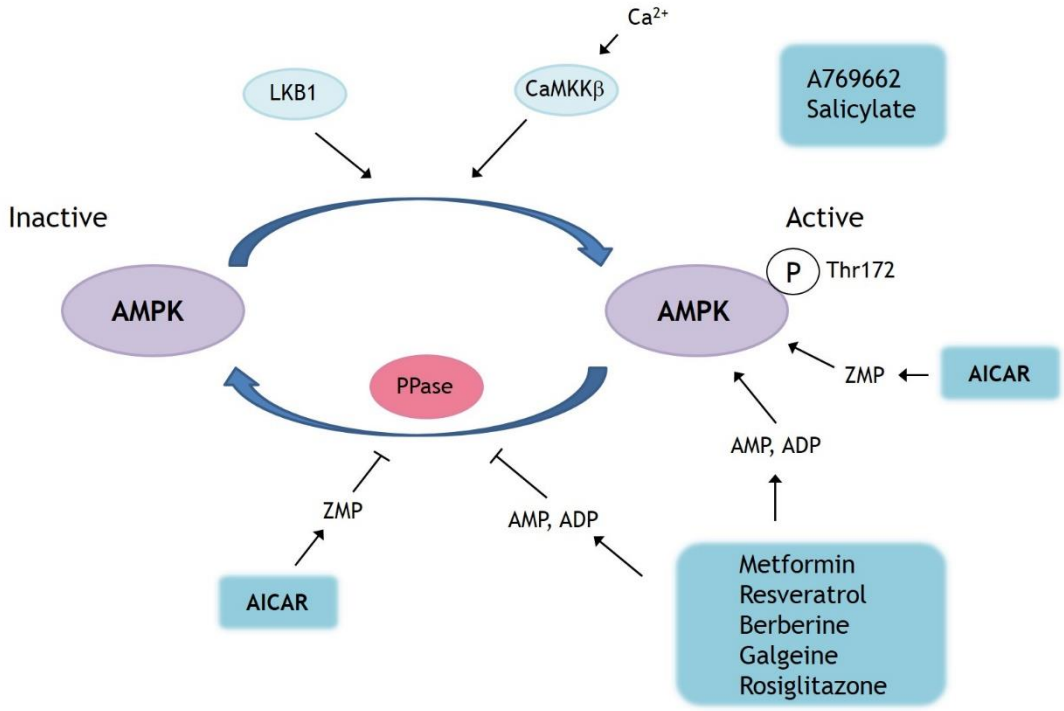

Figure 1-10: Regulation of AMPK

AMPK is activated by phosphorylation of the catalytic α subunit at Thr172 by LKB1 (liver kinase B1) or CaMKKβ (Ca^{2+}/calmodulin-dependent protein kinase kinase β) independently of adenine nucleotides. Increased AMP or ADP concentrations can allosterically activate AMPK and inhibit Thr172 dephosphorylation by protein phosphatases (PPase). A number of stimuli including xenobiotics and anti-diabetic agents activate AMPK via an increase in AMP/ATP or ADP/ADP concentrations. AICAR is phosphorylated to the AMP mimetic ZMP, thereby activating AMPK, whereas A769662 and salicylate are reported to active AMPK complexes containing the β1 regulatory subunit directly.

1.3.4 AMPK targets

AMPK regulates a wide range of different pathways in a variety of tissues via rapid phosphorylation of target proteins and longer-term effects on gene expression. Effects of AMPK are pleiotropic and can be observed in several tissues, such as adipose, liver, skeletal muscle, heart, brain and pancreas. Figure 1.11 below summarises many of the well-established downstream targets and effects of AMPK:

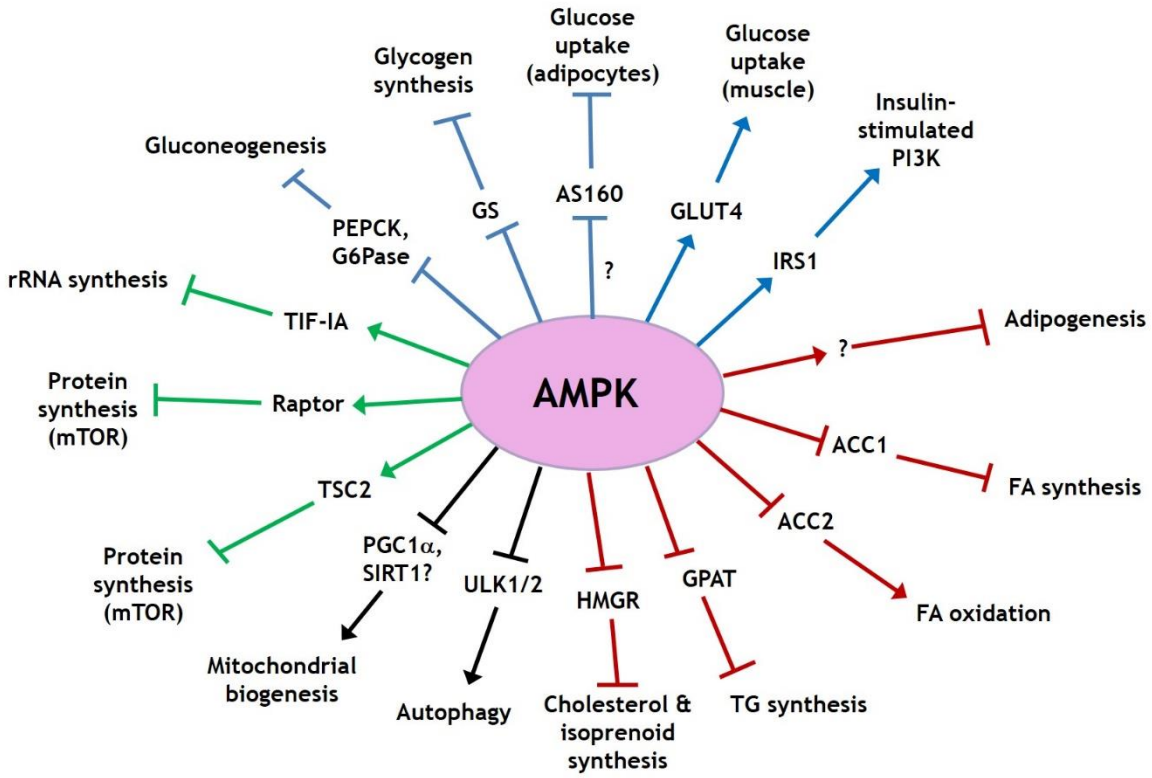

Figure 1-11: Targets for AMPK

AMPK regulates many target proteins and processes, including glucose metabolism (blue), lipid metabolism (red), mitochondrial biogenesis and autophagy (black) and protein metabolism (green). Abbreviations: AS160, Akt substrate of 160 kDa; G6Pase, glucose-6-phosphatase; GPAT, glycerol phosphate acyltransferase; GS, glycogen synthase; HMGR, 3-hydroxy-3-methyl-CoA reductase; IRS1, insulin resceptor substrate 1; mTOR, mammalian target of rapamycin; PEPCK, phosphoenolpyruvate carboxykinase; PGC1α, peroxisome proliferator-activated receptor-γ co-activator 1α; PI3K, phosphatidylinositol 3-kinase; SIRT1, sirtuin 1; TIF-1A, transcription initiation factor-1A; TSC2, tuberous sclerosis 2; ULK1/2, unc-51-like kinase.

1.3.5 Regulation of glucose homeostasis by AMPK

AMPK plays an important role in the regulation of glycogen synthesis, gluconeogenesis, glycolysis and glucose transport. AMPK has been reported to directly phosphorylate and inhibit muscle and liver GS (glycogen synthase), the key enzyme in the anabolic process of glycogen synthesis (Carling and Hardie 1989, Bultot et al. 2012). Interestingly, chronic activation of AMPK has been reported to increase glycogen storage in skeletal (Holmes, Kurth-Kraczek, and Winder 1999, Ojuka, Nolte, and Holloszy 2000) and cardiac (Arad, Seidman, and Seidman 2007)

muscle, suggested to be the result of allosteric activation of GS via increased glucose uptake and the subsequent rise in intracellular G6P (glucose-6-phosphate) concentrations (Hunter et al. 2011).

AMPK activators AICAR (Lochhead et al. 2000), metformin (Kim et al. 2008, Zhou et al. 2001), and adiponectin (Yamauchi et al. 2002) have all been reported to suppress hepatic gluconeogenesis via downregulation of gluconeogenic enzymes PEPCK (phosphoenolpyruvate carboxykinase) and G6Pase (glucose-6-phosphatase) in an AMPK-dependent manner. In contrast, a recent study by Foretz and co-workers reported that mice with a liver-specific AMPKα1/α2 double knockout still exhibited normal blood glucose and insulin, and metformin still suppressed glucose output and G6Pase expression (Foretz et al. 2010). Furthermore, AICAR was still able to inhibit expression of both PEPCK and G6Pase in isolated hepatocytes derived from these mice; thus indicating the possibility for metformin and AICAR to reduce expression of gluconeogenic enzymes via AMPK-independent mechanisms (Foretz et al. 2010).

PFK-2 (phosphofrucokinase-2) controls the synthesis and degradation of fructose 2,6-bisphosphate, which itself stimulates PFK-1, a key glycolytic enzyme. AMPK has been reported to phosphorylate and activate PFK-2 in ischaemic cardiac muscle, thereby stimulating glycolysis (Marsin et al. 2000).

Insulin-stimulated glucose uptake in striated muscle and adipocytes is mediated by the translocation of vesicles containing GLUT4 to the plasma membrane, with the resultant influx of glucose providing a substrate for glycogen synthesis in skeletal muscle and TG synthesis in adipocytes. AMPK activation in skeletal muscle has been demonstrated to increase both basal and insulin-stimulated glucose uptake by promoting GLUT4 translocation to the cell surface (Buhl et al. 2001, Koistinen et al. 2003, Fazakerley et al. 2010), and GLUT4 gene expression (Ojuka, Nolte, and Holloszy 2000, Holmes, Kurth-Kraczek, and Winder 1999). Interestingly, AMPK appears to have opposing effects in adipocytes, whereby it inhibits insulin-stimulated glucose uptake as will be described in more detail in 1.4.3.

1.3.6 Regulation of lipid metabolism by AMPK

A key metabolic target of AMPK is ACC, which is the rate-limiting enzyme in the conversion of acetyl CoA to malonyl CoA (Tong 2005). Malonyl CoA itself is both a precursor for the biosynthesis of FA as it provides acetyl groups (Wakil, Stoops, and Joshi 1983) and an inhibitor of FA oxidation via the allosteric inhibition of CPT1 (carnitine palmitoyl transferase 1) and the subsequent transport of long-chain FA into the mitochondrial matrix (McGarry 1995). Thus, phosphorylation and inhibition of ACC by AMPK suppresses the synthesis of malonyl CoA, reducing FA synthesis and relieving inhibition of CPT1, thereby facilitating the oxidation of FA to yield ATP (Figure 1.12). Furthermore, AMPK has been proposed to activate malonyl CoA decarboxylase, which catalyses the conversion of malonyl CoA to acetyl CoA, thus further propagating these effects (Assifi et al. 2005). There are two isoforms of ACC in mammals; ACC1 (265 kDa) is predominantly expressed in lipogenic tissues including liver, adipose tissue and lactating mammary gland (Ha et al. 1996, Abu-Elheiga et al. 2005), and as such is proposed to primarily regulate FA synthesis (Ruderman et al. 2003). ACC2 (280 kDa) is predominantly expressed in cardiac and skeletal muscle (Ha et al. 1996, Abu-Elheiga et al. 2005), and is proposed to be primarily involved in the regulation of FA oxidation (Merrill et al. 1997). Furthermore, long-term AMPK activation has been reported to reduce gene expression of ACC and FAS (Hardie 2008), thereby further increasing FA oxidation and reducing FA synthesis. The effect of AMPK activation on lipid metabolism in adipose tissue will be discussed in more detail in 1.4.4.

Finally, another anabolic process inhibited by AMPK activation is the biosynthesis of cholesterol and isoprenoids; AMPK can phosphorylate and inhibit HMGR (HMG-CoA reductase), the rate-limiting enzyme in this process (Beg, Stonik, and Brewer 1978).

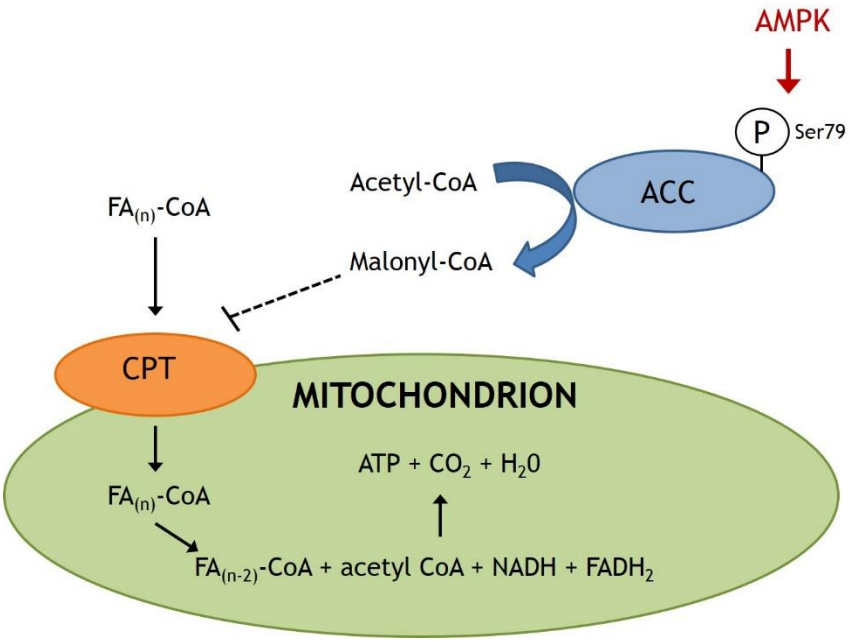

Figure 1-12: AMPK regulation of fatty acid oxidation

AMPK stimulates FA oxidation by phosphorylating and inactivating ACC, thus inhibiting the conversion of acetyl CoA to malonyl CoA and relieving the inhibitory effect of malonyl CoA on CPT (carnitine palmitoyl transferase). FA thereby enter into the mitochondrial matrix where they are oxidised to yield ATP.

1.3.7 Regulation of mitochondrial biogenesis and autophagy by AMPK

Mitochondrial biogenesis is the *de novo* formation of mitochondria, ultimately increasing the capacity for the oxidative catabolism of glucose and FA within the cell. AMPK activates PGC-1α (peroxisome proliferator-activated receptor-γ co-activator 1α), a co-activator which enhances the activity of several transcription factors leading to the increased transcription of mitochondrial genes (Lin, Handschin, and Spiegelman 2005). Indeed, rats treated with AICAR exhibited elevated expression of mitochondrial genes in muscle (Winder et al. 2000).

Autophagy is a catabolic process by which cellular components are degraded in order to maintain essential activity and cellular viability in response to energy depletion; thus, autophagy is promoted by AMPK activation. AMPK has been reported to directly phosphorylate and activate the mammalian autophagy-initiating kinase Ulk1 under conditions of glucose starvation (Kim et al. 2011).

1.3.8 Regulation of protein metabolism by AMPK

mTOR is a highly conserved Ser/Thr protein kinase that is ubiquitously expressed and exists as two complexes: mTORC1, in which mTOR associates with Raptor and mLST8; and mTORC2, in which mTOR associates with Rictor, mSIN1 and mLST8. Importantly, mTORC1 is sensitive to rapamycin, while mTORC2 is not; thus providing a way of distinguishing mTORC1 and mTORC2 functions. The two complexes differentially regulate protein targets; mTORC1 is by far the best characterised and is generally thought to promote protein synthesis via phosphoryalation of S6K1 (ribosomal protein S6 kinase) and 4E-BP1 (elongation factor-4E binding protein 1) (Inoki, Zhu, and Guan 2003), while mTORC2 has been suggested to regulate cell survival, metabolism and cytoskeletal organisation via phosphorylation of PKB, SGK1 (serum/glucocorticoid regulated kinase 1) and PKCα (protein kinase Cα) (Weber and Gutmann 2012).

AMPK activation has been shown to inhibit the mTORC1 pathway via phosphorylation and activation of the upstream TSC1/2 (tuberous sclerosis complex 1/2) (Inoki et al. 2006). Consistent with this, AICAR-mediated mTOR inhibition is attenuated in TSC1 or TSC2-deficient cells (Wolff et al. 2011). In addition, AMPK-mediated phosphorylation of Raptor may also negatively regulate mTORC1 activity; AICAR-induced mTOR inhibition was reported to be suppressed in cells with a phospho-defective Raptor mutant (Gwinn et al. 2008).

AMPK has been reported to suppress rRNA (ribosomal RNA) synthesis via phosphorylation of the RNA polymerase I (Pol I)-associated transcription factor TIF-IA, thereby inhibiting the formation of a functional transcription initiation complex (Hoppe et al. 2009).

Recent studies utilising AICAR or metformin in intact cells have suggested that AMPK may inhibit the anabolic process of cell proliferation via inhibition of mTOR (Grimaldi et al. 2012, Carling et al. 2012). In contrast, treatment with AICAR, A769662 or infection with viruses expressing a constitutively active AMPK mutant were revealed to inhibit endothelial cell proliferation via increased p21 and p27 expression (Peyton et al. 2012), while AICAR was reported to inhibit growth of a HepG2 cell line via phosphorylation of p53 (Imamura et al. 2001), all leading to

cell cycle arrest. Taken together, AMPK suppresses the anabolic processes of protein synthesis, cell growth and proliferation when cellular energy is depleted.

1.4 Role of AMPK in adipose tissue and obesity

1.4.1 Expression and activation of AMPK in adipose tissue

AMPKα1 has been reported to be the principal catalytic isoform expressed in cultured 3T3-L1 adipocytes (Salt, Connell, and Gould 2000), isolated epididymal rat adipocytes (Daval et al. 2005), human SCAT (Lihn et al. 2004) and mouse BAT (Mulligan et al. 2007), as assessed in immunoprecipitates using isoform-specific anti-AMPKα subunit antibodies which measure total cellular/tissue activity. AMPKα2 is only a minor isoform in adipocytes; however it is possible that complexes containing the α2 subunit isoform could play a role in specific subcellular compartments as has been proposed in endothelial cells, in which ablation of the α2 subunit isoform was associated with a marked increase in oxidative stress despite AMPKα1 being the major isoform (Wang, Zhang, et al. 2010). The AMPKβ1-specific pharmacological activators A769662 and salicylate have been reported to stimulate AMPK activity in 3T3-L1 adipocytes and mouse WAT, thus indicating adipocytes contain the β1 subunit isoform (Zhou, Wang, et al. 2009, Hawley et al. 2012). Furthermore, a modest reduction in AMPK Thr172 phosphorylation and activity was observed in adipose tissue of *AMPKβ1$^{-/-}$* mice (Dzamko et al. 2010). As the reduction in AMPK activity was not substantial, this could imply that β2 could represent the significant β isoform in adipose; however WAT from mice lacking the β2 subunit displayed no reduction in AMPK activity (Steinberg et al. 2010), thus β1 is likely to be the dominant β isoform in WAT. While there is a lack of published data describing the principal AMPK subunits in other cells which constitute adipose tissue, AMPKα1 is reported to be the dominant catalytic subunit expressed in human endothelial cells (Wang, Zhang, et al. 2010) and mouse macrophages (Yang et al. 2010). Furthermore, these cells also express β1 (Reihill, Ewart, and Salt 2011, Galic et al. 2011).

A number of stimuli have been reported to regulate adipose tissue AMPK activation under physiological and pathophysiological conditions. Caloric restriction

stimulates AMPK activation in rodent WAT (Daval et al. 2005, Sponarova et al. 2005), as does exercise (potentially via adrenergic stimulation) in human SCAT and rat epididymal adipose tissue (Watt et al. 2006, Park et al. 2002). Cold exposure has also been reported to activate AMPK in rodent WAT (Mulligan et al. 2007) and BAT (Mulligan et al. 2007, Vucetic et al. 2011). As previously mentioned, the adipocytokines adiponectin and leptin have been reported to activate adipocyte AMPK (Wu et al. 2003, Liu et al. 2010, Wang et al. 2005), thus highlighting the potential autocrine regulation of AMPK activity.

1.4.2 Role of AMPK in adipogenesis

Differentiation of preadipocytes involves a highly regulated transcriptional cascade induced by hormones, including insulin and glucocorticoids, and is characterised by expression of FAS and aP2 (adipocyte-specific FA-binding protein) in addition to increased expression of the PPAR and C/EBP (CCAAT/enhancer-binding protein) transcription factors (MacDougald and Lane 1995). The initial phase is known as mitotic clonal expansion (MCE), and involves re-entry of growth-arrested pre-adipocytes into the cell cycle where they undergo several rounds of mitosis. This is accompanied by the transient expression of C/EBPβ and C/EBPδ. These transcription factors subsequently stimulate transcription of PPARγ, which can in turn active C/EBPα (Figure 1.13). PPARγ and C/EBPα exist in a positive-feedback loop to propagate differentiation and induction of late adipogenic genes, including aP2 and FAS, in the terminal differentiation phase (Rosen et al. 2000).

Adipogenesis is an anabolic process, and AMPK has been suggested to inhibit it in the MCE phase. AMPK activation in adipocytes has been reported to reduce expression of C/EBPβ (which is essential for initiation of the adipogenic transcriptional cascade), and subsequent inhibition of PPARγ, C/EBPα and late adipogenic markers (Habinowski and Witters 2001, Zhou, Wang, et al. 2009, Giri et al. 2006). A769662 was reported to reduce the expression of C/EBPα, PPARγ and C/EBPβ, with a concomitant suppression of lipid droplet accumulation in 3T3-L1 adipocytes (Zhou, Wang, et al. 2009). AICAR was also reported to suppress adipogenesis, reducing expression of C/EBPα, PPARγ, SREBP-1c and aP2 (Habinowski and Witters 2001, Giri et al. 2006). Furthermore, a recently discovered novel synthetic compound structurally and functionally similar to

resveratrol has also been suggested to inhibit adipogenesis via AMPK activation, suppressing expression of C/EBPα, PPARγ, FAS and aP2 (Vingtdeux et al. 2011). While these studies all indicate that AMPK acts at the early proliferation phase to inhibit adipogenesis, the exact mechanism by which AMPK elicits these effects is still unclear.

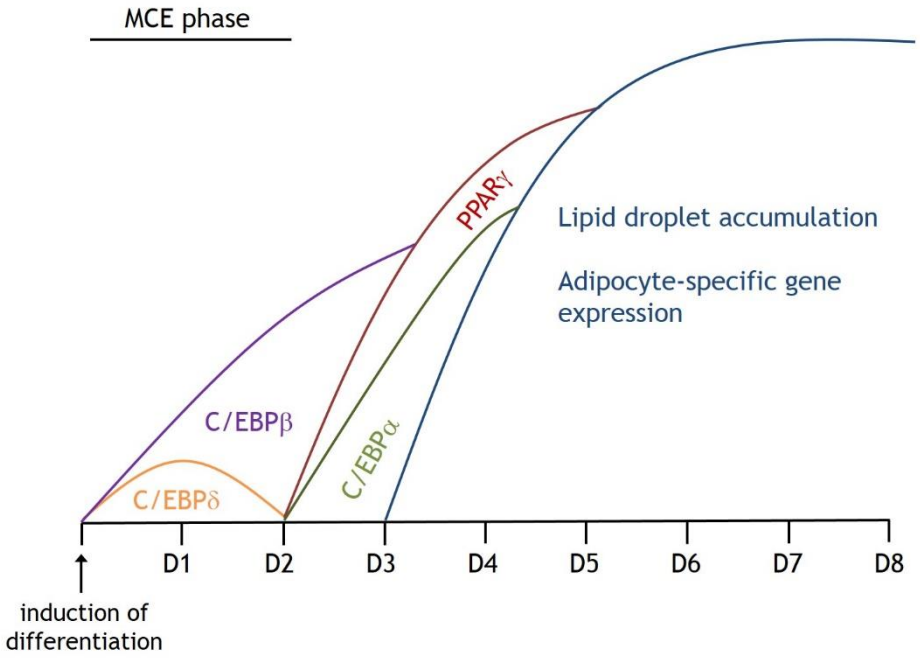

Figure 1-13: Temporal expression of key adipogenic genes

Upon induction of differentiation, growth-arrested adipocytes undergo several rounds of mitosis, known as the mitotic clonal expansion (MCE) phase, which is accompanied by the transient expression of C/EBPβ and C/EBPδ. C/EBPβ and C/EBPδ induce transcription of PPARγ, which in turn activates C/EBPα. PPARγ and C/EBPα exist in a positive feedback loop to propagate differentiation and induction of adipogenic genes in the terminal differentiation phase. D, number of days post-induction of differentiation.

1.4.3 Effect of AMPK on adipocyte cell size

An increase in adipose tissue mass during obesity can be the result of an increase in adipocyte number (hyperplasia), an increase in adipocyte cell size (hypertrophy), or both. The role of AMPK in altered adipose tissue mass has been previously examined utilising mice deficient in the alpha2 catalytic subunit isoform; HFD-fed *AMPKα2*$^{-/-}$ mice displayed an increased adipose tissue mass

compared with wild-type littermates (Villena et al. 2004). This was reported to be exclusively due to adipocyte hypertrophy, with no change in cell number or adipogenic marker expression observed (Villena et al. 2004). In contrast, Daval and co-workers reported a reduction in adipocyte size in *AMPK$\alpha 1^{-/-}$* mice; however it is important to note these mice were fed a chow diet and were not obese (Daval et al. 2005).

1.4.4 Effect of AMPK on adipocyte carbohydrate metabolism

AMPK has been shown to stimulate glucose uptake into muscle via upregulation of GLUT4 translocation as described in section 1.3.5; however the effect of AMPK activation on glucose uptake in adipocytes is less clear. Studies in 3T3-L1 adipocytes showed that AICAR increased basal (Salt, Connell, and Gould 2000, Sakoda et al. 2002) and inhibited insulin-stimulated glucose uptake (Salt, Connell, and Gould 2000, Boyle et al. 2011), while AICAR was reported to inhibit both basal and insulin-stimulated glucose uptake in isolated rat adipocytes (Gaidhu, Fediuc, and Ceddia 2006, Gaidhu et al. 2010). Although in direct contrast to its effects in muscle, multiple lines of evidence supports inhibition of insulin-stimulated glucose uptake by AMPK in adipocytes. Furthermore, this is proposed to be independent of any effects on the early steps in the insulin signalling pathway, including tyrosine phosphorylation of IRS-1 (Wu et al. 2003, Salt, Connell, and Gould 2000), PI3K recruitment to IRS-1 (Salt, Connell, and Gould 2000) or PKB activity/phosphorylation (Wu et al. 2003, Salt, Connell, and Gould 2000, Boyle et al. 2011, Gaidhu et al. 2010). The mechanism by which AMPK suppresses insulin-stimulated glucose transport is not yet fully understood; however it is thought to reduce the insulin-stimulated inhibitory phosphorylation of AS160 by PKB via a currently unknown mechanism (Gaidhu et al. 2010). Less is known about the long term effects of AMPK on glucose transport. 3T3-L1 adipocytes incubated with metformin for 24-48 h exhibited a reduction in the fold increase in insulin-stimulated glucose transport as a result of higher basal glucose uptake (Boyle et al. 2011). Interestingly, increased basal glucose uptake was also observed in human SCAT and VAT preadipocyte-derived adipocytes incubated for 24 h with metformin (Fischer et al. 2010). Furthermore, metformin was found to further enhance insulin-stimulated glucose uptake in human SCAT preadipocyte-derived adipocytes (Fischer et al. 2010). While it has been reported that AMPK activation

increases GLUT4 expression in muscle (Ojuka, Nolte, and Holloszy 2000, Holmes, Kurth-Kraczek, and Winder 1999), GLUT4 protein levels were unaffected following chronic AICAR or metformin treatment in 3T3-L1 adipocytes or in adipose biopsies from volunteers with Type 2 diabetes treated with metformin for 10 weeks (Boyle et al. 2011). Overall, AMPK activation in adipocytes appears to suppress insulin-stimulated glucose uptake; however further studies are necessary to fully understand the molecular mechanisms behind this.

1.4.5 Effect of AMPK on adipose lipid metabolism

1.4.5.1 Fatty acid oxidation

AMPK-mediated phosphorylation and inactivation of ACC promotes FA oxidation to yield ATP via a reduction in malonyl CoA concentrations as described in 1.3.6. Chronic activation of AMPK in adipocytes was associated with an increase in FA oxidation (Gaidhu et al. 2009, Luo et al. 2007) and mitochondrial content (Orci et al. 2004, Gaidhu et al. 2011). Moreover, sustained AICAR treatment increased WAT expression of PPARα, PPARδ and PGC-1α; these all influence expression of enzymes involved in FA oxidation and mitochondrial biogenesis (Gaidhu et al. 2009, Ahmadian et al. 2011). In contrast, acute stimulation with AICAR was reported to inhibit FA oxidation in isolated rat adipocytes (Gaidhu, Fediuc, and Ceddia 2006). Gaidhu and co-workers hypothesised that suppression of FA oxidation in adipocytes may spare FA for oxidation by other tissues in which local ATP production is more crucial (Gaidhu, Fediuc, and Ceddia 2006). Thus, the role of AMPK in the regulation of FA oxidation in WAT may be dependent upon the duration of AMPK stimulation, such that acute AMPK activation may inhibit FA oxidation, while sustained AMPK activation appears to stimulate FA oxidation.

1.4.5.2 Lipolysis

Lipolysis is the process by which TG are hydrolysed to glycerol and FA in response to adrenergic stimulation of PKA and the subsequent phosphorylation of HSL and perilipins in the fasted state, and is suppressed by insulin-mediated PKB phosphorylation and subsequent activation of PDE3B in the fed state as described in more detail in 1.1.3. AICAR-mediated AMPK activation was reported to

antagonise lipolysis via phosphorylation of HSL on Ser565, thus preventing PKA-stimulated phosphorylation and activation of HSL (Daval et al. 2005, Anthony, Gaidhu, and Ceddia 2009, Sullivan et al. 1994, Corton et al. 1995). Furthermore, an increase in lipolysis was found to activate AMPK (Gauthier et al. 2008). When the rate at which FA are liberated during lipolysis exceeds the rate at which they are being exported from the cells, they become re-esterified back into TG in an ATP-dependent manner. Therefore, it has been suggested that activation of AMPK and AMPK-mediated inhibition of lipolysis would prevent a futile cycling and depletion of ATP (Gauthier et al. 2008, Hardie, Ross, and Hawley 2012a).

In contrast to these reports suggesting an anti-lipolytic role for AMPK, other studies have proposed that AMPK may stimulate lipolysis. Adrenergic stimulation has been reported to activate AMPK which results in the stimulation of lipolysis in 3T3-L1 adipocytes (Yin, Mu, and Birnbaum 2003) and isolated rat adipocytes (Koh et al. 2007). Furthermore, the AMPK inhibitor Compound C was found to ameliorate β-adrenergic-stimulated lipolysis in rat adipocytes (Koh et al. 2007), suggesting that AMPK is necessary for adrenaline-induced lipolysis. Interestingly, AICAR has been reported to initially suppress lipolysis in isolated rat adipocytes and in rats *in vivo* as assessed by a reduction in serum FA, yet chronic AICAR treatment was found to stimulate lipolysis (Gaidhu et al. 2009). Thus, as with FA oxidation, the role of AMPK in the regulation of lipolysis may depend on the duration and mode of AMPK activation; however the overall effect of AMPK on lipolysis remains controversial.

1.4.5.3 Lipogenesis

Chronic activation of AMPK by AICAR in isolated rat adipocytes (Gaidhu, Fediuc, and Ceddia 2006, Gaidhu et al. 2009, Sullivan et al. 1994) and metformin in human adipose tissue (Boyle et al. 2011) markedly increased ACC phosphorylation and suppressed lipogenic gene expression. Furthermore, Sullivan and co-workers observed a decrease in the lipogenic rate concomitant with ACC phosphorylation (Sullivan et al. 1994). Conversely, adipocytes from *AMPKβ1*$^{-/-}$ mice displayed an increase in lipogenesis in adipose explants (Dzamko et al. 2010). It has been suggested that the AMPK-mediated inhibition of lipogenesis would conserve ATP under conditions of cellular stress (Gaidhu, Fediuc, and Ceddia 2006).

1.4.6 AMPK and brown adipose

Brown adipocytes have a high mitochondrial content and characteristically express UCP-1, allowing for thermogenesis as described in 1.1.1.2. The role of brown adipose and the involvement of AMPK in its regulation are currently poorly characterised. AMPK has been reported to be activated in mice and rat BAT following prolonged exposure to cold (Mulligan et al. 2007, Vucetic et al. 2011), while studies in cultured mouse brown adipocytes revealed an increase in AMPK activation and glucose transport following AICAR (Sakaue et al. 2003) or β-adrenergic (Hutchinson et al. 2005) stimulation. Furthermore, in mouse BAT, acute adrenergic signalling has been proposed to stimulate AMPK activation via an increase in Thr172 phosphorylation, while chronic adrenergic stimulation increases AMPK α subunit protein levels (Pulinilkunnil et al. 2011). Metformin has recently been reported to increase AMPKα1 expression and AMPK activity in both mouse BAT and cultured brown adipocytes (Geerling et al. 2013). Intriguingly, AMPK activity was found to be increased during differentiation in brown adipocytes; conversely siRNA-mediated knockdown of AMPK suppressed differentiation of brown adipocytes, indicating AMPK may promote differentiation in thermogenic BAT (Vila-Bedmar, Lorenzo, and Fernández-Veledo 2010). This is in direct contrast to the anti-adipogenic affect AMPK has in white adipocytes; the differential role of AMPK in white and brown adipocytes could be due to the fact that BAT specialises in lipid catabolism as opposed to energy storage. Interestingly, sustained AICAR treatment in mice was shown to increase the proportion of beige adipocytes within WAT deposits (Vila-Bedmar, Lorenzo, and Fernández-Veledo 2010), indicating AMPK activation may play a role in the remodelling of adipocyte metabolism by stimulating energy dissipation in WAT rather than lipid storage.

1.4.7 AMPK and Inflammation

1.4.7.1 Adipocytokines regulated by AMPK

Prior to this study, AMPK had been proposed to exert anti-inflammatory effects in different tissues and cell types, including endothelial cells (Ewart, Kohlhaas, and Salt 2008) and macrophages (Sag et al. 2008); however the effects of AMPK

activation on inflammatory pathways in adipocytes were not well understood. The first study to suggest an anti-inflammatory role for AMPK showed that AICAR inhibited both the protein and mRNA expression of LPS-induced TNF-α, IL-1β and IL-6 in rat primary astrocytes, microglia and macrophages (Giri et al. 2004). Other studies followed, providing further evidence that AMPK activation attenuates synthesis of proinflammatory cytokines TNF-α, IL-1β and IL-6 in macrophages (Yang et al. 2010, Jeong et al. 2009, Sag et al. 2008), and IL-6 and IL-8 in adipocytes (Lihn et al. 2008). Berberine was reported to reduce proinflammatory cytokine expression in adipose tissue of *db*/*db* mice (Jeong et al. 2009), while AICAR was demonstrated to inhibit secretion of TNF-α and IL-6 in human SCAT cultured *ex-vivo* (Lihn et al. 2004). A study utilising expression of a constitutively active AMPK in macrophages demonstrated a reduction in LPS-induced TNF-α synthesis together with a concomitant increase in the anti-inflammatory cytokine IL-10 (Sag et al. 2008). Conversely, downregulation of AMPK via either antisense oligonucleotides or expression of a dominant negative mutant AMPK led to an increase in both mRNA and protein expression of TNF-α and a reduction in IL-10 production (Sag et al. 2008). Furthermore, AICAR-mediated AMPK activation has been found to diminish immune responses in a range of *in vivo* models of inflammation, including a murine model of acute and chronic colitis (Bai et al. 2010), rat model of autoimmune encephalomyelitis (Prasad et al. 2006), and a murine lung injury model (Zhao et al. 2008).

While it is well established that adiponectin stimulates AMPK activation as described in 1.3.3.1, AMPK may also regulate adiponectin expression. AICAR reportedly stimulated an increase in adiponectin gene expression in human SCAT cultured *ex vivo* (Lihn et al. 2004). In contrast, however, adiponectin expression was found to be suppressed in 3T3-L1 adipocytes following AICAR or metformin treatment (Huypens, Quartier, et al. 2005); thus indicating the effect of AMPK on adiponectin expression is still unclear.

1.4.7.2 Inhibition of inflammation by AMPK

Prior to the beginning of this study, few groups had attempted to elucidate the molecular mechanisms by which AMPK may inhibit proinflammatory signalling in a variety of cell types; and the regulation of adipocyte inflammation by AMPK was

poorly characterised. Early studies found that activation of AMPK was associated with a decrease in NFκB reporter gene activity (Giri et al. 2004, Cacicedo et al. 2004). Several studies followed which supported this observation and found that AMPK activation attenuated cytokine-stimulated NFκB in multiple cell types, including cultured endothelial cells (Cacicedo et al. 2004), macrophages (Yang et al. 2010), neutrophils (Zhao et al. 2008), microglial cells, astrocytes (Giri et al. 2004) and hepatic stellate cells (Caligiuri et al. 2008). Furthermore, constitutively active AMPK suppresses LPS-stimulated degradation of IκBα and subsequent binding of NFκB p65 to the IL-6 promoter in macrophages (Yang et al. 2010, Sag et al. 2008) while conversely downregulation of AMPK with RNA interference reduces the ability of AICAR to inhibit binding of p65 to the IL-6 promoter (Yang et al. 2010). Finally, it has been suggested that AMPK may inhibit the NFκB signalling pathway at the level of IKK, as metformin has been reported to reduce TNF-α-stimulated IKKα/β S180/181 phosphorylation in HUVECs (human umbilical vein endothelial cells) in an AMPK-dependent manner (Huang et al. 2009). Inhibition of cytokine-stimulated MAPK phosphorylation by AMPK has previously been demonstrated in a small number of studies, however the mechanism had not been characterised. Berberine was found to inhibit LPS-stimulated phosphorylation of JNK, ERK1/2 and p38 MAPK in macrophages in an AMPK-dependent manner (Jeong et al. 2009), while increased JNK phosphorylation was observed not only in HUVECs following siRNA-mediated downregulation of either AMPKα1 or AMPKα2, but also in aortic endothelial cells isolated from *AMPKα2*$^{-/-}$ mice (Dong et al. 2010). AICAR and metformin were also reported to inhibit JNK activation in HUVECs in response to TNF-α or H_2O_2 (Schulz et al. 2008).

Before this study began, little was known about the effect of AMPK on IL-6 stimulated proinflammatory signalling. Handy and co-workers suggested AMPK activation triggered suppression of leptin-mediated STAT3 phosphorylation and SOCS-3 induction in hepatic stellate cells (Handy et al. 2010); however, to our knowledge the current study is the first to investigate the effect of AMPK on IL-6 signalling in adipocytes.

Sag and co-workers reported that transfection of a constitutively active mutant AMPK promoted polarisation of macrophages towards an M2 phenotype (Sag et al. 2008). Furthermore, inhibition of AMPKα expression with RNA interference or

transfection with a dominant negative mutant AMPK elevated mRNA and protein expression of proinflammatory cytokines TNF-α and IL-6; therefore macrophages displayed an M1 phenotype in the absence of AMPK (Sag et al. 2008). Adiponectin was also reported to prime human monocytes towards an M2 phenotype, as demonstrated by an inhibition of proinflammatory factors (Lovren et al. 2010). It should be noted that neither of these studies investigated whether AMPK activation had any effect on macrophages which were already of a proinflammatory, M1 phenotype (Sag et al. 2008, Lovren et al. 2010).

1.5 Aims

The overall aim of this study was to determine the functional consequences of AMPK activation in adipocytes subjected to proinflammatory stimuli and characterise the mechanisms by which AMPK exerts its actions. Although AMPK activation has been previously reported to inhibit inflammatory responses in endothelial cells and macrophages, an investigation into the consequences of AMPK activation on inflammatory signalling in adipocytes has yet to be undertaken. Elevated levels of proinflammatory cytokines are strongly associated with obesity, insulin resistance and Type 2 diabetes, and ablation of proinflammatory signalling has been demonstrated to improve insulin sensitivity.

The initial aim of this study was to investigate the temporal parameters of inhibition of intermediates of the cytokine-stimulated MAPK, NFκB and JAK/STAT signalling pathways by AMPK activation in 3T3-L1 adipocytes by immunoblotting and immunofluorescence. Furthermore, the mechanisms by which AMPK inhibits these proinflammatory signalling pathways was investigated by pharmacological and genetic manipulation of the signalling pathways. The proinflammatory profile of adipose tissue from *AMPKα1*$^{-/-}$ mice compared to litter-matched wild-type mice was also examined.

Functional consequences of AMPK activation in 3T3-L1 adipocytes and RAW 264.7 macrophages were investigated in this study as macrophages also contribute to the proinflammatory profile of adipose tissue. The effect of AMPK activation on cytokine and chemokine secretion from 3T3-L1 adipocytes and RAW 264.7 macrophages in response to proinflammatory stimuli was assessed in culture

medium using a mouse multiplex bead immunoassay kit and Luminex detection system. Furthermore, the effect of individual proinflammatory cytokines or conditioned medium from activated macrophages on insulin-stimulated glucose uptake in 3T3-L1 adipocytes was determined using 2-[^{3}H] deoxy-D-glucose. Downstream effects of AMPK activation on proinflammatory cytokine-stimulated gene expression of the chemokine MCP-1 was assessed using semi-quantitative PCR.

Finally, the effect of AMPK activation on 3T3-L1 adipocyte differentiation was investigated by immunoblotting and lipid staining with Oil red O. In addition, adipocyte cell size was examined in *AMPK*α*1*$^{-/-}$ mice by hematoxylin and eosin staining.

Chapter 2 - Materials and Methods

2.1 Materials

2.1.1 List of materials and suppliers

Abcam, Cambridge, UK
A769662 (6,7-Dihydro-4-hydroxy-3-(2'-hydroxy[1,1'-biphenyl]-4-yl)-6-oxo-thieno[2,3-*b*]pyridine-5-carbonitrile)

BBC Biochemical, Mt Vernon, WA, USA
Zinc formalin

Cambridge Biosciance Ltd, Cambridge, UK
Quick Titer™ Adenovirus Titer Immunoassay kit

Cayman Chemicals, Ann Arbor, MI, USA
PP242

Cell signalling Technology Inc, Danvers, MA, USA
Interleukin-1ß (IL-1ß)

BDH Laboratory Supplies, Poole, UK
Coomassie brilliant blue G-250
Tetrasodium pyrophosphate (Na_4PPi)

Bio-rad Laboratories Ltd, Hertfordshire, UK
Mini-PROTEAN® TGX™ precast gels

Eastman Kodak Company, Rochester, NY, USA
Kodak medical X-ray film

Fisher Scientific UK Ltd, Loughborough, Leicestershire, UK
Ammonium persulphate (APS)
Corning tissue culture T75/T150 flasks, 10 cm diameter dishes and 6 well plates
Ethidium bromide

Tris base (tris(hydroxymethyl)aminoethane)

Formendium, Hunstanton, Norfolk, UK

Bacterial Agar

Tryptone

Yeast extract powder

GE Healthcare, Little Chalfont, Buckinghamshire, UK

Protein G sepharose beads

Protein A sepharose beads

Invitrogen (Life Technologies Ltd), Paisley, UK

dNTPs (dATP, dCTP, dGTP, dTTP)

Lipofectamine 2000

Mouse cytokine 20-plex panel for Luminex® platform

S.O.C. medium

Taq PCRx® DNA Polymerase

One Shot chemically competent TOP10 *E.coli*

Invitrogen (GIBCO Life Technologies Ltd), Paisley, UK

Dulbecco's modified Eagles media (DMEM)

Foetal calf serum (FCS) (USA origin)

Foetal calf serum (FCS) (EU origin)

L-glutamine

Newborn calf serum (NCS)

Opti-MEM® I Reduced Serum Media

Penicillin/streptomycin

Trypsin

Melford Laboratories Ltd, Chelsworth, Ipswich, Suffolk, UK

Dithiothreitol (DTT)

Merck Chemicals Ltd, Nottingham, UK

Compound C

MG132

National Diagnostics (UK) Ltd, Hessle, East Riding of Yorkshire, UK
Ecoscint A

New England Biolabs, Ipswich, MA, USA
Gel loading dye (6x)
Low molecular weight DNA marker (100 bp)
Prestained protein marker (broad range 6-175 kDa)

PALL Life Sciences, Pensacola, FL, USA
Nitrocellulose transfer membrane, 0.45 μM pore size

Perkin Elmer, Beaconsfield, Buckinghamshire, UK
2-[^{3}H]-deoxy-D-glucose

Pierce, Perbio Science, UK Ltd, Tettenhall, Cheshire, UK
10,000 MWCO slide-a-lyzer

Premier International Foods, Cheshire, UK
Dried skimmed milk

Promega, Madison, WI, USA
ImProm-II™ Reverse Transcription System
Wizard® Plus SV Minipreps Kit

Qiagen Ltd, Crawley, West Sussex, UK
RNeasy Mini Kit

R & D Systems, Abingdon Science Park, Abingdon, Oxford, UK
Interleukin-6 (IL-6) (murine/human)
Soluble interleukin-6 receptor-α (sIL-6α) (murine/human)

Roche Diagnostic Ltd, Burgess Hill, UK
Agarose MP

Severn Biotech Ltd, Kidderminster, Hereford, UK
Acrylamide:Bisacrylamide (37.5:1; 30% (w/v) Acrylamide)

Sigma-Aldrich Ltd, Gillingham, Dorset, UK

5-Amino-2,3-dihydro-1,4-phthalazinedione (luminol)

Ampicillin

Bovine serum albumin (BSA)

Benzamidine

p-Coumaric acid

Cytochalasin B

Dexamethasone

D-mannitol

DPX mountant

Dulbecco's modified Eagles media (DMEM)

Eosin Y

Ethylenediamine tetraacetic acid (EDTA)

Ethylene glycol-bis (ß-amino-ethylether)-N,N,N',N'-tetraacetic acid (EGTA)

Haematoxylin solution

Hydrogen peroxide (H_2O_2)

Isobutylmethylxanthine (IBMX)

Lipopolysaccharide (LPS)

ß-mercaptoethanol

MCP-1 mouse forward and reverse primers

N_ω-Nitro-D-arginine methyl ester hydrochloride (D-NAME)

N_ω-Nitro-L-arginine methyl ester hydrochloride (L-NAME)

Oil red O

Paraformaldehyde

phenylmethylsulphonyl fluoride (PMSF)

Ponceau stain

Porcine Insulin

18S forward and reverse primers

Saponin

Sodium deoxycholate

Soyabean trypsin inhibitor (SBTI)

N,N,N',N'-Tetramethylethylenediamine (TEMED)

Triton X-100

Tumour necrosis factor-α (TNF-α)

Tween-20

Thermo Scientific, Waltham, MA, USA
Immunomount

Tocris Bioscience, Bristol, UK
NSC-87877 (SHP-2 inhibitor) (Chen et al. 2006)
Troglitazone

Toronto Research Chemicals Inc, Ontario, Canada
AICAR (5-aminoimidazole-4-carboxamide-1-beta-4-ribofuranoside)

VWR International Ltd., Lutterworth, Leicestershire, UK
Falcon tissue culture 10 cm diameter dishes and 6/12/24 well plates
HEPES (N-2-hydroxyethylpiperazine-N' 2-ethane sulphonic acid)

Worthington Biochemical Corporation, Lakewood, NJ, USA
Collagenase Type I

TC-PTP inhibitor was generously donated by Prof. Zhong-Yin Zhang (Department of Biochemistry and Molecular Biology, Indiana University School of Medicine, USA) (Zhang et al. 2009).

2.1.2 List of specialist equipment and suppliers

Beckman Coulter™, High Wycombe, UK
Optima™ XL-80K ultracentrifuge
SW40 rotor
Multi-Purpose scintillation counter LS 6500
Allegra® X-12 centrifuge

Bio-Rad Laboratories, Hemel Hempstead, UK
Protein gel casting and Western blotting equipment (Mini Protean III)
Agarose gel casting equipment (Mini-Sub/Wide Mini-Sub Cell GT gel system)
Luminex® 100™ detection system for mouse cytokine multiplex bead immunoassay analysis

Carl Ziess Ltd, Cambridge, UK
LSM Exciter laser scanning microscope
Axiovision light microscope

Fisher Scientific, Loughborough, UK
Polycarbonate freezing container

Optika Microscopes, Ponteranica, Italy
XDS-1B light microscope

Techne, Bibby Scientific Ltd, Staffordshire, UK
Progene FPR0G050 Thermocycler

Thermo Scientific, Waltham, MA, USA
Nanodrop spectrophotometer

WPA, Cambridge, UK
S2000 spectrophotometer

2.1.3 List of cells and suppliers

American Type Culture Collection, Manassas, VI, USA
3T3-L1 preadipocytes

3T3-L1 CAR (3T3-L1 adipocytes overexpressing the coxsackie virus and adenovirus receptor) were a kind gift from Prof. David Orlicky, University of Colorado (CO, USA) (Ross et al. 2003).

TC-PTP$^{+/+}$ and *TC-PTP*$^{-/-}$ MEFs were kind gifts from Dr. M. Tremblay, McGill University (Montreal, Canada) (Ibarra-Sánchez et al. 2001).

TSC2$^{+/+}$*p53*$^{-/-}$ and *TSC2*$^{-/-}$*p53*$^{-/-}$ MEFs were kind gifts from Dr. A. Tee, University of Cardiff (Cardiff, UK) (Kwiatkowski et al. 2002).

2.1.4 List of antibodies and conditions of use

2.1.4.1 Primary antibodies for western blotting

Table 2-1: Primary antibodies used for western blotting

n/a: not applicable; OBB: Odyssey® blocking buffer. All blots were incubated overnight at 4°C.

Epitope	Clonality	Host species	Dilution	Diluent ECL (w/v PBST) or LI-COR (v/v PBST	Source
ACC1	polyclonal	sheep	2 μg/ml	3% milk or 50% OBB	A generous gift from Prof. D.G. Hardie, University of Dundee, Dundee, UK. Raised against CQRDFTVASPAEFVT (C + residues 96-109 of rat ACC1 conjugated to KLH)
ACC S79	polyclonal	rabbit	1 :1000	5% BSA or 50% OBB	New England Biolabs, Hertfordshire, UK. (#3661)
ACRP	polyclonal	rabbit	1 :1000	50% OBB	Dr Mairi Clarke, University of Glasgow (Clarke et al. 2006)

AMPKα1	polyclonal	sheep	1 μg/ml	3% milk or 50% OBB	A generous gift from Prof. D.G. Hardie, University of Dundee, Dundee, UK. (Woods et al. 1996)
AMPKα2	polyclonal	sheep	1 μg/ml	3% milk or 50% OBB	A generous gift from Prof. D.G. Hardie, University of Dundee, Dundee, UK. (Woods et al. 1996)
AMPK phospho-T172	polyclonal	rabbit	1 :1000	5% BSA or 50% OBB	New England Biolabs, Hertfordshire, UK. (#2531)
C/EBPα	polyclonal	rabbit	1 :200	50% OBB	Santa Cruz Biotechnology, CA, USA. (#SC-61)
C/EBPβ	polyclonal	rabbit	1 :200	50% OBB	Santa Cruz Biotechnology, CA, USA. (#SC-150)
GAPDH	monoclonal clone:6C5	mouse	1 :80000	5% milk or 50% OBB	Ambion, Cambridgeshire, UK. (#4300)
IκBα	monoclonal clone:44D4	rabbit	1 :1000	5% BSA or 50% OBB	New England Biolabs, Hertfordshire, UK. (#4812)

IκBα (amino terminus)	monoclonal clone:L35A5	mouse	1 :1000	50% OBB	New England Biolabs, Hertfordshire, UK. (#4814)
IκBα phospho-S32	monoclonal clone:14D4	rabbit	1 :1000	5% BSA or 50% OBB	New England Biolabs, Hertfordshire, UK. (#2859)
IKKβ	monoclonal clone:2C8	rabbit	1 :1000	50% OBB	New England Biolabs, Hertfordshire, UK. (#2370)
IKKβ IP preferred	monoclonal clone:L570	rabbit	1 :50 (IP)	n/a	New England Biolabs, Hertfordshire, UK. (#2678)
IKKα	polyclonal	rabbit	1 :1000	50% OBB	New England Biolabs, Hertfordshire, UK. (#2682)
IKKα/β phospho-S176/S177	monoclonal clone:C84E11	rabbit	1 :1000	50% OBB	New England Biolabs, Hertfordshire, UK. (#2078)
JAK1	monoclonal clone: 73/JAK1	mouse	1 :1000	50% OBB	BD transduction laboratories, Oxford, UK. (#610232)
JAK1 phospho-Y1022/1023	polyclonal	rabbit	1 :200	50% OBB	Santa Cruz Biotechnology, CA, USA. (#SC-16773)
JAK2 XP®	monoclonal clone:D2E12	rabbit	1 :1000	50% OBB	New England Biolabs, Hertfordshire, UK. (#3230)

JAK2 phospho-Y1007/1008	polyclonal	rabbit	1 :1000	50% OBB	New England Biolabs, Hertfordshire, UK. (#3771)
JNK	polyclonal	rabbit	1 :1000	5% BSA or 50% OBB	New England Biolabs, Hertfordshire, UK. (#9252)
JNK phospho-T183/Y185	polyclonal	rabbit	1 :1000	5% BSA or 50% OBB	New England Biolabs, Hertfordshire, UK. (#9251)
JNK phospho-T183/Y185	monoclonal clone:G9	mouse	1 :1000	50% OBB	New England Biolabs, Hertfordshire, UK. (#9255)
p44/42 MAPK (Erk1/2)	polyclonal	rabbit	1 :1000	5% BSA or 50% OBB	New England Biolabs, Hertfordshire, UK. (#9102)
p44/42 MAPK (Erk1/2) phospho-T202/Y204	monoclonal clone:E10	mouse	1 :2000	5% BSA or 50% OBB	New England Biolabs, Hertfordshire, UK. (#9106)
NFκB p65 XP®	monoclonal clone: D14E12	rabbit	1 :1000	50% OBB	New England Biolabs, Hertfordshire, UK. (#8242)
NFκB p65 phospho-S536	monoclonal clone:93H1	rabbit	1 :1000	50% OBB	New England Biolabs, Hertfordshire, UK. (#3033)

p38 MAPK	polyclonal	rabbit	1 :1000	5% BSA or 50% OBB	New England Biolabs, Hertfordshire, UK. (#9212)
p38 MAPK phospho-T180/Y182 XP®	monoclonal clone:D3F9	rabbit	1 :1000	5% BSA or 50% OBB	New England Biolabs, Hertfordshire, UK. (#4511)
p53	monoclonal clone:D0-1	mouse	1 :200	50% OBB	Santa Cruz Biotechnology, CA, USA. (#SC-126)
p70 S6 kinase	monoclonal clone:49D7	rabbit	1 :1000	5% BSA or 50% OBB	New England Biolabs, Hertfordshire, UK. (#2708)
p70 S6 kinase phospho-S371	polyclonal	rabbit	1 :1000	5% BSA or 50% OBB	New England Biolabs, Hertfordshire, UK. (#9208)
PPARγ	monoclonal clone:E-8	mouse	1 :200	50% OBB	Santa Cruz Biotechnology, CA, USA. (#SC-7273)
phospho-tyrosine	monoclonal clone:4G10	mouse	1 :1000	50% OBB; 50% TBST	Millipore Corporation, Billerica, MA, USA. (#05-321)
SOCS-3	polyclonal	goat	1 :200	50% OBB	Santa Cruz Biotechnology, CA, USA. (#SC-7009)
STAT3	monoclonal clone:79D7	rabbit	1 :2000	5% BSA or 50% OBB	New England Biolabs, Hertfordshire, UK. (#4904)

STAT3 phospho-Y705	monoclonal clone:3E2	mouse	1 :1000	5% BSA or 50% OBB	New England Biolabs, Hertfordshire, UK. (#9138)
STAT3 phospho-S727	monoclonal clone:6E4	mouse	1 :1000	50% OBB	New England Biolabs, Hertfordshire, UK. (#9136)
STAT5	monoclonal clone:3H7	rabbit	1 :1000	50% OBB	New England Biolabs, Hertfordshire, UK. (#9358)
STAT5 phospho-Y694	monoclonal clone:14H2	mouse	1 :1000	50% OBB	New England Biolabs, Hertfordshire, UK. (#9356)
TC-PTP	monoclonal clone: 252294	mouse	1 :1000	5% milk	R&D Systems, Abingdon, UK. (#MAB1930)
Tuberin/ TSC2	monoclonal clone:D57A9	rabbit	1 :1000	50% OBB	New England Biolabs, Hertfordshire, UK. (#3990)
β-Tubulin	monoclonal clone:9F3	rabbit	1 :1000	50% OBB	New England Biolabs, Hertfordshire, UK. (#2128)

2.1.4.2 Primary antibodies for immunofluorescence

Table 2-2: Primary antibodies used for immunofluorescence

All coverslips were incubated in permeabilisation media (2% (w/v) BSA, 0.1% (w/v) Saponin, 20 mM glycine, PBS) for 45 min at room temperature.

Epitope	Clonality	Host species	Dilution	Source
c-myc	monoclonal clone : 9E10	mouse	1 :100	Santa Cruz Biotechnology, CA, USA. (#SC-40)
NFκB p65 XP®	monoclonal clone : D14E12	rabbit	1 :50	New England Biolabs, Hertfordshire, UK. (#8242)

2.1.4.3 Secondary detection agents for western blotting

Table 2-3: Secondary detection agents for western blotting

All blots were incubated for 1 h at room temperature.

Linked molecule	Epitope	Host species	Dilution	Diluent (w/v or v/v in PBST)	Source
HRP	mouse IgG	sheep	1 :2000	5% milk	GE Healthcare, Buckinghamshire, UK. (#NA931)
HRP	rabbit IgG	donkey	1 :2000	5% milk	GE Healthcare, Buckinghamshire, UK. (#NA934)
HRP	streptococcus sp. Protein G	n/a	1 :2000	5% milk	Sigma, St Louis, MO, USA. (#P8170)
IRDye® 800CW	mouse IgG	donkey	1 :5000	50% OBB	LI-COR Biosciences, Lincoln, NE, USA. (#926-32210)

IRDye® 800CW	rabbit IgG	donkey	1 :5000	50% OBB	LI-COR Biosciences, Lincoln, NE, USA. (#926-32213)
IRDye® 680LT	rabbit IgG	donkey	1 :5000	50% OBB	LI-COR Biosciences, Lincoln, NE, USA. (#926-68023)
IRDye® 680LT	goat IgG	donkey	1 :5000	50% OBB	LI-COR Biosciences, Lincoln, NE, USA. (#926-68074)
Alexa Fluor® 680 (red)	sheep IgG	donkey	1 :5000	50% OBB	Invitrogen, Life Technologies Ltd, Paisley, UK. (#A21102)

2.1.4.4 Secondary detection agents for immunofluorescence

Table 2-4: Secondary detection agents for immunofluorescence

All coverslips were incubated for in permeabilisation media (2% (w/v) BSA, 0.1% (w/v) Saponin, 20 mM glycine, PBS) for 30 min at room temperature.

Linked molecule	Epitope	Clonality	Host species	Dilution	Source
Alexa Fluor® 488 (green)	rabbit IgG	polyclonal	goat	1 :100	Invitrogen, Life Technologies Ltd, Paisley, UK. (#A11008)

Alexa Fluor® 565 (red)	rabbit IgG	polyclonal	goat	1 :100	Invitrogen, Life Technologies Ltd, Paisley, UK. (#A11011)
Alexa Fluor® 568 (red)	mouse IgG	polyclonal	goat	1 :100	Invitrogen, Life Technologies Ltd, Paisley, UK. (#A11004)

2.1.5 Standard solutions

Unless stated otherwise, all buffers and reagents were made up with distilled water.

Bradford's reagent

35.0 mg/l coomassie brilliant blue

5.0% (v/v) ethanol

5.1% (v/v) orthophosphoric acid

Bradford's reagent was filtered and stored in the dark.

Enhanced chemiluminescence (ECL) detection reagents

Solution 1:

0.1 mM Tris-HCl, pH 8.5

450 mg/l luminol in 2% (v/v) DMSO

130 mg/l coumaric acid in 1% (v/v) DMSO

Solution 2:

0.1 mM Tris-HCl, pH 8.5

0.02% (v/v) H_2O_2

Immunoprecipitation (IP) buffer

50 mM Tris-HCl, pH 7.4 at 4°C

150 mM NaCl

50 mM NaF

5 mM $Na_4P_2O_7$

1 mM EDTA

1 mM EGTA

1% (v/v) Triton-X-100
1% (v/v) glycerol
1 mM DTT
0.1 mM benzamidine added on day of use
0.1 mM PMSF
5 µg/mL SBTI
1 mM $Na_3 VO_4$

Krebs-Ringer HEPES (KRH) buffer
119.0 mM NaCl
20.0 mM HEPES-NaOH, pH 7.4
5.0 mM $NaHCO_3$
10.0 mM glucose
4.8 mM KCl
2.5 mM $CaCl_2$
1.2 mM $MgSO_4$
1.2 mM NaH_2PO_4

Krebs-Ringer phosphate (KRP) buffer
130 mM NaCl
4.8 mM KCl
5 mM NaH_2PO_4, pH 7.4
1.25 mM $MgSO_4$
1.25 mM $CaCl_2$

Lysis Buffer
50 mM Tris-HCl, pH 7.4 at 4°C
50 mM NaF
1 mM $Na_4P_2O_7$
1 mM EDTA
1 mM EGTA
1% (v/v) Triton-X-100

250 mM mannitol
1 mM DTT
1 mM $Na_3 VO_4$ added on day of use
0.1 mM benzamidine
0.1 mM PMSF
5 µg/mL SBTI

Phosphate-buffered saline (PBS) (pH 7.2)

85 mM NaCl
1.7 mM KCl
5 mM Na_2HPO_4
0.9 mM KH_2PO_4

Phosphate-buffered saline + Tween 20 (PBST)

85 mM NaCl
1.7 mM KCl
5 mM Na_2HPO_4
0.9 mM KH_2PO_4
0.1% (v/v) Tween 20

Ponceau S stain

0.2% (w/v) ponceau S
1% (v/v) acetic acid

Scott's tap water substitute

42 mM $NaHCO_3$
167 mM $MgSO_4$

SDS-polyacrylamide gel electrophoresis (SDS-PAGE) Running buffer

190 mM glycine
62 mM Tris base
0.1% (w/v) SDS

4 X SDS-PAGE sample buffer

200 mM Tris-HCl, pH 6.8
8% (w/v) SDS
40% (v/v) glycerol
0.4% (w/v) bromophenol blue
200 mM DTT

TAE buffer (pH 8.2)
40 mM Tris acetate
1 mM EDTA

Transfer buffer
25 mM Tris base
192 mM glycine
20% (v/v) ethanol

Tris-buffered saline (TBS)
20 mM Tris-HCl, pH 7.5
137 mM NaCl

Tris-buffered saline + Tween 20 (TBST)
20 mM Tris-HCl, pH 7.5
137 mM NaCl
0.1% (v/v) Tween 20

2 YT medium
1.6% (w/v) Tryptone
1% (w/v) Yeast extract
0.5% (w/v) NaCl

2.2 Methods

2.2.1 Cell Culture Procedures

2.2.1.1 Cell culture plastic ware

3T3-L1 and 3T3-L1 CAR (3T3-L1 adipocytes overexpressing the coxsackie virus and adenovirus receptor) cells were cultured in Corning T75 flasks and Falcon 10 cm diameter dishes, 6 well, 12 well and 24 well plates. Human embryonic kidney (HEK) 293 cells, mouse embryonic fibroblasts (MEFs) and HeLa cells were cultured in Corning T75 flasks and 6 well plates. RAW 264.7 macrophages were cultured in Corning T150 flasks and 10 cm diameter dishes.

2.2.1.2 Cell culture growth media for 3T3-L1 preadipocytes

Preadipocytes were maintained as fibroblasts (passage 2-12) in Dulbecco's modified Eagle's medium (DMEM) supplemented with 10% (v/v) newborn calf serum (NCS) and 100 U/ml (v/v) penicillin and streptomycin. Cells were cultured at 37°C in a humidified atmosphere of 10% (v/v) CO_2 in media replaced every 48 h.

2.2.1.3 Cell culture growth media for 3T3-L1 CAR preadipocytes

Preadipocytes were maintained as fibroblasts (passage 15-30) in DMEM supplemented with 10% (v/v) foetal calf serum (FCS) and 100 U/ml (v/v) penicillin and streptomycin. Cells were cultured at 37°C in a humidified atmosphere of 10% (v/v) CO_2 in media replaced every 48 h.

2.2.1.4 Cell culture growth media for HEK 293 and HeLa cells

HEK 293 cells and HeLa cells were each maintained in DMEM supplemented with 10% (v/v) FCS and 2 mM glutamine. Cells were cultured at 37°C in a humidified atmosphere of 5% (v/v) CO_2 in media replaced every 48 h.

2.2.1.5 Cell culture growth media for MEFs

MEFs were maintained in DMEM supplemented with 10% (v/v) FCS, 100 U/ml (v/v) penicillin and streptomycin and 2 mM glutamine. Cells were cultured at 37°C in a humidified atmosphere of 5% (v/v) CO_2 in media replaced every 48 h.

2.2.1.6 Cell culture growth media for RAW 264.7 macrophages

RAW 264.7 macrophages were maintained in RPMI 1640 supplemented with 10% (v/v) FCS, 100 U/ml (v/v) penicillin and streptomycin and 2 mM glutamine. Cells were cultured at 37°C in a humidified atmosphere of 5% (v/v) CO_2 in media replaced every 48 h.

2.2.1.7 Preparation of 3T3-L1 and 3T3-L1 CAR fibroblast differentiation medium

Differentiation was initiated using DMEM containing 10% (v/v) FCS, 0.5 mM methyl isobutylxanthine (IBMX), 0.25 µM dexamethasone, 5 µM troglitazone, and porcine insulin (1 µg/ml), prepared as outlined below.

A 2.5 mM solution of dexamethasone in ethanol was diluted 1:20 with 10% (v/v) FCS/DMEM medium immediately prior to use yielding a 500X stock solution. A 500X concentrated solution of IBMX was also prepared by dissolving 55 mg IBMX in 1 ml of 1M KOH. Insulin (1 mg/ml) was then prepared in 0.01 M HCl.

3T3-L1 differentiation medium was prepared by diluting both the dexamethasone and IBMX solutions to a 1X concentration in 10% (v/v) FCS/DMEM and then adding insulin and troglitazone to final concentrations of 1 µg/ml and 5 µM, respectively. The medium was then filter-sterilised prior to use.

2.2.1.8 3T3-L1 and 3T3-L1 CAR fibroblast differentiation protocol

To differentiate the 3T3-L1 and 3T3-L1 CAR fibroblast cells into adipocytes, the cells were grown to confluency in 10% (v/v) NCS/DMEM. At 48 hr post-confluence, cell medium was aspirated and replaced with differentiation medium consisting of 10% (v/v) FCS/DMEM containing 0.25 µM dexamethasone, 0.5 mM IBMX, 5 µM

troglitazone and insulin (1 µg/ml). After a further three days this medium was aspirated and replaced with 10% (v/v) FCS/DMEM containing 5 µM troglitazone and insulin (1 µg/ml). The cells were incubated in this medium for three days before the medium was aspirated and replaced with 10% (v/v) FCS/DMEM, in which the cells were then maintained in. At 8-12 days post-induction of differentiation, cells were used for experimentation.

2.2.1.9 Passaging of 3T3-L1 and 3T3-L1 CAR fibroblasts, MEFs, HEK 293 and HeLa cells

When cells in T75 flasks were 70-80% confluent, DMEM growth medium was aspirated and the cells briefly washed in sterile PBS before 3 ml of sterile trypsin (0.05% (v/v) in diaminothanetetra-acetic acid, disodium salt (EDTA)) was added to each T75 flask. Flasks were then incubated at 37°C until the cells began to lift off. Trypsin was titurated over the surface of the flask until all of the cells were detached. An appropriate volume of DMEM growth medium was added to the trypsin and used to seed cell culture plastic ware as detailed in 2.2.1.1.

2.2.1.10 Passaging of RAW 264.7 macrophages

When cells in T150 flasks were 70-80% confluent, a cell lifter was gently passed over the surface of the flask to detach adherent cells into the medium. Cells were counted using a haemocytometer and an appropriate volume of RPMI 1640 growth medium added for seeding T150 flasks and 10 cm diameter dishes at a density of 1×10^6 cells/dish.

2.2.1.11 Resurrection of frozen cell stocks from liquid nitrogen

Cell cryogenic vials were removed from liquid nitrogen and incubated in a water bath at 37°C until the cells were thawed. Vials were then transferred to a cell culture sterile flow hood where they were transferred to a T75 flask containing 10 ml of the appropriate growth medium for the cell type as described in sections 2.2.1.2 – 2.2.1.6 and maintained in an incubator at 37°C in an atmosphere of 5 or 10% (v/v) CO_2. The following day the medium was aspirated to remove dead cell debris and was replaced with fresh medium.

2.2.1.12 Preparation of 3T3-L1 and 3T3-L1 CAR fibroblasts, MEFs, HEK 293 and HeLa cells for freezing

DMEM medium was aspirated from T75 flasks and 3 ml of trypsin (0.05% (v/v) in EDTA) was added to each flask. Flasks were then incubated at 37°C until the cells began to lift off. Trypsin was titurated over the surface of the flask until all of the cells were detached. 7 ml of the appropriate DMEM growth medium was added to each flask. The cell suspension was then transferred to a 15 ml universal tube. The trypsin/cell mix was centrifuged at 350 x g for 5 min and the trypsin supernatant aspirated. The cell pellet was then resuspended in 1 mL of freeze medium; FCS containing 10% (v/v) dimethyl sulphoxide (DMSO). The re-suspended pellet was then transferred into 1.8 ml polypropylene cryogenic tubes. The cryogenic tubes were then placed in a polycarbonate container and stored overnight at -80°C. The following morning the vials were transferred to liquid nitrogen and stored until required.

2.2.1.13 Preparation of RAW 264.7 macrophages for freezing

A cell lifter was gently passed over the surface of the flask to detach adherent cells into the medium. The cell suspension was then transferred to a 15 ml universal tube. The trypsin/cell mix was centrifuged at 350 x g for 5 min and the trypsin supernatant aspirated. The cell pellet was then re-suspended in 1 ml of freeze medium; FCS containing 10% (v/v) DMSO. The re-suspended pellet was then transferred into 1.8 ml polypropylene cryogenic tubes. The cryogenic tubes were then placed in a polycarbonate container and stored overnight at -80°C. The following morning the vials were transferred to liquid nitrogen and stored until required.

2.2.2 Preparation of 3T3-L1 lysates

3T3-L1 cells cultured in 6 well Falcon tissue culture dishes were preincubated for 2 h in serum-free DMEM at 37°C before exchanging for 1 ml Krebs-Ringer phosphate (KRP) supplemented with 10 mM glucose per well. Test substances were then added to the wells for various durations at 37°C. The medium was removed and wells washed once with ice-cold PBS prior to addition of 0.1 ml lysis buffer to

each well on ice. The cell extract was scraped off using a cell lifter and transferred into pre-cooled 1.5 ml microcentrifuge tubes. The extracts were vortex-mixed and centrifuged (21,910 x g, 10 min, 4°C) on a bench top centrifuge. The supernatants were stored at -80°C.

2.2.3 Preparation of MEF, HEK 293 and HeLa lysates

MEFs, HEK 293 or HeLa cells cultured in 6 well Corning tissue culture dishes were preincubated for 2 h in serum-free DMEM at 37°C before adding test substances to the wells for various durations at 37°C. The medium was removed and wells washed once with ice-cold PBS prior to addition of 0.1 ml lysis buffer to each well on ice. The cell extract was scraped off using a cell lifter and transferred into pre-cooled 1.5 ml microcentrifuge tubes. The extracts were vortex-mixed and centrifuged (21,910 x g, 5 min, 4°C) on a bench top centrifuge. The supernatants were stored at -80°C.

2.2.4 Preparation of RAW 264.7 macrophage lysates

RAW 264.7 macrophages cultured in 10 cm Corning tissue culture dishes were incubated in serum-free RPMI 1640 and test substances added to the dishes for various durations at 37°C. The medium was removed and wells washed once with ice-cold PBS prior to addition of 0.6 ml lysis buffer to each dish on ice. The cell extract was scraped off using a cell lifter and transferred into pre-cooled 1.5 ml microcentrifuge tubes. The extracts were vortex-mixed and centrifuged (21,910 x g, 5 min, 4°C) on a bench top centrifuge. The supernatants were stored at -80°C.

2.2.5 Protein concentration determination

Spectrophotometric analysis of cell lysates according to the Bradford method (Bradford 1976) was carried out at 595 nm in a spectrophotometer using disposable plastic cuvettes. Duplicates of 1 µg, 2 µg, 4 µg and 6 µg bovine serum albumin (BSA) were made up to 100 µl with H_20 and utilised as reference standards. Lysates, analysed in duplicate, were diluted (1:10 – 3T3-L1 and HEK lysates; 1:5 – MEF, Hela and RAW 264.7 macrophage lysates) using distilled water. 5 µl of diluted lysate was then added to 95 µl of distilled water in a cuvette. To all samples and reference standards, 1 ml Bradford's reagent was added and spectrophotometric

analysis performed in a WPA S2000 spectrophotometer within 10 min of reagent addition. The mean absorbance for each sample duplicate was calculated and the protein concentration determined by comparison to the calculated mean A_{595}/µg BSA derived from the linear portion of the BSA reference standard curve.

2.2.6 Immunoprecipitation

2.2.6.1 Immunoprecipitation of AMPKα1/α2 or IKKß from 3T3-L1 adipocytes

5 µl packed volume (per sample) of protein G-sepharose beads were washed 3 times in screw cap microcentrifuge tubes using 1 ml of immunoprecipitation (IP) buffer (21,910 x g, 1 min at 4°C). AMPKα1 (1 µg/sample) and AMPKα2 (1 µg/sample), or anti-IKKβ (1:50) were then added to the beads. 250 µl IP buffer was then added and mixed by rotation for 1 h at 4°C. The beads were pelleted (21,910 x g, 1 min at 4°C) and resuspended in IP buffer (25% v/v). In 1.5 ml microcentrifuge tubes, 3T3-L1 adipocyte lysate (200 µg) was added to 20 µl of the protein G-sepharose bead slurry pre-bound to either sheep anti-AMPKα1/α2 or rabbit anti-IKKβ antibody. The volume was made up to 250 µl with IP buffer and was mixed for 4 h at 4°C on a rotating mixer. The beads were then pelleted (21,910 x g, 1 min at 4°C) and the immunodeplete retained. The pellet was washed five times (21,910 x g, 1 min at 4°C) with 1 ml IP buffer. The pellets were stored at -20°C.

2.2.6.2 Immunoprecipitation of JAK2 from 3T3-L1 adipocytes

3T3-L1 adipocyte lysate (200 µg) was added to rabbit anti-JAK2 antibody (1:100), and made up to 250 µl with IP buffer and mixed by rotation overnight at 4°C in 1.5 ml screw cap microcentrifuge tubes. The following morning, 5 µl packed volume (per sample) of protein A-sepharose beads were washed 3 times (21,910 x g, 1 min at 4°C) with 1 ml IP buffer. The beads were then resuspended in IP buffer (50% v/v). 20 µl of the protein A-sepharose bead slurry was added to the lysate/antibody mixture which was then mixed by rotation for 3 h at 4°C. The beads were then pelleted (21,910 x g, 1 min at 4°C) and the immunodeplete

retained. The pellet was washed five times (21,910 x g, 1 min at 4°C) with 1 ml IP buffer. The pellets were stored at -20°C.

2.2.7 SDS-Polyacrylamide Gel Electophoresis

Sodium dodecyl sulphate-polyacrylamide gel electrophoresis (SDS-PAGE) was performed using 1.5 mm thick vertical slab gels containing between 8 and 12% acrylamide. Slab gels were prepared using Bio-Rad mini-Protean III gel units, with a stacking gel of approximately 2 cm deep. The stacking gel consisted of 5% (v/v) acrylamide/0.136% (v/v) bisacrylamide in 125 mM Tris-HCl, pH 6.8, 0.1% SDS, polymerised with 0.1% (w/v) ammonium peroxidisulphate (APS) and 0.05% (v/v) tetramethylethylenediamine (TEMED). Cell lysates were mixed 3:1 with 4 X SDS-containing sample buffer and heated to 95°C in a heating block for 5 min prior to separation by SDS-PAGE on Tris buffered gels. Prestained broad range (6-175 kDa) protein markers were used as a standard. Gels were electrophoresed using the Bio-Rad Protean III system at a constant voltage of 80 V for stacking and 180 V through the separating gel. Gels were electrophoresed until the tracking dye had migrated to the bottom of the gel and good separation of the molecular weight markers had been obtained.

2.2.8 Western Blotting of Proteins

2.2.8.1 Electrophoretic transfer of proteins from gels onto nitrocellulose membranes

Proteins were separated by SDS-PAGE as previously described (2.2.7). The gels were removed from the plates and placed on top of an equal-sized sheet of nitrocellulose (0.45 µm pore size), pre-wetted with transfer buffer and then placed between 2 layers of 3 mm filter paper also pre-wetted with transfer buffer. The ‘sandwich’ was then inserted between the plates of the gel holder cassette and transfer was performed using a Bio-Rad mini Protean III trans-blot electrophoretic transfer cell at a constant current of 40 mA overnight or at 60 V for 2.5 h. The nitrocellulose membranes were then removed from the transfer cassette and the efficiency of transfer determined by the presence and intensity

of pre-stained molecular weight standards. Membranes were also briefly stained with Ponceau to assess equal loading of protein.

2.2.8.2 Blocking of membranes and probing with primary antibodies

Non-specific sites on nitrocellulose membranes were blocked by incubation with shaking in phosphate-buffered saline (PBS)/5% (w/v) milk for 30 min at room temperature. After washing (3 x 5 min) the membrane in PBS, the primary antibody was applied to the blot and incubated, with shaking, overnight at 4°C in phosphate-buffered saline tween (PBST)/5% (w/v) milk or PBST/5% (w/v) BSA or PBST/50% (v/v) Odyssey® blocking buffer.

2.2.8.3 Secondary antibodies and immunodetection of proteins using western blotting and the ECL detection system

Following an overnight incubation in primary antibody, the membranes were washed (3 x 5 min) in PBST prior to incubation, with shaking, for 1 h at room temperature with the appropriate horseradish peroxidase (HRP)-conjugated secondary antibody in PBST/5% (w/v) milk. The membranes were then washed (2 x 5 min high salt (0.5 M NaCl) PBST, 2 x 5 min PBST, 1 x 5 min PBS).

Equal volumes of 'detection reagent 1' and 'detection reagent 2' were mixed and the membranes, prepared as described in 2.2.7.2, were immersed in the mix with shaking for 60 seconds. The detection reagents were then removed, membranes wrapped in cling-film and exposed to Kodak film. The films were developed using the X-OMAT processor.

2.2.8.4 Secondary antibodies and immunodetection of proteins using western blotting and the LI-COR detection system

Following an overnight incubation in primary antibody, the membranes were washed (3 x 5 min) in PBST prior to incubation, with shaking, for 1 h at room temperature with the appropriate fluorescent IRDye®-conjugated secondary antibody in PBST/50% (v/v) Odyssey® blocking buffer. The membranes were then

washed (3 x 5 min) in PBST followed by (1 x 5 min) PBS. If required, membranes were initially washed (2 x 5 min) in high salt (0.5 M NaCl) PBST.

2.2.8.5 Stripping of nitrocellulose membranes

Nitrocellulose membranes were incubated in stripping buffer (2% (w/v) SDS, 63 mM Tris-HCL (pH 6.8), 0.7% (v/v) β-mercaptoethanol) at 50°C for 30 min with shaking. Membranes were then washed (3 x 5 min) in PBST followed by (1 x 5 min) PBS.

2.2.8.6 Densitometric quantification of protein bands

The antibody-detected bands on the developed film were scanned on a Mercury 1200c scanner, using Adobe Photoshop software. The antibody-detected bands detected using the LI-COR Odyssey® Sa system were exported into Adobe Photoshop software. The intensity of the immune-detected protein bands was measured using ImageJ software.

2.2.9 2-deoxy-D-glucose uptake assay

Glucose uptake was measured by the uptake of 2-[^{3}H]-deoxy-D-glucose according to the method of Gibbs (Gibbs, Lienhard, and Gould 1988). 3T3-L1 adipocytes were cultured on 12 well plates and incubated at 37°C in 1 ml/well of serum free DMEM for 2 h prior to use. Cells were subsequently incubated at 37°C in 475 µl/well of Krebs-Ringer phosphate (KRP) for 1 h and test substances added to the plates for various durations at 37°C. When longer incubations were required, test substances were added directly to serum-free DMEM with no prior serum starvation. Cells were then washed and incubated in KRP for 20 min prior to insulin stimulation.

The cells were then stimulated with 10 nM insulin for 15 min. Glucose transport was initiated by the addition of 2-[^{3}H]-deoxy-D-glucose (final concentration 50 µmol/l and 1 µCi/ml) to each well. The reaction was terminated after 3 min by inverting the plates rapidly to remove the incubation buffer, and then by immersing them sequentially in 2 x 2 L and 1 L of ice-cold PBS. After air drying the plates for 1 h, 0.5 ml of 1% (v/v) Triton X-100/H_20 was added to the cell monolayers for 24 h. A Beckman Multi-Purpose scintillation counter LS6500 was

used to measure 2-[^{3}H]-deoxy-D-glucose uptake. 5 ml of scintillation fluid was used per sample. Non-specific association of radioactivity was determined in parallel incubations in the presence of 10 µmol/l cytochalasin B.

2.2.10 RNA extraction and reverse transcription polymerase chain reaction (RT-PCR)

2.2.10.1 Extraction of RNA from 3T3-L1 adipocytes

3T3-L1 cells grown in 10 cm Falcon cell culture dishes were incubated in serum-free DMEM at 37°C before test substances were added and incubated for various durations at 37°C. The media was removed and total RNA was isolated according to the RNeasy Mini Kit (Qiagen) centrifugation protocol, utilising 15 second centrifugation steps (13,226 x g) in a bench top centrifuge) for the lysate application and wash steps, discarding the flowthrough between each step.

Briefly, cells were lysed by addition of 0.6 ml lysis (RLT) buffer to each dish and collected with a cell scraper. Lysates were homogenised by passing through a sterile 23-guage needle and syringe 10 times. Each lysate was mixed gently with an equal volume of 70% (v/v) ethanol and applied to separate RNeasy mini columns in 700 µl aliquots until the entire lysate had been passed over the column. Columns were washed with 350 µl of wash buffer 1 (RW1) twice and transferred to fresh 2 ml collection tubes prior to addition of 2 x 500 µl wash buffer 2 (RPE). After discarding the flowthrough, columns were centrifuged at 13,226 x g for 2 min to dry the RNeasy silica gel membrane and to eliminate any chance of accidental carryover of buffer RPE. Columns were transferred to fresh, 1.5 ml collection tubes and RNA was eluted with 50 µl RNase-free water by centrifuging at 13,226 x g for 1 minute. The RNA concentration was determined at A_{260} in a Nanodrop spectrophotometer (Thermo Scientific) prior to storage at -80°C.

2.2.10.2 Reverse transcription

For cDNA synthesis, total RNA extracted from 3T3-L1 adipocytes was reverse transcribed using the ImProm-II™ Reverse Transcription System (Promega) and a thermocycler. Per reaction, ~0.1–1 µg DNase-free RNA was added to 5x reaction

buffer, 6 mM $MgCl_2$, 0.5 mM dNTPs, 20U recombinant RNasin ribonuclease inhibitor, 1 µl random primers and 1 µl ImProm-II™ reverse transcriptase. RNase-free water was used to make up the reaction volume to 20 µl. For initial 'no RT' controls, the reverse transcriptase was replaced with 1 µl RNase-free water. Synthesis of cDNA was initiated by a primer extension step (5 min at 25°C), followed by a cDNA synthesis step (1 h at 42°C). The reverse transcriptase was inactivated during a reaction termination step (15 min at 70°C). Resulting cDNA was stored at -20°C.

2.2.10.3 PCR and gel resolution of PCR products

For amplification of gene transcripts, 2 µl of cDNA was mixed with a PCR mastermix (see below), and gene-specific primers to the transcript of interest were added. The PCR mastermix contained 1x Taq buffer, 0.25 mM dNTPs, 1.5 mM $MgCl_2$, 0.5 µM primer mix, 1 µl Taq DNA polymerase, and RNase-free water to a total volume of 50 µl. PCR reactions were carried out in a thermocycler under the following conditions:

.

94°C	3 min	
94°C	30 s	30 Cycles
55°C	30 s	
72°C	90 s	
72°C	10 min	
4°C	Hold	

18S Forward Sequence: 5'-ACCGCGGTTCTATTTTGTTG

18S Reverse Sequence: 5'-AGTCGGCATCGTTTATGGTC

Mouse MCP-1 Forward Sequence: 5'-AGCCAACTCTCACTGAAGCC

Mouse MCP-1 Reverse Sequence: 5'-CATTCAAAGGTGCTGAAGACC

Analysis of PCR products was performed on 1% (w/v) agarose gels, resolved for 30 minutes at 100 V, using a Mini-Sub Cell GT gel system (Bio-Rad). PCR products

were mixed 5:1 with 6x DNA loading buffer, and equal volumes (10 µl) of PCR products were applied to the agarose gels. The gels were then visualised by ethidium bromide staining.

2.2.11 Plasmid DNA transformation and Purification

2.2.11.1 Plasmid DNA transformation

A JAK2 V617F plasmid (James et al. 2005) was a kind gift from Dr William Sands (University of Glasgow) and was maintained and propagated in TOP10 (Invitrogen) *E. coli*. Chemically-competent cells were defrosted on ice for 15 min. DNA was added (1-10 µl) and the cells incubated on ice for a further 15 min. The cells were then heat-shocked for 1 min at 42°C before recovering on ice for a further minute. SOC media (250 µl) was added and the tubes incubated at 37°C for at least 1 h with shaking. After incubation, the mixture was plated onto agar plates containing ampicillin. The plates were inverted and incubated overnight at 37°C.

2.2.11.2 Small-scale DNA preparations from *E.coli* (Miniprep)

A single colony from a fresh bacterial transformation was used to inoculate 5 ml 2 YT media (1.6% (w/v) tryptone, 1% (w/v) yeast extract. 0.5% (w/v) NaCl) containing 0.1 mg/ml ampicillin, and the culture grown overnight with shaking at 37°C. DNA purification was carried out using Promega Wizard® Plus SV Miniprep Kit. The DNA concentration was determined at A_{260} using a Nanodrop spectrophotometer (Thermo Scientific) prior to storage at -20°C.

2.2.11.3 Transfection of HEK 293 or Hela cell lines with JAK2 V617F plasmid

HEK 293 or Hela cells were seeded in 6 well Corning tissue culture dishes and grown to 90-95% confluency before the medium was replaced with 500 µl/well of growth medium. For each well of cells to be transfected, 4 µg JAK2 V617F or empty pRK5 plasmid DNA was diluted in Opti-MEM® I Reduced Serum Media and complexed with Lipofectamine 2000 (Invitrogen) in a 1:1 (w/v) ratio. Following incubation, the DNA-Lipofectamine 2000 complex was added to appropriate wells

and incubated at 37°C in a humidified atmosphere of 5% (v/v) CO_2 for 48h prior to treatment. Non-specific transfection was determined in parallel incubations in the presence of 4 µl/well Lipofectamine 2000.

2.2.12 Recombinant adenoviruses

2.2.12.1 AMPK adenoviruses

Adenoviruses encoding a dominant negative AMPK mutant (Ad.α1-DN, full-length AMPKα1 containing a D157A mutation), and a constitutively active AMPK mutant (Ad.$\alpha1^{312}$, residues 1-312 of AMPKα1 containing a T172D mutation) have been described previously (Woods et al. 2000) and were a generous gift from Dr F. Foufelle, Centre Biomédical des Cordeliers, Paris.

2.2.12.2 Adenovirus propagation

HEK 293 cells in T75 flasks were cultured in DMEM growth media (see 2.2.1.3) and passaged at 70-80% confluency (see 2.2.1.8). Each T75 flask was split into 5 x T150 flasks. Once 20 x T150 flasks were obtained, and grown to 70-80% confluency, recombinant adenoviruses were propagated in the HEK 293 cells. Detached cells were then pelleted in 50 ml falcon tubes (6 min at 604 x g). 100 mL of the supernatant was retained to infect more HEK 293 cells, and the pellets pooled and resuspended in 10 ml of sterile PBS.

2.2.12.3 Adenovirus purification

In order to lyse the HEK 293 cells containing the adenovirus particles, 10 mL of Arklone P (trichlorotrifluroethane) was added to the HEK 293 cell suspension (2.2.10.2) and mixed gently by inverting the tube for about 10 seconds. The mixture was then centrifuged at 340 x g for 15 min. The upper layer containing virus was separated from cell debris (interface) and the Arklone P layer (bottom layer). The upper layer was transferred to a clean 50 ml Falcon tube. 10 ml PBS was added to the left-over Arklone P layer, which was mixed and centrifuged as before, and the upper layer collected and added to the upper layer previously obtained.

2.5 ml sterile CsCl dissolved in Tris/EDTA (5 mM Tris-HCl, 1 mM EDTA pH 7.8) at a density of 1.33 g/ml was added to a sterile centrifuge tube. This was underlaid with 1.5 ml of sterile 1.45 g/ml CsCl. The virus layer was loaded on the CsCl gradient and centrifuged at 100,000 x g in a SW40 rotor using an Optima™ XL-80K ultracentrifuge at 8°C for 90 min. The tube was then punctured just below the virus band with a 21 guage needle, and withdrawn into a 2.5 ml syringe. The virus was transferred to a 10 micron Slide-A-Lyzer cassette and dialysed against cold Tris/EDTA buffer at 4°C overnight, and against fresh buffer containing 10% (v/v) glycerol for a further 2 h the following morning. The purified virus was removed and stored at -80°C.

2.2.12.4 Adenovirus titration

The Quick Titer™ Adenovirus Titer Immunoassay kit was used to titre the virus. Briefly, HEK cells were plated onto a 24 well plate. After 1 h 100 µl of 10^{-3}, 10^{-4}, 10^{-5} and 10^{-6} diluted virus solutions were added to the wells. The cells were then incubated for 48 h at 37°C, 5% (v/v) CO_2. To fix the cells the media was removed and replaced with 0.5 ml cold methanol and incubated for 20 min at 20°C. Cells were washed three times in PBS containing 1% (w/v) BSA. 250 µl of anti-Hexon antibody was added to each well and incubated for 1 h at room temperature. The cells were then washed 3 times in PBS prior to the addition of 250 µl of HRP-conjugated secondary antibody to each well and incubated for 1 h at room temperature. The cells were then washed five times in PBS. 250 µl of diaminobenzidine (DAB) was added to each well and incubated for 10 min at room temperature. DAB was then aspirated and the cells were washed twice with PBS. 1 ml of PBS was added to each well. The positive stained cells were counted for a minimum of five separate fields per well using a light microscope and 10X objective. Calculation of adenovirus titre was determined (Infectious Units/ml).

2.2.12.5 3T3-L1 adipocyte adenovirus infection

6 days post-differentiation, 500 µl of serum-free DMEM was added to 3T3-L1 CAR cells cultured on 6 well plates. Adenovirus was added (Ad.Null and Ad.α1-DN: 600 IFU/cell; Ad.GFP and Ad.$\alpha1^{312}$: 100 IFU/cell) to the dishes and incubated for 4 h at 37°C in a humidified atmosphere of 10% (v/v) CO_2. 500 µl of DMEM / 20% FCS

was added to the cells for a further 48 h before experiments were conducted, cell lysates prepared (see section 2.2.2) and conditioned medium collected (see section 2.2.13).

2.2.12.6 MEF adenovirus infection

Adenovirus encoding human wild-type p53 (Riccioni et al. 1998) was a kind gift from Prof Andrew Baker. At 70-80% confluency, 500 µl/well of serum-free DMEM was added to MEFs cultured on 6 well plates. Adenovirus was added (Ad.Null and Ad.p53: 100 IFU/cell) to the dishes and incubated for 4 h at 37°C in a humidified atmosphere of 5% (v/v) CO_2. DMEM / 20% FCS (500 µl/well) was added to the cells for a further 24 h before experiments were conducted.

2.2.13 Stimulation of 3T3-L1 CAR cytokine/chemokine production

3T3-L1 CAR adipocytes grown in 6-well Falcon plates infected with adenovirus (see section 2.2.12.5) were incubated in serum-free DMEM and stimulated with 10 ng/ml IL-1β or IL-6 and sIL-6Rα (5 ng/ml and 25 ng/ml, respectively) for 6 h with or without 30 min preincubation with 300 µM A769662. After this incubation period, cells were washed three times in serum-free DMEM and incubated with 0.4 ml/well SF-DMEM for 1 h at 37°C, 10% (v/v) CO_2. After 1 h, the conditioned serum free DMEM was collected and stored at -20°C.

2.2.14 Stimulation of RAW 264.7 macrophage cytokine/chemokine production

RAW 264.7 macrophages grown in 10 cm diameter Corning dishes were incubated in serum-free RPMI 1640 medium and stimulated with 1 µg/ml lipopolysaccharide (LPS) for 6 h with or without 30 min preincubation with 100 µM A769662. After this incubation period, cells were washed three times in serum free RPMI 1640 and incubated with 0.4 ml/well serum-free RPMI 1640 for 1 h at 37°C, 5% (v/v) CO_2. After 1 h, the conditioned serum-free RPMI 1640 was collected and stored at -20°C.

2.2.15 Analysis of 3T3-L1 CAR / RAW 264.7 macrophage cytokine and chemokine production

Conditioned medium from infected 3T3-L1 CAR adipocytes and RAW 264.7 macrophages (see sections 2.2.13 and 2.2.14) was used for cytokine and chemokine analysis with a Multiplex Bead Immunoassay (mouse cytokine 20-Plex panel, Invitrogen), testing for the presence of murine basic-FGF, GM-CSF, IFN-γ, IL-1α, IL-1β, IL-2, IL-4, IL-5, IL-6, IL-10, IL-12 (p40/p70), IL-13, IL-17, IP-10, KC, MCP-1, MIG, MIP-1α, TNF-α and VEGF. This assay allows the simultaneous detection of several molecules bound specifically to beads coated with different antibodies. These beads have distinct spectral properties and are linked to fluorophores, which permit the Luminex® 100™ detection system to distinguish between different beads, and thus, different antibody-bound molecules, while simultaneously measuring the quantity of associated fluorophore.

The assay was carried out following manufacturer's instructions, but antibodies and enzyme substrates were used at half the recommended concentration. All steps were carried out at room temperature and in the dark. Briefly, 50 µl per sample of conditioned medium was added to 50 µl assay diluent and 50 µl incubation buffer, and incubated with primary antibody-coated beads for 2 h with shaking. After two washes with wash solution, biotinylated detector antibody was added for 1 h with agitation. Two further washes preceded incubation with streptavidin-RPE for 30 min. Prior to detection in a Bio-Plex system (Bio-Rad), the assay was washed three times with wash solution. Serial dilutions of cytokine and chemokine standards were included in duplicate as a reference, from which the cytokine and chemokine concentrations in each sample were then calculated.

2.2.16 TCA precipitation

3T3-L1 adipocytes grown in 10 cm diameter Falcon dishes were incubated in serum-free DMEM and stimulated with TNF-α (10 ng/ml) or IL-6/sIL-6Rα (5 ng/ml; 25 ng/ml) for 6 h with or without 30 min preincubation with 300 μM A769662. The supernatant was centrifuged (1500 rpm, 15 min) to remove dead cells. 50 μl sodium deoxycholate (0.15% w/v) was added per ml of supernatant and incubated for 5 min at room temperature before addition of 100 μl trichloroacetic acid (TCA)

(72% w/v) per ml of supernatant. After 20 min on ice, the mixture was centrifuged (21,910 x g, 15 min at 4°C) before aspirating the supernatant. Pellets were resuspended in 1 ml chilled acetone and centrifuged (21,910 x g, 15 min at 4°C). Supernatant was removed and pellets air dried before resuspending in 60 μl 1x SDS-PAGE sample buffer. Resuspended pellets were stored at -20°C.

2.2.17 Oil Red O staining of 3T3-L1 adipocytes

3T3-L1 adipocytes were grown on glass coverslips and differentiated as described in section 2.2.1, but in the absence of troglitazone. Duplicate coverslips were incubated with either A769662 or DMSO from the point of differentiation until cells were fixed and stained at various intervals. At appropriate time points, differentiation medium was aspirated and cells were incubated in 10% (v/v) formalin for 5 min, which was replaced with fresh formalin for 1h at room temperature in the dark. After 1 h, coverslips were washed once in 60% (v/v) isopropanol and left to dry completely. Oil red O working solution was prepared ((60% (v/v) Oil red O stock (8.57 mM Oil red O (Sigma) in isopropanol) in dH_2O) and placed in wells for 10 min, before coverslips were washed four times with dH_20 and left to dry. Dry coverslips were then dipped in Mayers Hematoxylin (193.64 mM aluminium potassium alum, 16.54 mM hematoxylin, 2.02 mM sodium iodate, 2% (v/v) glacial actetic acid) then dipped in 3% (v/v) ammonium hydroxide, pH 10 in water, for 10 s. Coverslips were then mounted onto slides using Immumount adhesive and images captured using an Axiovision light microscope.

2.2.18 Confocal microscopy and staining

3T3-L1 adipocytes and 3T3-L1 CAR adipocytes were grown and differentiated on glass coverslips using the method described previously (see section 2.2.1.). 3T3-L1 CAR adipocytes were infected with adenoviruses as described in section 2.2.12.5 and utilised on Day 8 post-differentiation. 3T3-L1 adipocytes were utilised between day 8 to day 12 post-differentiation. Cells were stimulated with IL-1β (10 ng/ml for 15 min) with or without 30 min preincubation with A769662 (300 μM). Cells were then washed twice with PBS and fixed in 3% (w/v) paraformaldehyde at room temperature for 20 min. Coverslips were then washed twice in PBS and twice in 20 mM glycine in PBS to quench paraformaldehyde. Cells

were permeabilised in permeabilisation media (2% (w/v) BSA, 0.1% (w/v) Saponin, 20 mM glycine, PBS) for 20 min. Primary antibody was added in permeabilisation media for 45 min. Coverslips were then washed in permeabilisation media four times and the secondary antibody, also in permeabilisation media, was applied and the coverslips were incubated for 30 min in the dark. Cells were washed four times in permeabilisation media, and then washed once in PBS before being mounted on microscope slides using Immunomount adhesive. Slides were left overnight at 4°C before being visualised using a Ziess LSM exciter laser scanning microscope.

2.2.18.1 Image acquisition and quantification of fluorescence intensity

Immunolabelled samples were analysed using a Ziess LSM Exciter laser scanning microscope and LSM imaging software. Cells were visualised with a Plan-Apochromat X63/1.4 Oil DIC objective and the relevant filter. Quantification of nuclear fluorescence was assessed using ImageJ to obtain values corresponding to density from multiple points within the nucleus and calculating the mean density of nuclear fluorescence for each individual cell. A minimum of 50 cells were analysed for each treatment in each experiment, and an average taken.

2.2.19 Isolation of adipocytes from rat adipose

Male WKY rats were housed under standard conditions with free access to food and water. At approximately 12 weeks of age, mice were sedated and sacrificed by cardiac puncture. Epididymal adipose tissue was harvested and primary adipocytes isolated by digestion with collagenase type I (Worthington). Adipocyte preparation was performed in collaboration with Dr Silvia Bijland, University of Glasgow. Cells (10% v/v cytocrit in 1% (w/v) BSA, 0.2 μM adenosine, 10 mM glucose in KRH) were incubated in either IL-1β (10 ng/ml for 15 min), TNF-α (10 ng/ml for 15 min) or IL-6/sIL-6Rα (5 ng/ml; 25 ng/ml, respectively, for 1 h) with or without 30 min preincubation with A769662 (300 μM). Lysates were made and separated by SDS-PAGE and immunoblotted for proteins of interest.

2.2.20 Murine adipose tissue analysis

Female *AMPKα1$^{-/-}$* and wild-type sv129 mice were housed under standard conditions with free access to food and water. At approximately 4 months of age, mice were sacrificed by cervical dislocation. Organs were harvested (omental, subcutaneous and gonadal adipose). Lysates were made and separated by SDS-PAGE and immunoblotted for proteins of interest. Sections were also taken for immunohistological analysis of adipocyte cell size.

Omental and subcutaneous adipose tissue were fixed (10 % zinc formalin) for 24 h, and transferred to ethanol before being embedded in paraffin and sliced to produce 5 µm sections using a microtome. Sections were heated at 60°C for 35 min to soften before staining with haematoxylin and eosin. Briefly, sections were deparaffinised in Xylene then rehydrated through graded ethanol to water. Sections were then stained with Harris haematoxylin for 2 min followed by washing in water. Background staining was reduced by briefly submerging sections in 1% (v/v) HCl in 70% (v/v) ethanol followed by washing in Scotts tap water substitute for 30 s. Sections were counter stained in 1% (w/v) Eosin for 2 min before washing in water. Sections were then dehydrated through graded ethanol and then incubated in Xylene (3 min x 2). Tissue sections were mounted on coverslips using DPX mountant and images captured using an Axiovision light microscope.

2.2.21 Statistical Analysis

Results are expressed as mean ± SEM. Statistically significant differences were determined using a two-tail t-test, or one or two-way ANOVA where appropriate, with $p < 0.05$ as significant.

Chapter 3 – The effect of AMPK on TNF-α / IL-1β-stimulated proinflammatory signalling

3.1 Introduction

3.1.1 TNF-α and IL-1β signalling to NFκB and MAP kinases

TNF-α and IL-1β are proinflammatory cytokines which are secreted primarily by macrophages and monocytes, and have been reported to be elevated in WAT in obese states (Gustafson 2010). These cytokines trigger proinflammatory effects via simultaneous activation of the canonical NFκB and MAPK intracellular signalling cascades (see 1.2.2.1). Briefly, TNF-α or IL-1β binding its cognate receptor stimulates an increase in IκB kinase (IKK) activity, which in turn phosphorylates IκBα. Under basal conditions, IκBα is bound to the transcription factor NFκB in the cytoplasm; however upon phosphorylation by IKK, NFκB is released and translocates to the nucleus. The MAPK pathway is activated in parallel following cytokine stimulation, leading to the phosphorylation and activation of JNK, ERK and p38 MAPK. These pathways stimulate the transcription of genes involved in inflammation (e.g. IL-1β, TNF-α, IL-6 and MCP-1), survival (e.g. cFLIP) and adhesion (e.g. E-selectin, VCAM-1).

3.1.2 Regulation of proinflammatory signalling by AMPK

AMPK has been suggested to inhibit proinflammatory signalling in different cell types, including endothelial cells (Ewart, Kohlhaas, and Salt 2008) and macrophages (Sag et al. 2008); however the effect of AMPK activation on the MAPK and NFκB signalling pathways in adipocytes was poorly characterised. Prior to the beginning of this study, AMPK activation had been reported to suppress cytokine-stimulated NFκB activation in multiple cell types, including cultured endothelial cells (Cacicedo et al. 2004), macrophages (Yang et al. 2010), neutrophils (Zhao et al. 2008), microglial cells, astrocytes (Giri et al. 2004) and hepatic stellate cells (Caligiuri et al. 2008). Only a very small number of studies had previously examined inhibition of MAPK by AMPK. Berberine was reported to inhibit LPS-

stimulated phosphorylation of JNK, ERK1/2 and p38 MAPK in macrophages in an AMPK-dependent manner (Jeong et al. 2009), while elevated JNK phosphorylation was observed in aortic endothelial cells of *AMPKα2*$^{-/-}$ mice and HUVECs with an siRNA-mediated ablation of AMPKα1 or α2 (Dong et al. 2010). Furthermore, little was known about the mechanism by which AMPK might suppress proinflammatory cytokine signalling; however it was suggested that AMPK may inhibit the NFκB signalling pathway at the level of IKK, as metformin has been reported to reduce TNF-α-stimulated IKKα/β S180/181 phosphorylation in HUVECs in an AMPK-dependent manner (Huang et al. 2009).

3.1.3 Aims

While AMPK has been reported to have anti-inflammatory effects in a few different cell types, its role in adipocytes has not yet been fully investigated. In the current study the ability of AMPK to modulate cytokine-stimulated MAPK and NFκB signalling pathways in adipocytes was assessed. Furthermore, the effect of AMPK activation on the nuclear translocation of transcription factor NFκB was determined. Finally, the molecular mechanism by which AMPK may elicit these anti-inflammatory effects was investigated.

3.2 Results

3.2.1 AMPK activation in 3T3-L1 adipocytes

To examine whether TNF-α altered AMPK activity in 3T3-L1 adipocytes, cells were incubated with A769662 (a specific AMPK activator), Compound C (AMPK inhibitor) or TNF-α and the extent of AMPK Thr172 phosphorylation was determined by western blotting analysis of 3T3-L1 adipocyte lysates.

Incubation of 3T3-L1 adipocytes with A769662 (Fig. 3.1A) caused a significant ($p < 0.05$) increase, compared to the basal level, in AMPK Thr172 phosphorylation. This was significantly inhibited following preincubation with Compound C ($p < 0.001$). Incubation of 3T3-L1 adipocytes with TNF-α did not alter AMPK Thr172 phosphorylation compared to the basal level when data were normalised to A769662 (Fig. 3.1A); however TNF-α was found to cause a significant ($p < 0.01$) reduction in AMPK Thr172 phosphorylation compared to the basal level when data were normalised to vehicle (Fig. 3.1B).

3.2.2 Effect of AMPK activation by A769662 on IL-1β and TNF-α-stimulated MAPK activation in 3T3-L1 adipocytes

To determine whether AMPK activation influenced MAPK stimulation by proinflammatory stimuli, MAPK activation parameters in response to IL-1β or TNF-α in the presence or absence of A769662 were assessed in 3T3-L1 adipocytes. The extent of p38, ERK1/2 and JNK MAPK phosphorylation was assessed as a measure of activation by western blotting using phosphorylation site-specific antibodies.

Incubation of 3T3-L1 adipocytes with IL-1β in the absence of A769662 (Fig. 3.2) caused a significant ($p < 0.05$) increase, compared to the basal level, in p38 MAPK T180/Y182 phosphorylation after 3 min, peaking at 5 and 10 min ($p < 0.001$). Statistically significant ($p < 0.01$) reductions in p38 MAPK phosphorylation were observed at 5 and 10 min in the presence of A769662 compared to IL-1β treatment alone.

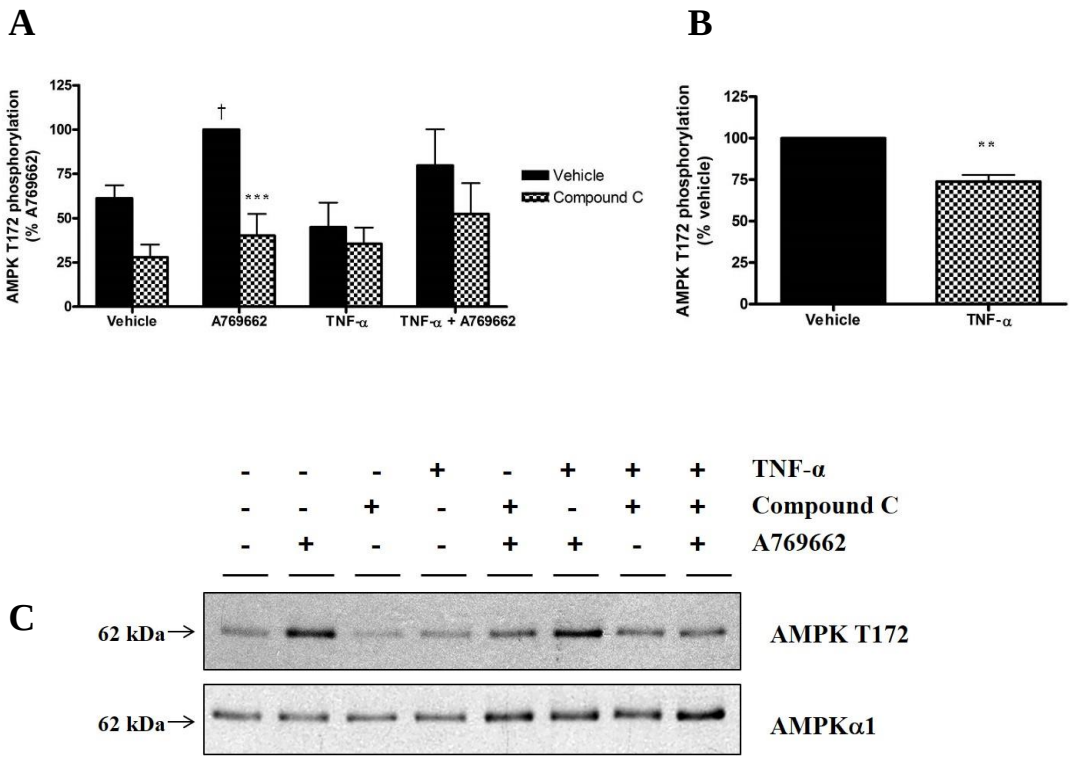

Figure 3-1: Effect of A769662 and Compound C on AMPK phosphorylation

*3T3-L1 adipocytes were incubated with TNF-α (10 ng/ml) for 15 min following preincubation for 30 min in the presence or absence of A769662 (300 μM) and 60 min in the presence or absence of Compound C (60 μM) and lysates prepared. Lysates were resolved by SDS-PAGE and subjected to immunoblotting with the antibodies indicated. (A) & (B) Quantification of AMPKα Thr172 phosphorylation was determined by comparison with total AMPK using densitometric analysis (A) Data shown represent the mean ± SEM % A769662-stimulated AMPK phosphorylation of six independent experiments. †p < 0.05 (one-way ANOVA), increase in AMPKα Thr172 phosphorylation, relative to vehicle. ***p < 0.001 (one-way ANOVA), reduction in AMPKα1 Thr172 phosphorylation, relative to the absence of Compound C. (B) Data shown represent the mean ± SEM % vehicle AMPK phosphorylation of three independent experiments. **p < 0.01 (two-tail t-test), reduction in AMPK Thr172 phosphorylation, relative to vehicle. (C) Representative western blot.*

Incubation of 3T3-L1 adipocytes with TNF-α in the absence of A769662 (Fig. 3.3) caused a significant ($p < 0.01$) increase, compared to the basal level, in p38 MAPK T180/Y182 phosphorylation after 5, 10 and 360 min. Preincubation with A769662 caused significant reductions in p38 MAPK phosphorylation after 3 min ($p < 0.05$) and 360 min ($p < 0.01$), compared to TNF-α treatment alone. A statistically significant ($p < 0.05$) reduction in basal p38 MAPK phosphorylation was observed following A769662 treatment.

Incubation of 3T3-L1 adipocytes with IL-1β in the absence of A769662 (Fig. 3.4) caused a significant increase, compared to the basal level, in ERK1/2 T202/Y204 phosphorylation after 10 and 15 min ($p < 0.001$ and $p < 0.01$, respectively). A statistically significant ($p < 0.01$) reduction in ERK1/2 phosphorylation was observed at 10 min in the presence of A769662 compared to IL-1β treatment alone. A statistically significant ($p < 0.05$) reduction in basal ERK1/2 T202/Y204 phosphorylation was observed following A769662 treatment. Incubation of 3T3-L1 adipocytes with TNF-α in the absence of A769662 (Fig. 3.5) caused a significant ($p < 0.05$) increase, compared to the basal level, in ERK1/2 T202/Y204 phosphorylation after 10 and 360 min. Preincubation with A769662 caused significant reductions in ERK1/2 T202/Y204 phosphorylation in ERK1 after 3, 10 ($p < 0.05$) and 360 ($p < 0.01$) min, and in ERK2 after 3 ($p < 0.05$), 10 ($p < 0.01$) and 360 ($p < 0.001$) min compared to TNF-α treatment alone. A statistically significant ($p < 0.05$) reduction in basal ERK1/2 T202/Y204 phosphorylation was observed following A769662 treatment.

Incubation of 3T3-L1 adipocytes with IL-1β in the absence of A769662 (Fig. 3.6) caused a significant increase, compared to the basal level, in JNK T183/Y185 phosphorylation (54 and 46 kDa isoforms) after 15 and 30 min ($p < 0.001$ and $p < 0.01$, respectively) and JNK 54 kDa subunit phosphorylation after 10 min ($p < 0.01$). A statistically significant ($p < 0.05$) reduction in phosphorylation of both JNK subunits was observed at 15 min in the presence of A769662 compared to IL-1β treatment alone. TNF-α displayed a tendency to increase JNK T183/Y185 phosphorylation (Fig. 3.7) in 3T3-L1 adipocytes, compared to the basal level, although this did not reach statistical significance. Similarly, A769662 displayed a tendency to reduce TNF-α-stimulated JNK T183/Y185 phosphorylation, although this did not reach statistical significance.

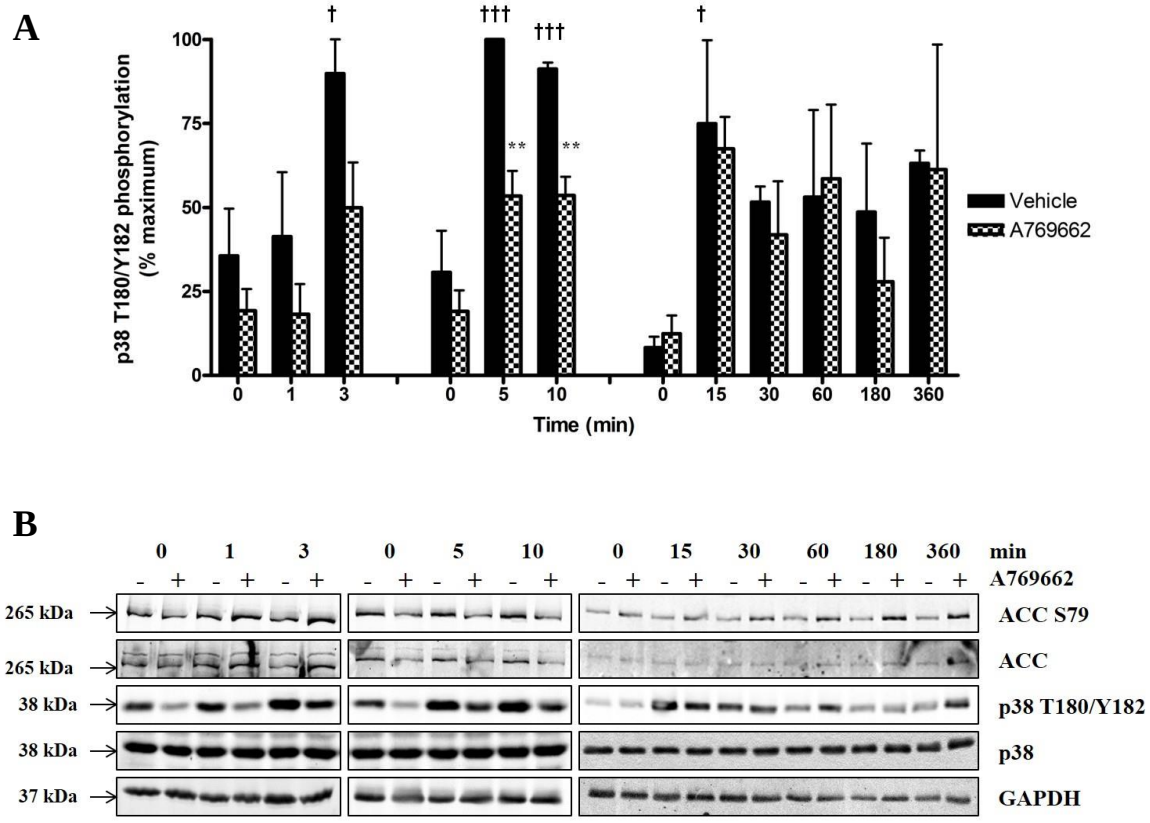

Figure 3-2: Effect of A769662 on IL-1β-stimulated p38 MAPK phosphorylation

3T3-L1 adipocytes were incubated with IL-1β (10 ng/ml) for various durations following preincubation for 30 min in the presence or absence of A769662 (300 μM) and lysates prepared. Lysates were resolved by SDS-PAGE and subjected to immunoblotting with the antibodies indicated. (A) Quantification of p38 MAPK T180/Y182 phosphorylation was determined by comparison with total p38 MAPK using densitometric analysis. Data shown represent the mean ± SEM % maximum p38 phosphorylation of three independent experiments. $^{\dagger}p < 0.05$, $^{\dagger\dagger\dagger}p < 0.001$ (two-way ANOVA), increase in p38 MAPK T180/Y182 phosphorylation, relative to vehicle. $^{**}p < 0.01$ (two-way ANOVA), reduction in p38 MAPK T180/Y182 phosphorylation, relative to the absence of A769662. (B) Representative western blot.

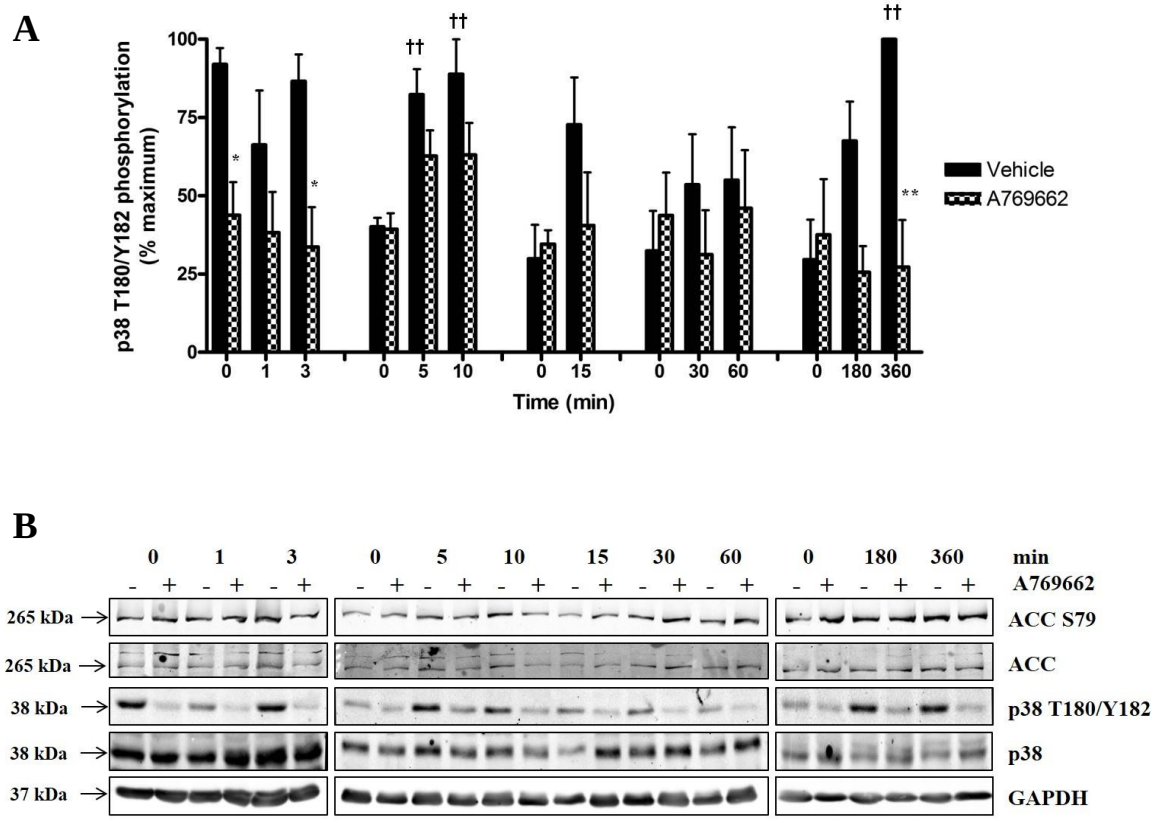

Figure 3-3: Effect of A769662 on TNF-α-stimulated p38 MAPK phosphorylation

*3T3-L1 adipocytes were incubated with TNF-α (10 ng/ml) for various durations following preincubation for 30 min in the presence or absence of A769662 (300 μM) and lysates prepared. Lysates were resolved by SDS-PAGE and subjected to immunoblotting with the antibodies indicated. (A) Quantification of p38 MAPK T180/Y182 phosphorylation was determined by comparison with total p38 MAPK using densitometric analysis. Data shown represent the mean ± SEM % maximum p38 phosphorylation of three independent experiments. ††p < 0.01 (two-way ANOVA), increase in p38 MAPK T180/Y182 phosphorylation, relative to vehicle. *p < 0.05, **p < 0.01 (two-way ANOVA), reduction in p38 MAPK T180/Y182 phosphorylation, relative to the absence of A769662. (B) Representative western blot.*

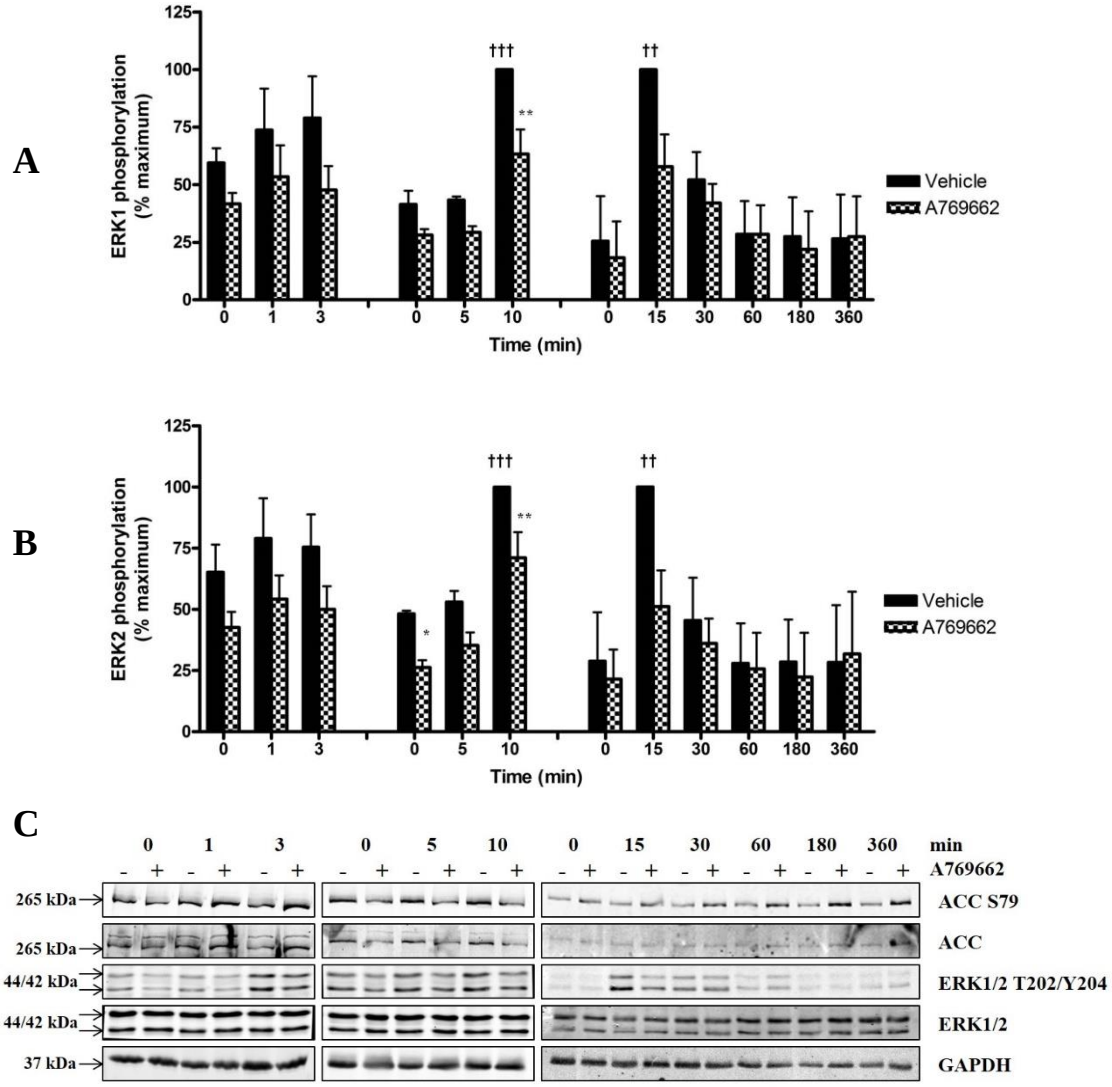

Figure 3-4: Effect of A769662 on IL-1β-stimulated ERK1/2 phosphorylation

3T3-L1 adipocytes were incubated with IL-1β (10 ng/ml) for various durations following preincubation for 30 min in the presence or absence of A769662 (300 μM) and lysates prepared. Lysates were resolved by SDS-PAGE and subjected to immunoblotting with the antibodies indicated. (A) & (B) ERK1 and ERK2, respectively. Quantification of ERK1/2 T202/Y204 phosphorylation was determined by comparison with total ERK1/2 using densitometric analysis. Data shown represent the mean ± SEM % maximum ERK1/2 phosphorylation of three independent experiments. $^{††}p < 0.01$, $^{†††}p < 0.001$ (two-way ANOVA), increase in ERK1/2 T202/Y204 phosphorylation, relative to vehicle. $^{*}p < 0.05$, $^{**}p < 0.01$ (two-way ANOVA), reduction in ERK1/2 T202/Y204 phosphorylation, relative to the absence of A769662. (C) Representative western blot.

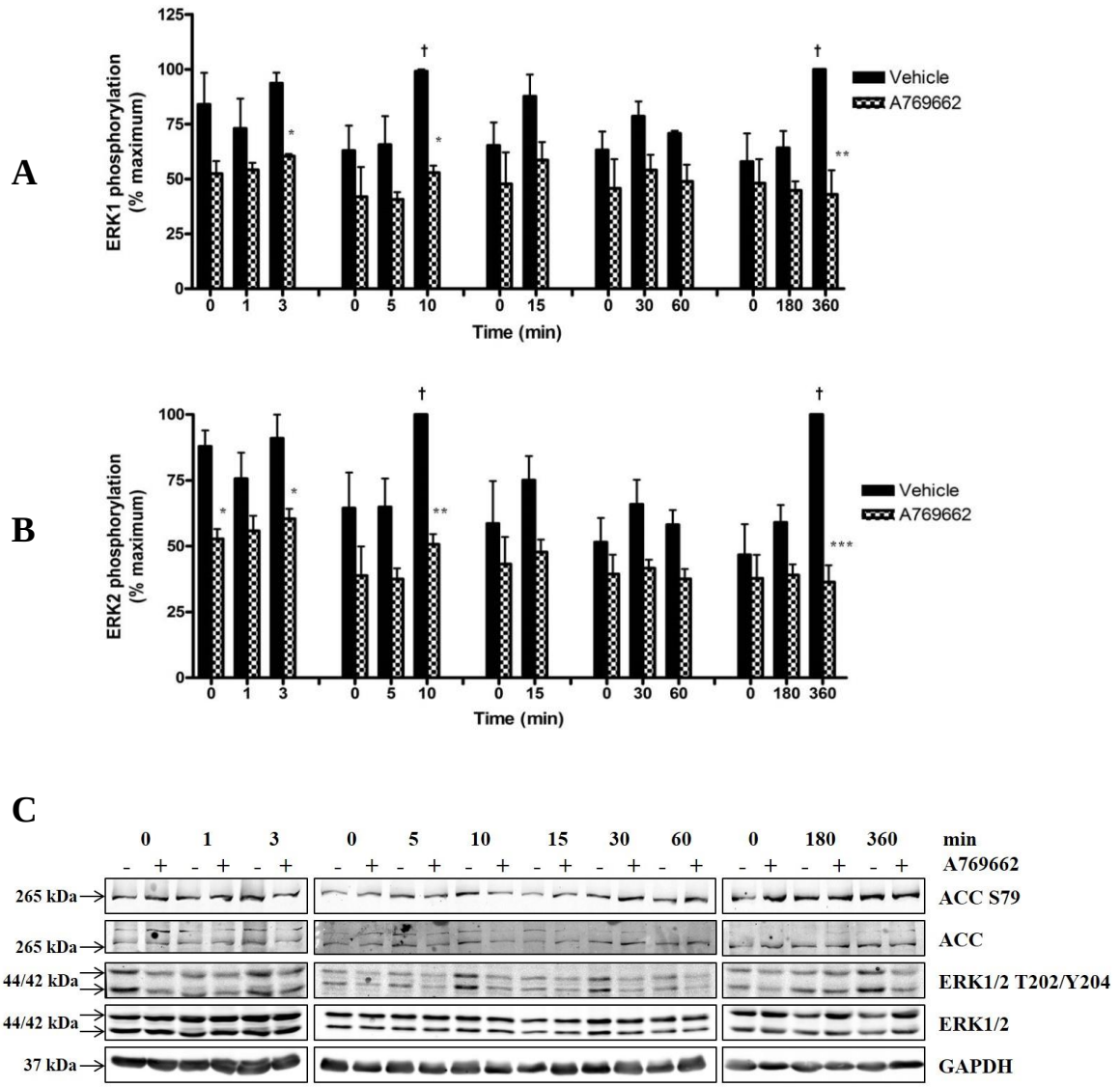

Figure 3-5: Effect of A769662 on TNF-α-stimulated ERK1/2 phosphorylation

*3T3-L1 adipocytes were incubated with TNF-α (10 ng/ml) for various durations following preincubation for 30 min in the presence or absence of A769662 (300 μM) and lysates prepared. Lysates were resolved by SDS-PAGE and subjected to immunoblotting with the antibodies indicated. (A) & (B) ERK1 and ERK2, respectively. Quantification of ERK1/2 T202/Y204 phosphorylation was determined by comparison with total ERK1/2 using densitometric analysis. Data shown represent the mean ± SEM % maximum ERK1/2 phosphorylation of three independent experiments. (A) †p < 0.05, (two-way ANOVA), increase in ERK1/2 T202/Y204 phosphorylation, relative to vehicle. *p < 0.05, **p < 0.01, ***p < 0.001 (two-way ANOVA), reduction in ERK1/2 T202/Y204 phosphorylation, relative to the absence of A769662. (C) Representative western blot.*

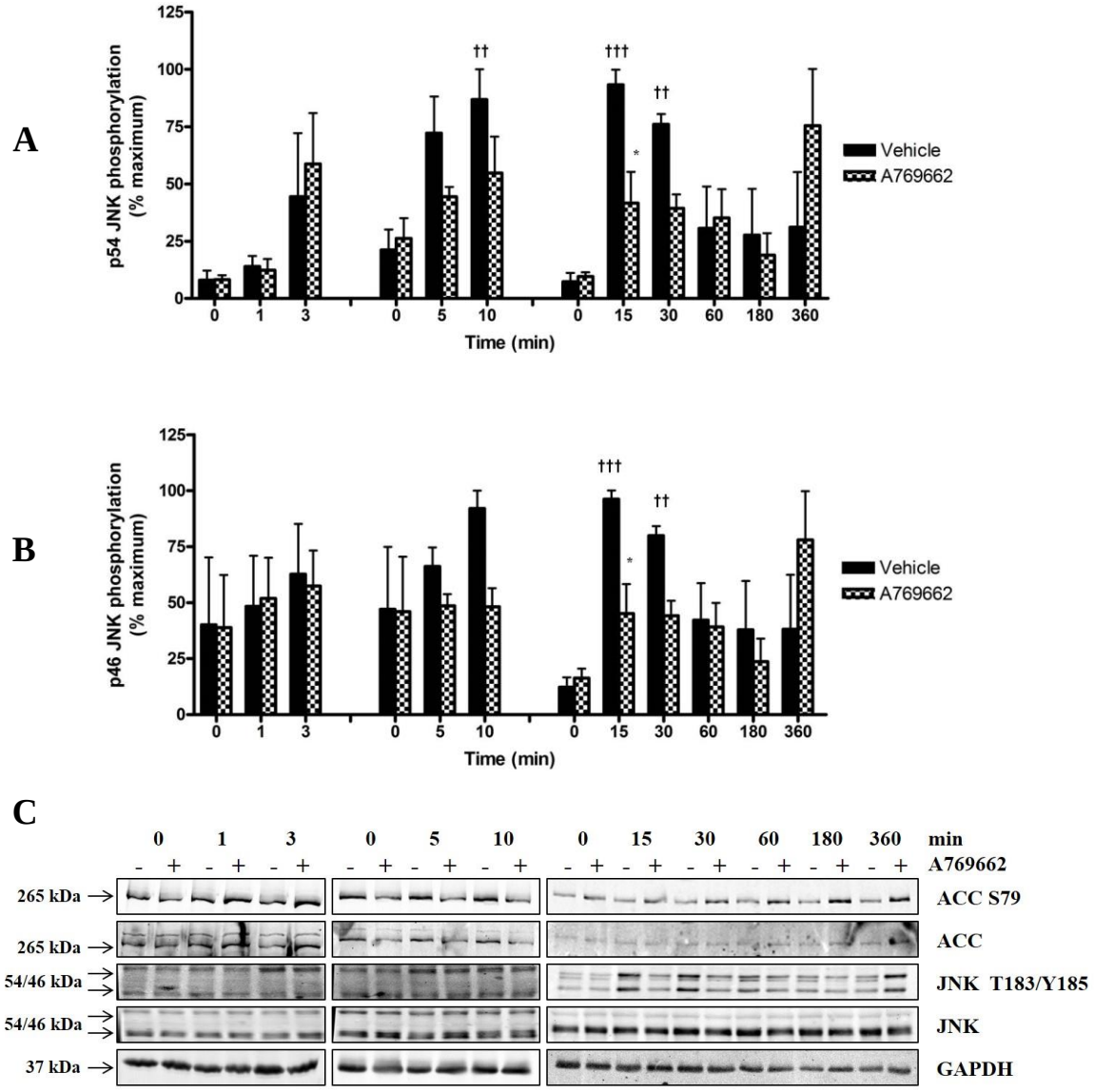

Figure 3-6: Effect of A769662 on IL-1β-stimulated JNK phosphorylation

3T3-L1 adipocytes were incubated with IL-1β (10 ng/ml) for various durations following preincubation for 30 min in the presence or absence of A769662 (300 μM) and lysates prepared. Lysates were resolved by SDS-PAGE and subjected to immunoblotting with the antibodies indicated. (A) & (B) p54 JNK and p46 JNK, respectively. Quantification of JNK T183/Y185 phosphorylation was determined by comparison with total JNK using densitometric analysis. Data shown represent the mean ± SEM % maximum JNK phosphorylation of three independent experiments. $^{††}p < 0.01$, $^{†††}p < 0.001$ (two-way ANOVA), increase in JNK T183/Y185 phosphorylation, relative to vehicle. $^{*}p < 0.05$ (two-way ANOVA), reduction in JNK T183/Y185 phosphorylation, relative to the absence of A769662. (C) Representative western blot.

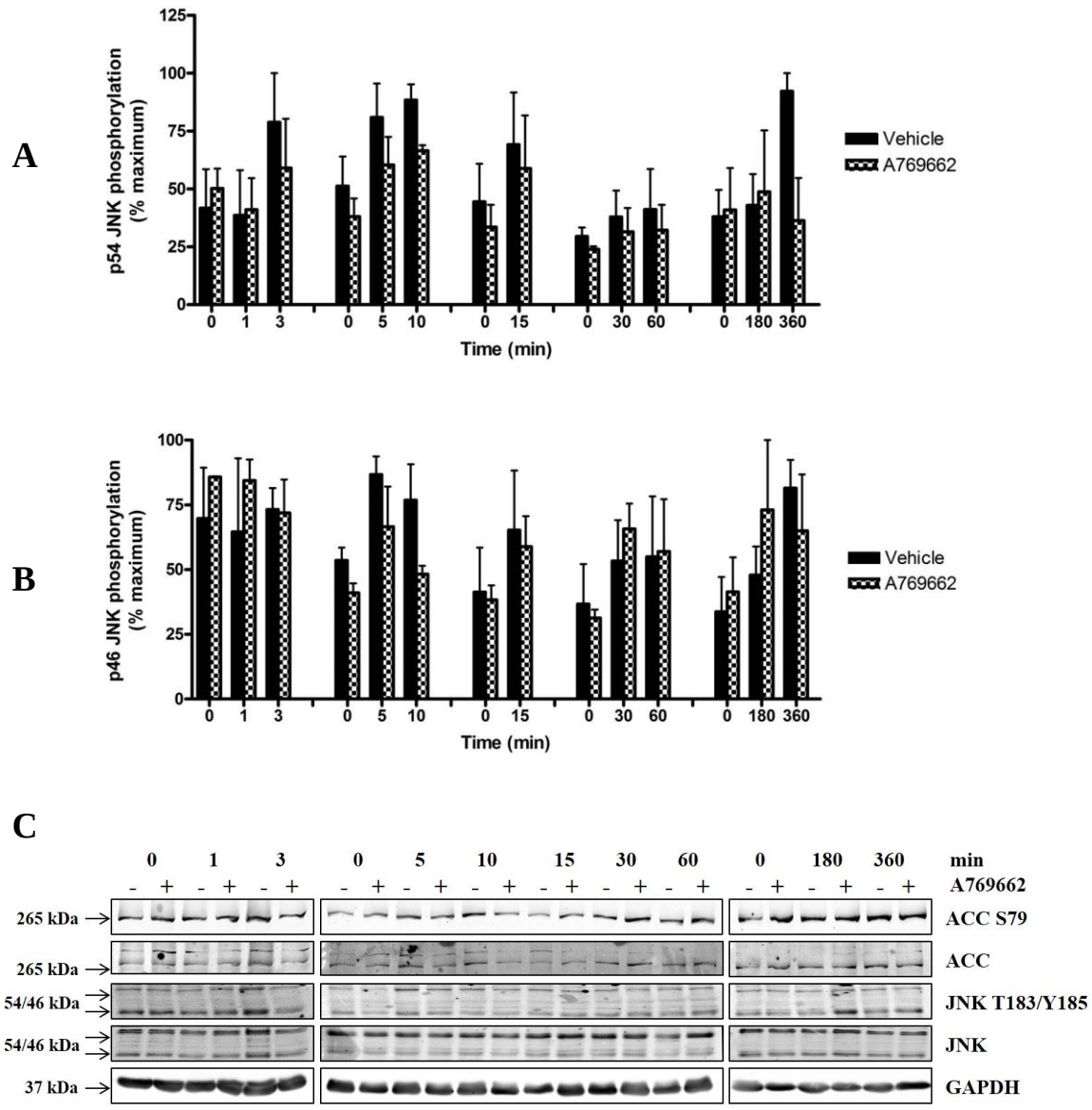

Figure 3-7: Effect of A769662 on TNF-α-stimulated JNK phosphorylation

3T3-L1 adipocytes were incubated with TNF-α (10 ng/ml) for various durations following preincubation for 30 min in the presence or absence of A769662 (300 μM) and lysates prepared. Lysates were resolved by SDS-PAGE and subjected to immunoblotting with the antibodies indicated. (A) & (B) p54 JNK and p46 JNK, respectively. Quantification of JNK T183/Y185 phosphorylation was determined by comparison with total JNK using densitometric analysis. Data shown represent the mean ± SEM % maximum JNK phosphorylation of three independent experiments. (C) Representative western blot.

3.2.3 Investigating whether inhibition of MAPK signalling by A769662 is dependent on AMPK activation

3.2.3.1 Effect of Compound C on A769662-mediated inhibition of MAPK signalling

The pharmacological AMPK inhibitor, Compound C, was utilised to determine whether the A769662-mediated inhibition of TNF-α-stimulated p38 MAPK phosphorylation was dependent upon AMPK activation. Incubation of 3T3-L1 adipocytes with TNF-α caused a 67.6 $\pm$ 23.6 % or 39.3 $\pm$ 15.2 % stimulation of p38 MAPK T180/Y182 phosphorylation (Fig. 3.8), compared to the basal level in the absence or presence of Compound C, respectively. Preincubation with A769662 caused a 51.3 $\pm$ 17.7 % reduction in p38 MAPK phosphorylation relative to TNF-α treatment alone, while this was reduced to 39.3 $\pm$ 28.5 % in the presence of Compound C (Fig. 3.8).

3.2.3.2 Effect of a DN or CA AMPK mutant on A769662-mediated inhibition of MAPK signalling

Adenovirus-mediated gene transfer was used to overexpress a dominant negative AMPK mutant (Ad.α1DN) or a constitutively active AMPK mutant (Ad.α1CA) in 3T3-L1 CAR adipocytes in order to investigate the effect of down- or up-regulation of AMPK on A769662-mediated inhibition of MAPK signalling.

Incubation with A769662 caused a 29.2 $\pm$ 47.4 % increase in ACC S79 phosphorylation in Ad.Null infected cells and a 2 $\pm$ 22.9 % reduction in Ad.α1DN infected cells, relative to the basal level (Fig. 3.9A). Ad.α1CA infected cells exhibited an 68.4 $\pm$ 6.8 % increase in basal ACC Ser79 phosphorylation compared with the basal level in cells infected with Ad.GFP, however this was not statistically significant (Fig. 3.9C). As neither the A769662 nor Ad.α1CA were able to significantly stimulate AMPK activity, it was not possible to assess the effect of adenovirus mediated up- or down-regulation of AMPK on IL-1β-stimulated MAPK phosphorylation.

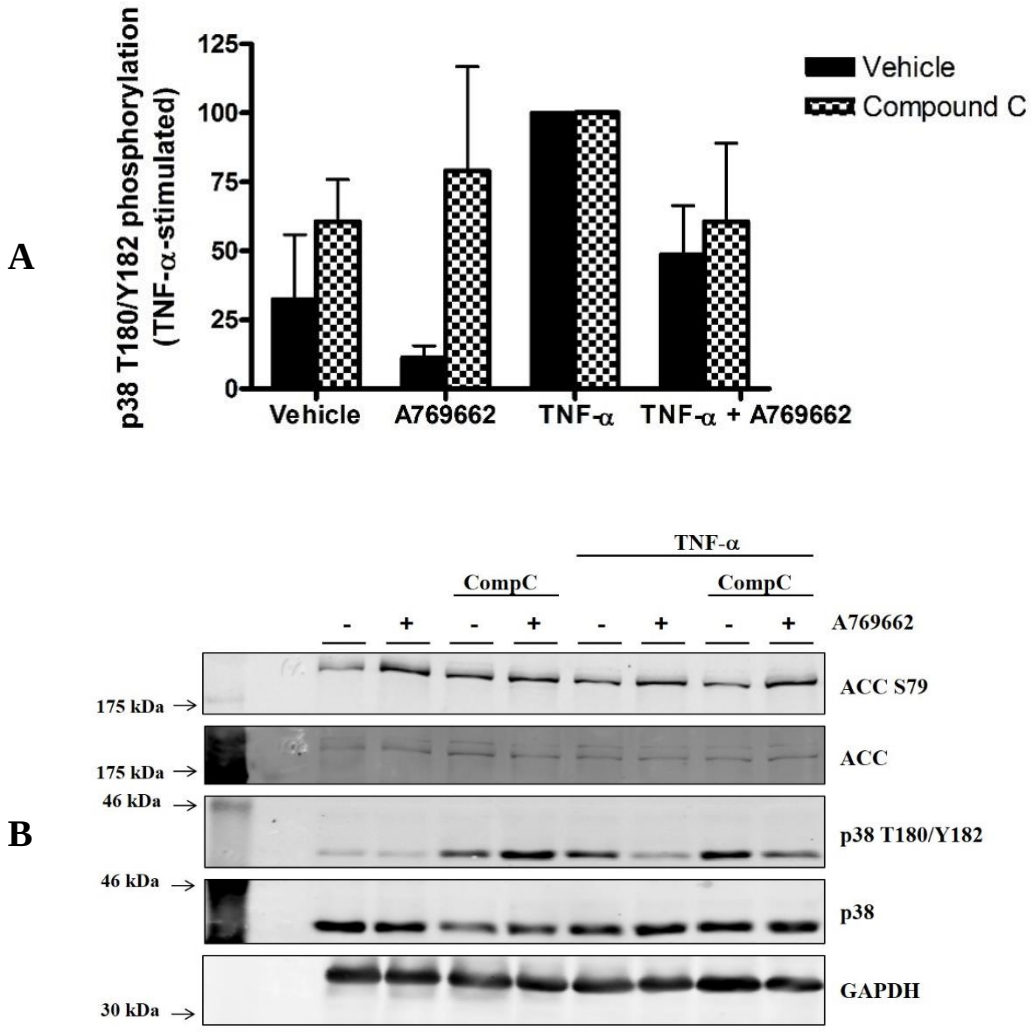

Figure 3-8: Effect of Compound C on A769662-mediated p38 MAPK inhibition

3T3-L1 adipocytes were incubated with TNF-α (10 ng/ml) for 15 min following preincubation for 30 min in the presence or absence of A769662 (300 μM) and 60 min in the presence or absence of Compound C (60 μM) and lysates prepared. Lysates were resolved by SDS-PAGE and subjected to immunoblotting with the antibodies indicated. (A) Quantification of p38 MAPK T180/Y182 phosphorylation was determined by comparison with p38 MAPK using densitometric analysis. Data shown represent the mean ± SEM % TNF-α-stimulated p38 phosphorylation of three independent experiments. (B) Representative western blot.

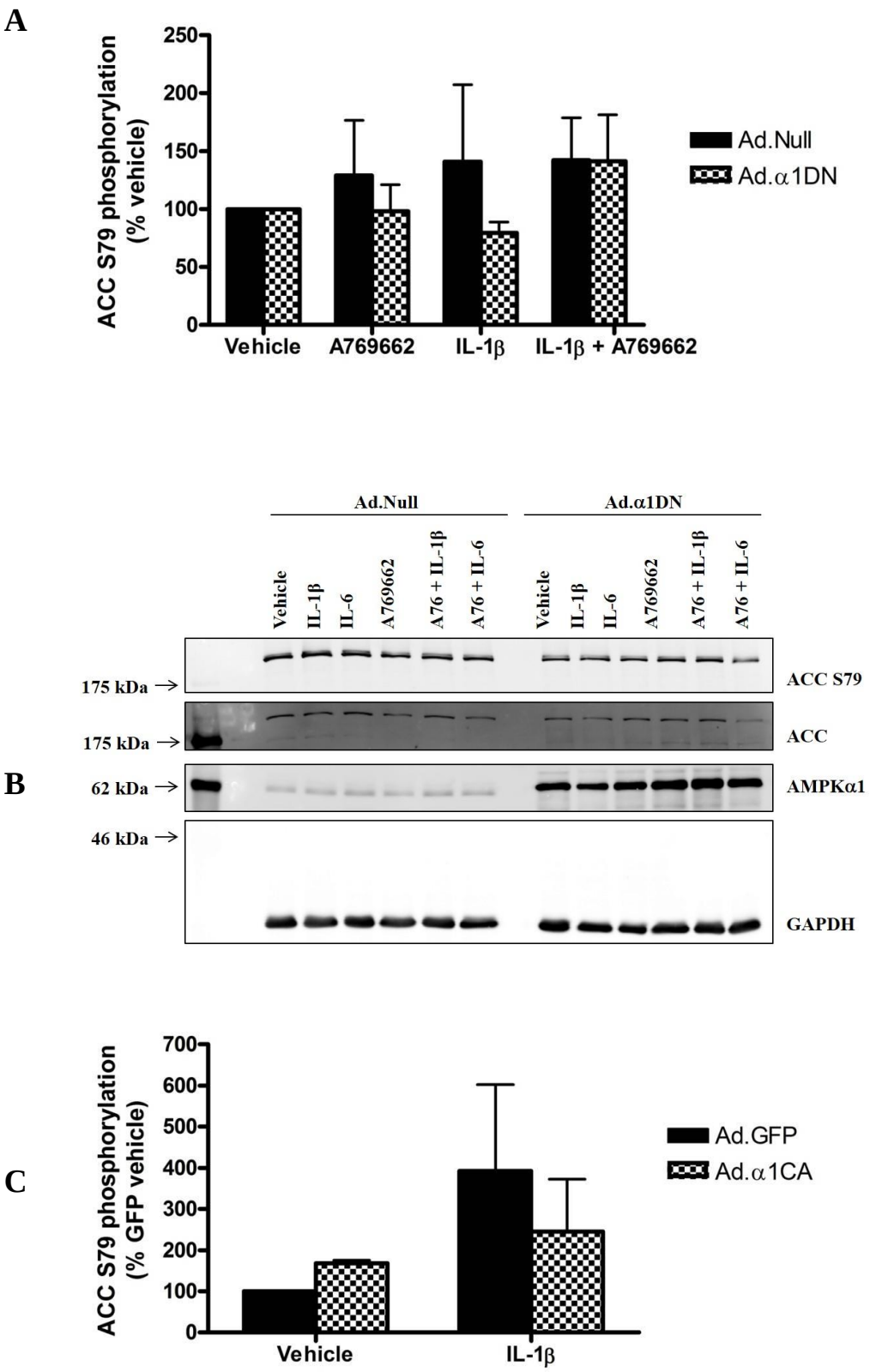

Figure 3-9: Effect of overexpression of a dominant negative or constitutively active AMPK mutant on ACC phosphorylation in 3T3-L1 CAR adipocytes

(continued overleaf)

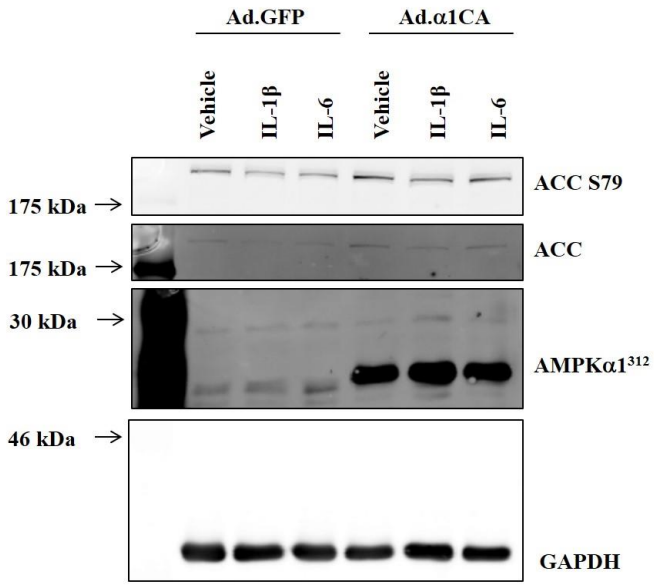

D

Figure 3-9: Effect of overexpression of a dominant negative or constitutively active AMPK mutant on ACC phosphorylation in 3T3-L1 CAR adipocytes

(A) 3T3-L1 CAR adipocytes were infected with (600 ifu/cell) for 48 h with Ad.α1DN or Ad.null prior to stimulation for 10 min with IL-1β (10 ng/ml) following preincubation for 30 min in the presence or absence of A769662 (300 μM) and cell lysates prepared. Lysates were resolved by SDS-PAGE and subjected to immunoblotting with the antibodies indicated. Quantification of ACC Ser79 phosphorylation was determined by comparison with ACC using densitometric analysis. Data shown represent the mean ± SEM % vehicle ACC phosphorylation of three independent experiments. (B) Representative western blot. (C) 3T3-L1 CAR adipocytes were infected with (100 ifu/cell) for 48 h with Ad.α1CA or Ad.GFP prior to stimulation for 10 min with IL-1β (10 ng/ml) and cell lysates prepared. Quantification of ACC Ser79 phosphorylation was determined by comparison with ACC using densitometric analysis. Data shown represent the mean ± SEM % vehicle GFP ACC phosphorylation of three independent experiments. (D) Representative western blot.

3.2.4 Endogenous MAPK phosphorylation in adipose tissue

To examine the role of AMPK in the basal inflammatory status of adipose tissue, gonadal and subcutaneous adipose tissue was collected from female *AMPKα1$^{-/-}$* and litter-matched wild-type sv129 mice. The extent of JNK and p38 MAPK phosphorylation in lysates was assessed as a measure of activation by western blotting using phosphorylation site-specific antibodies. ERK1/2 phosphorylation was undetectable in either gonadal or subcutaneous tissues (data not shown). Lane 2 of *AMPKα1$^{-/-}$* was omitted for analysis purposes as AMPKα1 was detectable in the lysate.

Phosphorylation of JNK p54 was significantly ($p < 0.01$) increased in *AMPKα1$^{-/-}$* gonadal adipose tissue compared to wild-type (Fig. 3.10A). Similarly, Fig. 3.11A shows JNK p54 phosphorylation was significantly ($p < 0.05$) increased in *AMPKα1$^{-/-}$* subcutaneous adipose tissue compared to wild-type. Phosphorylation of JNK p46 was undetectable in either wild-type or *AMPKα1$^{-/-}$* tissues.

Phosphorylation of p38 MAPK was increased 1.22 fold in *AMPKα1$^{-/-}$* gonadal adipose tissue compared to wild-type (Fig. 3.10B), however this did not reach significance. Similarly, it can be seen from Fig. 3.11B that p38 phosphorylation was increased 1.43 fold in *AMPKα1$^{-/-}$* subcutaneous adipose tissue compared to wild-type, but failed to reach significance.

3.2.5 Effect of AMPK activation by A769662 on IL-1β/TNF-α-stimulated MAPK activation in rat epididymal adipocytes

Data thus far have demonstrated that A769662 inhibits proinflammatory signalling in 3T3-L1 adipocytes. It was of interest, therefore, to investigate if this could be recapitulated in primary cells. Adipocytes isolated from rat epididymal adipose were incubated with IL-1β in the presence or absence of A769662. The extent of ACC, JNK, ERK1/2 and p38 MAPK phosphorylation in lysates was assessed as a measure of activation by western blotting using phosphorylation site-specific antibodies. JNK phosphorylation was undetectable (data not shown).

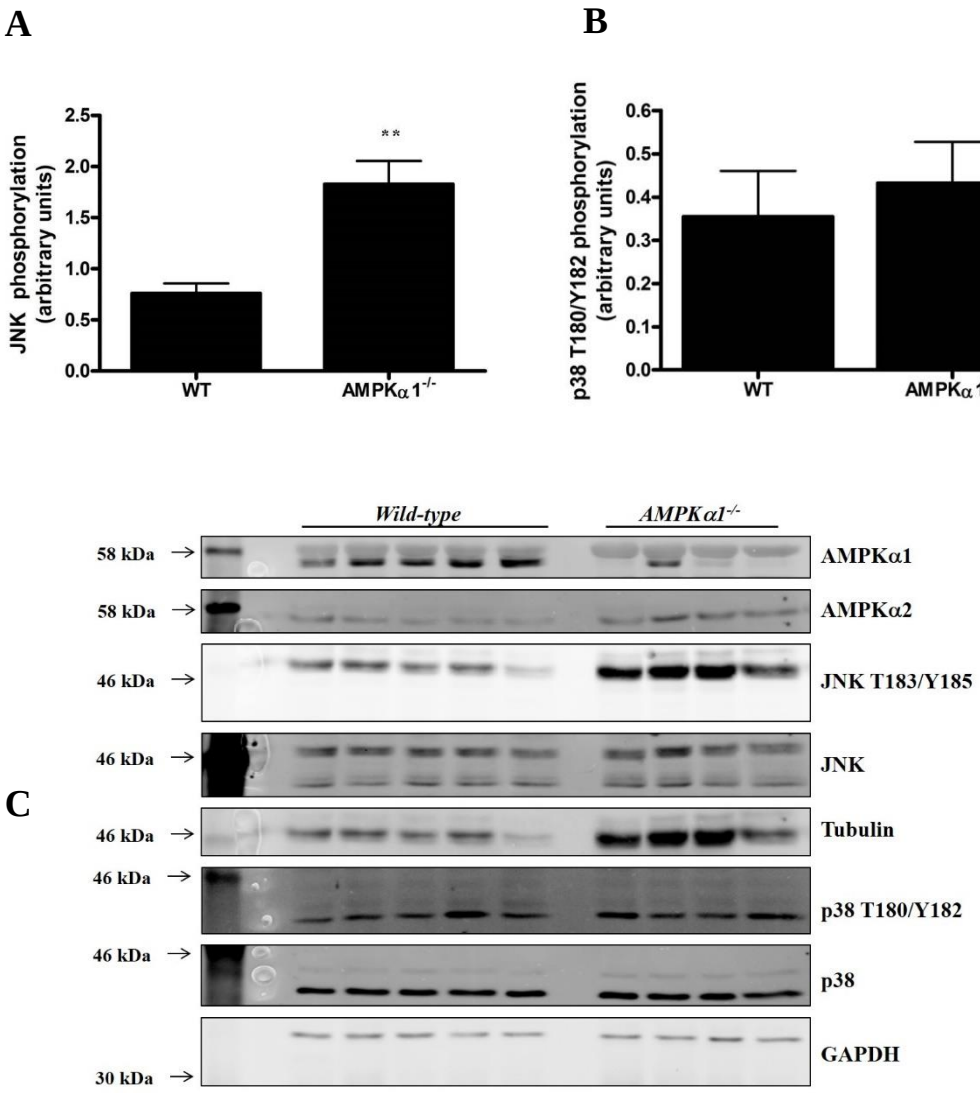

Figure 3-10: Basal JNK and p38 MAPK phosphorylation in gonadal adipose tissue from *AMPKα1*$^{+/+}$ and *AMPKα1*$^{-/-}$ mice

Gonadal adipose tissue obtained from AMPKα1$^{-/-}$ *and wild-type mice was resolved by SDS-PAGE and subjected to immunoblotting with the antibodies indicated. Data shown represent the mean ± SEM arbitrary units of 5 wild-type and 3 AMPKα1*$^{-/-}$ *samples. (A) Quantification of JNK T183/Y185 phosphorylation was determined by comparison with JNK using densitometric analysis. **p < 0.01 (two-tail t-test) increase in JNK T183/Y185 phosphorylation, relative to wild-type. (B) Quantification of p38 MAPK T180/Y182 phosphorylation was determined by comparison with p38 MAPK using densitometric analysis. (C) Representative western blot.*

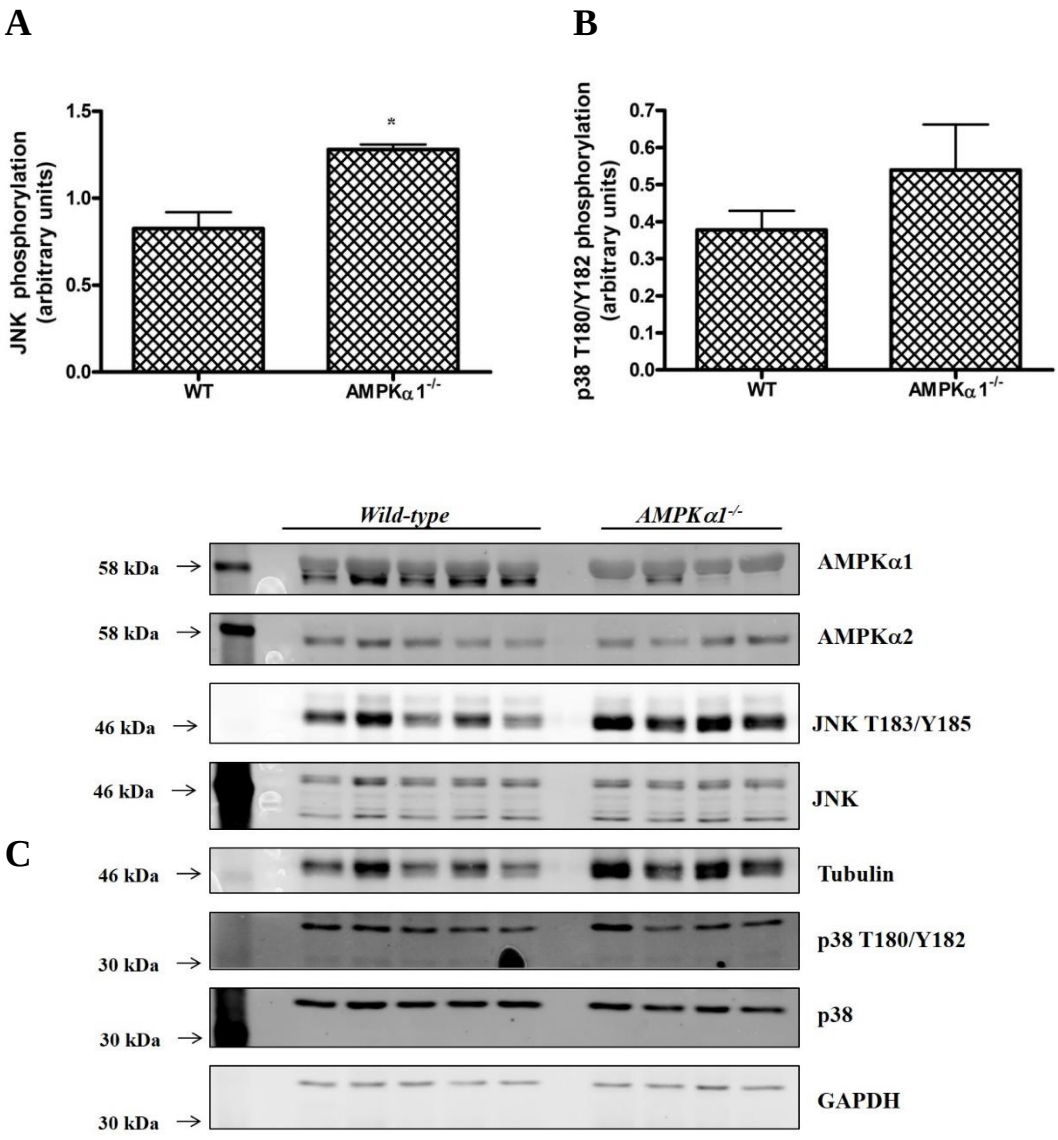

Figure 3-11: Basal JNK and p38 MAPK phosphorylation in subcutaneous adipose tissue from *AMPKα1*$^{+/+}$ and *AMPKα1*$^{-/-}$ mice

*Subcutaneous adipose tissue obtained from AMPKα1$^{-/-}$ and wild-type was resolved by SDS-PAGE and subjected to immunoblotting with the antibodies indicated. Data shown represent the mean ± SEM arbitrary units of 5 wild-type and 3 AMPKα1$^{-/-}$ samples. (A) Quantification of JNK T183/Y185 phosphorylation was determined by comparison with JNK using densitometric analysis. *p < 0.05 (two-tail t-test) increase in JNK T183/Y185 phosphorylation, relative to wild-type. (B) Quantification of p38 MAPK T180/Y182 phosphorylation was determined by comparison with p38 MAPK using densitometric analysis. (C) Representative western blot.*

Incubation with A769662 caused a 30.4 ± 17.5 % increase in ACC Ser79 phosphorylation compared to the basal level (Fig. 3.12); however this was not statistically significant ($p = 0.1$). IL-1β treatment induced a 190.2 ± 17.3 % increase in ERK1 T202/Y204 phosphorylation, relative to the basal level. Preincubation with A769662 caused a 19.6 ± 3.6 % inhibition of ERK1 phosphorylation, compared to IL-1β treatment alone (Fig. 3.13A). ERK2 phosphorylation was increased by 137.6 ± 2.1 % in response to IL-1β, relative to the basal level. Pretreatment with A769662 caused a 30.6 ± 6.5 % inhibition of ERK2 phosphorylation, compared to IL-1β treatment alone (Fig. 3.13B).

IL-1β treatment induced a 97.1 ± 15.1 % increase in p38 MAPK phosphorylation relative to the basal level, however this did not reach statistical significance. Preincubation with A769662 caused a 23 ± 21.8 % inhibition of p38 MAPK phosphorylation, compared to IL-1β treatment alone (Fig. 3.13C).

3.2.6 Effect of AMPK on IL-1β/TNF-α - stimulated NFκB nuclear translocation

3.2.6.1 Temporal parameters of NFκB nuclear localisation in 3T3-L1 adipocytes

3T3-L1 adipocytes were incubated with IL-1β or TNF-α for various durations to ascertain the optimum incubation time for subsequent experiments examining cytokine-induced nuclear translocation of NFκB. Fig. 3.14 demonstrated that NFκB nuclear translocation peaks at 15 min incubation with IL-1β or TNF-α, with a 10.6 or 2.5 fold increase, respectively.

3.2.6.2 Effect of A769662 on IL-1ß/TNF-α - stimulated NFκB nuclear translocation in 3T3-L1 adipocytes

Translocation of NFκB to the nucleus induces transcription of a variety of proinflammatory genes; therefore it was of interest to determine whether activation of AMPK by A769662 attenuated nuclear localisation of this transcription factor.

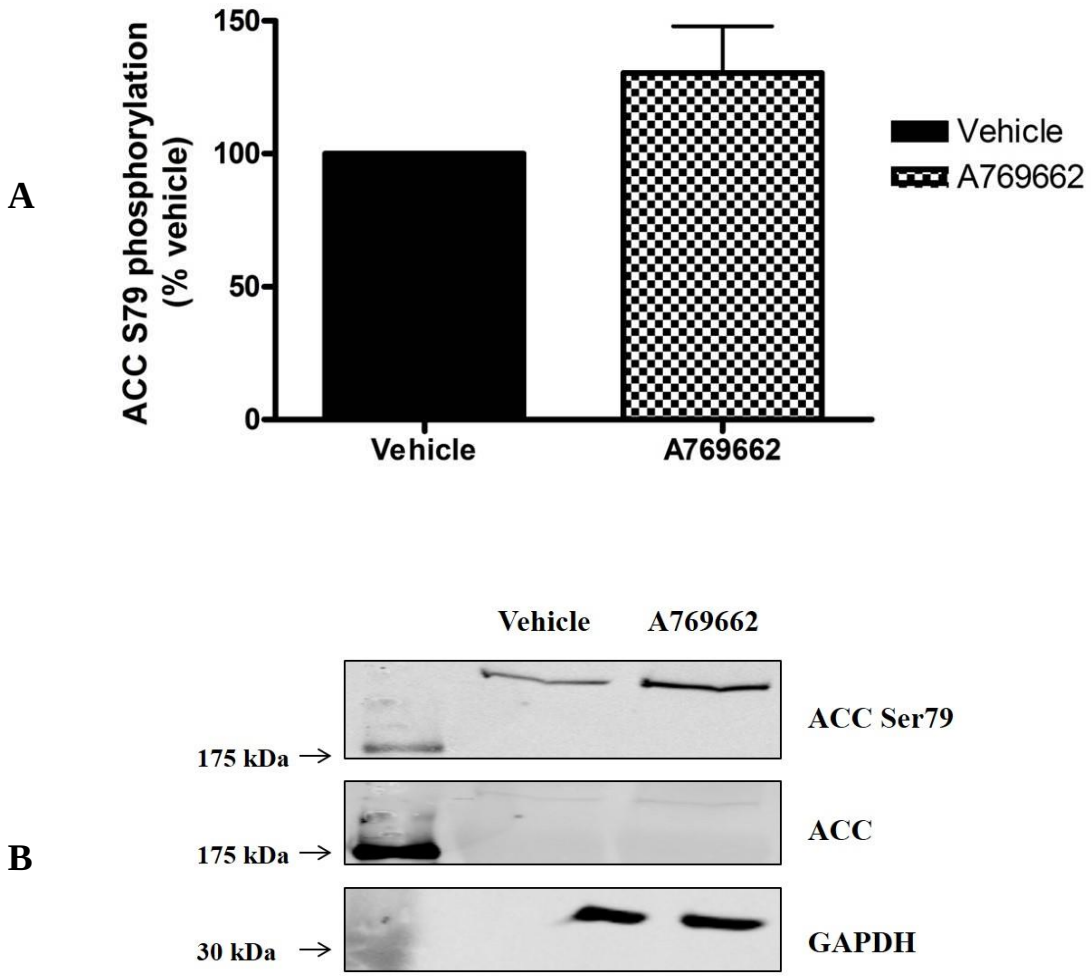

Figure 3-12: Effect of A769662 on AMPK activation in primary rat adipocytes

Adipocytes isolated from rat epididymal adipose tissue were incubated for 30 min with A769662 (300 μM) and lysates prepared. Lysates were resolved by SDS-PAGE and subjected to immunoblotting with the antibodies indicated. (A) Quantification of ACC Ser79 phosphorylation was determined by comparison with total ACC using densitometric analysis. Data shown represent the mean ± SEM % vehicle ACC phosphorylation of nine independent experiments. (B) Representative blot.

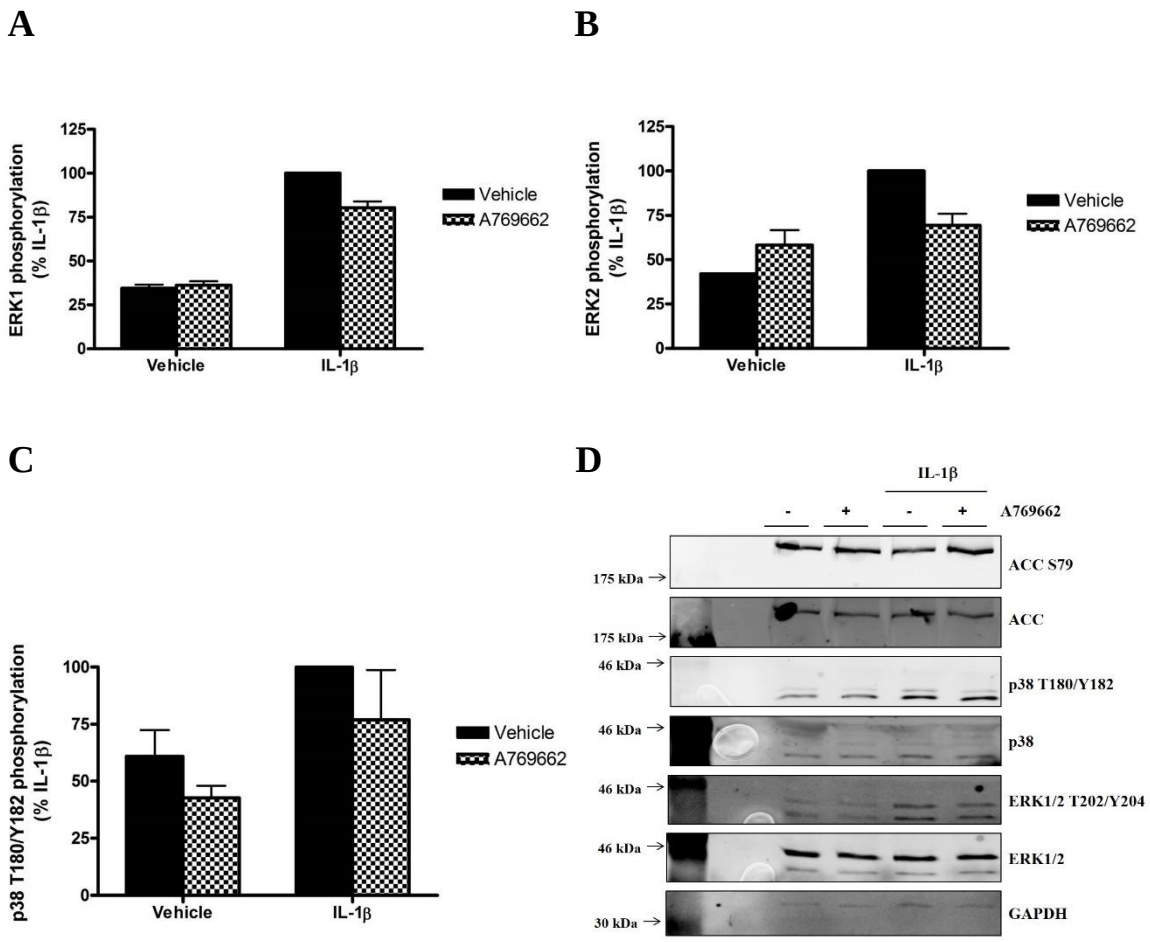

Figure 3-13: Effect of A769662 on IL-1β-stimulated ERK1/2 and p38 MAPK phosphorylation in rat adipocytes

Adipocytes isolated from rat epididymal adipose tissue were incubated with IL-1β (10 ng/ml) for 10 min following preincubation for 30 min in the presence or absence of A769662 (300 μM) and lysates prepared. Lysates were resolved by SDS-PAGE and subjected to immunoblotting with the antibodies indicated. (A & B) Quantification of ERK1 and ERK2 T202/Y204 phosphorylation respectively was determined by comparison with total ERK1/2 using densitometric analysis. Data shown represent the mean ± SEM % IL-1β-stimulated ERK1/2 phosphorylation of two independent experiments. (C) Quantification of p38 MAPK T180/Y182 phosphorylation was determined by comparison with total p38 MAPK using densitometric analysis. Data shown represent the mean ± SEM % IL-1β-stimulated p38 phosphorylation of three independent experiments. (D) Representative western blot.

A

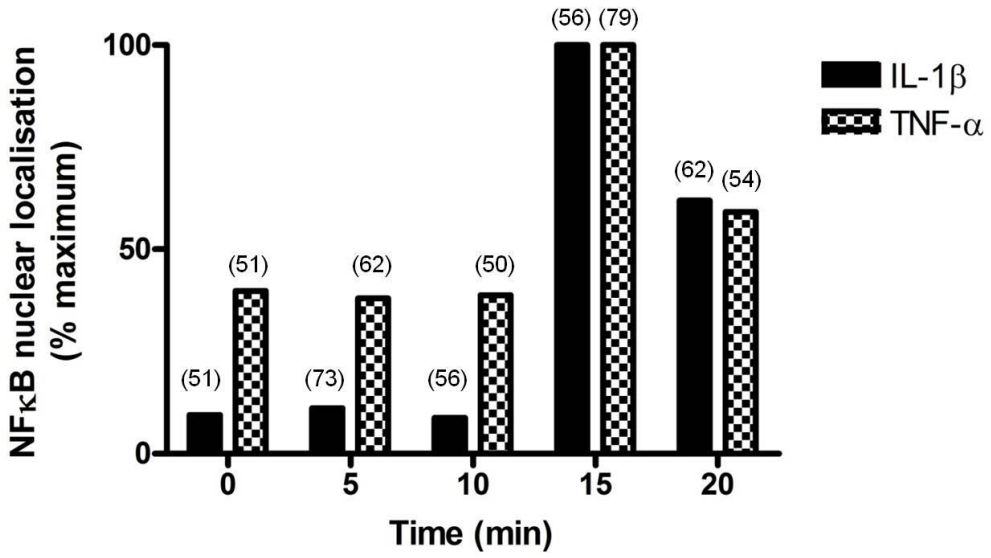

B

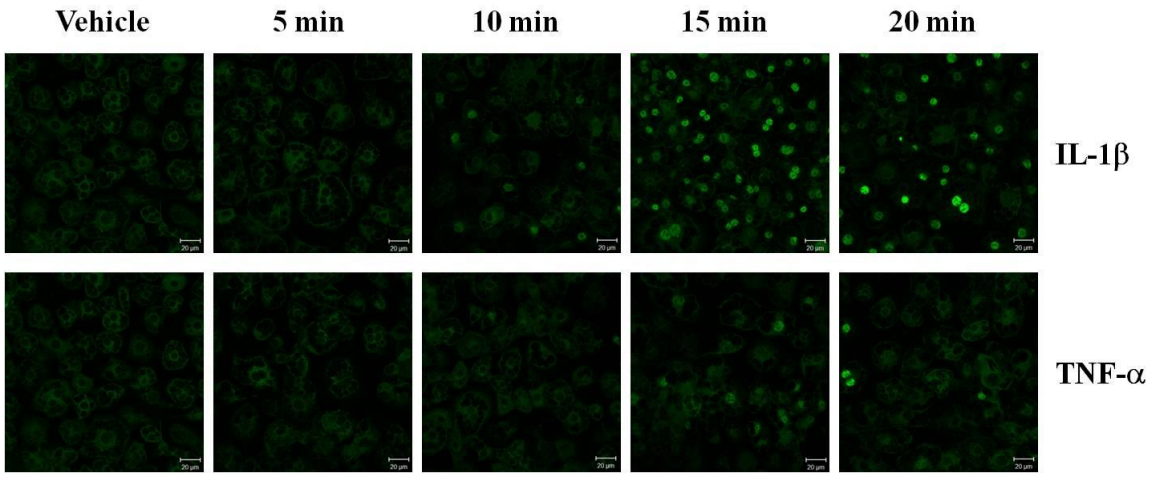

Figure 3-14: Temporal parameters of IL-1β and TNF-α - stimulated NFκB nuclear translocation in 3T3-L1 adipocytes

3T3-L1 adipocytes were incubated with IL-1β (10 ng/ml) or TNF-α (10 ng/ml) for various durations and stained for NFκB. Quantification of nuclear NFκB was determined by densitometric analysis of nuclear fluorescence. Data shown represent the % maximum IL-1β or TNF-α stimulated nuclear fluoresence, respectively, of a single experiment where a minimum of 50 cells were analysed for each treatment.

Incubation of 3T3-L1 adipocytes with IL-1β caused a significant ($p < 0.001$) increase, compared to the basal level, in translocation of NFκB to the nucleus (Fig. 3.15). A significant ($p < 0.001$) 68.4 ± 8.4 % inhibition of IL-1β-stimulated NFκB nuclear translocation was observed following preincubation with A769662 (Fig. 3.15).Similarly, incubation of 3T3-L1 adipocytes with TNF-α caused a significant ($p < 0.001$) increase, compared to the basal level, in NFκB nuclear translocation (Fig. 3.16). Preincubation with A769662 caused a more modest, but still statistically significant ($p < 0.05$) 33.3 ± 8.9 % inhibition of NFκB nuclear translocation compared to TNF-α treatment alone (Fig. 3.16).

3.2.6.3 Effect of a DN or CA AMPK mutant on A769662 – mediated inhibition of NFκB nuclear translocation

Adenovirus-mediated gene transfer was used to overexpress a dominant negative AMPK mutant (Ad.α1DN) or a constitutively active AMPK mutant (Ad.α1CA) in 3T3-L1 CAR adipocytes in order to investigate the effect of down- or up-regulation of AMPK on A769662 mediated inhibition of NFκB nuclear translocation.

IL-1β caused a 3.1 fold increase in nuclear translocation of NFκB in Ad.Null infected cells and a 2.5 fold increase in Ad.α1DN infected cells, relative to the basal level (Fig. 3.17). This was inhibited 3 fold in Ad.Null infected cells following preincubation with A769662 (Fig. 3.17). In contrast, preincubation with A769662 in Ad.α1DN infected cells caused a 1.3 fold increase in NFκB nuclear translocation relative to IL-1β treatment alone (Fig. 3.17).

Efficiency of Ad.α1DN viral infection was estimated to be approximately 60-70 %, as demonstrated by staining for the myc tag. Incubation with IL-1β caused a 2.5 and 1.22 fold stimulation of NFκB nuclear translocation in Ad.GFP and Ad.α1CA infected cells, respectively, relative to the basal level (Fig. 3.18). This corresponded to a 2 fold reduction in IL-1β-stimulated NFκB nuclear translocation in Ad.α1CA compared to Ad.GFP infected cells (Fig. 3.18). Efficiancy of Ad.α1CA viral infection was detected by the presence of GFP and estimated to be approximately 50 %.

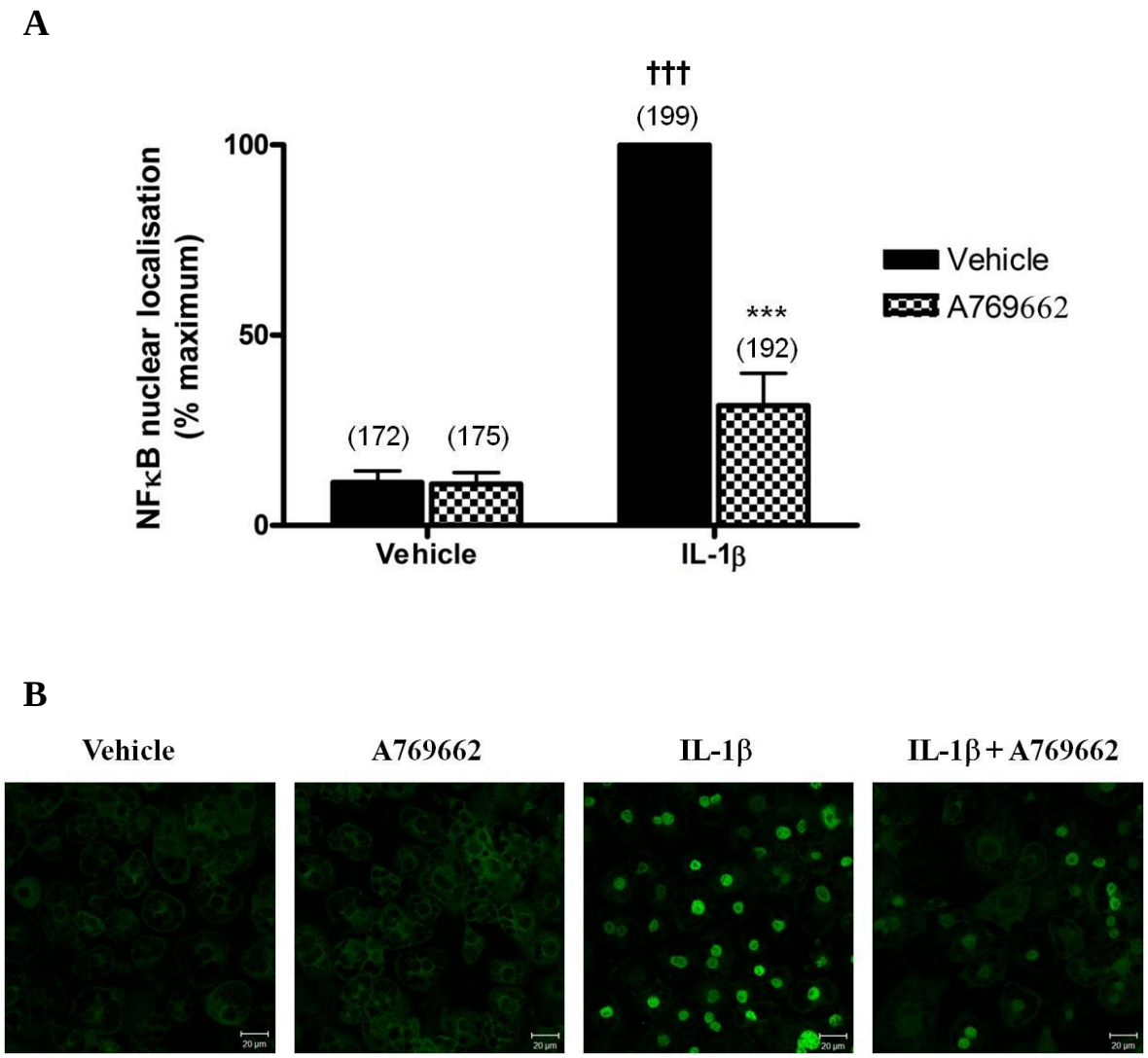

Figure 3-15: Effect of A769662 on IL-1β - stimulated NFκB nuclear translocation in 3T3-L1 adipocytes

*3T3-L1 adipocytes were incubated with IL-1β (10 ng/ml) for 15 min following preincubation for 30 min in the presence or absence of A769662 (300 μM) and stained for NFκB. (A) Quantification of nuclear NFκB was determined by densitometric analysis of nuclear fluorescence. Data shown represent the mean ± SEM % maximum nuclear fluorescence of three independent experiments with > 50 cells analysed for each treatment in each experiment. †††p < 0.001 (one-way ANOVA), increase in nuclear NFκB, relative to vehicle. ***p < 0.001 (one-way ANOVA), reduction in nuclear NFκB, relative to the absence of A769662. (B) Representative confocal images.*

A

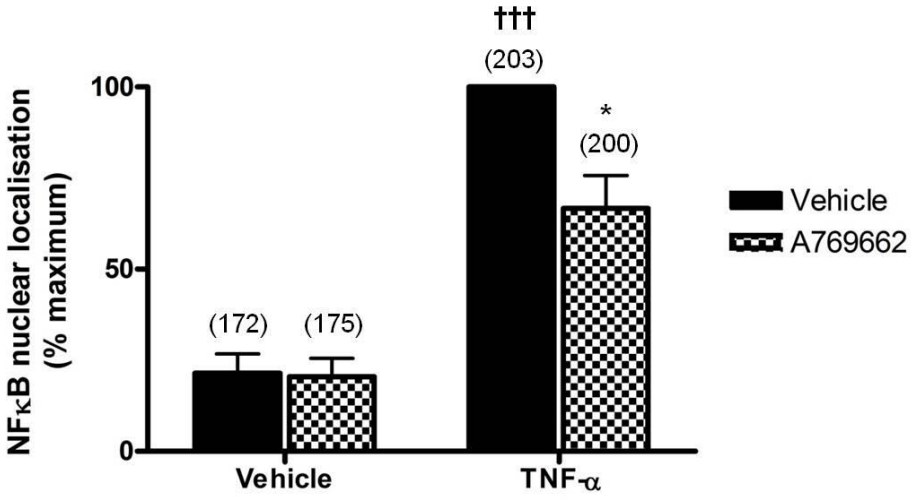

B

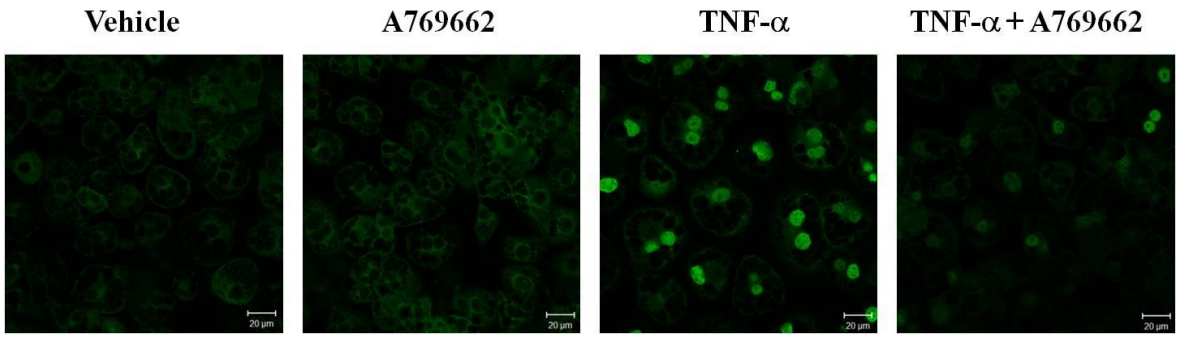

Figure 3-16: Effect of A769662 on TNF-α - stimulated NFκB nuclear translocation in 3T3-L1 adipocytes

*3T3-L1 adipocytes were incubated with TNF-α (10 ng/ml) for 15 min following preincubation for 30 min in the presence or absence of A769662 (300 μM) and fluorescently stained for NFκB. (A) Quantification of nuclear NFκB was determined by densitometric analysis of nuclear fluorescence. Data shown represent the mean ± SEM % maximum nuclear fluorescence of three independent experiments with > 50 cells analysed for each treatment in each experiment. †††p < 0.001 (one-way ANOVA), increase in nuclear NFκB, relative to vehicle. *p < 0.05 (one-way ANOVA), reduction in nuclear NFκB, relative to the absence of A769662. (B) Representative confocal images.*

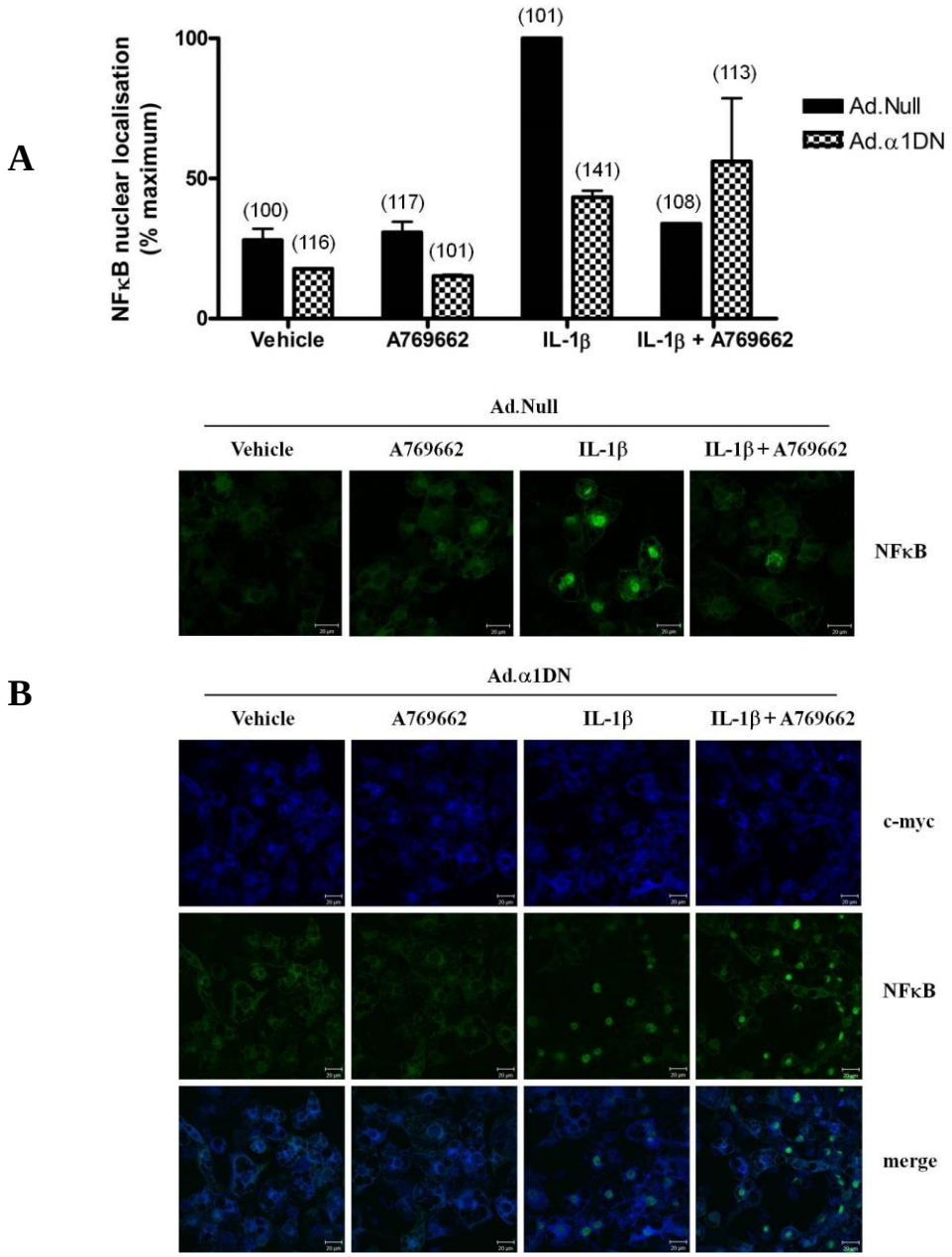

Figure 3-17: Effect of overexpression of a dominant negative AMPK mutant on IL-1β-stimulated NFκB nuclear translocation in 3T3-L1 CAR adipocytes

3T3-L1 CAR adipocytes were infected with (600 ifu/cell) Ad.α1DN or Ad.null for 48 h prior to stimulation for 15 min with IL-1β (10 ng/ml) following preincubation for 30 min in the presence or absence of A769662 (300 μM) and fluorescently stained for NFκB (green) and c-myc (blue). (A) Quantification of nuclear NFκB was determined by densitometric analysis of nuclear fluorescence. Data shown represent the mean ± SEM % maximum nuclear fluorescence of two independent experiments with > 50 cells analysed for each treatment in each experiment. (B) Representative confocal images (NFκB green, c-myc blue).

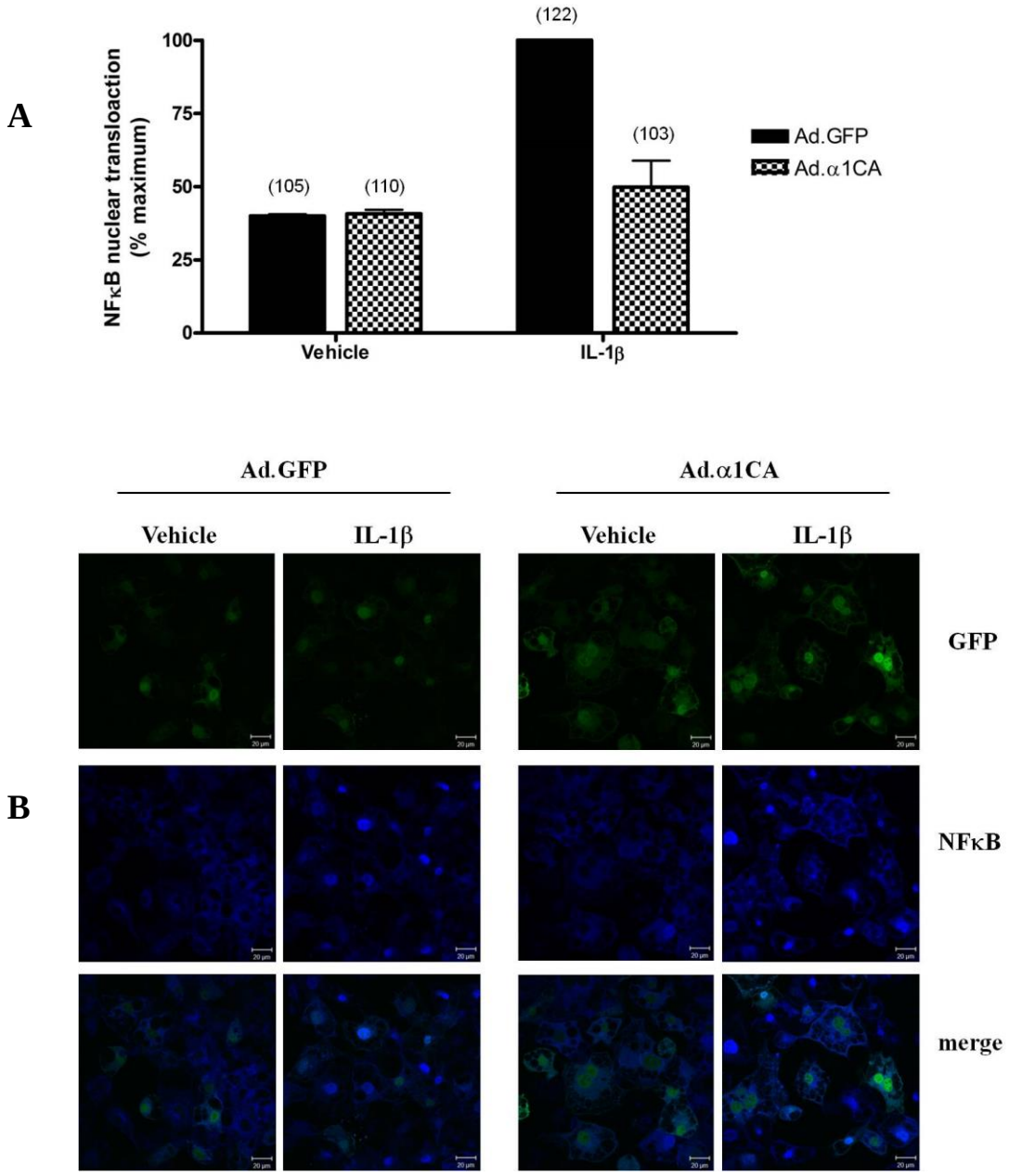

Figure 3-18: Effect of overexpression of a constitutively active AMPK mutant on IL-1β-stimulated NFκB nuclear translocation in 3T3-L1 CAR adipocytes

3T3-L1 CAR adipocytes were infected with (100 ifu/cell) Ad.α1CA or Ad.GFP for 48 h prior to stimulation for 15 min with IL-1β (10 ng/ml) following preincubation for 30 min in the presence or absence of A769662 (300 μM) and fluorescently stained for NFκB (blue). (A) Quantification of nuclear NFκB was determined by densitometric analysis of nuclear fluorescence. Data shown represent the mean ± SEM % maximum nuclear fluorescence of two independent experiments with > 50 cells analysed for each treatment in each experiment. (B) Representative confocal images (GFP green, NFκB blue).

3.2.7 Effect of AMPK activation by A769662 on TNF-α and IL-1β-stimulated NFκB pathway activation in 3T3-L1 adipocytes

In light of the AMPK-mediated inhibition of cytokine-stimulated NFκB nuclear translocation, NFκB pathway activation parameters in response to IL-1β or TNF-α in the presence or absence of A769662 were assessed in 3T3-L1 adipocytes. The extent of IκBα and NFκB phosphorylation was assessed as a measure of activation by western blotting using phosphorylation site-specific antibodies.

Incubation of 3T3-L1 adipocytes with IL-1β in the absence of A769662 caused a significant increase, compared to the basal level, in IκBα Ser32 phosphorylation after 3, 5, 10, 15, 30 and 60 min (Figure 3.19A). Statistically significant reductions in IκBα phosphorylation were observed at 3 ($p < 0.05$), 5 and 10 ($p < 0.001$) min in the presence of A769662 compared to IL-1β treatment alone (Fig. 3.19A). Furthermore, total IκBα protein levels were significantly diminished following 10 ($p < 0.05$), 15 and 30 ($p < 0.01$) min IL-1β treatment (Fig. 3.19B). A769662-mediated AMPK activation demonstrated a tendency to increase IκBα protein levels; however this did not reach significance (Fig. 3.19B). Incubation of 3T3-L1 adipocytes with TNF-α in the absence of A769662 caused a significant increase, compared to the basal level, in IκBα Ser32 phosphorylation after 3, 5 and 10 min ($p < 0.001$) and 15 min ($p < 0.05$) (Fig. 3.20A). Preincubation with A769662 caused significant reductions in IκBα Ser32 phosphorylation after 3 and 5 min ($p < 0.001$) and 10 min ($p < 0.01$), compared to TNF-α treatment alone (Fig. 3.20A). Incubation of 3T3-L1 adipocytes with IL-1β in the absence of A769662 caused a significant increase, compared to the basal level, in NFκB Ser536 phosphorylation after 3 ($p < 0.01$), 5 ($p < 0.001$), 10 ($p < 0.01$) and 15 ($p < 0.05$) min (Fig. 3.19C). Preincubation with A769662 caused a tendency to inhibit NFκB phosphorylation compared to IL-1β treatment alone; however this did not reach statistical significance (Fig. 3.19C). Incubation of 3T3-L1 adipocytes with TNF-α in the absence of A769662 caused a significant increase, compared to the basal level, in NFκB Ser536 phosphorylation after 3 min ($p < 0.01$), 5 and 10 min ($p < 0.001$), and 15 min ($p < 0.01$) (Fig. 3.20B). Preincubation with A769662 caused significant reductions after 3 and 5 min ($p < 0.05$) in NFκB phosphorylation, compared to TNF-α treatment alone (Fig. 3.20B).

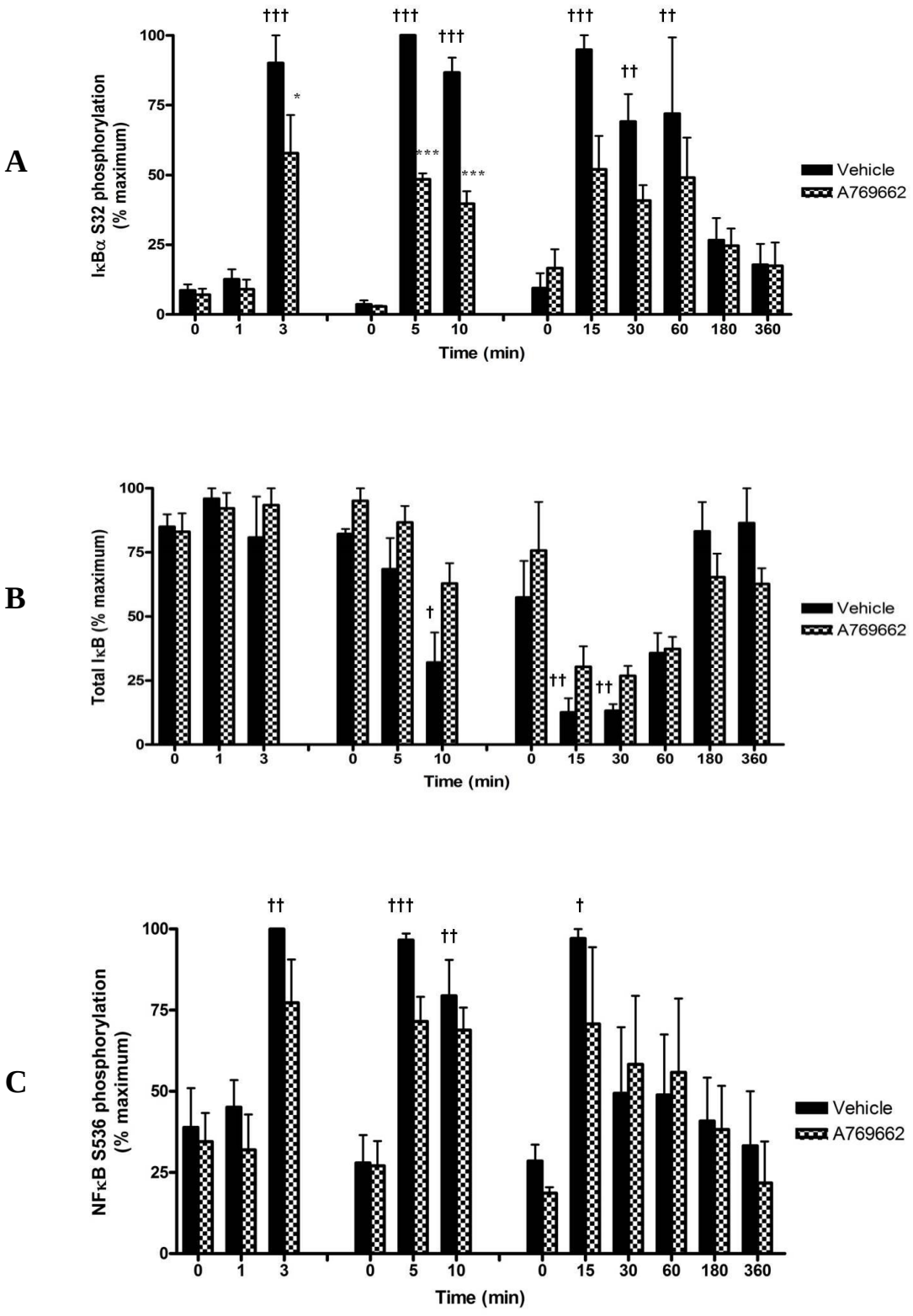

Figure 3-19: Effect of A769662 on IL-1β - stimulated IκBα and NFκB phosphorylation *(continued overleaf)*

D

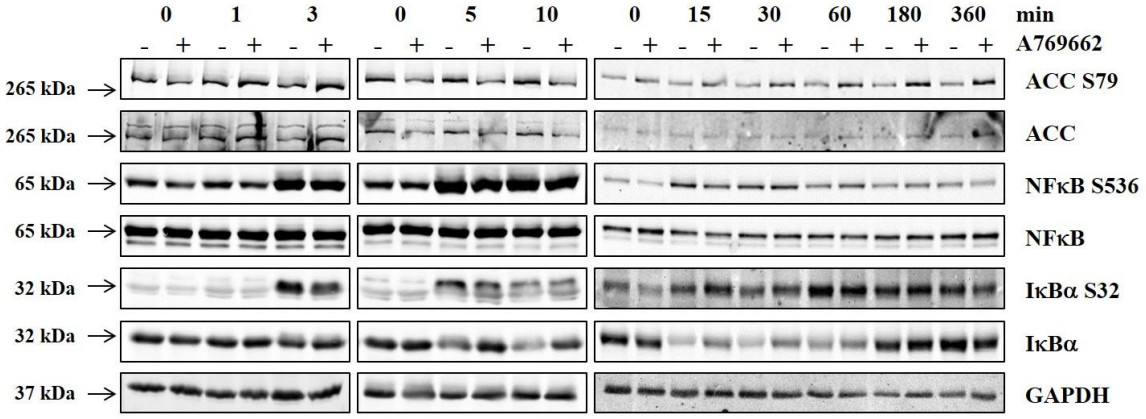

Figure 3-19: Effect of A769662 on IL-1β - stimulated IκBα and NFκB phosphorylation

3T3-L1 adipocytes were incubated with IL-1β (10 ng/ml) for various durations following preincubation for 30 min in the presence or absence of A769662 (300 μM) and lysates prepared. Lysates were resolved by SDS-PAGE and subjected to immunoblotting with the antibodies indicated. Data shown represent the mean ± SEM % maximum of three independent experiments. (A) Quantification of IκBα Ser32 phosphorylation was determined by comparison with total IκBα using densitometric analysis. $^{\dagger\dagger}p < 0.01$, $^{\dagger\dagger\dagger}p < 0.001$ (two-way ANOVA), increase in IκBα Ser32 phosphorylation, relative to vehicle. $^{*}p < 0.05$, $^{***}p < 0.001$ (two-way ANOVA), reduction in IκBα Ser32 phosphorylation, relative to the absence of A769662. (B) Quantification of total IκBα was determined by comparison with GAPDH using densitometric analysis. $^{\dagger}p < 0.05$, $^{\dagger\dagger}p < 0.01$ (two-way ANOVA), reduction in IκBα expression, relative to vehicle. (C) Quantification of NFκB Ser536 phosphorylation was determined by comparison with total NFκB using densitometric analysis. $^{\dagger}p < 0.05$, $^{\dagger\dagger}p < 0.01$, $^{\dagger\dagger\dagger}p < 0.001$ (two-way ANOVA), increase in NFκB Ser536 phosphorylation, relative to vehicle. (D) Representative western blot.

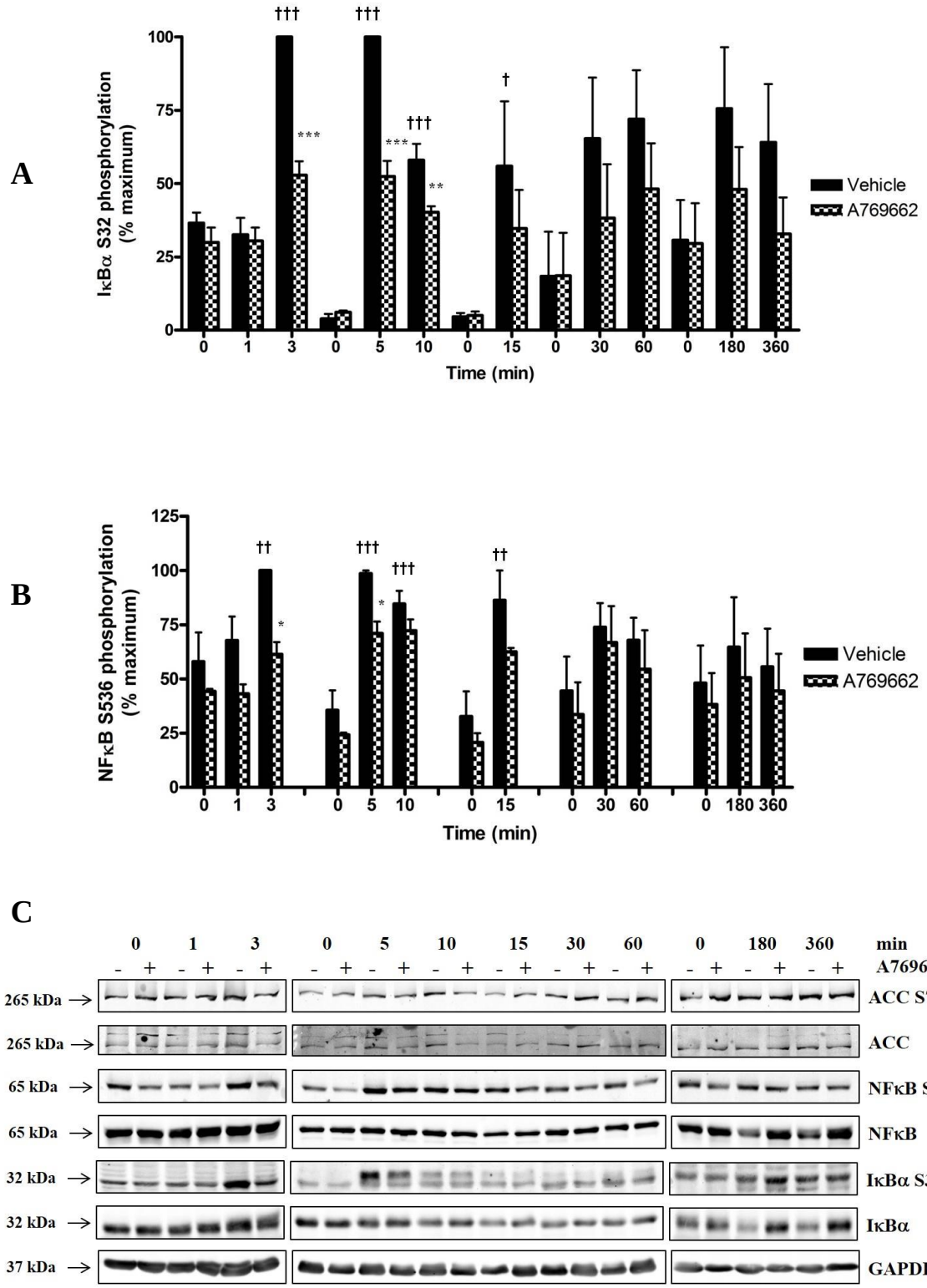

Figure 3-20: Effect of A769662 on TNF-α - stimulated IκBα and NFκB phosphorylation *(legend overleaf)*

Figure 3-20: Effect of A769662 on TNF-α - stimulated IκBα and NFκB phosphorylation

3T3-L1 adipocytes were incubated with IL-1β (10 ng/ml) for various durations following preincubation for 30 min in the presence or absence of A769662 (300 μM) and lysates prepared. Lysates were resolved by SDS-PAGE and subjected to immunoblotting with the antibodies indicated. Data shown represent the mean ± SEM % maximum of three independent experiments (A) Quantification of IκBα Ser32 phosphorylation was determined by comparison with total IκBα using densitometric analysis. $^{\dagger}p < 0.05$, $^{\dagger\dagger\dagger}p < 0.001$ (two-way ANOVA), increase in IκBα Ser32 phosphorylation, relative to vehicle. $^{**}p < 0.01$, $^{***}p < 0.001$ (two-way ANOVA), reduction in IκBα Ser32 phosphorylation, relative to the absence of A769662. (B) Quantification of NFκB Ser536 phosphorylation was determined by comparison with total NFκB using densitometric analysis. $^{\dagger\dagger}p < 0.01$, $^{\dagger\dagger\dagger}p < 0.001$ (two-way ANOVA), increase in NFκB Ser536 phosphorylation, relative to vehicle. $^{*}p < 0.05$ (two-way ANOVA), reduction in NFκB Ser536 phosphorylation, relative to the absence of A769662 (C) Representative western blot.

3.2.8 Investigating the mechanism of AMPK-mediated inhibition of IL-1β/TNF-α signalling

3.2.8.1 Effect of L-NAME on AMPK-mediated inhibition of IL-1β/TNF-α signalling

AMPK has been reported to stimulate the phosphorylation and activation of eNOS (Morrow et al. 2003), therefore it was of interest to determine whether the effects of AMPK on the MAPK signalling pathway are sensitive to eNOS inhibition by L-NAME, with the inactive isomer D-NAME utilised as a control.

IL-1β stimulated a significant ($p < 0.001$) increase in p38 T180/Y182 phosphorylation (Fig. 3.21A) in the presence of either L-NAME or D-NAME compared to the basal level. Preincubation with A769662 caused a significant ($p < 0.01$) 24 ± 1.5 % and 24.1 ± 3 % inhibition of p38 MAPK phosphorylation in D-NAME and L-NAME – treated cells, respectively, compared to IL-1β treatment alone (Fig. 3.21A). Incubation with TNF-α was also found to cause a significant ($p < 0.001$) increase in p38 MAPK phosphorylation in the presence of either L-NAME or D-NAME compared to the basal level (Fig. 3.21B). Preincubation with A769662 caused a significant ($p < 0.05$) 30.2 ± 4.6 % inhibition of p38 MAPK phosphorylation in L-NAME – treated cells compared to TNF-α stimulation alone; however no such inhibition was observed with A769662 preincubation in cells incubated with D-NAME, compared to TNF-α treatment alone (Fig. 3.21B).

IL-1β stimulated a significant ($p < 0.001$) increase in ERK1/2 T202/Y204 phosphorylation (Fig. 3.21C/D) in the presence of either L-NAME or D-NAME, compared to the basal level. Preincubation with A769662 caused a significant ($p < 0.001$) 54 ± 13.7 % and 47.6 ± 3.4 % inhibition of ERK1 phosphorylation (Fig. 3.21C) and 58.1 ± 7.6 % and 49.7 ± 9.2 % inhibition of ERK2 phosphorylation in D-NAME and L-NAME – treated cells respectively, compared to treatment with IL-1β alone (Fig. 3.21D). Incubation with TNF-α was also found to cause a significant ($p < 0.01$) increase in ERK1/2 T202/Y204 phosphorylation in the presence of either D-NAME or L-NAME, respectively, compared to the basal level (Fig. 3.21E/F). Preincubation with A769662 caused a 45.2 ± 17.5 % and 13.6 ± 14.4 % reduction in

ERK1 phosphorylation and 24.1 ± 17.8 % and 29.3 ± 9.9 % reduction in ERK2 phosphorylation in D-NAME and L-NAME – treated cells, respectively, compared to TNF-α treatment alone; however this was not statistically significant (Fig. 3.21E/F).

3.2.8.2 Investigating effect of AMPK on IKK activation

Data thus far demonstrate AMPK inhibits the NFκB signalling pathway as far upstream as IκBα (as demonstrated by inhibition of IκBα phosphorylation, Fig. 3.19 and 3.20). It was of interest, therefore, to investigate the effect of AMPK on upstream IKK activation.

Incubation of 3T3-L1 adipocytes with IL-1β in the absence of A769662 caused a significant ($p < 0.001$) increase, compared to the basal level, in IKKα/β Ser176/177 phosphorylation after 3 and 15 min. A modest, but significant ($p < 0.05$) increase was still observed after 30 min IL-1β treatment (Fig. 3.22). Statistically significant reductions in IKKα/β phosphorylation were observed at 3 min ($p < 0.01$) and 15 min ($p < 0.01$) in the presence of A769662 compared to IL-1β treatment alone (Fig. 3.22). IKKα/β expression/phosphorylation was undetectable in TNF-α-treated lysates (data not shown). In order to determine whether a potential interaction may occur between AMPK and IKK, AMPK or IKKβ was immunoprecipitated from 3T3-L1 adipocyte lysates that had been incubated with IL-1β in the presence or absence of A769662 in order to determine whether AMPK activation induced a detectable interaction with cytokine-stimulated IKKβ. As shown in Fig. 3.23, IKKβ was successfully immunoprecipitated from lysates, with no observable levels found in the immunodeplete. AMPK was detected in the IKKβ immunoprecipitate only when cells were incubated with A769662 compared to the basal level, however AMPK was not found to be present in the immunodeplete of lysates under any condition. In this preliminary experiment there was found to be only a modest immunoprecipitation of AMPK from the aforementioned lysates, while there was none present in the immunodeplete (Fig. 3.23). IKKβ was undetectable in the AMPK immunoprecipitate; however it was absent in the immunodeplete.

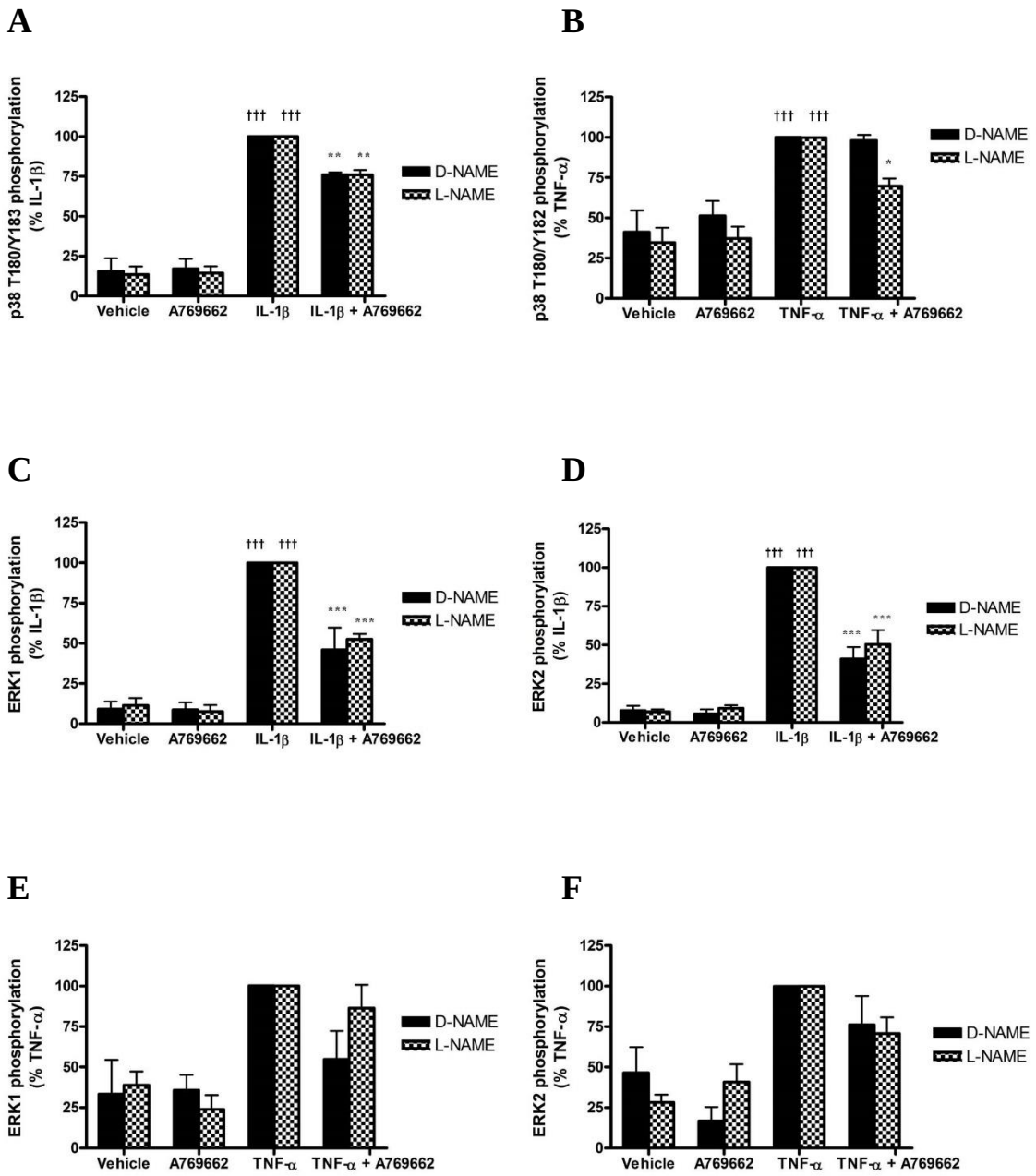

Figure 3-21: Effect of eNOS inhibition by L-NAME on AMPK-mediated inhibition of IL-1β or TNF-α-stimulated ERK1/2 and p38 MAPK phosphorylation *(continued overleaf)*

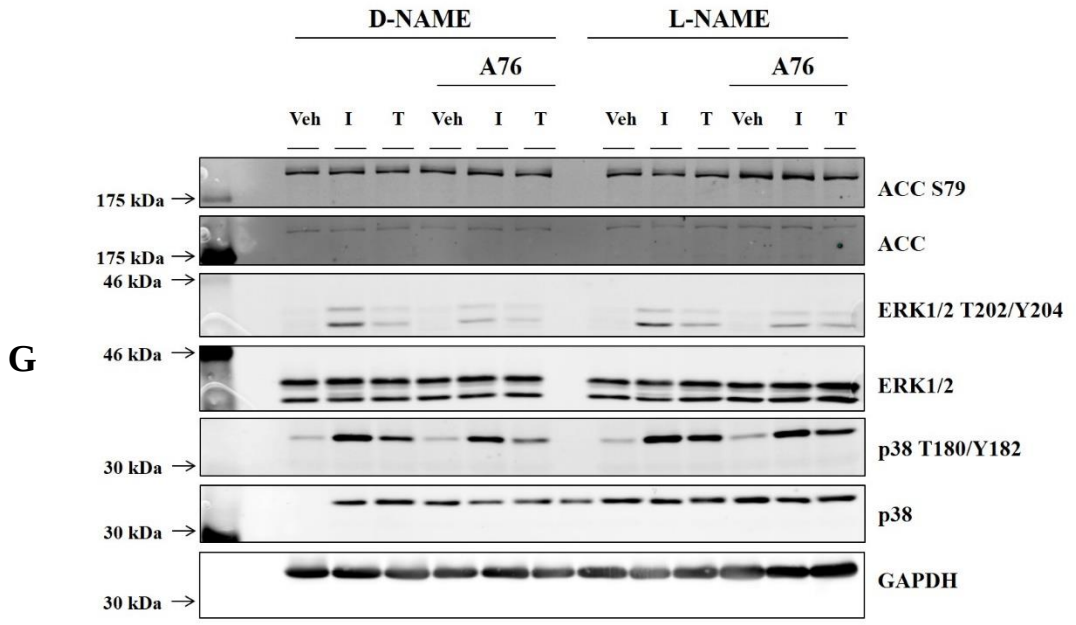

G

Figure 3-21: Effect of eNOS inhibition by L-NAME on AMPK-mediated inhibition of IL-1β-stimulated ERK1/2 and p38 MAPK phosphorylation

3T3-L1 cells were incubated with IL-1β (10 ng/ml) or TNF-α (10 ng/ml) for 15 min following preincubation for 30 min in the presence or absence of A769662 (300 μM) and 2 h in the presence or absence of L-NAME (1 mM) and lysates prepared. Lysates were resolved by SDS-PAGE and subjected to immunoblotting with the antibodies indicated. Quantification of p38 MAPK T180/Y182 and ERK1/2 T202/Y204 phosphorylation was determined by comparison with p38 MAPK and ERK1/2, respectively, using densitometric analysis. (A & B) Data shown represent the mean ± SEM % IL-1β or TNF-α stimulated of three independent experiments. $^{\dagger\dagger\dagger}p < 0.001$ (one-way ANOVA), increase in p38 MAPK T180/Y182 phosphorylation, relative to respective vehicle. $^{**}p < 0.01$, $^{*}p < 0.05$ (one-way ANOVA), reduction in p38 MAPK T180/Y182 phosphorylation, relative to respective absence of A769662. (C & D) ERK1 and ERK2, respectively. Data shown represent the mean ± SEM % IL-1β stimulated of three independent experiments. $^{\dagger\dagger\dagger}p < 0.001$ (one-way ANOVA), increase in ERK1/2 T202/Y204 phosphorylation, relative to respective vehicle. $^{***}p < 0.001$ (one-way ANOVA), reduction in ERK1/2 T202/Y204 phosphorylation, relative to respective absence of A769662. (E & F) ERK1 and ERK2, respectively. Data shown represent the mean ± SEM % TNF-α stimulated of two independent experiments. (G) Representative blot.

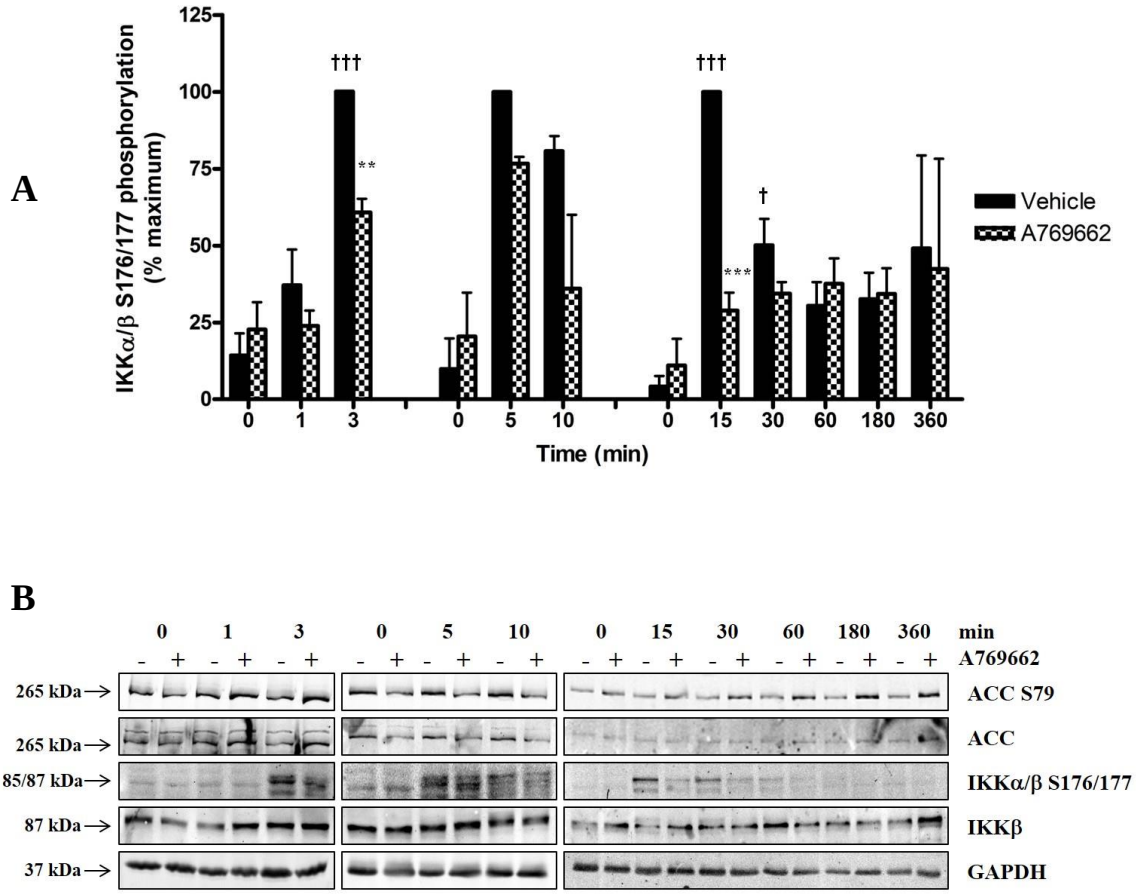

Figure 3-22: Effect of A769662 on IL-1β - stimulated IKKα/β phosphorylation

*3T3-L1 cells were incubated with IL-1β (10 ng/ml) for various durations following preincubation for 30 min in the presence or absence of A769662 (300 μM) and lysates prepared. Lysates were resolved by SDS-PAGE and subjected to immunoblotting with the antibodies indicated. (A) Quantification of IKKα/β Ser176/177 phosphorylation was determined by comparison with total IKKβ using densitometric analysis. Data shown represent the mean ± SEM % maximum IKKα/β phosphorylation of three independent experiments. †p < 0.05, †††p < 0.001 (two-way ANOVA), increase in IKKα/β S176/177 phosphorylation, relative to vehicle. **p < 0.01, ***p < 0.001 (two-way ANOVA), reduction in IKKα/β S176/177 phosphorylation, relative to absence of A769662. (B) Representative western blot.*

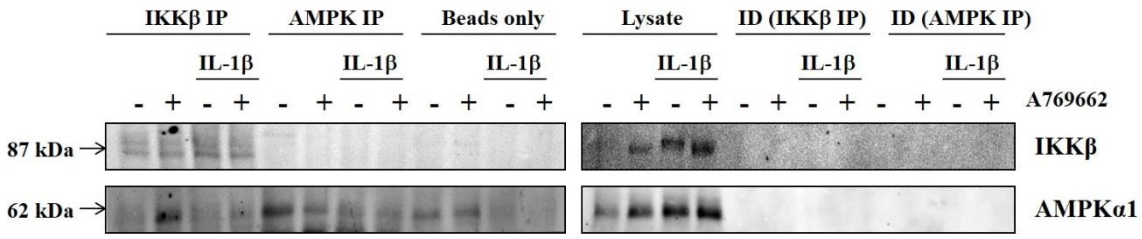

Figure 3-23: Effect of IL-1β and A769662 on IKKβ and AMPK interaction

Total AMPKα1 and α2 and IKKβ were immunoprecipitated with a mixture of AMPKα1 and α2 and IKKβ antibodies, respectively, from 3T3-L1 lysates (80-200 μg) obtained from cells incubated with IL-1β (10 ng/ml) for 15 min following 30 min preincubation with A769662 (300 μM). Immunoprecipitates were resolved on 7% SDS-PAGE, transferred to nitrocellulose and probed with anti-IKKβ and anti-AMPKα antibodies. Western blot from a single experiment. ID, immunodeplete; IP, immunoprecipitate.

3.3 Discussion

The key findings of this chapter are that AMPK activation in adipocytes inhibited both IL-1β and TNF-α - stimulated phosphorylation of MAPK and NFκB signalling pathway intermediates. Furthermore, NFκB nuclear translocation was attenuated in an AMPK-dependent manner as demonstrated by the utilisation of AMPK adenoviruses. The mechanism by which AMPK elicits these anti-inflammatory effects in adipocytes is unlikely to be mediated by eNOS, but does occur upstream of or directly at the level of IKK and MAP kinases p38, ERK and JNK.

Initial studies were undertaken to investigate activation of AMPK in adipocytes. This study found that A769662 significantly ($p < 0.05$) stimulated AMPK Thr172 phosphorylation in 3T3-L1 adipocytes (Fig. 3.1A), which supports previous studies reporting stimulation of AMPK activity in 3T3-L1 adipocytes by A769662 (Zhou, Wang, et al. 2009). Furthermore, Fig. 3.1A shows A769662-mediated AMPK Thr172 phosphorylation is significantly ($p < 0.001$) ablated in the presence of the AMPK inhibitor Compound C, which acts by competing for ATP. It is important to note, however, that Compound C is not specific for AMPK, therefore data generated using Compound C should be interpreted with care. Bain and co-workers found that it also inhibits several other protein kinases *in vitro* including ERK 8, MAPK-interacting-kinase 1 (MNK1), phosphorylase kinase (PHK), dual specificity tyrosine phosphorylation and regulated kinase (DYRK) isoforms, homeodomain-interacting protein kinase 2 (HIPK2), sarcoma kinase (Src), and lymphocyte cell-specific protein-tyrosine kinase (Lck) (Bain et al. 2007).

In order to investigate whether the ability of A769662 to stimulate AMPK activation could be recapitulated in primary cells, adipocytes were isolated from rat epididymal adipose tissue. AMPK activity was assessed as a measure of phosphorylation of the AMPK target protein acetyl CoA carboxylase (ACC), at Ser79. There are a number of lines of evidence demonstrating that AICAR stimulates an increase in AMPK activation in rat primary adipocytes (Daval et al. 2005, Gaidhu et al. 2010, Sullivan et al. 1994), however the effect of A769662 has, to our knowledge, not been examined. The current study found that A769662 appeared to induce a small increase in ACC Ser79 phosphorylation in rat adipocytes; however this did not reach significance (Fig. 3.12). It is possible that

a high degree of basal AMPK activation or variability between animals could account for the modest effect of A769662 in this study; alternatively, A769662 may not be particularly effective in primary adipocytes.

A small number of studies have suggested that AMPK activation can be modulated by proinflammatory cytokines including TNF-α in certain cells. The reports are conflicting, with TNF-α shown to activate AMPK in endothelial and kidney cell lines (Tang et al. 2010), while it has been demonstrated to be inhibitory in myotubes and muscle (Steinberg et al. 2006). To our knowledge, the effect of TNF-α on AMPK activation in adipocytes has not previously been assessed. This study found that in 3T3-L1 adipocytes TNF-α had no effect on AMPK Thr172 phosphorylation when data were normalised to A769662 (Fig. 3.1A); interestingly, however, TNF-α significantly ($p < 0.01$) reduced AMPK Thr172 phosphorylation compared to the basal level when data were normalised to vehicle (Fig. 3.1B). An inhibition of AMPK Thr172 phosphorylation by TNF-α could be the result of an increase in protein phosphatase 2C (PP2C) which dephosphorylates AMPK Thr172. Indeed, Steinberg and co-workers reported the TNF-α-mediated suppression of AMPK activity via transcriptional upregulation of PP2C in cultured skeletal muscle cells (Steinberg et al. 2006).

AMPK and MAPK

Proinflammatory cytokines TNF-α and IL-1β have been found to be upregulated in obese adipose tissue (Guilherme et al. 2008, Schenk, Saberi, and Olefsky 2008). In this study the temporal activation of components of the TNF-α/IL-1β - stimulated MAPK and NFκB pathways and their subsequent inhibition by AMPK was assessed in 3T3-L1 adipocytes.

Figures 3.2 – 3.7 demonstrated that both IL-1β and TNF-α were found to acutely stimulate MAPK signalling in 3T3-L1 adipocytes, with phosphorylation of ERK1/2 and p38 MAPK signalling intermediates peaking within 15 min of cytokine stimulation (Fig. 3.2 – 3.5). Furthermore, p38 and ERK1/2 MAPK appeared to undergo biphasic activation in response to TNF-α, with the disappearance of phosphorylation following 10-15 min cytokine stimulation which increased again after 6 h (Fig. 3.3 and 3.5). This is not unexpected; ERK1/2 and p38 MAPK have been reported to undergo biphasic activation in response to adenosine (Haq,

Clerk, and Sugden 1998) and oxidative stress (Jayakumar et al. 2006). In addition, IL-1β significantly ($p < 0.01$) stimulated phosphorylation of JNK (Fig. 3.6), while this did not reach significance in response to TNF-α due to a high degree of variability (Fig. 3.7). IL-1β appeared to be a more potent activator of the MAPK pathways than TNF-α, which correlates with recent data suggesting that IL-1β may be more relevant than TNF-α in terms of adipose tissue inflammation (Wieser, Moschen, and Tilg 2013). Activation of AMPK with A769662 significantly reduced IL-1β-stimulated p38 MAPK, ERK1/2 and JNK phosphorylation (Fig. 3.2, 3.4 and 3.6). Similarly, A769662 significantly inhibited TNF-α - stimulated p38 and ERK1/2 MAPK phosphorylation (Fig. 3.3 and 3.5), with a tendency to inhibit JNK activation (Fig. 3.7). These data support the few studies to date investigating the effect of AMPK on cytokine-stimulated MAPK phosphorylation and activation. Elevated JNK phosphorylation has been reported in macrophages of *AMPKβ1*$^{-/-}$ mice (Galic et al. 2011), and endothelial cells of mice deficient in AMPKα2 (Dong et al. 2010). Similarly, LPS-stimulated JNK, ERK1/2 and p38 MAPK phosphorylation was found to be reduced by berberine in an AMPK-dependent manner in macrophages (Jeong et al. 2009). To our knowledge, inhibition of cytokine-stimulated MAPK activation by AMPK in adipocytes had not been explored prior to this study.

Interestingly, while the finding that AMPK inhibited p38 MAPK phosphorylation in this study fits with the anti-inflammatory paradigm, it contradicts some published studies which suggest that AMPK may in fact activate p38 MAPK phosphorylation (Li et al. 2005, Xi, Han, and Zhang 2001). In contrast, Jacquet and co-workers found that while AMPK and p38 activation were temporally related in myocardial ischemia, p38 MAPK activation was independent of AMPK (Jacquet et al. 2007). Thus, it is possible that cell-type specific mechanisms may exist.

The effect of A769662 on IL-1β-stimulated ERK1/2 and p38 MAPK was also assessed in primary adipocytes isolated from rat epididymal adipose tissue. It can be seen in Fig. 3.13B/C that there appeared to be a tendency for A769662 to suppress IL-1β-stimulated ERK1/2 phosphorylation in isolated rat adipocytes. While A769662-mediated AMPK activation did not significantly reduce IL-1β-stimulated p38 MAPK phosphorylation (Fig. 3.13A), there did appear to be a subtle reduction. This marginal effect of A769662 on inhibition of MAPK phosphorylation is likely to relate to the very modest stimulation of AMPK activation in isolated adipocytes (Fig.

3.12). This study was carried out in a small number of independent experiments due to availability; therefore it is possible that more convincing data could be generated with a greater number of animals.

It was of importance to ascertain whether the inhibition of proinflammatory signalling could be directly attributed to AMPK, therefore the pharmacological AMPK inhibitor Compound C and adenoviruses to up- or downregulate AMPK were utilised. While Compound C showed a slight tendency to suppress A769662-mediated inhibition of p38 phosphorylation in 3T3-L1 adipocytes (Fig. 3.8), a significant degree of variability was observed across experimental replicates. Furthermore, Compound C was not found to significantly suppress A769662-mediated AMPK activation within these experimental replicates (data not shown); thus it is not feasible to draw any conclusions from these data. Adenoviruses overexpressing a dominant negative (Ad.α1DN) or constitutively active (Ad.α1CA) AMPK were also used to investigate whether the effect of A769662 on proinflammatory signalling in 3T3-L1 adipocytes is mediated by AMPK activation (Fig. 3.9). Differentiated adipocytes are relatively genetically intractable due to the abundance of lipid droplets and lack of CAR receptors required for adenoviral entry into the cell. To address this, 3T3-L1 adipocytes overexpressing the CAR receptor were utilised (Ross et al. 2003). Fig. 3.9A shows that A769662 failed to stimulate ACC Ser79 phosphorylation in cells infected with Ad.α1DN or Ad.Null control infected cells, indicating that A769662 failed to produce the expected effect. Similarly, there was no significant increase in ACC Ser79 phosphorylation in cells infected with Ad.α1CA virus compared to the Ad.GFP control (Fig. 3.9C). These data demonstrate that viral transfection in these experiments was likely to have been insufficient to manipulate AMPK activity as assessed in whole cell lysates, as implied by the lack of ACC Ser79 phosphorylation in Ad.α1CA infected cells. AMPK adenoviruses and Compound C have been successfully utilised in other cell lines to demonstrate AMPK-dependent inhibition of proinflammatory signalling. A study by Jeong and co-workers reported that inhibition or downregulation of AMPK with Compound C or Ad.α1DN infection, respectively, ablated berberine-mediated inhibition of proinflammatory gene expression in macrophages (Jeong et al. 2009). Taken together, this study was unable to show in whole cell lysates that the inhibition of cytokine-stimulated MAPK phosphorylation by A769662 was dependent upon AMPK activation, as not only did

A769662 fail to activate AMPK in control Ad.Null-infected cells, but AMPK activation in Ad.α1CA infected cells could not be convincingly demonstrated. No conclusions regarding the extent of MAPK phosphorylation could therefore be drawn from these experiments.

Nitric oxide has been reported to attenuate proinflammatory signalling via the S-nitrosylation of p65 and subsequent inhibition of NFκB DNA binding (Kelleher et al. 2007). AMPK has been reported to phosphorylate and activate endothelial nitric oxide synthase (eNOS) (Morrow et al. 2003), thereby providing a possible mechanism by which AMPK could inhibit proinflammatory signalling pathway activation. Expression of eNOS in 3T3-L1 adipocytes has been reported (Tanaka et al. 2003) and its activity can be inhibited using L-NAME. As Fig. 3.21A and 3.21C/D demonstrated, statistically significant inhibition of IL-1β-stimulate p38 MAPK ($p < 0.01$) or ERK1/2 ($p < 0.001$) phosphorylation by A769662 was not affected by inhibition of eNOS with L-NAME. TNF-α treatment induced a clear increase in ERK1/2 phosphorylation, which was modestly reduced following A769662 preincubation in both L-NAME and D-NAME-treated cells (Fig.3.21E/F). Curiously, while TNF-α significantly stimulated p38 MAPK phosphorylation, A769662-mediated AMPK activation appeared to significantly reduce TNF-α-stimulated p38 MAPK phosphorylation in L-NAME, but not D-NAME control treated cells (Fig. 3.21B). This is likely to be a result of very faint bands compared to those observed with IL-1β treatment, and proved difficult to analyse. Overall, these data indicate that AMPK-mediated inhibition of MAPK signalling is likely to be independent of NO production. It should be noted that positive controls were lacking in these experiments; nitrotyrosine, which is an indicator of NO production, was undetectable in lysates (data not shown). These data support the findings of Bess and co-workers, who reported that AMPK activation was sufficient to inhibit TNF-α-stimulated phosphorylation of IκBα and NFκB p65 in COS-7 cells which do not express endogenous eNOS (Bess et al. 2011).

AMPK and NFκB

The current study investigated the effect of AMPK on the cytokine-stimulated translocation of proinflammatory transcription factor NFκB to the nucleus. An initial time course revealed that both TNF-α and IL-1β-induced nuclear translocation of NFκB in 3T3-L1 adipocytes occurred following 15 min cytokine

treatment (Fig. 3.14), with IL-1β being the more potent activator. A769662 significantly reduced IL-1β ($p < 0.001$) and TNF-α ($p < 0.05$) – stimulated NFκB nuclear localisation (Fig. 3.15 and 3.16, respectively). In order to establish AMPK dependency, IL-1β-stimulated NFκB nuclear translocation was examined using DN or CA AMPK adenoviruses. The Ad.α1DN and Ad.α1CA viruses were myc and GFP-tagged, respectively; thereby providing a means to identify successfully infected cells for analysis and the efficiency of the viral infection (approximately 60-70% and 50%, respectively). It is clear from Fig. 3.17 that A769662 effectively reduced IL-1β-stimulated NFκB nuclear translocation in cells infected with Ad.Null, but crucially, had no effect in Ad.α1DN infected cells. IL-1β did not appear to stimulate NFκB nuclear translocation in Ad.α1DN infected cells to the same extent as in Ad.Null infected cells. Likewise, Fig. 3.18 demonstrated a clear reduction in NFκB nuclear translocation in Ad.α1CA infected cells compared to the Ad.GFP infected control. Despite these data being generated from only two independent experiments, it is clear that, taken together with the results generated with A769662, AMPK activation inhibited cytokine-stimulated NFκB nuclear translocation in 3T3-L1 adipocytes. These data support previous findings that there was an increase in NFκB present in the nuclear fraction of endothelial cells deficient in AMPKα2 (Wang, Zhang, et al. 2010).

It was important to elucidate the effect of AMPK activation on signalling intermediates upstream of NFκB. IL-1β and TNF-α were shown to rapidly stimulate the IKK/IκBα/NFκB signalling pathway in 3T3-L1 adipocytes, with phosphorylation of IκBα peaking within 15 min of cytokine stimulation with a concomitant reduction in total protein levels. A769662-mediated AMPK activation caused a significant reduction in IκBα phosphorylation (Fig. 3.19A and 3.20A) and reduced total protein degradation (Fig. 3.19B), in line with NFκB nuclear localisation findings (Fig. 3.15 - 3.18). Furthermore, AMPK activation significantly ablated the rapidly induced IL-1β-stimulated IKKα/β phosphorylation (Fig. 3.22); however TNF-α-stimulated IKKα/β phosphorylation was undetectable (data not shown). It is unlikely that TNF-α was unable to induce IKKα/β phosphorylation, as activation of downstream components IκBα and NFκB were observed. Thus, it is more likely that it simply was not detected by the antibody. Activation of AMPK significantly reduced TNF-α-stimulated NFκB phosphorylation (Fig. 3.20B), and while there

appeared to be a tendency for A769662 to inhibit IL-1β-stimulated NFκB phosphorylation, this did not reach statistical significance ($p < 0.05$) (Fig. 3.19C). Recent studies have suggested a number of different mechanisms for the inhibition of NFκB signalling by AMPK. Firstly, it has been reported in COS-7 cells that hyperphosphorylation of IKKβ by constitutively active AMPK resulted in the inhibition of IκBα phosphorylation, NFκB p65 activation and subsequent NFκB-mediated gene transcription (Bess et al. 2011). In contrast, this study demonstrated AMPK acutely and significantly reduced IKK phosphorylation in 3T3-L1 adipocytes (Fig. 3.22). This observation supports recent studies reporting the AMPK-mediated inhibition of IKK phosphorylation in different cell types. Metformin or AICAR were reported to attenuate TNF-α-stimulated IKKα/β Ser180/181 phosphorylation in HUVECs in an AMPK-dependent manner (Huang et al. 2009), while A769662 was reported to reduce IKKα/β phosphorylation in myocytes from obese individuals with type 2 diabetes (Green et al. 2011). The current study also found that there may be a potential interaction between AMPK and IKKβ in 3T3-L1 adipocytes (Fig. 3.23), as a preliminary experiment suggested AMPK may co-immunoprecipitate with IKKβ following A769662 stimulation. The reverse (IKKβ co-immunoprecipitating with AMPK) was not observed; however there was no detectable IKKβ in the immunodeplete, which could potentially be a result of it being co-immunoprecipitated with AMPK but not being detected on the western blot. These data suggest it is possible IKKβ and AMPK could interact, which may indicate a potential mechanism; however this data has yet to be replicated care should be taken in interpreting the results. While AMPK has been reported to modulate IKK phosphorylation, it has not, to our knowledge, been found to physically interact with it.

Alternatively, it has been suggested that AMPK may inhibit DNA binding directly. Zhang and co-workers reported that in endothelial cells AMPK phosphorylates the transcriptional coactivator p300, blocking acetylation of p65 which is required for full transcriptional activation of NFκB; however, this report did not investigate the effect of AMPK activation upstream of NFκB (Zhang et al. 2011). Similarly, it has been reported that AMPK may inhibit NFκB-mediated gene transcription via activation of the deacetylase SIRT1 which was demonstrated to deacetylate Lys310 of p65, stimulating Ser9-mediated methylation of Lys314/315 (Yang, Tajkhorshid, and Chen 2010). This leads to the polyubiquitination and subsequent

proteasomal degradation of p65, thus ablating transcription of NFκB target genes. The rapid inhibition of IKK/IκBα/NFκB phosphorylation and NFκB nuclear translocation by AMPK observed in the current study suggests the existence of a more acute mechanism of inhibition occurring upstream of, or at the level of, IKK in adipocytes. Finally, AICAR-mediated AMPK activation had no effect on LPS-stimulated IκBα phosphorylation or degradation in either macrophages (Kuo et al. 2008) or mesangial cells (Peairs et al. 2009), which suggests that the mechanism by which AMPK inhibits cytokine-stimulated NFκB signalling may be cell-type specific.

Finally, to explore the importance of AMPK on the basal inflammatory status of adipose tissue, subcutaneous and gonadal depots were obtained from *AMPKα1*$^{-/-}$ and genetically matched wild-type mice. Basal phosphorylation of JNK was found to be significantly increased in both adipose depots from *AMPKα1*$^{-/-}$ mice compared to wild-type (Fig. 3.10A and 3.11A). This correlates with a study by Galic and co-workers, which reported elevated JNK phosphorylation in *AMPKβ1*$^{-/-}$ mouse macrophages in response to palmitate exposure (Galic et al. 2011). There was no significant difference in p38 MAPK phosphorylation between the phenotypes (Fig. 3.10B and 3.11B), although there did appear to be a tendency toward increased p38 MAPK phosphorylation in *AMPKα1*$^{-/-}$ adipose compared to wild-type (Fig. 3.10B and 3.11B). These are convincing data indicating an anti-inflammatory role of AMPK in adipose tissue, particularly as gonadal is a form of visceral adipose, which is central to the production of proinflammatory mediators in obesity (Gauthier et al. 2011). While the anti-inflammatory role of AMPK in adipose tissue has not previously been well characterised, these data correlate with a report suggesting that berberine reduced cytokine expression in adipose tissue of obese *db*/*db* mice; however the AMPK dependence of this was not confirmed (Jeong et al. 2009). Likewise, AICAR has been reported to inhibit TNF-α secretion in human subcutaneous adipose tissue cultured *ex vivo* (Lihn et al. 2004).

Overall, this current work demonstrates for the first time in adipocytes that AMPK suppresses cytokine-stimulated MAPK and NFκB signalling pathways and subsequent nuclear translocation of NFκB via a mechanism likely to be upstream of IKK and MAPKs and independent of NO production.

Chapter 4 - The effect of AMPK on IL-6-stimulated proinflammatory signalling

4.1 Introduction

4.1.1 IL-6 signalling via the JAK/STAT pathway

In most cell types, IL-6 initially forms a complex with a soluble receptor (sIL-6Rα) before binding to the signal-transducing gp130 receptor subunits, stimulating activation of JAK, which phosphorylates tyrosine residues on the cytoplasmic tails of gp130. These phospho-tyrosine residues function as docking sites for SH2-containing proteins including STAT proteins and SHP-2, which are subsequently phosphorylated by JAK (Heinrich et al. 1998). Phosphorylated STAT proteins dimerise and translocate to the nucleus where they regulate the transcription of target genes, including CRP (Zhang et al. 1996) and MCP-1 (Fasshauer, Klein, et al. 2004), which are involved in the inflammatory response. SHP-2 activation stimulates the ERK MAPK cascade (Fukada et al. 1996).

4.1.2 IL-6 inflammatory signalling in disease and regulation by AMPK

IL-6 is produced by multiple cell types including macrophages and adipocytes; indeed, increased concentrations are found to be secreted by WAT in obesity (Sopasakis et al. 2004, Gustafson 2010). Interestingly, it has been reported that IL-6 secretion is greater in visceral, rather than subcutaneous adipocytes (Fried, Bunkin, and Greenberg 1998). Furthermore, plasma concentrations of IL-6 are positively correlated with body mass and insulin resistance (Lee et al. 2009). It is well established that elevated levels of IL-6 are associated with the development of some chronic inflammatory and autoimmune diseases, such as diabetes (Pradhan et al. 2001), atherosclerosis (Amar et al. 2006) and rheumatoid arthritis (Nishimoto 2006); indeed, IL-6 is often considered a marker or predictor for these diseases. Prior to the beginning of this study, very little was known about the effect of AMPK on IL-6-stimulated proinflammatory signalling. AMPK activation was reported to suppress leptin-mediated STAT3 phosphorylation and SOCS-3

induction in hepatic stellate cells (Handy et al. 2010); however, to our knowledge, the current study was the first to investigate the effect of AMPK on IL-6 signalling in adipocytes.

4.1.3 Aims

While AMPK has been found to inhibit MAPK/NFκB proinflammatory pathways triggered by cytokines such as TNF-α and IL-1β in different cell types, its ability to regulate IL-6-stimulated JAK/STAT proinflammatory signalling in adipocytes remains to be investigated.

In the current study the ability of AMPK to modulate the IL-6-stimulated JAK/STAT signalling pathway in adipocytes was assessed. Furthermore, the molecular mechanism by which AMPK may elicit these anti-inflammatory effects was investigated.

4.2 Results

4.2.1 Effect of IL-6 on AMPK activation in 3T3-L1 adipocytes

To examine whether IL-6 altered AMPK activity in 3T3-L1 adipocytes, cells were incubated with A769662, Compound C or IL-6/sIL-6Rα and the extent of AMPK Thr172 and ACC Ser79 phosphorylation was determined by western blotting analysis of 3T3-L1 and rat epididymal adipocyte lysates, respectively.

Incubation of 3T3-L1 adipocytes with A769662 (Fig. 4.1A) caused a 37 ± 7 % increase in AMPK Thr172 phosphorylation, compared to the basal level. This was significantly reduced following preincubation with Compound C ($p < 0.001$). Incubation of 3T3-L1 adipocytes with IL-6/sIL-6Rα did not alter AMPK Thr172 phosphorylation compared to the basal level when data were normalised to A769662-stimulated (Fig. 4.1A) or vehicle (Fig. 4.1B). Similarly, incubation with IL-6/sIL-6Rα did not alter ACC Ser79 phosphorylation in adipocytes isolated from rat epididymal adipose tissue (Fig. 4.1D/E).

4.2.2 Effect of AMPK activation by A769662 on IL-6-stimulated STAT3 and ERK1/2 in 3T3-L1 adipocytes

To determine whether AMPK activation influenced stimulation of downstream components of the IL-6 signalling pathway, STAT3 and ERK1/2 activation parameters in response to IL-6/sIL-6Rα in the presence or absence of A769662 were assessed in 3T3-L1 adipocytes. The extent of STAT3 and ERK1/2 phosphorylation was assessed as a measure of activation by western blotting using phosphorylation site-specific antibodies. Incubation of 3T3-L1 adipocytes with IL-6/sIL-6Rα (Fig. 4.2) caused a significant increase, compared to the basal level, in STAT3 Y705 phosphorylation at 15, 30 and 60 min ($p < 0.001$) and 360 min ($p < 0.05$). A769662 caused a statistically significant reduction in IL-6-stimulated STAT3 phosphorylation at 15, 30, 60 and 360 min ($p < 0.001$) and 180 min ($p < 0.05$). In contrast, incubation with IL-6/sIL-6Rα did not stimulate ERK1/2 phosphorylation in 3T3-L1 adipocytes (Fig. 4.3); similarly preincubation with A769662 was found to have no effect on ERK1/2 phosphorylation.

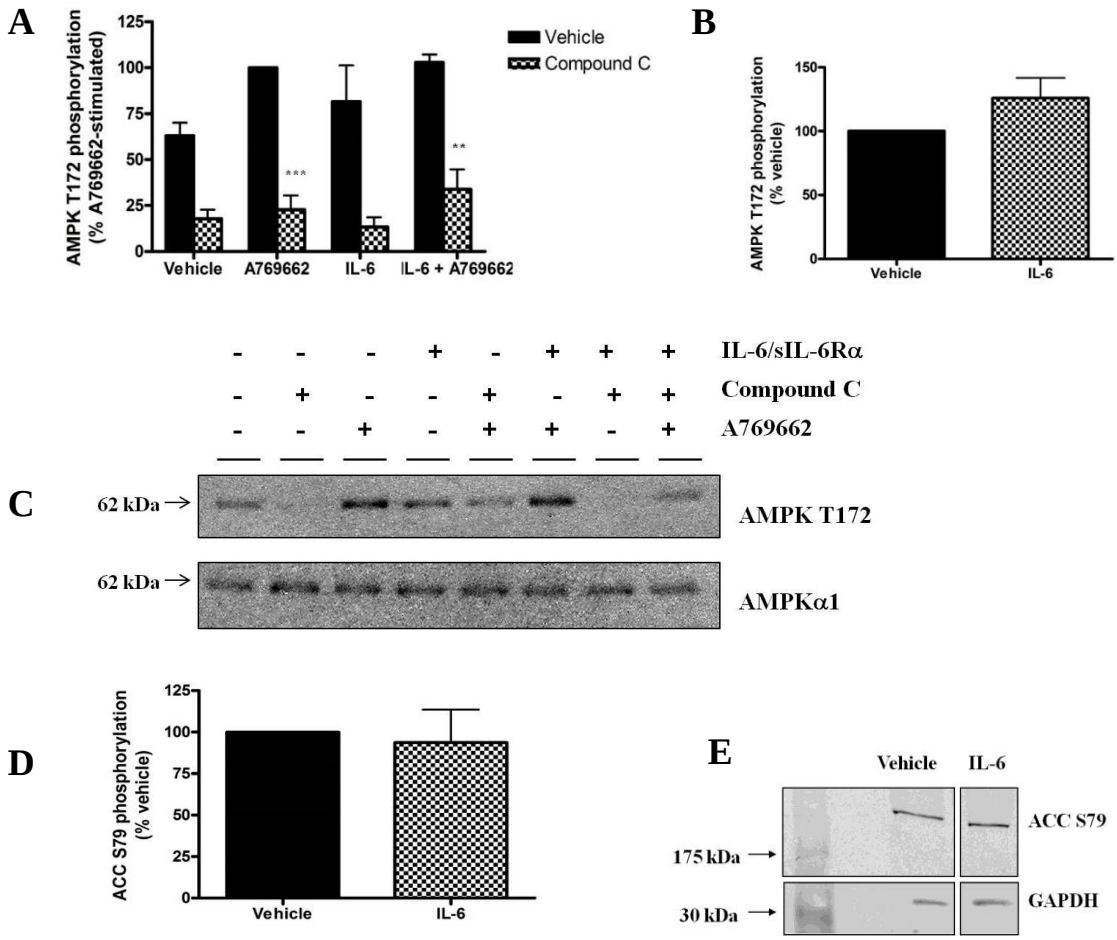

Figure 4-1: Effect of IL-6/sIL-6Rα on AMPK phosphorylation

*(A – C) 3T3-L1 adipocytes were incubated with IL-6/sIL-6Rα (5 ng/ml; 25 ng/ml) for 60 min following preincubation for 30 min in the presence or absence of A769662 (300 μM) and 60 min in the presence or absence of Compound C (60 μM); (D – E) adipocytes isolated from rat epididymal adipose were incubated for 60 min with IL-6/sIL-6Rα (5 ng/ml; 25 ng/ml) and lysates prepared. Lysates were resolved by SDS-PAGE and subjected to immunoblotting with the antibodies indicated. (A & B) Quantification of AMPK Thr172 phosphorylation relative to total AMPKα1 and (D) Quantification of ACC S79 phosphorylation relative to GAPDH was determined by densitometric analysis. (A) Data shown represent the mean ± SEM % A769662-stimulated AMPK phosphorylation of three independent experiments. **p < 0.01, ***p < 0.001 (one-way ANOVA), reduction in AMPKα1 Thr172 phosphorylation, relative to the absence of Compound C. (B) Data shown represent the mean ± SEM % vehicle AMPK phosphorylation of three independent experiments. (C) Representative western blot. (D) Data shown represent the mean ± SEM % vehicle of three independent experiments. (E) Representative blot; samples resolved on the same SDS-PAGE gel.*

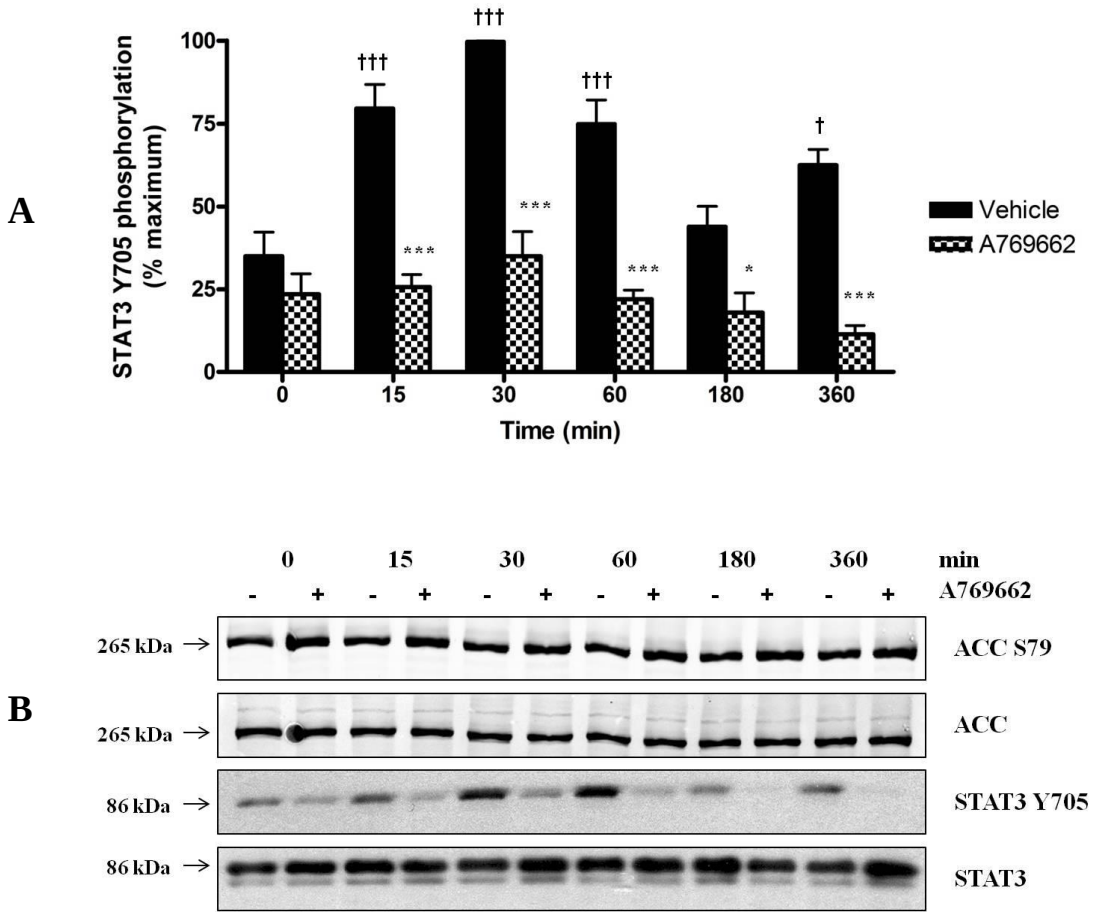

Figure 4-2: Effect of A769662 on IL-6-stimulated STAT3 phosphorylation

3T3-L1 adipocytes were incubated with IL-6/sIL-6Rα (5 ng/ml; 25 ng/ml) for various durations following preincubation for 30 min in the presence or absence of A769662 (300 μM) and lysates prepared. Lysates were resolved by SDS-PAGE and subjected to immunoblotting with the antibodies indicated. (A) Quantification of STAT3 Y705 phosphorylation relative to total STAT3 was determined by densitometric analysis. Data shown represent the mean ± SEM % maximum STAT3 phosphorylation of six independent experiments. $^{\dagger}p < 0.05$, $^{\dagger\dagger\dagger}p < 0.001$ (two-way ANOVA), increase in STAT3 Y705 phosphorylation, relative to vehicle. $^{*}p < 0.05$, $^{***}p < 0.001$ (two-way ANOVA), reduction in STAT3 Y705 phosphorylation, relative to the absence of A769662. (B) Representative western blot.

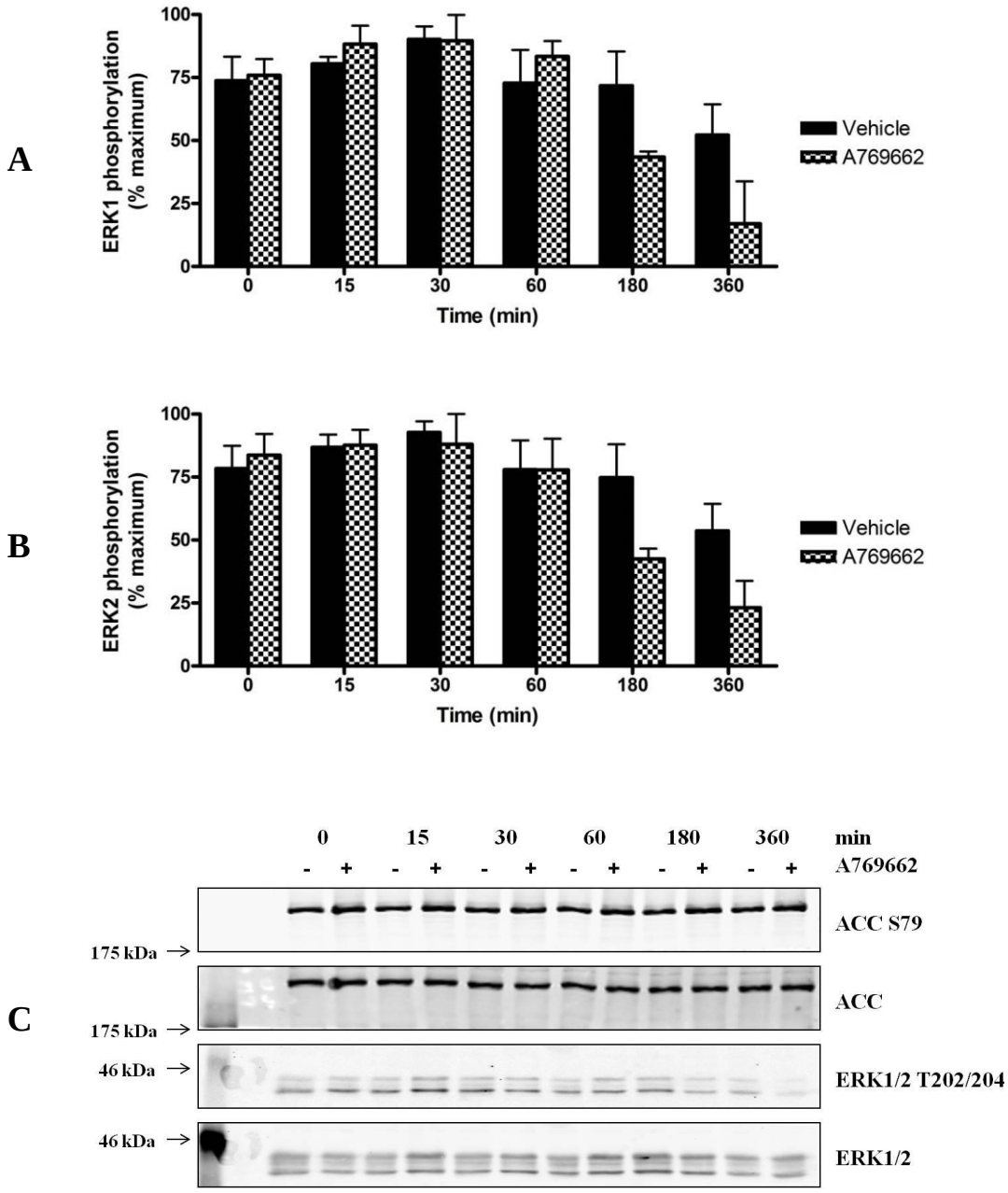

Figure 4-3: Effect of A769662 on IL-6-stimulated ERK1/2 phosphorylation

3T3-L1 adipocytes were incubated with IL-6/sIL-6Rα (5 ng/ml; 25 ng/ml) for various durations following preincubation for 30 min in the presence or absence of A769662 (300 μM) and lysates prepared. Lysates were resolved by SDS-PAGE and subjected to immunoblotting with the antibodies indicated. (A) & (B) ERK1 and ERK2, respectively. Quantification of ERK1/2 T202/Y204 phosphorylation relative to total ERK1/2 was determined by densitometric analysis. Data shown represent the mean ± SEM % maximum ERK1/2 phosphorylation of three independent experiments. (C) Representative western blot.

4.2.3 Investigating whether inhibition of IL-6 signalling is dependent upon AMPK activation

The pharmacological AMPK inhibitor, Compound C, was utilised to determine whether the A769662-mediated inhibition of IL-6-stimulated STAT3 phosphorylation was dependent upon AMPK activation. Incubation of 3T3-L1 adipocytes with IL-6/sIL-6Rα caused a 59.4 ± 18.4 % or 52.6 ± 20.1 stimulation of STAT3 Y705 phosphorylation, compared to the basal level in the absence or presence of Compound C, respectively. Preincubation with A769662 caused a subtle 36 ± 20.2 % reduction in STAT3 phosphorylation relative to IL-6/sIL-6Rα treatment alone, while this was reduced to 28.5 ± 29.2 % in the presence of Compound C (Fig. 4.4).

3T3-L1 adipocytes are relatively genetically intractable; however siRNA-mediated AMPKα1 knockdown in HUVECs caused a reduction in the ability of AICAR to suppress IL-6-stimulated STAT3 phosphorylation (Fig. 4.5). Moreover, three compounds which activate AMPK via diverse mechanisms all suppressed IL-6/sIL-6Rα-stimulated STAT3 phosphoryaltion in HUVECs (Fig. 4.6). The data shown in Figures 4.5 and 4.6 were generated and analysed by Dr Claire Rutherford, University of Glasgow.

4.2.4 Endogenous STAT3 phosphorylation in adipose tissue

To examine the role of AMPK in the basal inflammatory status of adipose tissue, gonadal and subcutaneous adipose tissue was collected from female *AMPKα1*$^{-/-}$ and litter-matched wild-type sv129 mice. The extent of STAT3 phosphorylation in lysates was assessed as a measure of activation by western blotting using phosphorylation site-specific antibodies. Lane 2 of *AMPKα1*$^{-/-}$ was omitted for analysis purposes as AMPK was detectable in the lysates suggesting it may have been heterozygous or wild type with respect to AMPKα1.

Phosphorylation of STAT3 was increased 2 fold in *AMPKα1*$^{-/-}$ gonadal adipose tissue compared to wild-type ($p < 0.05$) (Fig. 4.7). STAT3 phosphorylation was increased 1.28 fold in *AMPKα1*$^{-/-}$ subcutaneous adipose tissue compared to wild-type (Fig. 4.8), however this did not reach significance ($p = 0.17$).

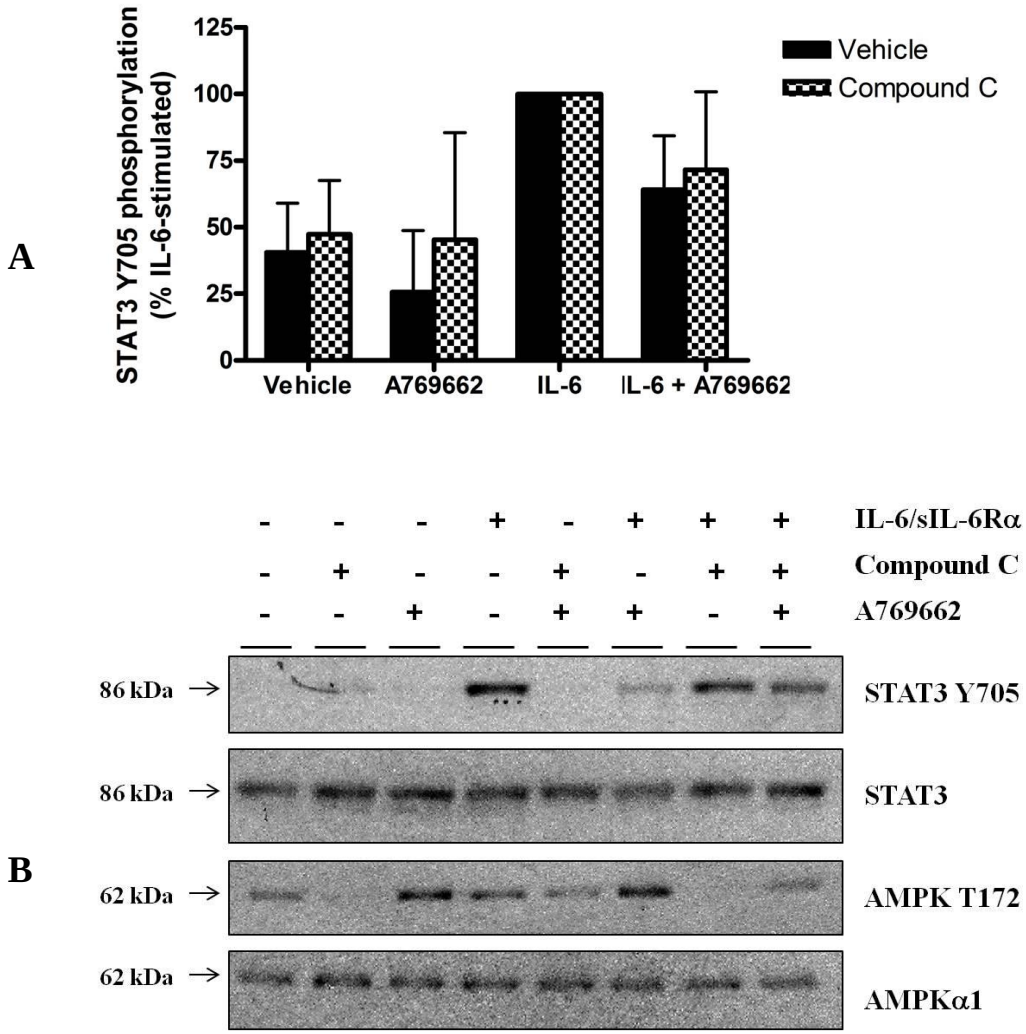

Figure 4-4: Effect of Compound C on A769662-mediated STAT3 inhibition

3T3-L1 adipocytes were incubated with IL-6/sIL-6Rα (5 ng/ml; 25 ng/ml) for 60 min following preincubation for 30 min in the presence or absence of A769662 (300 μM) and 60 min in the presence or absence of Compound C (60 μM) and lysates prepared. Lysates were resolved by SDS-PAGE and subjected to immunoblotting with the antibodies indicated. (A) Quantification of STAT3 Y705 phosphorylation relative to total STAT3 was determined by densitometric analysis. Data shown represent the mean % ± SEM IL-6-stimulated STAT3 phosphorylation of three independent experiments. (B) Representative western blot.

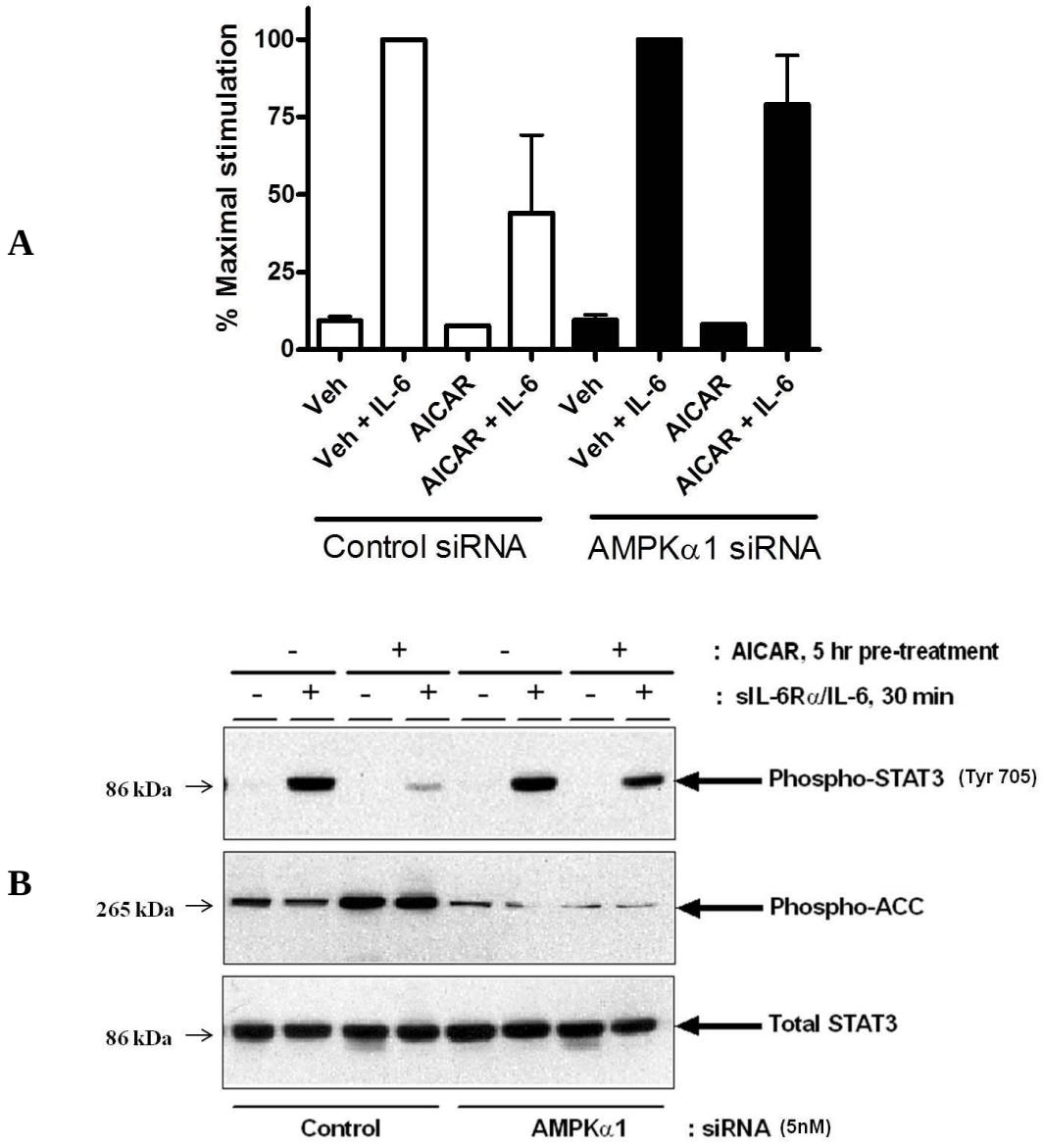

Figure 4-5: Effect of AMPKα1 knockdown on AICAR-mediated STAT3 inhibition in HUVECs

HUVECs transfected with AMPKα1 or scrambled control siRNA were incubated with IL-6/sIL-6Rα (5 ng/ml; 25 ng/ml) for 30 min following preincubation for 5 h in the presence or absence of AICAR (1 mM) and lysates prepared. Lysates were resolved by SDS-PAGE and subjected to immunoblotting with the antibodies indicated. (A) Quantification of STAT3 Y705 phosphorylation relative to total STAT3 was determined by densitometric analysis. Data shown represent the mean % ± SEM maximum of two independent experiments. (B) Representative western blot. (Data generated and analysed by Dr Claire Rutherford, University of Glasgow)

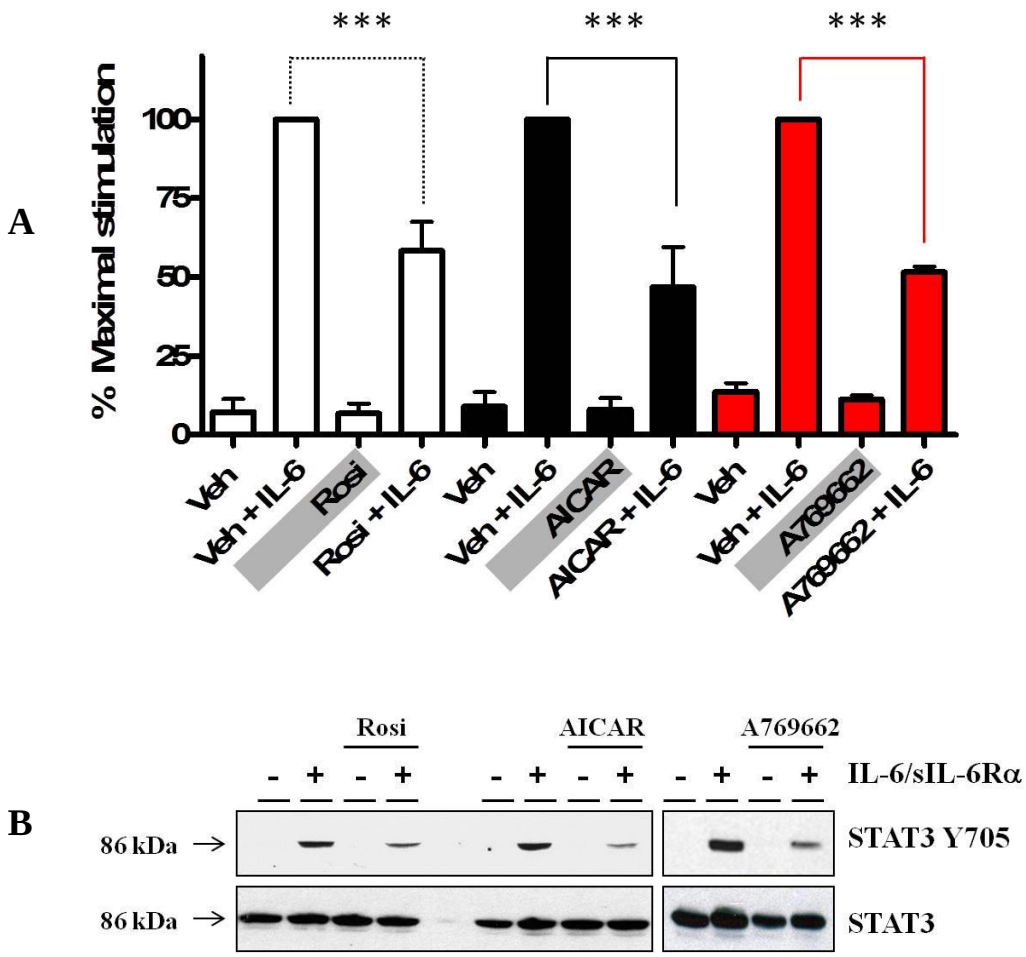

Figure 4-6: Effect of AMPK activators on STAT3 inhibition in HUVECs

HUVECs were incubated with IL-6/sIL-6Rα (5 ng/ml; 25 ng/ml) for 30 min following preincubation in the presence or absence of Rosiglitazone (Rosi) (10 μM; 24 h), AICAR (1 mM; 2 h) or A769662 (100 μM; 40 min) and lysates prepared. Lysates were resolved by SDS-PAGE and subjected to immunoblotting with the antibodies indicated. (A) Quantification of STAT3 Y705 phosphorylation relative to total STAT3 was determined by densitometric analysis. Data shown represent the mean % ± SEM maximum of three independent experiments. (B) Representative western blots. (Data generated and analysed by Dr Claire Rutherford, University of Glasgow)

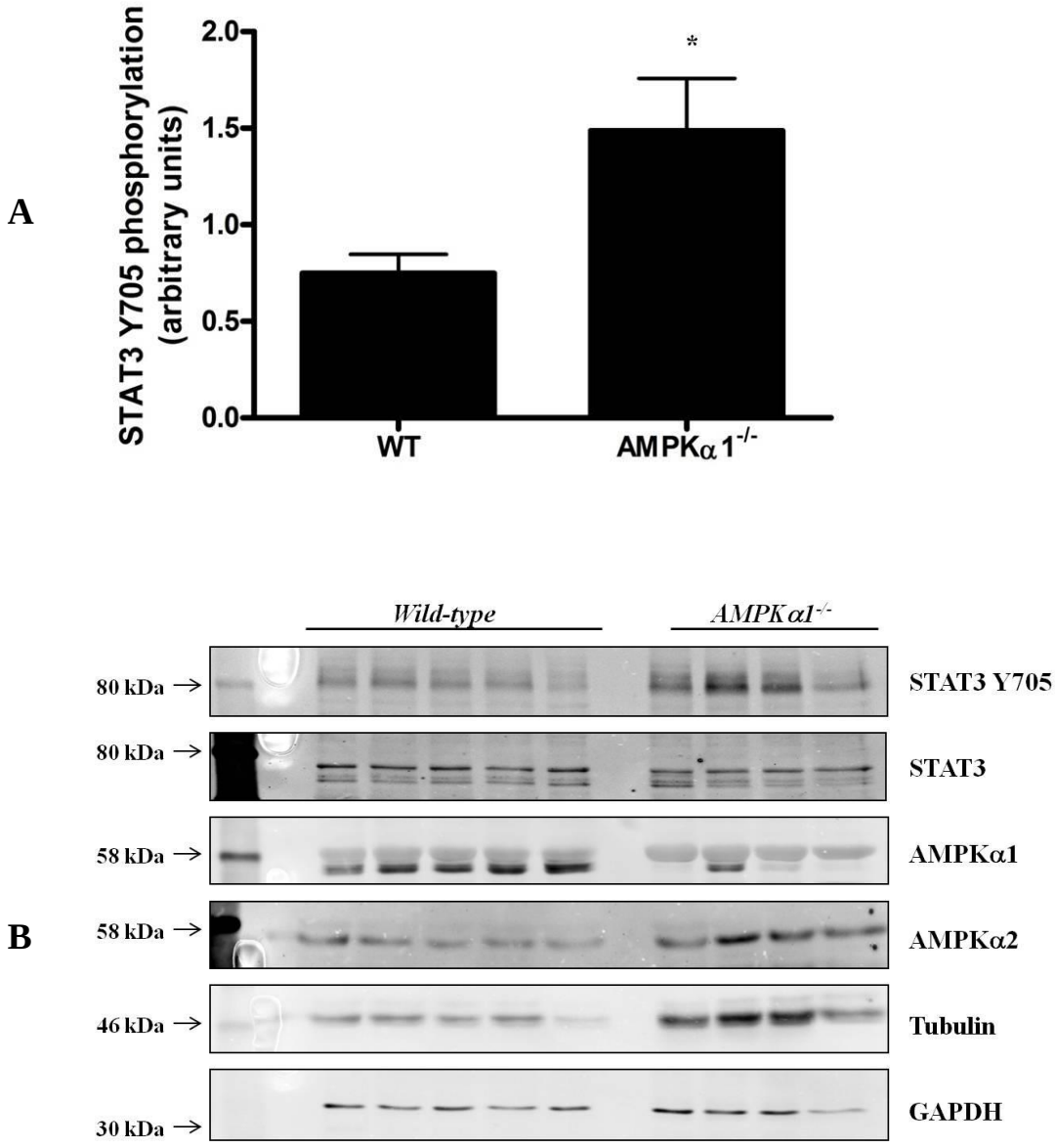

Figure 4-7: Basal STAT3 phosphorylation in gonadal adipose tissue from *AMPKα1*$^{+/+}$ and *AMPKα1*$^{-/-}$ mice

Gonadal adipose tissue obtained from AMPKα1$^{-/-}$ *and wild-type mice was resolved by SDS-PAGE and subjected to immunoblotting with the antibodies indicated. Data shown represent the mean ± SEM arbitrary densitometry units of 5 wild-type and 3 AMPKα1*$^{-/-}$ *samples. (A) Quantification of STAT3 Y705 phosphorylation relative to total STAT3 was determined by densitometric analysis. *p < 0.05 increase in STAT3 phosphorylation, relative to wild-type. (B) Representative western blot.*

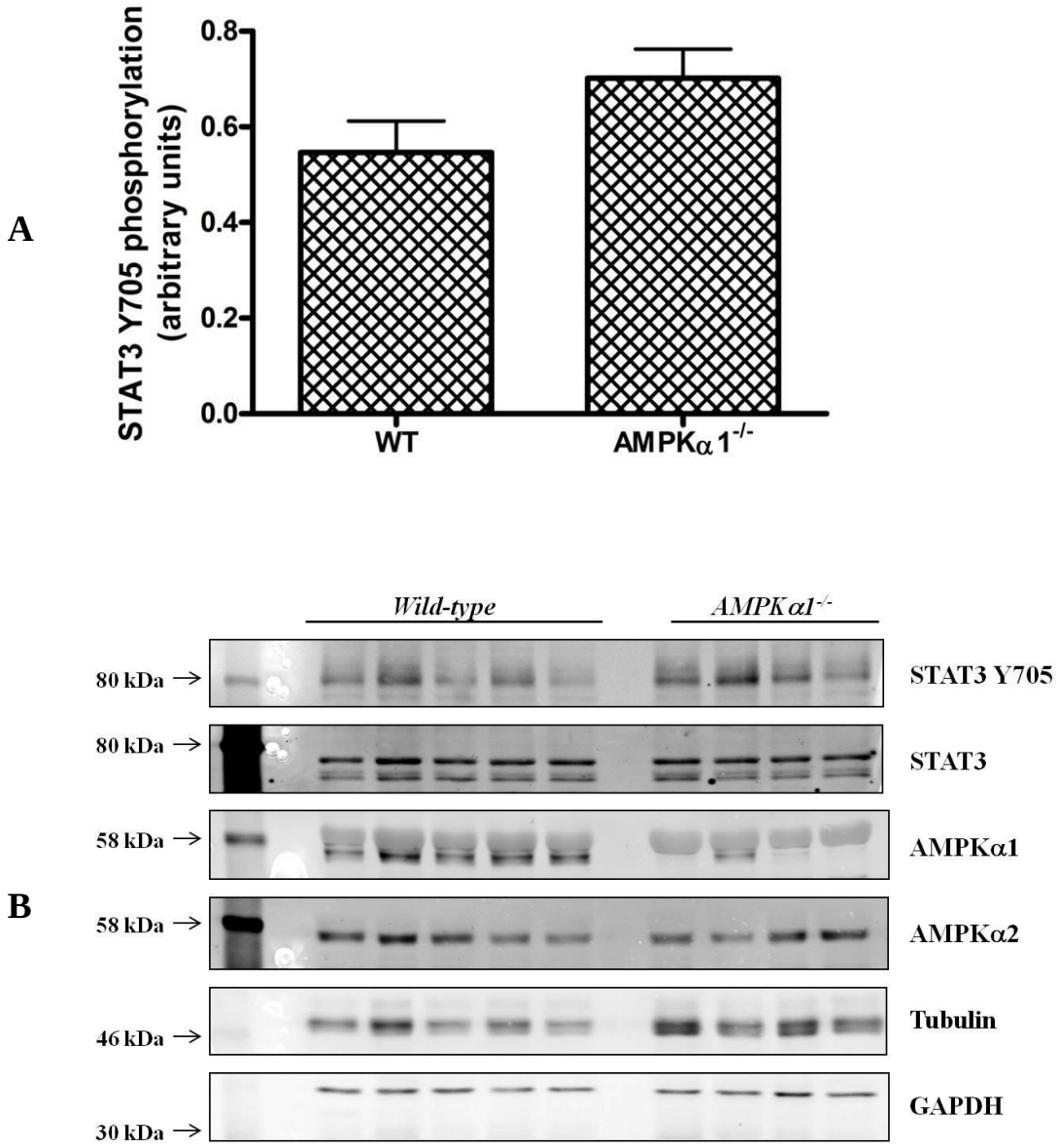

Figure 4-8: Basal STAT3 phosphorylation in subcutaneous adipose tissue from *AMPKα1*$^{+/+}$ and *AMPKα1*$^{-/-}$ mice

Subcutaneous adipose tissue obtained from AMPKα1$^{-/-}$ *and wild-type was resolved by SDS-PAGE and subjected to immunoblotting with the antibodies indicated. Data shown represent the mean ± SEM arbitrary densitometry units of 5 wild-type and 3 AMPKα1*$^{-/-}$ *samples. (A) Quantification of STAT3 Y705 phosphorylation relative to total STAT3 was determined by densitometric analysis. (B) Representative western blot.*

4.2.5 Investigating the mechanism: TSC2/mTOR/TC-PTP

4.2.5.1 Effect of mTOR inhibition on IL-6 signalling

AMPK has been reported to inhibit the mammalian target of rapamycin (mTOR) via activation of tuberous sclerosis protein 1/2 (TSC1/2) (Inoki, Zhu, and Guan 2003, Shaw et al. 2004). Furthermore, it has been suggested that mTOR mediates phosphorylation of STAT3 S727 (Yokogami et al. 2000); serine phosphorylation of STAT3 at this site has been proposed to promote full transcriptional activation of STAT3 (Wen, Zhong, and Darnell 1995). Thus, it was of interest to investigate the role of mTOR in the regulation of IL-6-stimulated STAT3 phosphorylation. PP242 was chosen as a pharmacological inhibitor of mTOR, and it specifically inhibits both mTORC1 and mTORC2, as it binds directly to the ATP binding site of either (Feldman et al. 2009). Incubation of 3T3-L1 adipocytes with IL-6/sIL-6Rα caused a significant ($p < 0.001$) stimulation of STAT3 Y705 phosphorylation, compared to the basal level. A769662 modestly decreased IL-6-stimulated STAT3 phosphorylation although this did not reach significance (Fig. 4.9A). Preincubation with PP242 caused a significant ($p < 0.05$) reduction in STAT3 Y705 phosphorylation, relative to IL-6/sIL-6Rα treatment alone, to which A769662 had no additional effect (Fig. 4.9A). Phosphorylation of STAT3 S727 was unaffected by IL-6/sIL-6Rα, A769662 or PP242 in 3T3-L1 adipocytes (Fig. 4.9B). Phosphorylation of a well-characterised downstream target of mTOR, p70 S6 kinase (p70 S6K), was found to be significantly ($p < 0.05$) reduced following treatment with PP242 compared to the absence of PP242. In contrast, incubation with A769662 caused a trend toward increased p70 S6K S371 phosphorylation compared to the absence of A769662; however, this did not reach significance (Fig. 4.9C). To determine whether the effects of A769662 and PP242 were specific to adipocytes, these experiments were repeated in MEFs. Incubation of MEFs with IL-6/sIL-6Rα caused a significant ($p < 0.001$) stimulation of STAT3 Y705 phosphorylation, compared to the basal level. Preincubation with A769662 caused a significant ($p < 0.001$) inhibition of STAT3 Y705 phosphorylation, relative to the absence of A769662 (Fig. 4.10A). Preincubation with PP242 induced a subtle 18.6 $\pm$ 4.9 % reduction in STAT3 Y705 phosphorylation compared to IL-6/sIL-6Rα treatment alone; however this did not reach significance when analysed using one-way ANOVA.

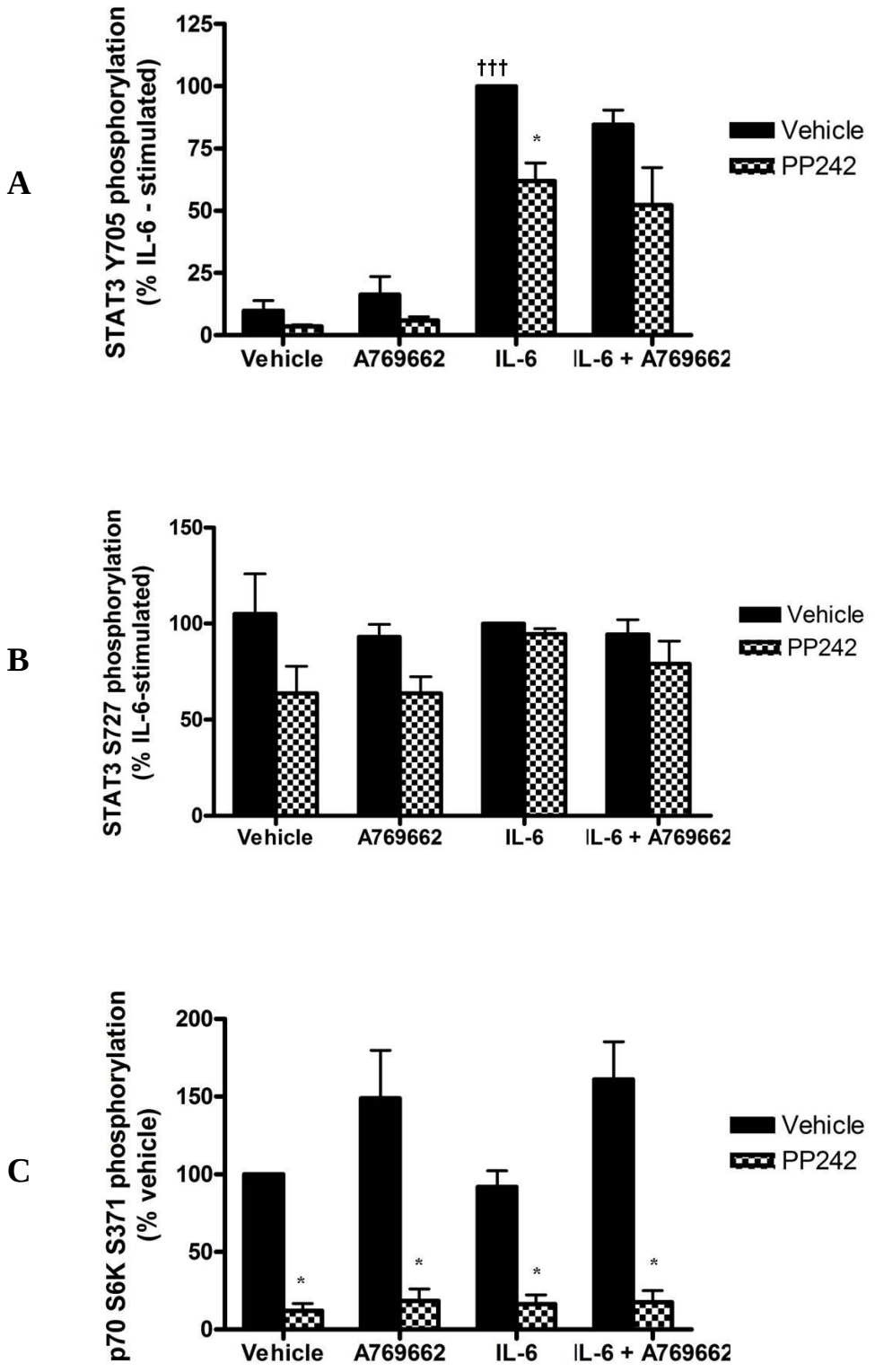

Figure 4-9: Effect of mTOR inhibition on IL-6 signalling in 3T3-L1 adipocytes

(continued overleaf)

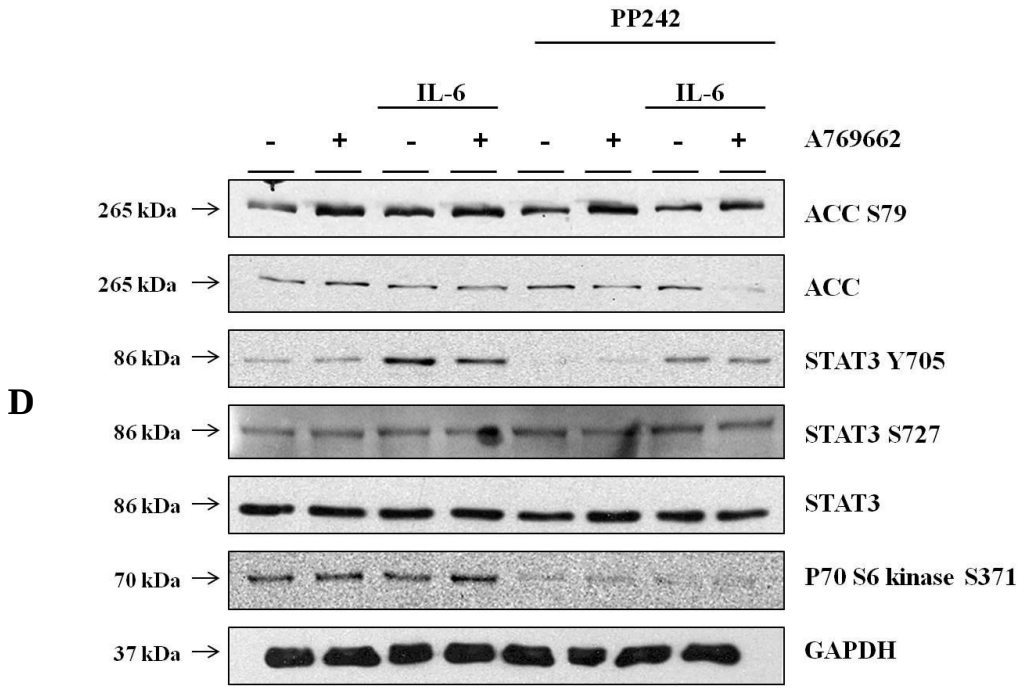

Figure 4-9: Effect of mTOR inhibition on IL-6 signalling in 3T3-L1 adipocytes

3T3-L1 adipocytes were incubated with IL-6/sIL-6Rα (5 ng/ml; 25 ng/ml) for 60 min following preincubation for 30 min in the presence or absence of A769662 (300 μM) and 3 h in the presence or absence of PP242 (2 μM) and lysates prepared. Lysates were resolved by SDS-PAGE and subjected to immunoblotting with the antibodies indicated. (A) Quantification of STAT3 Y705 phosphorylation relative to total STAT3 was determined by densitometric analysis. Data shown represent the mean ± SEM % IL-6-stimulated STAT3 Y705 phosphorylation of three independent experiments. $^{\dagger\dagger\dagger}p < 0.001$ (one-way ANOVA), increase in STAT3 Y705 phosphorylation, relative to vehicle. $^{*}p < 0.05$, (one-way ANOVA) reduction in STAT3 Y705 phosphorylation, relative to the absence of A769662. (B) Quantification of STAT3 S727 phosphorylation relative to total STAT3 was determined by densitometric analysis. Data shown represent the mean ± SEM % IL-6-stimulated STAT3 S727 phosphorylation of three independent experiments. (C) Quantification of p70 S6K S371 phosphorylation relative to total p70 S6K was determined by densitometric analysis. Data shown represent the mean ± SEM % vehicle p70 S6K phosphorylation of three independent experiments. $^{*}p < 0.05$ (one-way ANOVA), increase in p70 S6K S371 phosphorylation, relative to vehicle. (D) Representative western blot.

A two-tail t-test yielded a *p* value of 0.02, indicating there may be a tendency toward a PP242-mediated inhibition of STAT3 phosphorylation in MEFs. The inhibition of STAT3 phosphorylation observed following preincubation with A769662 remained unaffected in the presence of PP242 (Fig. 4.10A). Phosphorylation of STAT3 S727 was unaffected by IL-6/sIL-6Rα, A769662 or PP242 in MEFs (Fig. 4.10B). Phosphorylation of p70 S6K S371 was significantly ($p < 0.01$) reduced following preincubation with PP242 compared to the absence of PP242 (Fig. 4.10C).

4.2.5.2 Effect of TSC2 knockout on A769662-mediated inhibition of STAT3 phosphorylation

To determine whether the reduction in STAT3 phosphorylation by A769662 was mediated to any degree via inhibition of mTOR, *TSC2*$^{-/-}$*p53*$^{-/-}$ MEFs and wild type control *TSC2*$^{+/+}$*p53*$^{-/-}$ MEFs were incubated with IL-6/sIL-6Rα in the presence or absence of A769662 and the extent of STAT3 Y705 phosphorylation was determined by western blotting analysis of lysates. Incubation with A769662 caused a significant increase, compared to the basal level, in ACC Ser79 phosphorylation in both *TSC2*$^{+/+}$*p53*$^{-/-}$ and *TSC2*$^{-/-}$*p53*$^{-/-}$ MEFs (Fig. 4.11A). IL-6/sIL-6Rα treatment caused a clear increase, compared to the basal level, in STAT3 phosphorylation in both *TSC2*$^{+/+}$*p53*$^{-/-}$ and *TSC2*$^{-/-}$*p53*$^{-/-}$ MEFs; however this did not reach statistical significance with one-way ANOVA analysis. Using an alternative method of statistical analysis STAT3 Y705 phosphorylation was found to be significantly increased, compared to the basal level, in both *TSC2*$^{+/+}$*p53*$^{-/-}$ ($p < 0.001$) and *TSC2*$^{-/-}$*p53*$^{-/-}$ ($p < 0.05$) MEFs (two-tail t-test). Preincubation with A769662 had no effect on IL-6/sIL-6Rα-stimulated STAT3 Y705 phosphorylation in either *TSC2*$^{+/+}$*p53*$^{-/-}$ or *TSC2*$^{-/-}$*p53*$^{-/-}$ MEFs compared to the absence of A769662 (Fig. 4.9B). *TSC2*$^{-/-}$*p53*$^{-/-}$ MEFs displayed a tendency towards increased IL-6/sIL-6Rα-stimulated STAT3 Y705 phosphorylation compared to *TSC2*$^{+/+}$*p53*$^{-/-}$ MEFs; however this did not reach significance (Fig. 4.11B).

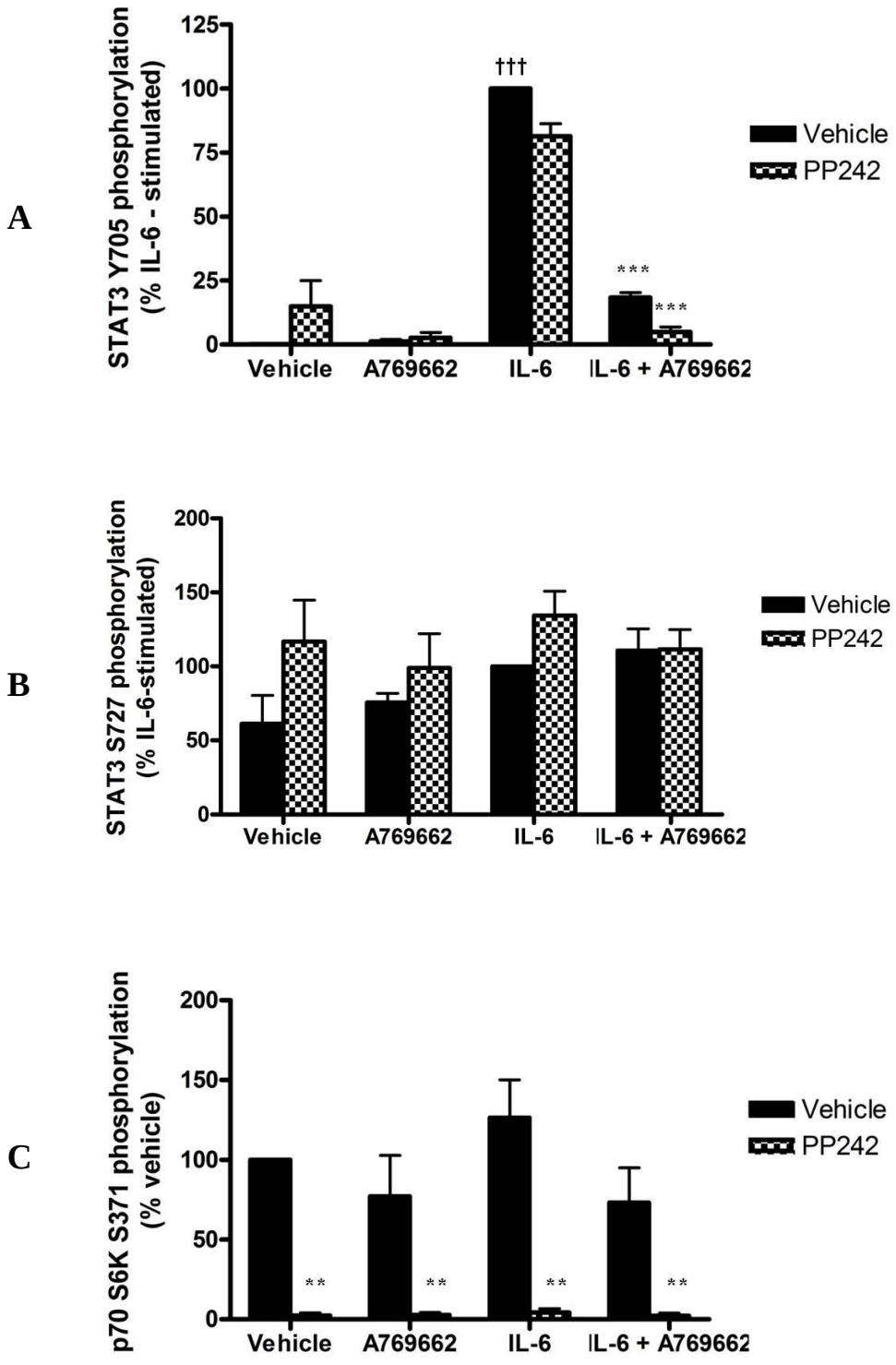

Figure 4-10: Effect of mTOR inhibition on IL-6 signalling in mouse embryonic fibroblasts *(continued overleaf)*

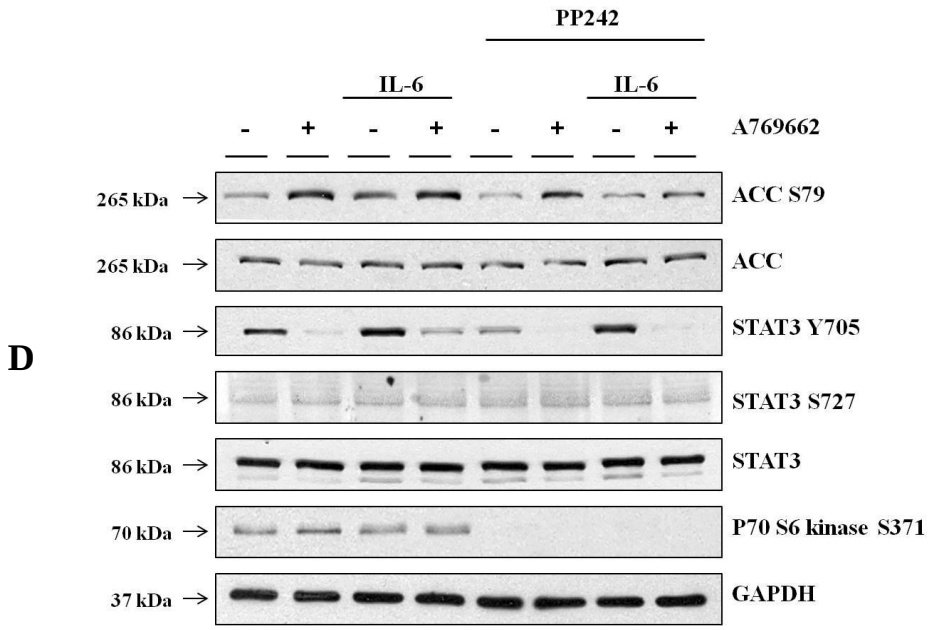

D

Figure 4-10: Effect of mTOR inhibition on IL-6 signalling in mouse embryonic fibroblasts

MEFs were incubated with IL-6/sIL-6Rα (5 ng/ml; 25 ng/ml) for 60 min following preincubation for 30 min in the presence or absence of A769662 (300 μM) and 3 h in the presence or absence of PP242 (2 μM) and lysates prepared. Lysates were resolved by SDS-PAGE and subjected to immunoblotting with the antibodies indicated. (A) Quantification of STAT3 Y705 phosphorylation relative to total STAT3 was determined by densitometric analysis. Data shown represent the mean ± SEM % IL-6-stimulated STAT3 Y705 phosphorylation of three independent experiments. $^{\dagger\dagger\dagger}p < 0.001$ (one-way ANOVA), increase in STAT3 Y705 phosphorylation, relative to vehicle. $^{***}p < 0.001$, (one-way ANOVA) reduction in STAT3 Y705 phosphorylation, relative to the absence of A769662. (B) Quantification of STAT3 S727 phosphorylation relative to total STAT3 was determined by densitometric analysis. Data shown represent the mean ± SEM % IL-6-stimulated STAT3 S727 phosphorylation of three independent experiments. (C) Quantification of p70 S6K S371 phosphorylation relative to total p70 S6K was determined by densitometric analysis. Data shown represent the mean ± SEM % vehicle p70 S6K phosphorylation of three independent experiments. $^{**}p < 0.01$ (one-way ANOVA), increase in p70 S6K S371 phosphorylation, relative to vehicle. (D) Representative western blot.

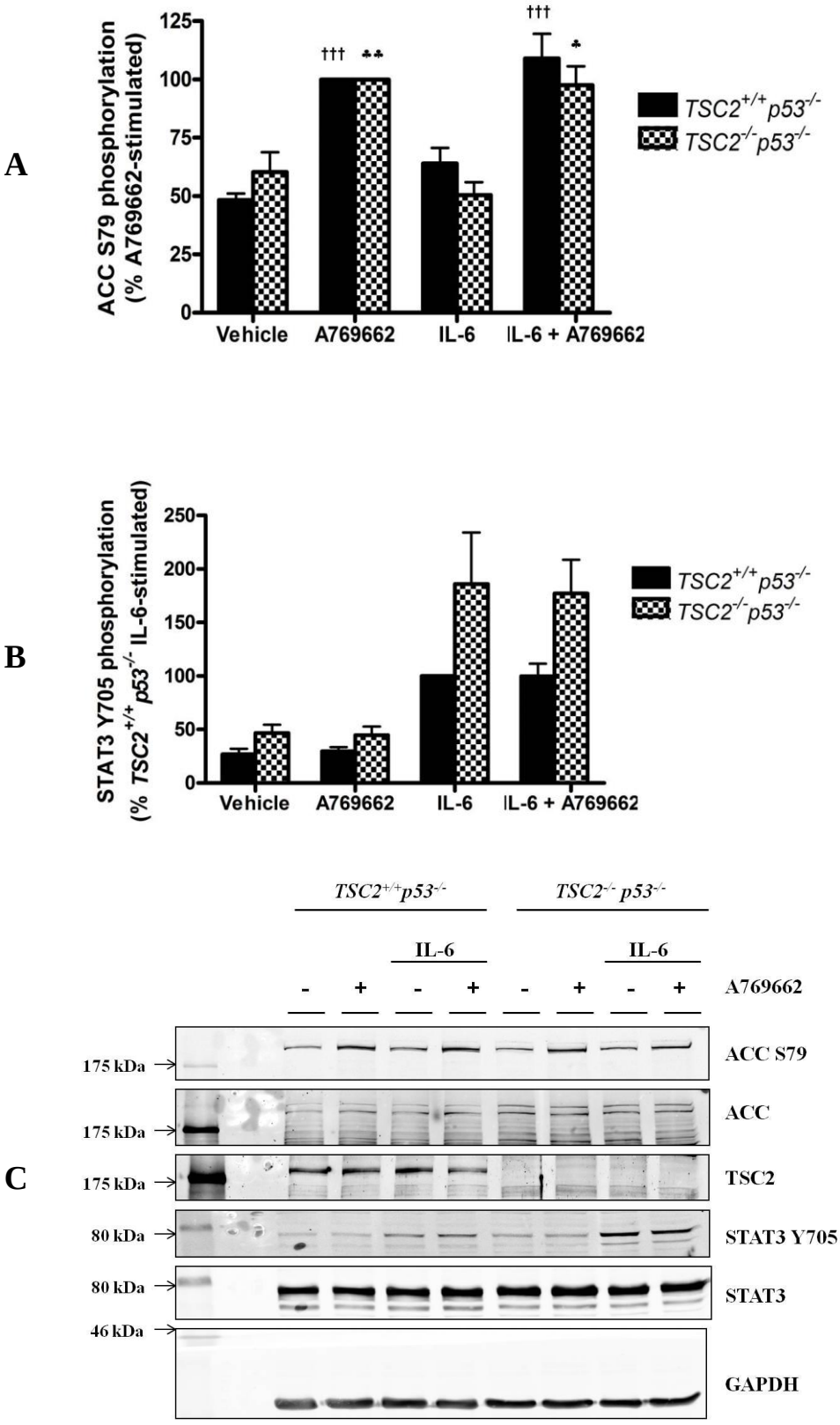

Figure 4-11: Effect of TSC2 knockout on AMPK-mediated inhibition of STAT3 phosphorylation *(legend overleaf)*

Figure 4-11: Effect of TSC2 knockout on AMPK-mediated inhibition of STAT3 phosphorylation

$TSC2^{+/+}p53^{-/-}$ or $TSC2^{-/-}p53^{-/-}$ MEFs were incubated with IL-6/sIL-6Rα (5 ng/ml; 25 ng/ml) for 60 min following preincubation for 30 min in the presence or absence of A769662 (300 μM) and lysates prepared. Lysates were resolved by SDS-PAGE and subjected to immunoblotting with the antibodies indicated. (A) Quantification of ACC S79 phosphorylation relative to ACC was determined by densitometric analysis. Data shown represent the mean ± SEM % A769662-stimulated ACC phosphorylation of three independent experiments. $^{\dagger\dagger\dagger}p < 0.001$, $^{*}p < 0.05$, $^{**}p < 0.01$ (one-way ANOVA), increase in ACC S79 phosphorylation, relative to $TSC2^{+/+}p53^{-/-}$ or $TSC2^{-/-}p53^{-/-}$ vehicle, respectively. (B) Quantification of STAT3 Y705 phosphorylation relative to STAT3 was determined by densitometric analysis. Data shown represent the mean ± SEM % $TSC2^{+/+}p53^{-/-}$ IL-6 stimulated STAT3 phosphorylation of three independent experiments. (C) Representative western blot.

4.2.5.3 Potential role of p53 in AMPK-mediated reduction in STAT3 phosphorylation

As IL-6/sIL-6Rα-stimulated STAT3 phosphorylation was not inhibited by A769662 in *TSC2*$^{+/+}$*p53*$^{-/-}$ MEFs, it was important to determine whether p53 was necessary for AMPK-mediated regulation of STAT3 phosphorylation. Adenovirus-mediated gene transfer was used to express wild-type p53 in *TSC2*$^{+/+}$*p53*$^{-/-}$ mouse embryonic fibroblasts in order to investigate the effect of p53 in AMPK-mediated inhibition of IL-6/sIL-6Rα-stimulated STAT3 Y705 phosphorylation.

Incubation with A769662 caused a significant increase in ACC Ser79 phosphorylation in both Ad.Null and Ad.p53 infected *TSC2*$^{+/+}$*p53*$^{-/-}$ MEFs ($p < 0.05$ and $p < 0.001$, respectively) (Fig. 4.12A). IL-6/sIL-6Rα caused a significant ($p < 0.001$) increase in STAT3 Y705 phosphorylation in both Ad.Null and Ad.p53 infected *TSC2*$^{+/+}$*p53*$^{-/-}$ MEFs; however preincubation with A769662 failed to reduce STAT3 Y705 phosphorylation in either Ad.Null or Ad.p53 infected *TSC2*$^{+/+}$*p53*$^{-/-}$ MEFs (Fig. 4.12B).

4.2.6 Effect of phosphatases on AMPK-mediated regulation of IL-6 signalling

In order to determine whether inhibition of IL-6-stimulated STAT3 phosphorylation by AMPK was mediated by the increased action of a phosphatase, genetic and pharmacological approaches were utilised to ablate the action of two key phosphatases known to be upstream of STAT3 in the JAK/STAT pathway.

4.2.6.1 T-cell protein tyrosine phosphatase (TC-PTP)

STAT3 and JAK1 have been reported to be substrates of TC-PTP (Fukushima et al. 2010), while AMPK activation has been reported to alter cellular localisation of TC-PTP (Lam et al. 2001). This study therefore sought to determine whether inhibition or ablation of T cell protein tyrosine phosphatase (TC-PTP) altered AMPK or mTOR-mediated inhibition of STAT3 phosphorylation.

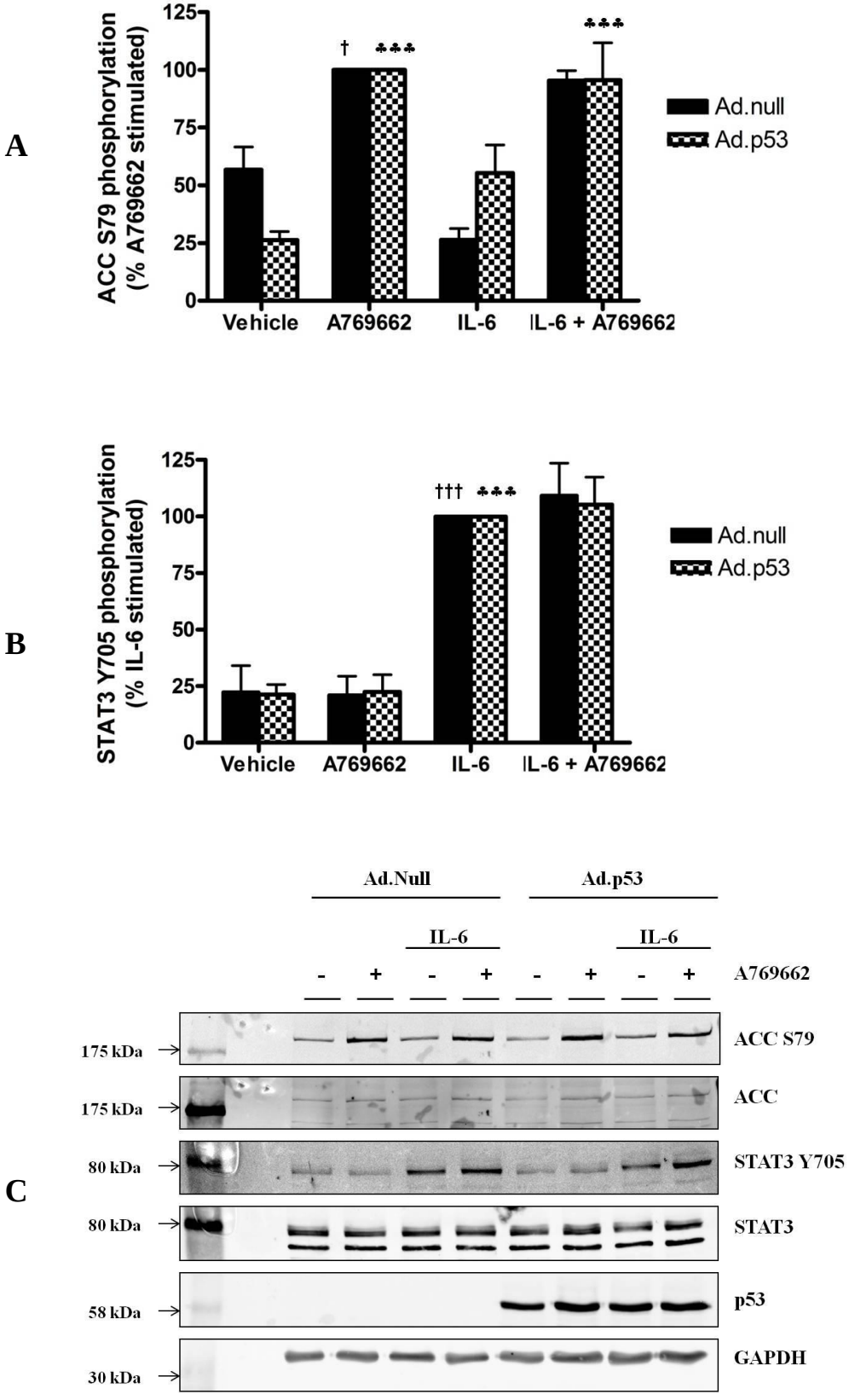

Figure 4-12: Effect of p53 on AMPK-mediated inhibition of STAT3 phosphorylation *(legend overleaf)*

Figure 4-12: Effect of p53 on AMPK-mediated inhibition of STAT3 phosphorylation

$TSC2^{+/+}p53^{-/-}$ MEFs were infected with 100 ifu/cell for 48 h with Ad.p53 or Ad.Null prior to stimulation with IL-6/sIL-6Rα (5 ng/ml; 25 ng/ml) for 60 min following preincubation for 30 min in the presence or absence of A769662 (300 μM) and lysates prepared. Lysates were resolved by SDS-PAGE and subjected to immunoblotting with the antibodies indicated. (A) Quantification of ACC S79 phosphorylation relative to total ACC was determined by densitometric analysis. Data shown represent the mean $\pm$ SEM % A769662-stimulated ACC phosphorylation of three independent experiments. $^{\dagger}p < 0.05$, $^{***}p < 0.001$, (one-way ANOVA), increase in ACC S79 phosphorylation, relative to Ad.Null or Ad.p53 vehicle, respectively. (B) Quantification of STAT3 Y705 phosphorylation relative to total STAT3 was determined by densitometric analysis. Data shown represent the mean $\pm$ SEM % IL-6 stimulated STAT3 phosphorylation of three independent experiments. $^{\dagger\dagger\dagger}p < 0.001$, $^{***}p < 0.001$ (one-way ANOVA), increase in STAT3 Y705 phosphorylation, relative to Ad.Null or Ad.p53 vehicle, respectively. (C) Representative western blot.

AMPK

Incubation of 3T3-L1 adipocytes with IL-6/sIL-6Rα caused a significant ($p < 0.001$) increase, compared to the basal level, in STAT3 Y705 phosphorylation. This was significantly inhibited following preincubation with A769662 ($p < 0.01$) (Fig. 4.13). Preincubation with a pharmacological TC-PTP inhibitor (Zhang et al. 2009) had no effect on either IL-6/sIL-6Rα-stimulated STAT3 phosphorylation or the A769662-mediated reduction in IL-6/sIL-6Rα-stimulated STAT3 phosphorylation (Fig. 4.13). IL-6/sIL-6Rα induced a significant ($p < 0.001$) increase, compared to the basal level, in STAT3 Y705 phosphorylation in both *TC-PTP*$^{+/+}$ (wild-type) and *TC-PTP*$^{-/-}$ MEFs (Fig. 4.14). Preincubation with A769662 caused a significant ($p < 0.001$) reduction in STAT3 Y705 phosphorylation in both wild-type and *TC-PTP*$^{-/-}$ MEFs, relative to IL-6/sIL-6Rα treatment alone (Fig. 4.14).

mTOR

IL-6/sIL-6Rα induced a significant ($p < 0.05$) increase, compared to the basal level, in STAT3 Y705 phosphorylation in wild-type, but not *TC-PTP*$^{-/-}$ MEFs (Fig. 4.15A). In wild-type MEFs, preincubation with PP242 caused a 36.9 ± 9.2 % reduction in phosphorylation of STAT3 Y705, compared to IL-6/sIL-6Rα treatment alone; however PP242 had no effect on IL-6/sIL-6Rα-stimulated STAT3 Y705 phosphorylation in *TC-PTP*$^{-/-}$ MEFs (Fig. 4.15A). STAT3 protein expression was significantly ($p < 0.001$) increased in *TC-PTP*$^{-/-}$ MEFs compared to wild-type *TC-PTP*$^{+/+}$ MEFs (Fig. 4.15B).

4.2.6.2 SH2-containing tyrosine phosphatase (SHP-2)

SHP-2 has been reported to negatively regulate IL-6-stimulated STAT3 phosphorylation (Ohtani et al. 2000). Thus, in order to determine whether inhibition of SHP-2 in 3T3-L1 adipocytes could ablate the AMPK-mediated inhibition of IL-6-stimulated STAT3 phosphorylation, 3T3-L1 adipocytes were incubated with a SHP-2 pharmacological inhibitor NSC 87877 (Chen et al. 2006), IL-6/sIL-6Rα or A769662 and the extent of STAT3 Y705 phosphorylation was assessed as a measure of activation by western blotting using phosphorylation site-specific antibodies. IL-6/sIL-6Rα induced a significant ($p < 0.001$) increase, compared to the basal level, in STAT3 Y705 phosphorylation in both the presence and absence of NSC 87877 (Fig. 4.16).

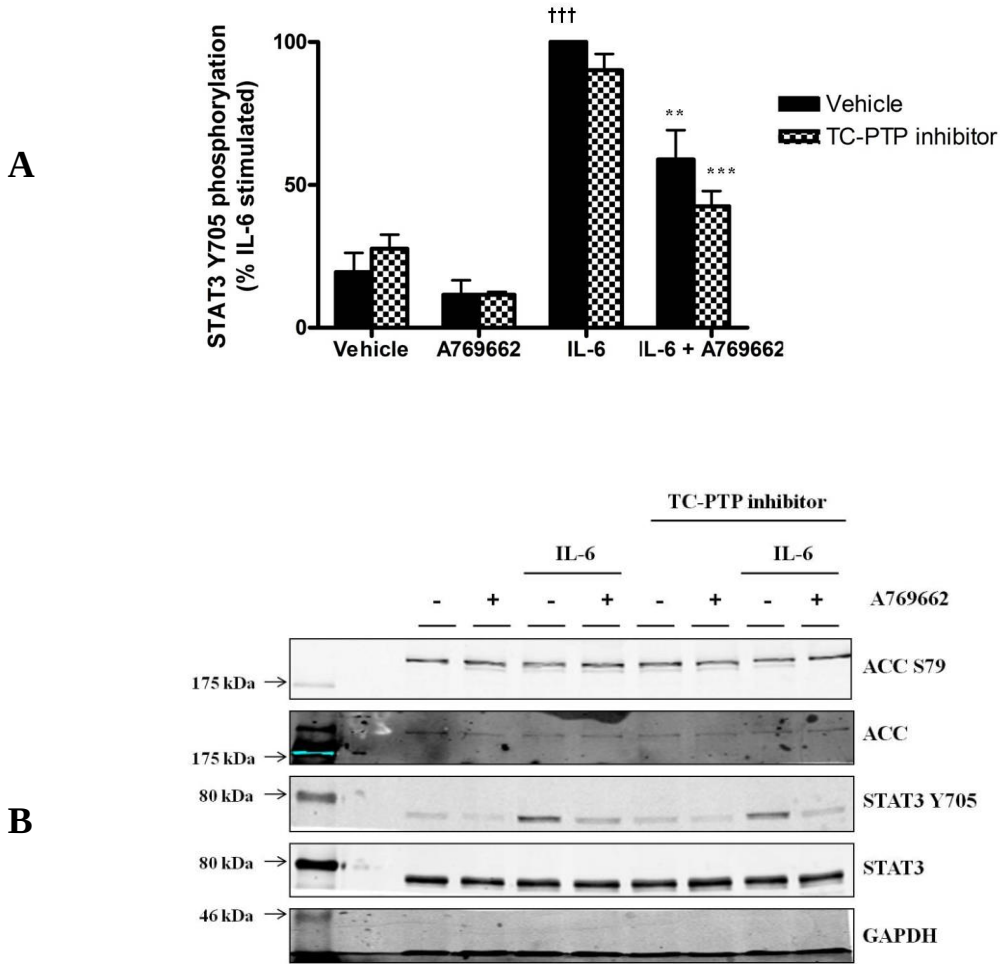

Figure 4-13: Effect of TC-PTP on AMPK-mediated inhibition of STAT3 phosphorylation in 3T3-L1 adipocytes

3T3-L1 adipocytes were incubated with IL-6/sIL-6Rα (5 ng/ml; 25 ng/ml) for 60 min following preincubation for 30 min in the presence or absence of A769662 (300 μM) and 2 h in the presence or absence of TC-PTP inhibitor (Lysates were resolved by SDS-PAGE and subjected to immunoblotting with the antibodies indicated. (A) Quantification of STAT3 Y705 phosphorylation relative to total STAT3 was determined by densitometric analysis. Data shown represent the mean ± SEM % IL-6-stimulated STAT3 phosphorylation of three independent experiments. $^{†††}p < 0.001$ (one-way ANOVA), increase in STAT3 Y705 phosphorylation, relative to vehicle. $^{**}p < 0.01$, $^{***}p < 0.001$, (one-way ANOVA) reduction in STAT3 Y705 phosphorylation, relative to the absence of A769662. (B) Representative western blot.

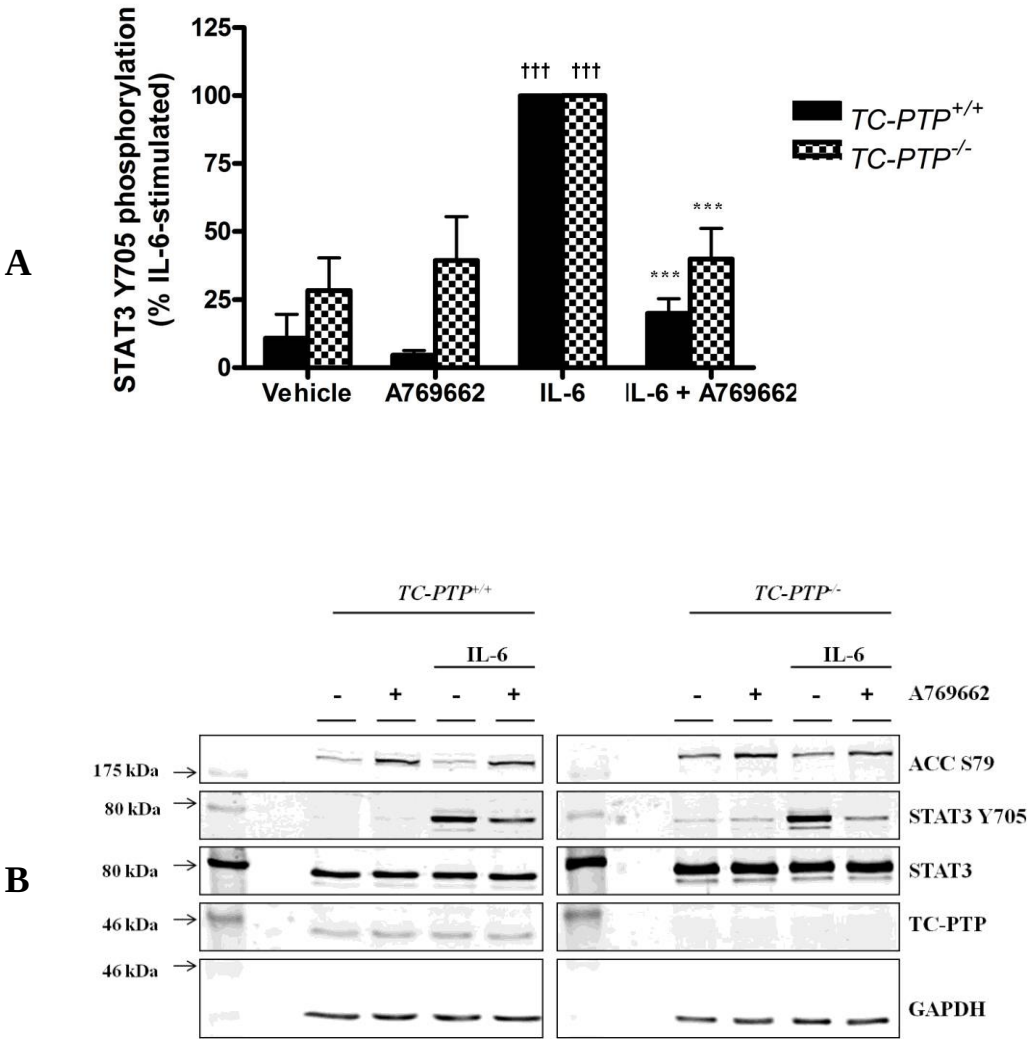

Figure 4-14: Effect of TC-PTP on AMPK-mediated inhibition of STAT3 phosphorylation in mouse embryonic fibroblasts

TC-PTP$^{+/+}$ (wild-type) and TC-PTP$^{-/-}$ MEFs were incubated with IL-6/sIL-6Rα (5 ng/ml; 25 ng/ml) for 60 min following preincubation for 30 min in the presence or absence of A769662 (300 μM) and lysates prepared. Lysates were resolved by SDS-PAGE and subjected to immunoblotting with the antibodies indicated. (A) Quantification of STAT3 Y705 phosphorylation relative to total STAT3 was determined by densitometric analysis. Data shown represent the mean ± SEM % IL-6-stimulated STAT3 phosphorylation of six independent experiments. $^{†††}p < 0.001$ (one-way ANOVA), increase in STAT3 Y705 phosphorylation, relative to vehicle. $^{***}p < 0.001$, (one-way ANOVA) reduction in STAT3 Y705 phosphorylation, relative to the absence of A769662. (B) Representative western blot with samples resolved at the same time on separate gels.

A

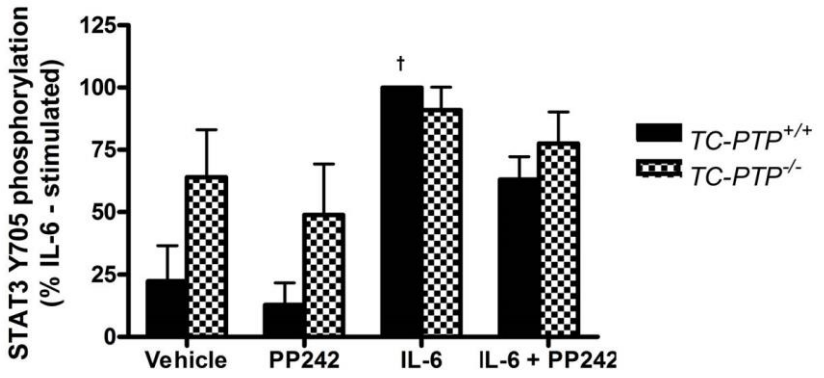

B

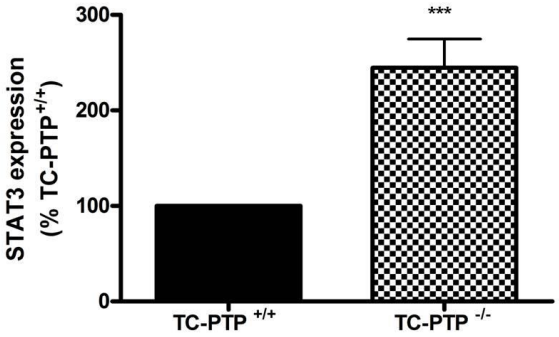

C

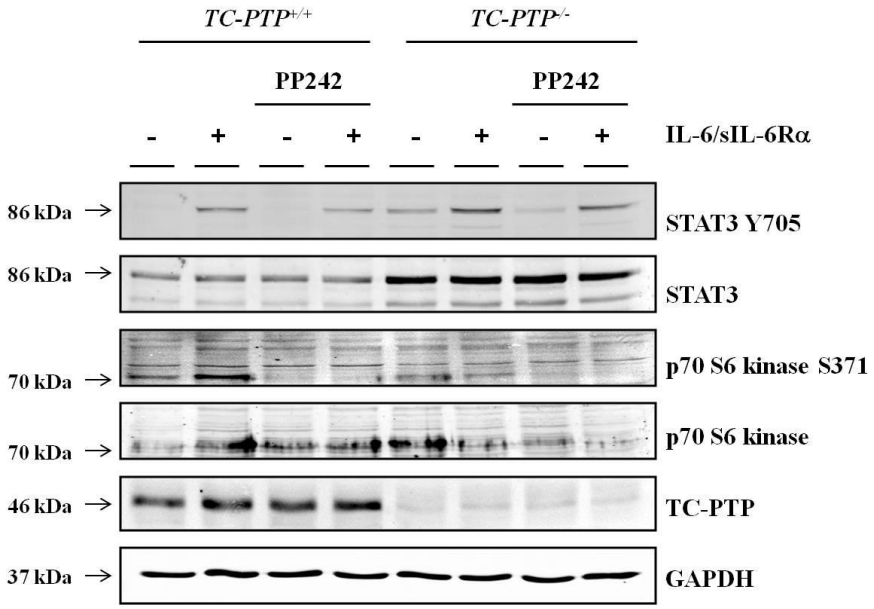

Figure 4-15: Effect of TC-PTP on mTOR-mediated inhibition of STAT3 phosphorylation *(legend overleaf)*

Figure 4-15: Effect of TC-PTP on mTOR-mediated inhibition of STAT3 phosphorylation

*TC-PTP$^{+/+}$ (wild-type) and TC-PTP$^{-/-}$ MEFs were incubated with IL-6/sIL-6Rα (5 ng/ml; 25 ng/ml) for 60 min following preincubation for 3 h in the presence or absence of PP242 (2 μM) and lysates prepared. Lysates were resolved by SDS-PAGE and subjected to immunoblotting with the antibodies indicated. (A) Quantification of STAT3 Y705 phosphorylation relative to total STAT3 was determined by densitometric analysis. Data shown represent the mean ± SEM % IL-6-stimulated STAT3 phosphorylation of three independent experiments. $^{\dagger}p < 0.05$ (one-way ANOVA), increase in STAT3 Y705 phosphorylation, relative to vehicle. (B) Quantification of STAT3 expression was determined relative to GAPDH by densitometric analysis. Data shown represent the mean ± SEM % wild-type STAT3 expression of three independent experiments. ***p < 0.001 (two-tail t-test), increase in STAT3 expression, relative to wild-type. (C) Representative western blot.*

Preincubation with A769662 caused a significant reduction in STAT3 Y705 phosphorylation, in both the presence and absence of NSC 87877 ($p < 0.01$ and $p < 0.05$, respectively), compared to IL-6/sIL-6Rα treatment alone (Fig. 4.16).

4.2.6.3 Sodium orthovanadate

In order to determine whether AMPK inhibited IL-6-stimulated STAT3 phosphorylation via a dephosphorylation mechanism in 3T3-L1 adipocytes, cells were incubated with the tyrosine phosphatase inhibitor sodium orthovanadate, A769662 or IL-6/sIL-6Rα and the extent of STAT3 Y705 phosphorylation determined by western blotting analysis.

Incubation of 3T3-L1 adipocytes with IL-6/sIL-6Rα caused a significant ($p < 0.05$) increase, compared to the basal level, in STAT3 Y705 phosphorylation (Fig. 4.17). IL-6/sIL-6Rα-stimulated STAT3 Y705 phosphorylation was further increased in the presence of sodium orthovanadate ($p < 0.001$), compared to IL-6/sIL-6Rα treatment alone. Preincubation with A769662 caused a 49.3 ± 9.9 % reduction in STAT3 Y705 phosphorylation, relative to IL-6/sIL-6Rα treatment alone. This did not reach significance upon analysis using one-way ANOVA; however a two-tail t-test generated a p value of 0.008. A769662 treatment significantly ($p < 0.001$) reduced IL-6/sIL-6Rα-stimulated STAT3 Y705 phosphorylation in the presence of sodium orthovanadate, compared to the absence of A769662 (Fig. 4.17). The presence of total phosphorylated tyrosine in these experiments was examined in order to confirm the effectiveness of sodium orthovanadate as a tyrosine phosphatase inhibitor. The representative blot (Fig. 4.17C) demonstrated an increase in phosphorylated tyrosine following sodium orthovanadate treatment, relative to the absence of the compound.

4.2.7 Role of JAK2 in AMPK-mediated inhibition of STAT3 phosphorylation

To determine whether AMPK activation influenced JAK stimulation by IL-6, JAK activation parameters in response to IL-6/sIL-6Rα in the presence or absence of A769662 were assessed in 3T3-L1 adipocytes.

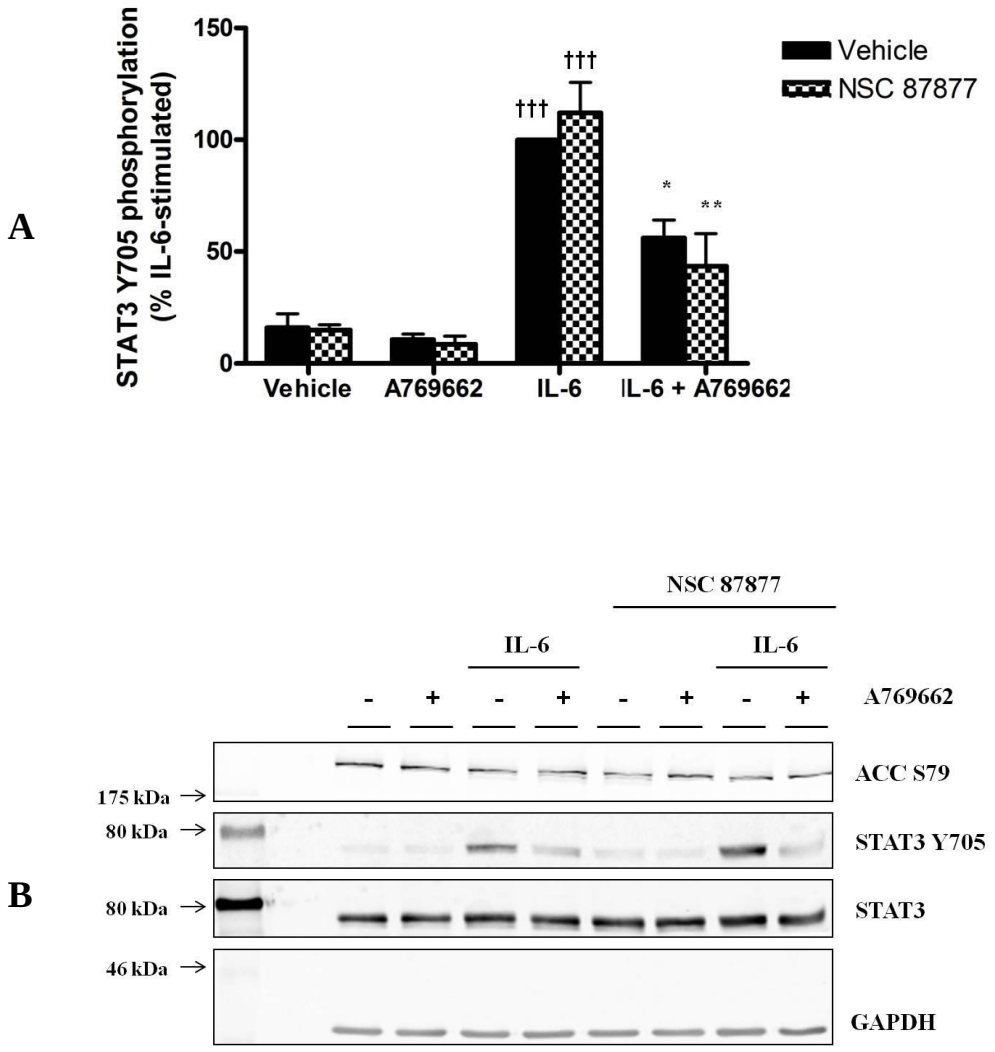

Figure 4-16: Effect of SHP-2 on AMPK-mediated inhibition of STAT3 phosphorylation

3T3-L1 adipocytes were incubated with IL-6/sIL-6Rα (5 ng/ml; 25 ng/ml) for 60 min following preincubation for 30 min in the presence or absence of A769662 (300 μM) and 1 h in the presence or absence of the SHP-2 inhibitor NSC 87877 (50 μM) and lysates prepared. Lysates were resolved by SDS-PAGE and subjected to immunoblotting with the antibodies indicated. (A) Quantification of STAT3 Y705 phosphorylation relative to total STAT3 was determined by densitometric analysis. Data shown represent the mean ± SEM % IL-6-stimulated STAT3 phosphorylation of three independent experiments. $^{†††}p < 0.001$ (one-way ANOVA), increase in STAT3 Y705 phosphorylation, relative to vehicle. $*p < 0.05$, $**p < 0.01$, (one-way ANOVA) reduction in STAT3 Y705 phosphorylation, relative to the absence of A769662. (B) Representative western blot.

A

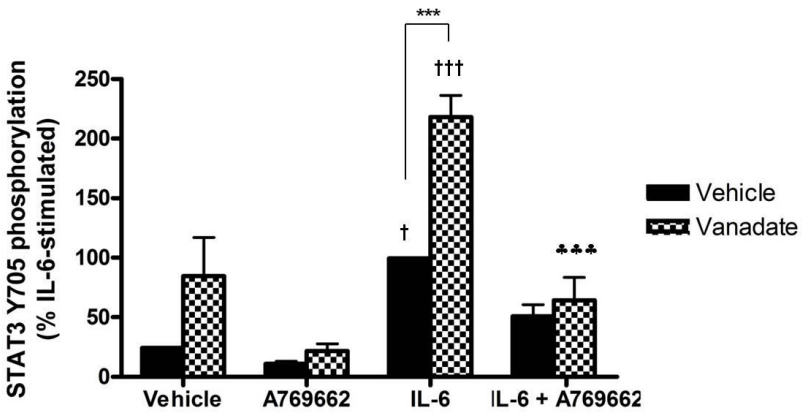

B

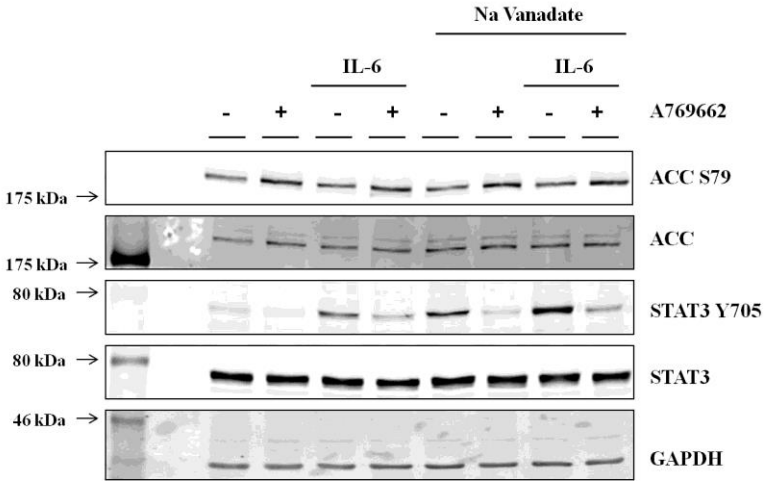

C

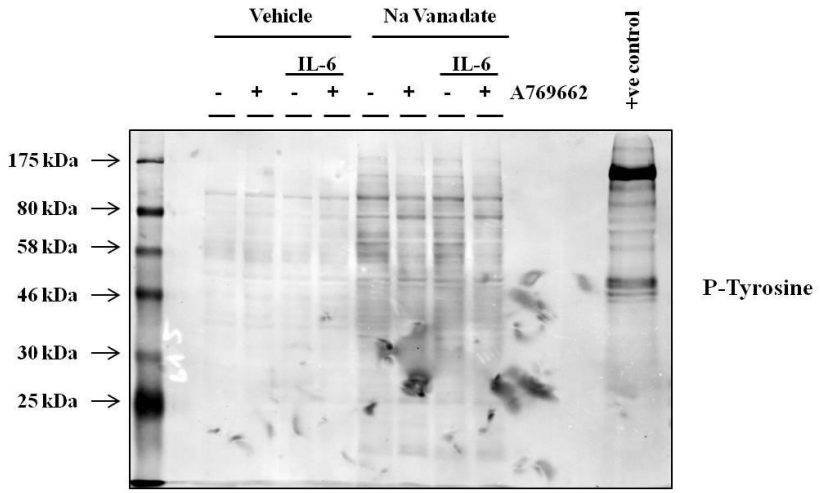

Figure 4-17: Effect of sodium orthovanadate on AMPK-mediated inhibition of STAT3 phosphorylation *(legend overleaf)*

Figure 4-17: Effect of sodium orthovanadate on AMPK-mediated inhibition of STAT3 phosphorylation

*3T3-L1 adipocytes were incubated with IL-6/sIL-6Rα (5 ng/ml; 25 ng/ml) for 60 min following preincubation for 30 min in the presence or absence of A769662 (300 μM) and 30 min in the presence or absence of sodium orthovanadate (2 mM) and lysates prepared. Lysates were resolved by SDS-PAGE and subjected to immunoblotting with the antibodies indicated. (A) Quantification of STAT3 Y705 phosphorylation relative to total STAT3 was determined by densitometric analysis. Data shown represent the mean % IL-6-stimulated STAT3 phosphorylation of three independent experiments. $^{\dagger}p < 0.05$, $^{\dagger\dagger\dagger}p < 0.001$ (one-way ANOVA), increase in STAT3 Y705 phosphorylation, relative to vehicle. $^{***}p < 0.001$ (one-way ANOVA) reduction in STAT3 Y705 phosphorylation, relative to the absence of A769662. ***p < 0.001, (one-way ANOVA) increase in STAT3 Y705 phosphorylation, relative to the absence of sodium orthovanadate. (B & C) Representative western blots.*

The extent of JAK1 and JAK2 phosphorylation was assessed as a measure of activation by western blotting using phosphorylation site-specific antibodies. Incubation of 3T3-L1 adipocyte lysates with IL-6/sIL-6Rα in the absence of A769662 induced an increase in an immunoreactive band of approximately 70-75 kDa at 15 and 30 min when probed with an antibody raised against JAK2 Y1007/1008 (Fig. 4.18A). Preincubation with A769662 reduced the intensity of these bands. In contrast, incubation with an antibody raised against total JAK2 produced bands of the predicted molecular mass (125 kDa) (Fig. 4.18E). Incubation with IL-6/sIL-6Rα did not alter JAK1 Y1022/1023 phosphorylation in 3T3-L1 adipocytes (Fig. 4.18C). Furthermore, there was no difference in total protein levels of JAK1 (Fig. 4.18B) or JAK2 (4.18D).

As the anti-JAK2 Y1007/1008 antibody detected bands of the incorrect size, it was of interest to immunoprecipitate JAK2 from the whole cell lysate to avoid any potential cross-reactivity with another protein. JAK2 was immunoprecipitated from 3T3-L1 adipocyte lysates in which cells had been incubated in the presence or absence of IL-6/sIL-6Rα for 15 min. JAK2 was detected at approximately 125 kDa in the lysate and the immunoprecipitate; however there appeared to be less immunoprecipitated in the presence of IL-6/sIL-6Rα, relative to unstimulated cells. JAK2 was also detected in the immunodeplete, indicating incomplete immunoprecipitation (Fig. 4.19). JAK2 Y1007/1008 was undetectable in the whole cell lysate; however a band which could correspond to JAK2 Y1007/1008 was detected in the JAK2 immunoprecipitate; however this appeared reduced in the presence of IL-6/sIL-6Rα, compared to vehicle. Interestingly, the band corresponding to 70-75 kDa was also present in the whole cell lysate, immunodeplete and JAK2 immunoprecipitate when probed with anti-JAK2 Y1007/1008, and was increased in the presence of IL-6/sIL-6Rα relative to the basal level (Fig. 4.19).

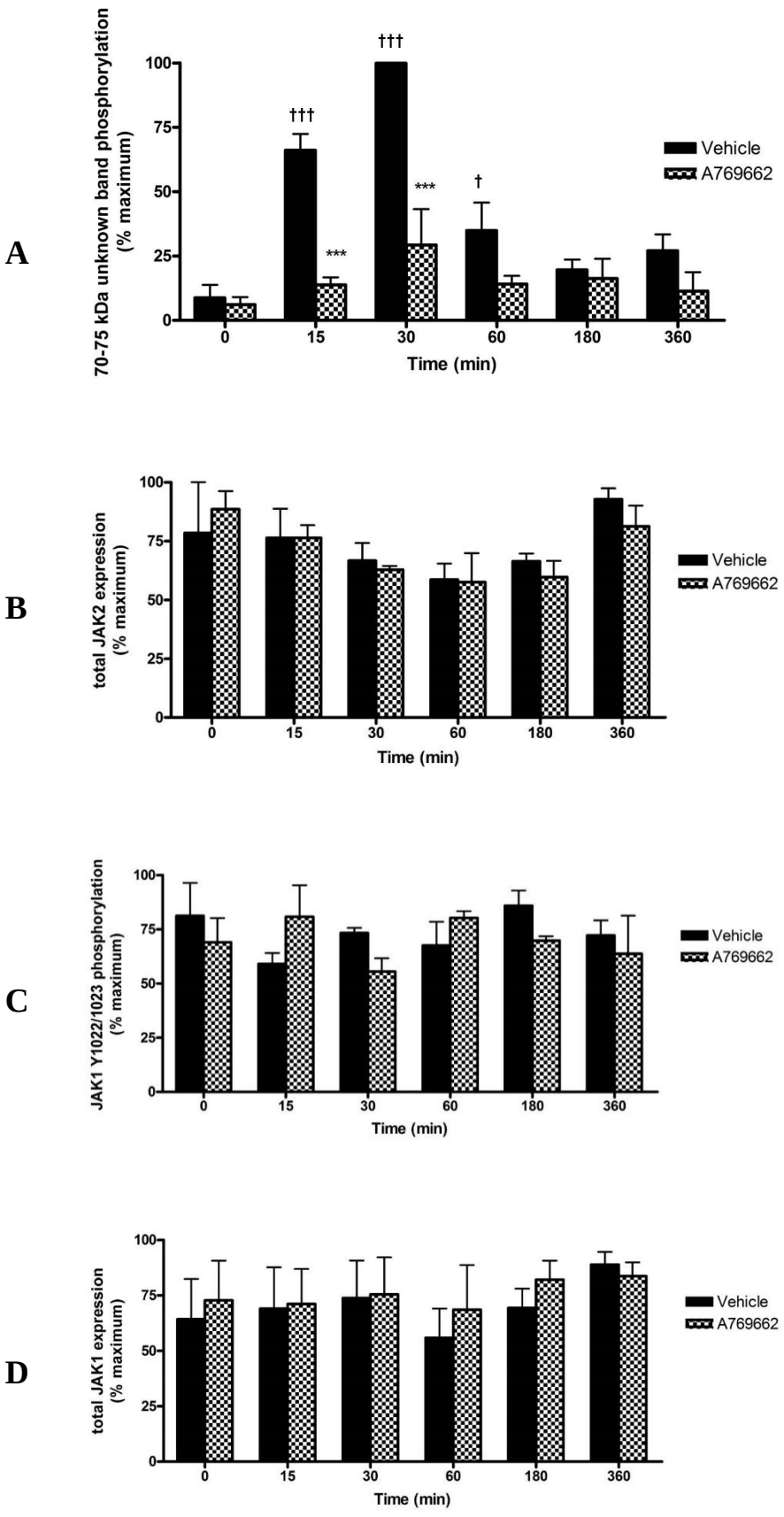

Figure 4-18: Effect of A769662 on IL-6-stimulated JAK phosphorylation *(continued overleaf)*

E

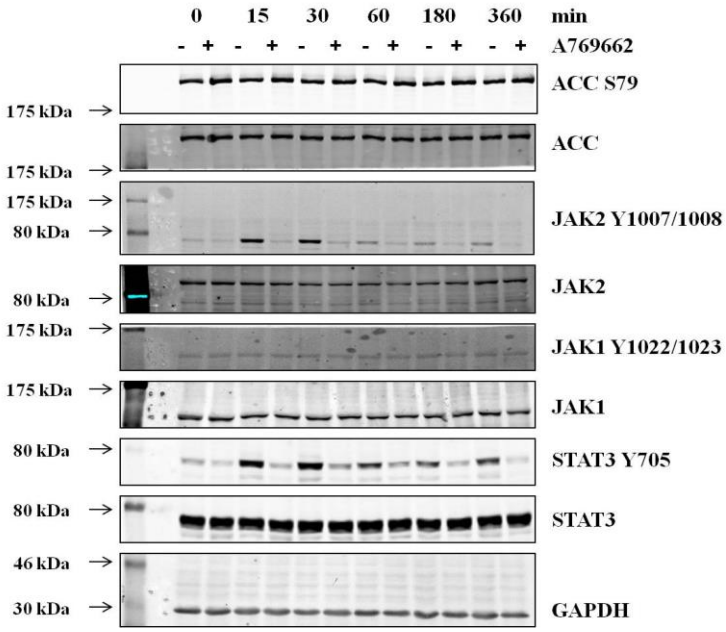

Figure 4-18: Effect of A769662 on IL-6-stimulated JAK phosphorylation

3T3-L1 adipocytes were incubated with IL-6/sIL-6Rα (5 ng/ml; 25 ng/ml) for various durations following preincubation for 30 min in the presence or absence of A769662 (300 μM) and lysates prepared. Lysates were resolved by SDS-PAGE and subjected to immunoblotting with the antibodies indicated. The unknown band refers to the band detected at 70-75 kDa with anti-JAK2 Y1007/1008. (A) Quantification of unknown band phosphorylation relative to GAPDH was determined by densitometric analysis. Data shown represent the mean ± SEM % maximum unknown band phosphorylation of three independent experiments. $^{\dagger}p < 0.05$, $^{\dagger\dagger\dagger}p < 0.001$ (two-way ANOVA), increase in unknown band phosphorylation, relative to vehicle. $^{***}p < 0.001$ (two-way ANOVA), reduction in unknown band phosphorylation, relative to the absence of A769662. (B) Quantification of JAK2 expression relative to GAPDH was determined by densitometric analysis. Data shown represent the mean ± SEM % maximum JAK2 of three independent experiments. (C) Quantification of JAK1 Y1022/1023 phosphorylation relative to total JAK1 was determined by densitometric analysis. Data shown represent the mean ± SEM % maximum JAK1 phosphorylation of three independent experiments. (D) Quantification of JAK1 expression relative to GAPDH was determined by densitometric analysis. Data shown represent the mean % maximum JAK1 of three independent experiments. (E) Representative western blot.

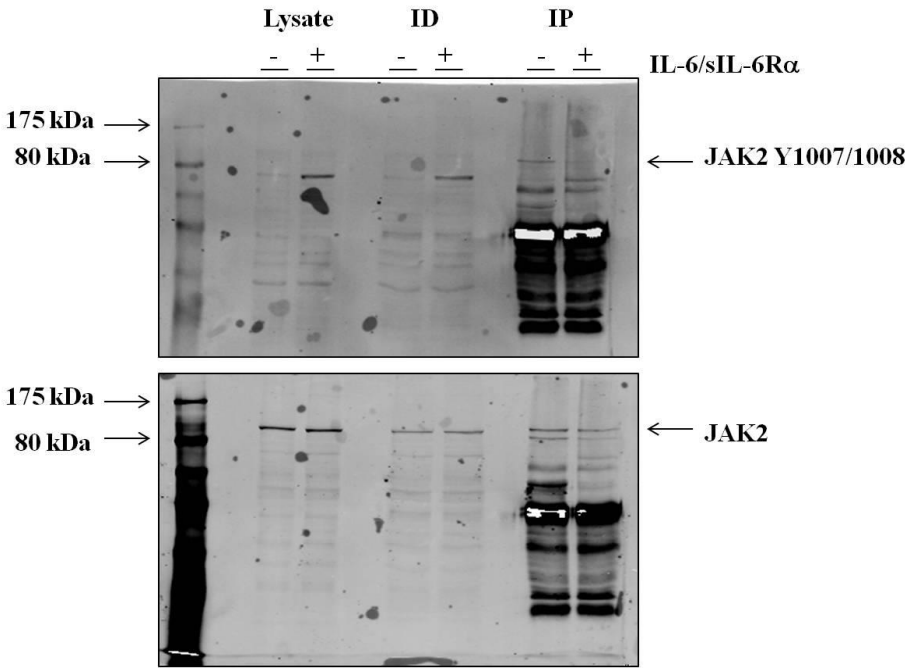

Figure 4-19: Effect of IL-6 on JAK2 phosphorylation

JAK2 was immunoprecipitated from 3T3-L1 lysates (200 μg) obtained from cells incubated in the presence or absence of IL-6/sIL-6Rα (5 ng/ml; 25 ng/ml) for 15 min. Immunoprecipitates (IP) and immunodepleted lysates (ID) were resolved on 10 % SDS-PAGE, transferred to nitrocellulose and probed with anti-JAK2 and anti-JAK2 Y1007/1008 antibodies. Western blot from a single experiment.

4.2.8 Effect of JAK2 V617F mutant on AMPK-mediated inhibition of JAK/STAT phosphorylation

4.2.8.1 HEK-293 cells

The data presented in Figures 4.18 and 4.19 suggest that JAK2 phosphorylation may be altered by A769662 stimulation. In order to determine whether AMPK may reduce STAT3 phosphorylation via direct inhibition of JAK2, a mutant JAK2 (V617F) which is essentially constitutively active, or the empty plasmid control pRK5, was transfected into HEK-293 cells. Cells were incubated in the presence or absence of A769662 and the extent of ACC S79, JAK2 Y1007/1008, STAT3 Y705 and STAT5 Y694 phosphorylation were determined by western blotting analysis of HEK-293 lysates.

Incubation of HEK-293 cells with A769662 caused a significant ($p < 0.001$) increase, compared to the basal level, in ACC S79 phosphorylation in both JAK2 V617F and pRK5 transfected cells (Fig. 4.20A). Transfection of HEK-293 cells with the JAK2 V617F mutant caused a significant ($p < 0.001$) increase in phosphorylation of JAK2 Y1007/1008, STAT3 Y705 and STAT5 Y694, compared to control cells transfected with pRK5 (Fig. 4.20B, 4.20C and 4.20D, respectively). Preincubation with A769662 had no effect on the extent of JAK2 Y1007/1008, STAT3 Y705 or STAT5 Y694 phosphorylation in HEK-293 cells transfected with the JAK2 V617F mutant, relative to the absence of A769662 (Fig. 4.20B, 4.20C and 4.20D, respectively). Incubation with IL-6/sIL-6Rα did not stimulate phosphorylation of JAK2 Y1007/1008, STAT3 Y705 or STAT5 Y694 in HEK-293 cells (Fig. 4.20E).

4.2.8.2 HeLa cells

In this study, HEK-293 cells did not respond to IL-6/sIL-6Rα. It was therefore of interest to determine whether AMPK could inhibit IL-6-stimulated STAT3 phosphorylation in the presence of the JAK2 V617F mutant. In this preliminary experiment the JAK2 V617F mutant or pRK5 empty plasmid were transfected into HeLa cells, which were then incubated with IL-6/sIL-6Rα in the presence or absence of A769662 and the extent of ACC S79 and STAT3 Y705 phosphorylation was determined by western blotting analysis of HeLa lysates.

Incubation of HeLa cells with A769662 caused an increase, compared to the basal level, in ACC S79 phosphorylation in untransfected, JAK2 V617F, pRK5 and mock transfected cells (Fig. 4.21A). Transfection of HeLa cells with the JAK2 V617F mutant caused an increase in STAT3 Y705 phosphorylation, compared to control cells transfected with pRK5 (Fig. 4.21B). Incubation with IL-6/sIL-6Rα clearly increased STAT3 Y705 phosphorylation, relative to the absence of IL-6/sIL-6Rα in both JAK2 V617F and pRK5 control transfected HeLa cells. Preincubation with A769662 had no effect on STAT3 Y705 phosphorylation in HeLa cells transfected with the JAK2 V617F mutant, compared to the absence of A769662 (Fig. 4.21B). In untransfected, mock and pRK5 transfected cells, preincubation with A769662 inhibited IL-6/sIL-6Rα-stimulated STAT3 Y705 phosphorylation relative to the absence of A769662 (Fig. 4.21B).

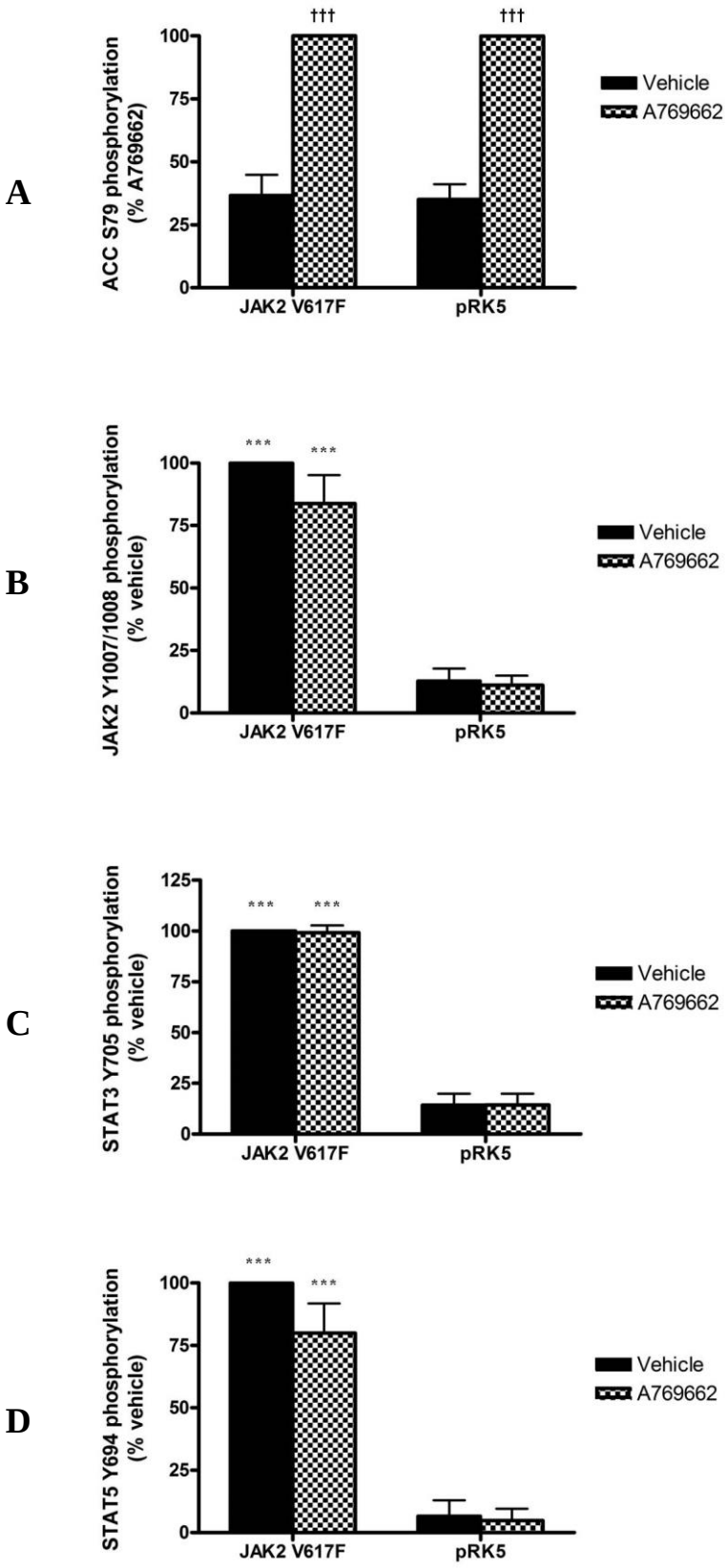

Figure 4-20: Effect of JAK2 mutant on AMPK-mediated inhibition of JAK/STAT signalling in HEK-293 cells *(continued overleaf)*

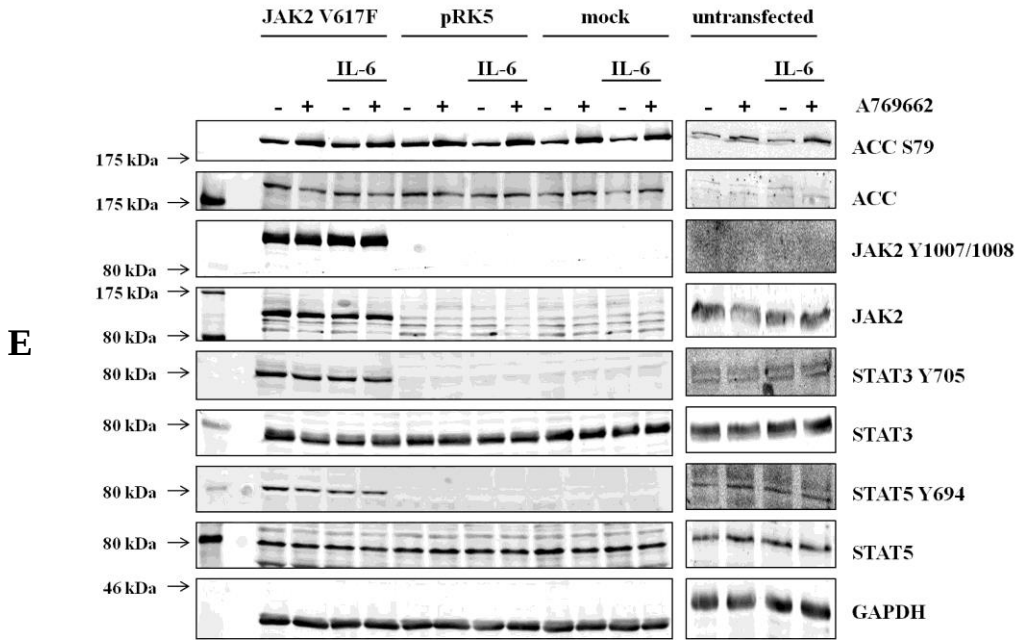

Figure 4-20: Effect of JAK2 mutant on AMPK-mediated inhibition of JAK/STAT signalling in HEK-293 cells

*HEK-293 cells were transfected with mutant JAK2 V617F or pRK5 for 48 h prior to stimulation for 30 min with A769662 (300 μM) and cell lysates prepared. Lysates were resolved by SDS-PAGE and subjected to immunoblotting with the antibodies indicated. (A) Quantification of ACC S79 phosphorylation relative to total ACC was determined by densitometric analysis. Data shown represent the mean ± SEM % A769662 stimulated phosphorylation of five independent experiments. $^{\dagger\dagger\dagger}p < 0.001$ (one-way ANOVA), increase in ACC S79 phosphorylation, relative to vehicle. (B – D) Data shown represent the mean ± SEM % vehicle stimulated phosphorylation of five independent experiments. (B) Quantification of JAK2 Y1007/1008 phosphorylation relative to total JAK2 was determined by densitometric analysis. ***p < 0.001 (one-way ANOVA), increase in JAK2 Y1007/1008 phosphorylation, relative to pRK5-transfected. (C) Quantification of STAT3 Y705 phosphorylation relative to total STAT3 was determined by densitometric analysis. ***p < 0.001 (one-way ANOVA), increase in STAT3 Y705 phosphorylation, relative to pRK5-transfected. (D) Quantification of STAT5 Y694 phosphorylation relative to total STAT5 was determined by densitometric analysis. ***p < 0.001 (one-way ANOVA), increase in STAT5 Y694 phosphorylation, relative to pRK5-transfected. (E) Representative western blot.*

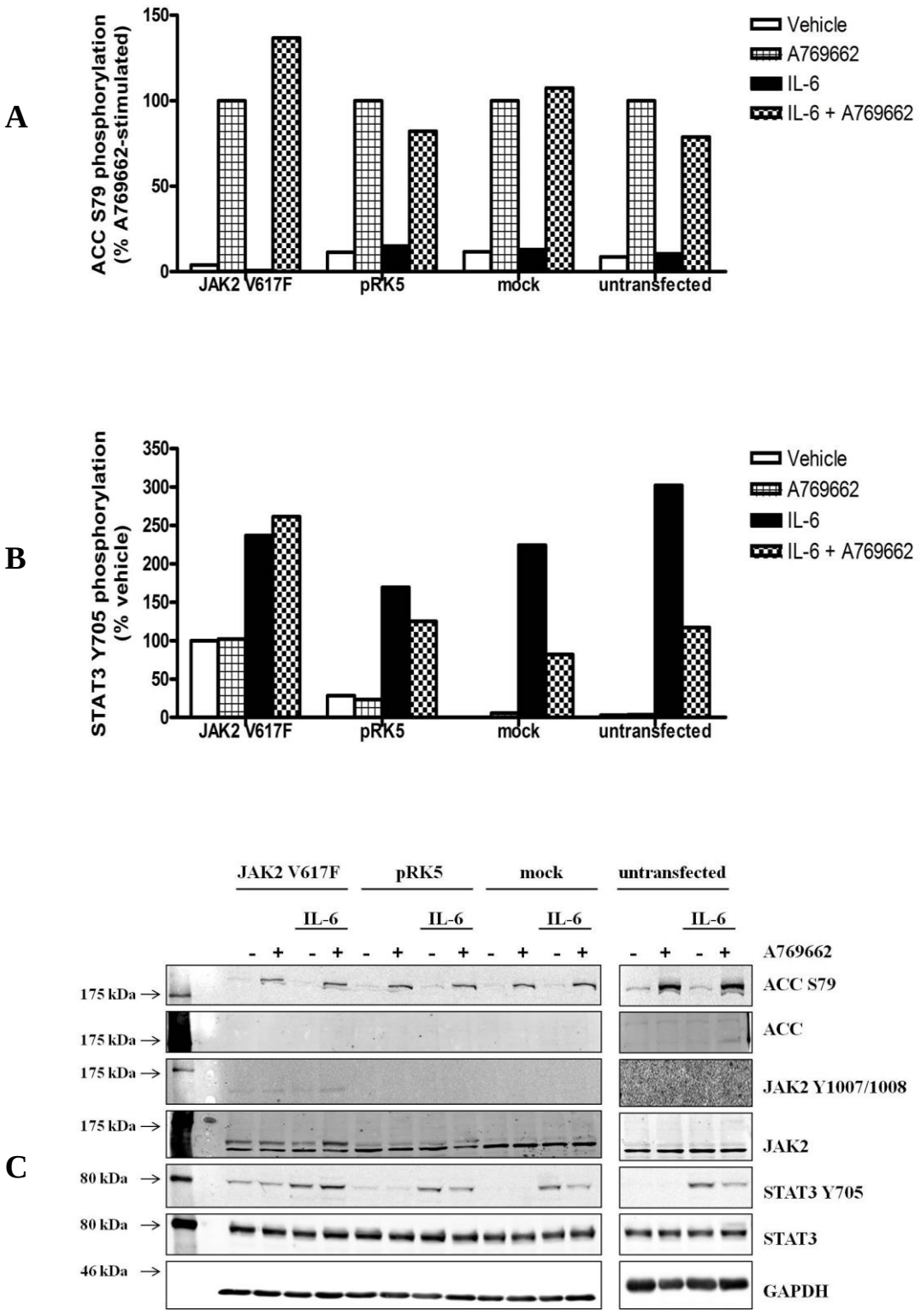

Figure 4-21: Effect of JAK2 mutant on AMPK-mediated inhibition of JAK/STAT signalling in HeLa cells *(legend overleaf)*

Figure 4-21: Effect of JAK2 mutant on AMPK-mediated inhibition of JAK/STAT signalling in HeLa cells

HeLa cells were transfected with mutant JAK2 V617F or pRK5 for 48 h prior to stimulation for 60 min with IL-6/sIL-6Rα (5 ng/ml; 25 ng/ml) following preincubation for 30 min with A769662 (300 μM) and cell lysates prepared. Lysates were resolved by SDS-PAGE and subjected to immunoblotting with the antibodies indicated. (A) Quantification of ACC S79 phosphorylation relative to total ACC was determined by densitometric analysis. Data shown represent the % A769662 stimulated phosphorylation of a single experiment. (B) Quantification of STAT3 Y705 phosphorylation relative to total STAT3 was determined by densitometric analysis. Data shown represent the % vehicle stimulated phosphorylation of a single experiment. (C) Western blot from a single experiment.

4.3 Discussion

The key findings of this chapter are that AMPK activation in adipocytes inhibited IL-6-stimulated phosphorylation of STAT3, by a mechanism likely to be via inhibition of JAK phosphorylation, and not via the action of a phosphatase. Furthermore, inhibition of mTOR also inhibited IL-6-stimulated STAT3 phosphorylation, and this may be mediated, at least in part, via TC-PTP, and is likely to occur independently of AMPK activation.

Initial studies were undertaken to initially assess whether IL-6 could induce AMPK activation in 3T3-L1 adipocytes. IL-6 has been reported to have a varied influence on AMPK activity in different cell types, with multiple lines of evidence suggesting IL-6 stimulates AMPK in muscle (Kelly et al. 2004, Carey et al. 2006); conversely, IL-6-deficient mice have been reported to have reduced AMPK activity in muscle and adipose tissue (Kelly et al. 2004). Furthermore, Wan and co-workers recently reported increased IL-6-stimulated phosphorylation of AMPK and ACC in cultured epididymal adipose tissue (Wan et al. 2012), while in contrast, there was reported to be no difference in AMPK activity in SCAT of both wild-type and IL-6-deficient mice (Brandt et al. 2012). IL-6 has been reported to inhibit AMPK activity in endothelial cells (Yuen et al. 2009), while it has recently been found that IL-6 has no effect on AMPK activity in HepG2 cells (Nerstedt et al. 2010, Nerstedt et al. 2013) or rat primary hepatocytes (Kim et al. 2012). In this study, Figure 4.1 demonstrated that IL-6 had no effect on AMPK Thr172 phosphorylation in 3T3-L1 adipocytes, either relative to A769662-stimulated (Fig. 4.1A) or vehicle (Fig. 4.1B). Furthermore, ACC Ser79 phosphorylation remained unaltered following IL-6 treatment in adipocytes isolated from rat epididymal adipose tissue (Fig. 4.1D). Taken together, these data strongly suggest AMPK activity is not influenced acutely by IL-6 in adipocytes. IL-6 may, however, influence AMPK activity in other tissues, particularly muscle during exercise by an as yet uncharacterised mechanism.

In addition to proinflammatory cytokines such as TNF-α and IL-1β, IL-6 has also been found to be upregulated in obese adipose tissue. In this study the temporal activation of downstream components of the IL-6 signalling pathway and their subsequent inhibition by AMPK was examined. Figure 4.2 demonstrated that the

IL-6/sIL-6Rα complex stimulated the JAK-STAT pathway in 3T3-L1 adipocytes, with increased phosphorylation of STAT3 Y705 over the duration of the experiment, peaking at 30 to 60 min of cytokine stimulation. In contrast, treatment with the IL-6/sIL-6Rα complex did not stimulate ERK1/2 T202/204 phosphorylation (Fig. 4.3). This is consistent with previous reports in 3T3-L1 adipocytes and isolated human adipocytes (Andersson et al. 2007, Rotter, Nagaev, and Smith 2003). A769662 significantly reduced IL-6-stimulated STAT3 phosphorylation (Fig. 4.2). Prior to this study, very little was known about the regulation of IL-6-stimulated inflammatory signalling by AMPK. Shortly after this study began, Nerstedt and co-workers reported that AICAR-mediated AMPK activation inhibited IL-6-stimulated inflammatory signalling in the human hepatocarcinoma cell line HepG2 via inhibition of STAT3 phosphorylation (Nerstedt et al. 2010). Moreover, it has recently been reported that both AICAR and metformin suppressed IL-6-stimulated STAT3 phosphorylation in both HepG2 and mouse liver cells (Nerstedt et al. 2013), thus data generated in the current study supports these published findings. In contrast, a recent study found that metformin, but not AICAR, reduced STAT3 phosphorylation in a STAT3-positive lung cancer cell line (Lin et al. 2013), thereby suggesting an AMPK-independent mechanism of metformin. Interestingly, adiponectin has been reported to suppress STAT3 S727 phosphorylation in an AMPK-dependent manner; however STAT3 Y705 was not examined (Wu et al. 2012). The role of serine phosphorylation of STAT3 is controversial: it has been reported to promote full transcriptional activation of STAT3 (Wen, Zhong, and Darnell 1995), while others propose that serine phosphorylation may negatively regulate STAT3 Y705 phosphorylation, dimerisation, nuclear translocation and subsequent transcriptional activity (Chung et al. 1997, Wakahara et al. 2012). In the current study STAT3 S727 phosphorylation was not altered by IL-6 or A769662 treatment in 3T3-L1 adipocytes or mouse embryonic fibroblasts (Fig. 4.9B and Fig. 4.10B, respectively); these data support similar findings recently reported by Nerstedt and co-workers, in which STAT3 S727 phosphorylation was not affected by acute IL-6, AICAR or metformin treatment in HepG2 cells (Nerstedt et al. 2013). In contrast, sustained (24 h) IL-6 treatment has been reported to induce STAT3 S727 phosphorylation in 3T3-L1 adipocytes, with a simultaneous increase in Y705 phosphorylation (Serrano-Marco et al. 2011). Taken together, the mechanism and consequences of serine phosphorylation of STAT3 are still poorly understood;

however these data suggest that IL-6 does not acutely stimulate STAT3 S727 phosphorylation in 3T3-L1 adipocytes.

In order to determine whether the ability of A769662 to suppress IL-6-stimulated STAT3 phosphorylation was dependent upon AMPK activation, the pharmacological inhibitor Compound C was utilised. Figure 4.4 suggested that the tendency toward A769662-mediated inhibition of STAT3 phosphorylation may be abolished in the presence of Compound C; however there was a high degree of variability associated with these particular experiments. This is likely due to the reduced number of replicates, as it was necessary to only select data where inhibition of AMPK activation by Compound C was also observed (Fig. 4.1A). As discussed in Chapter 3, results generated using Compound C should be interpreted with care as it has been found to inhibit other protein kinases. 3T3-L1 adipocytes are relatively intractable to transient transfection or infection with adenoviruses, as discussed in Chapter 3. siRNA-mediated knockdown of AMPKα1 in HUVECs ameliorated suppression of STAT3 phosphorylation by AICAR, relative to cells transfected with the scrambled control (Fig. 4.5). Furthermore, IL-6-stimulated STAT3 phosphorylation was reduced following activation of AMPK by rosiglitazone, AICAR and A769662. This further supports the AMPK dependence of inhibition of STAT3 phosphorylation as these compounds all activate AMPK via different mechanisms.

Adipose tissue obtained from *AMPKα1$^{-/-}$* and genetically matched wild-type mice provided further evidence for the anti-inflammatory role of AMPK in adipose tissue. Basal phosphorylation of STAT3 was found to be significantly increased in gonadal adipose tissue from *AMPKα1$^{-/-}$* mice compared to wild-type (Fig. 4.7), while there appeared to be a subtle increase in STAT3 phosphorylation in subcutaneous adipose tissue from *AMPKα1$^{-/-}$* mice compared to wild-type (Fig. 4.8). These data support the finding that adipose tissue from *AMPKα1$^{-/-}$* mice exhibited increased basal JNK phosphorylation compared to wild-type (Fig. 3.10 and 3.11). To our knowledge, this is the first time such an observation has been made in adipose tissue. Taken together, these data demonstrate for the first time that basal JNK and STAT3 signalling are increased in adipose tissue the absence of AMPKα1. This could suggest a role for AMPK in the suppression of basal cytokine synthesis or signalling; however it is important to note that adipose-specific

AMPKα1$^{-/-}$ mice do not currently exist, therefore these observations could be the result of secondary indirect effects from other tissues in which AMPKα1 is ablated.

Another member of the STAT family, STAT4, has recently been proposed to play a key role in the development of inflammation and insulin resistance in adipocytes. Dobrian and co-workers found that while STAT4-deficient mice developed obesity similar to their wild-type controls when challenged with a high-fat diet, they exhibited greater insulin sensitivity. Furthermore, they displayed improved adipocyte inflammation and insulin signalling (Dobrian et al. 2013). STAT4 is primarily activated by IL-12, and while the source and temporal production of IL-12 in WAT remains unclear (Knudsen and Lee 2013), this work further implicates the JAK/STAT pathway in the development of inflammation and insulin resistance in adipocytes.

mTOR is a serine/threonine kinase found as two structurally and functionally different complexes, mTORC1 and mTORC2, and regulates cell growth and proliferation, controlling energy-consuming processes such as mRNA translation and ribosomal biogenesis. The presence of amino acids are required for mTOR activation, while under low cellular energy conditions AMPK has been found to reduce mTOR activity, as measured by phosphorylation of downstream target p70 S6 kinase (Kimura et al. 2003). AMPK has been proposed to do so indirectly via phosphorylation of TSC2, a negative regulator of mTOR (Inoki, Zhu, and Guan 2003), or directly via raptor, a component of mTORC1 (Gwinn et al. 2008).

Studies utilising TSC2-deficient cells or siRNA-mediated knockdown of TSC2 have reported an increase in STAT3 Y705 and S727 phosphorylation; conversely, inhibition of mTOR with rapamycin ameliorated STAT3 phosphorylation with a subsequent reduction in transcriptional activity (Weichhart et al. 2008, Onda et al. 2002, Goncharova et al. 2009, Chen et al. 2012). It was of interest, therefore, to investigate the role of mTOR in the regulation of IL-6-stimulated STAT3 phosphorylation in adipocytes using the pharmacological mTORC1/2 inhibitor PP242. In the current study phosphorylation of STAT3 S727 was not found to be altered by PP242 treatment in either 3T3-L1 adipocytes or MEFs (Fig. 4.9B and Fig. 4.10B, respectively). mTORC1 has previously been reported to stimulate phosphorylation of STAT3 at S727 in CNTF-stimulated neuroblastoma cells (Yokogami et al. 2000), though as described above, the mechanism and the effects

of STAT3 serine phosphorylation are largely poorly understood. PP242-mediated mTOR inhibition significantly reduced IL-6-stimulated STAT3 Y705 phosphorylation in 3T3-L1 adipocytes (Fig. 4.9A) and A769662 had no further effect on PP242-mediated suppression of STAT3 phosphorylation (Fig. 4.9A). The same experiments performed in MEFs demonstrated a significant reduction in IL-6-stimulated STAT3 phosphorylation in response to A769662 (Fig. 4.10A); while inhibition of mTOR with PP242 induced a tendency toward a reduction in STAT3 phosphorylation ($p < 0.02$, two-tail t-test), and had no further effect on A769662-mediated inhibition (Fig. 4.10A). It can be seen in Fig 4.9C and 4.10C that PP242 successfully inhibited mTOR activity in both 3T3-L1 adipocytes and MEFs, respectively, as measured by p70 S6 kinase phosphorylation. A769662-mediated AMPK activation was not found to reduce phosphorylation of p70 S6 kinase in either cell type. This was unexpected as AMPK has been reported to suppress mTOR activation (Kimura et al. 2003); however basal levels of phosphorylated p70 S6 kinase were low due to the lack of serum in the experimental media.

To our knowledge, this is the first time mTOR inhibition has been linked to a reduction in STAT3 phosphorylation in adipocytes, and supports previous reports that inhibition of mTOR with rapamycin suppressed STAT3 phosphorylation in other cell types (Weichhart et al. 2008, Onda et al. 2002, Goncharova et al. 2009, Chen et al. 2012). It is not possible from these data to ascertain whether the reduction in IL-6-stimulated STAT3 phosphorylation previously observed with AMPK activation in 3T3-L1 adipocytes is mediated by mTOR inhibition, or whether AMPK activation and mTOR inhibition act independently to suppress STAT3 phosphorylation, as unusually, A769662 was not found to significantly reduce STAT3 phosphorylation in these experiments (Fig. 4.9A).

In order to further explore the mTOR pathway as a potential mechanism for inhibition of IL-6-stimulated STAT3 phosphorylation, TSC2-deficient MEFs were utilised together with genetically-matched wild-type cells. In order for the *TSC2*$^{-/-}$ MEFs to be viable and grow without undergoing premature senescence, they (in addition to the wild-type control cells) were generated as *p53*$^{-/-}$ (Zhang et al. 2003). If the inhibition of STAT3 Y705 phosphorylation by AMPK occurred at least in part via the TSC/mTOR pathway, a reduction in the degree of inhibition of STAT3 phosphorylation by AMPK when TSC2 is no longer present would be expected.

IL-6 stimulated STAT3 Y705 phosphorylation in both *TSC2*$^{+/+}$*p53*$^{-/-}$ and *TSC2*$^{-/-}$*p53*$^{-/-}$ MEFs, with further increased STAT3 phosphorylation in *TSC2*$^{-/-}$*p53*$^{-/-}$ MEFs compared with *TSC2*$^{+/+}$*p53*$^{-/-}$ (Fig. 4.11B). These data support numerous reports that STAT3 is hyper-activated in the absence of TSC2 (Weichhart et al. 2008, Onda et al. 2002, Goncharova et al. 2009, Chen et al. 2012), which is consistent with the constitutive activation of mTOR in the *TSC2 null* MEFs. A769662 was found to successfully activate AMPK in both *TSC2*$^{+/+}$*p53*$^{-/-}$ and *TSC2*$^{-/-}$*p53*$^{-/-}$ MEFs, as measured by ACC S79 phosphorylation (Fig. 4.11A); however IL-6-stimulated STAT3 phosphorylation was completely unaffected by AMPK activation, not only in *TSC2*$^{-/-}$*p53*$^{-/-}$ cells but also in *TSC2*$^{+/+}$*p53*$^{-/-}$ cells (Fig. 4.11B). This was unexpected, as it has previously been demonstrated in this study that A769662-mediated AMPK activation abolished IL-6-stimulated STAT3 phosphorylation in MEFs (Fig. 4.10). These findings implied a potential requirement for the presence of p53 in the AMPK-mediated inhibition of STAT3 phosphorylation. The relationship between AMPK and p53 in cancer is well established (Hardie 2004, Lee et al. 2012); however to our knowledge there have been no reports to suggest an interaction between AMPK and p53 is necessary for inhibition of inflammatory signalling. To investigate this further, an adenovirus overexpressing human wild-type p53 was utilised in order to determine whether p53 expression is necessary for the AMPK-mediated inhibition of STAT3 phosphorylation. Mouse and human p53 share a strong sequence homology, reported to be approximately 81 % (Zakut-Houri et al. 1985). IL-6 significantly stimulated STAT3 Y705 phosphorylation in both Ad.Null and Ad.p53 infected MEFs; however, this was not diminished in MEFs infected with either Ad.Null or Ad.p53 following AMPK activation (Fig. 4.12B). It has been reported that p53 may induce transcription of AMPKβ1 in human, but not in mouse (Feng et al. 2007); therefore is unlikely to underlie any potential effect of p53 in MEFs. The same study reported that TSC2 is also regulated by p53 in both human and mouse (Feng et al. 2007), so while it is possible that TSC2 may not be functioning properly in *TSC2*$^{+/+}$*p53*$^{-/-}$ MEFs, this is unlikely as Figure 4.9B demonstrated a tendency toward hyperphosphorylation of STAT3 in *TSC2*$^{-/-}$*p53*$^{-/-}$ relative to the wild-type *TSC2*$^{+/+}$*p53*$^{-/-}$ MEFs, indicating TSC2 is functional in the *TSC2*$^{+/+}$*p53*$^{-/-}$ MEFs. Moreover, if TSC2 was functionally impaired in the *TSC2*$^{+/+}$*p53*$^{-/-}$ MEFs, this would imply that TSC2 was essential for the A769662-mediated inhibition of STAT3 phosphorylation as A769662 had no effect on IL-6-stimulated STAT3 phosphorylation in *TSC2*$^{+/+}$*p53*$^{-/-}$ MEFs (Fig. 4.11B); however there is no

evidence to suggest this. AMPK was functional in *TSC2*$^{+/+}$*p53*$^{-/-}$ MEFs infected with either ad.null or ad.p53 adenoviruses, as measured by phosphorylation of ACC Ser79 (Fig. 4.12A); however, ACC was phosphorylated to a greater extent in *TSC2*$^{+/+}$*p53*$^{-/-}$ MEFs infected with ad.p53 adenovirus, relative to ad.null infected cells (Fig. 4.12A). This could suggest that AMPK activation was retarded in the absence of p53; however adenoviral-mediated p53 expression did not restore the ability of A769662 to inhibit IL-6-stimulated STAT3 phosphorylation. It is not possible to elucidate from these experiments whether the level of p53 expressed in the *TSC2*$^{+/+}$*p53*$^{-/-}$ MEFs infected with Ad.p53 was in line with endogenous p53, or that it was functional, as we were unable to examine MEFs from the original mice they were derived from. Therefore these data suggest that p53 may regulate the transcription of a gene involved in the AMPK-mediated inhibition of the JAK/STAT pathway, and that simply expressing p53 using adenovirus in *TSC2*$^{+/+}$*p53*$^{-/-}$ MEFs may not be sufficient to restore its function, possibly due to expression levels or species difference.

Taken together, these data suggest that both AMPK activation and mTOR inhibition suppress IL-6-stimulated STAT3 phosphorylation, and this is likely to occur via mutually exclusive mechanisms.

Protein phosphorylation and dephosphorylation are key processes which control the JAK/STAT pathway, mainly occurring at tyrosine residues and carried out by protein tyrosine kinases and protein tyrosine phosphatases (PTP), respectively (Shuai and Liu 2003, Tonks and Neel 2001). While the expression of some PTPs, including SHP-1 and CD45 are restricted to hematopoietic cells (Hermiston, Zikherman, and Zhu 2009), others such as TC-PTP, PTP1B and SHP-2 are more ubiquitously expressed (Xu and Qu 2008). In the current study it was of interest to investigate whether inhibition of IL-6-stimulated STAT3 phosphorylation by AMPK was mediated by the action of a phosphatase.

TC-PTP has been demonstrated to negatively regulate the JAK/STAT pathway via dephosphorylation of target substrates. JAK1 and JAK3 were reported to be directly dephosphorylated by TC-PTP (Simoncic et al. 2002), while Yamamoto and co-workers employed a similar substrate-trapping technique to identify STAT3 as a substrate for TC-PTP (Yamamoto et al. 2002). In line with JAK as a substrate for TC-PTP, TC-PTP was reported to suppress IL-2-stimulated STAT5 phosphorylation,

while conversely, TC-PTP-deficient lymphocytes exhibited increased STAT5 phosphorylation upon IL-2 treatment, compared to wild-type control cells (Simoncic et al. 2002). Two isoforms of TC-PTP exist: an endoplasmic reticulum-targeted 48 kDa form (TC48) and a nuclear 45 kDa form (TC45); overexpression of TC45 in 293T cells was reported to ameliorate IL-6-stimulated STAT3 phosphorylation (Yamamoto et al. 2002). Conversely, isolated hepatocytes deficient in TC-PTP displayed elevated STAT3 phosphorylation in response to IL-6 treatment compared to wild-type control cells (Fukushima et al. 2010). Furthermore, TC-PTP has recently been reported to be expressed in WAT (Loh et al. 2011). Interestingly, TC-PTP has recently been identified as a substrate of mTOR in a screen defining the mTOR-regulated phosphoproteasome (Hsu et al. 2011). In the current study pharmacological and genetic approaches were utilised to investigate whether TC-PTP mediated the inhibition of STAT3 phosphorylation by AMPK activation or mTOR inhibition observed in Figures 4.9 and 4.10.

Figure 4.13 demonstrated that inhibition of TC-PTP in 3T3-L1 adipocytes using a pharmacological inhibitor did not ameliorate the ability of AMPK to reduce IL-6-stimulated STAT3 phosphorylation. The inhibitor has been reported to confer specificity to TC-PTP as it was designed to recognise residues surrounding the active site, rather than the active site itself (Zhang et al. 2009); however these data should be interpreted with care as a positive control for these experiments did not exist. Similar observations were made in MEFs; IL-6-stimulated STAT3 phosphorylation was significantly ablated following AMPK activation in both wild-type and *TC-PTP*$^{-/-}$ MEFs (Fig. 4.14). As TC-PTP was identified as a substrate of mTOR (Hsu et al. 2011), it was of interest to ascertain whether the moderate reduction in STAT3 Y705 phosphorylation observed following mTOR inhibition could be attributed to TC-PTP. Inhibition of mTOR by PP242 suppressed IL-6-stimulated STAT3 phosphorylation in wild-type MEFs; however this was abolished in *TC-PTP*$^{-/-}$ MEFs (Fig. 4.15). Furthermore, protein expression of STAT3 was significantly increased in *TC-PTP*$^{-/-}$ MEFs compared to wild-type control cells (Fig. 4.15B); this is not unexpected, as these cells are deficient in a negative regulator of STAT3 signalling. Taken together, these data suggest that AMPK activation and mTOR inhibition both suppress IL-6-stimulated STAT3 Y705 phosphorylation via independent mechanisms. It is likely that the moderate reduction in STAT3 phosphorylation following mTOR inhibition may be mediated by TC-PTP, as

suppression of mTOR activity may relieve the inhibitory phosphorylation of TC-PTP, thereby facilitating the subsequent dephosphorylation of STAT3.

SH2-containing protein tyrosine phosphatase (SHP-2) is another ubiquitously expressed PTP which has been implicated in multiple signalling pathways downstream of a variety of growth factors and cytokines, including IL-6 (Neel and Tonks 1997). It has been reported to be involved in the Ras/Raf/MAPK, PI3 kinase, NFκB and JAK/STAT pathways, where it can either enhance or diminish signal transduction; thus is thought to have dual functions in growth factor and cytokine transduction (Kim and Baumann 1999). IL-6 signalling leads to the induction of both the SHP-2/ERK MAPK and JAK/STAT pathways with SHP-2 being proposed to play a role in the negative regulation of the JAK/STAT pathway via dephosphorylation of JAK and STAT proteins (You, Yu, and Feng 1999, Chen et al. 2003). *SHP-2*$^{-/-}$ fibroblasts have been reported to exhibit elevated IFN-γ-stimulated JAK1 phosphorylation (You, Yu, and Feng 1999), while SHP-2 has been found to dephosphorylate STAT5 in the cytoplasm; conversely, this is inhibited in *SHP-2*$^{-/-}$ cells (Chen et al. 2003).

The compound curcumin has been reported to suppress LPS- and IFN-γ-stimulated phosphorylation of JAK1, JAK2, STAT1 and STAT3 via activation of SHP-2 in brain microglial cells (Kim et al. 2003). Interestingly, curcumin was later identified to elicit many of its anti-inflammatory effects via activation of AMPK in a variety of cells (Kim et al. 2009, Yu et al. 2008, Xiao et al. 2013). In contrast, it has recently been reported that both AICAR and metformin reduced IL-6-stimulated SHP-2 phosphorylation in HepG2 cells (Nerstedt et al. 2013). In the current study, pharmacological inhibition of SHP-2 in 3T3-L1 adipocytes did not attenuate the AMPK-mediated inhibition of IL-6-stimulated STAT3 phosphorylation (Fig. 4.16). The role of SHP-2 in signal transduction is complex, as it plays a role as both a positive and a negative regulator of different pathways depending on the stimuli, and compared to tyrosine kinases, much less is known regarding the actions of particular PTPs on specific pathways in response to different stimuli. Previous reports suggesting that SHP-2 dephosphorylated components of the JAK/STAT pathway involved stimulation with IFN-γ or IL-3 rather than IL-6 (You, Yu, and Feng 1999, Chen et al. 2003). It is possible IL-6 may not stimulate the SHP/ERK arm in 3T3-L1 adipocytes; a suggestion supported by Figure 4.3, which demonstrated a

lack of ERK1/2 activation by IL-6. These data lack direct evidence, however, that SHP-2 was activated by IL-6 in these cells. It is also possible that AMPK simply may not have any effect on the action of SHP-2 in 3T3-L1 adipocytes. As with previous data (Fig. 4.13), there was no positive control for this experiment demonstrating the inhibition of SHP-2 by NSC 87877, therefore data should be interpreted with care.

Taken together, it appeared that the mechanism by which AMPK inhibited IL-6-stimulated STAT3 phosphorylation may not have been via the action of a phosphatase. In order to further confirm this, 3T3-L1 adipocytes were incubated with the tyrosine phosphatase inhibitor sodium orthovanadate. If AMPK-mediated inhibition of STAT3 phosphorylation was indeed mediated via the action of a tyrosine phosphatase, then this would be expected to be abolished upon incubation with a phosphatase inhibitor. Figure 4.17 demonstrated that inhibition of PTPs with sodium orthovanadate did not ablate the AMPK-mediated suppression of IL-6-stimulated STAT3 phosphorylation. STAT3 phosphorylation was significantly increased following incubation with IL-6 in combination with sodium orthovanadate; this was not unexpected, as tyrosine phosphorylation was being maintained. Furthermore, probing the cell lysates with anti-phosphotyrosine confirmed that sodium orthovanadate effectively blocked tyrosine dephosphorylation (Fig. 4.17C). Taken together, these data have demonstrated that AMPK inhibited IL-6-stimulated STAT3 phosphorylation via a mechanism independent of protein tyrosine phosphatases.

Next, this study sought to determine whether the mechanism underlying the inhibition of STAT3 phosphorylation by AMPK involved regulation of the upstream JAKs. During the course of this study, to our knowledge there was no evidence in the literature regarding the effect of AMPK on JAK regulation; indeed evidence concerning the regulation of proinflammatory IL-6 signalling by AMPK was sparse, and virtually non-existent in adipocytes. Proteasomal degradation of JAK has been suggested to negatively regulate the JAK/STAT pathway (Yu and Burakoff 1997); however no difference in total protein level of JAK1 or JAK2 was observed following AMPK activation with A769662 in this study (Fig. 4.18B and 4.18D). These data support a recent study in which JAK1 and JAK2 protein levels were unaffected by AICAR or metformin in HepG2 cells (Nerstedt et al. 2013). Relatively few studies exist focussing on the expression, activation and function of JAKs in adipocytes;

however there is evidence suggesting JAK1 and JAK2 are expressed at similar levels in 3T3-L1 adipocytes (Stewart et al. 1999), and have been found to be expressed in adipose tissue *in vivo* (Hellgren et al. 2001). Furthermore, JAK3 and Tyk2 have also been reported to be expressed in adipose tissue (Hellgren et al. 2001, Derecka et al. 2012); however adipose tissue is comprised of several cell types as discussed previously (1.1.1), therefore these proteins are not necessarily expressed in adipocytes *in vivo*. In the current study, JAK1 phosphorylation remained unaltered following incubation with IL-6 or A769662 (Fig. 4.18C). Curiously, immunoblotting of 3T3-L1 lysates with anti-JAK2 Y1007/1008 revealed a band of around 70-75 kDa in size (4.18E), while JAK2 has a predicted mass of 125 kDa. This unknown band appeared to resolve at a mass similar to STAT3 and followed a similar pattern as observed in Figure 4.2. To further investigate this, JAK2 was immunoprecipitated from lysates where 3T3-L1 adipocytes had been incubated with or without IL-6/sIL-6Rα for 15 min. Immunoblotting revealed bands corresponding to 125 kDa, indicating JAK2 had been successfully immunoprecipitated; however there appeared to be a slight decrease in JAK2 in the presence of IL-6 compared to vehicle. This was consistent with a subtle increase in JAK2 detected in the corresponding immunodepleted lysate. Phosphorylated JAK2 was detected in the immunoprecipitate at a mass which coincided with that observed with total JAK2. The level appeared diminished in the presence of IL-6 relative to vehicle, which was the converse of what would be expected; however this was consistent with the appearance of reduced total JAK2 immunoprecipitated from this sample. Interestingly, the unknown band previously observed with IL-6 treatment in the lysate was also present in the immunoprecipitate when immunoblotted with anti-JAK2 Y1007/1008. Taken together, these data indicate the presence of a protein closely associated with phospho-JAK2, which was of a molecular mass comparable to STAT3 and responded to IL-6 and A769662 in a similar manner to STAT3. Curiously, JAK2 Y1007/1008 was observed at the predicted molecular mass of 125 kDa in HEK-293 and HeLa cell lysates (Fig. 4.20 and 4.21), suggesting JAK2 Y1007/1008 may be recognised in cell lines derived from human and not mouse.

To further address the role of JAK2 in the AMPK-mediated inhibition of STAT3 phosphorylation, a mutant JAK2 was utilised, whereby the valine at position 617 had been mutated to a phenylalanine, rendering it essentially constitutively

active. JAKs are composed of seven JH (JAK homology) domains: the JH3-7 segment of the protein contains a FERM and SH2 domain, and is essential for receptor binding. At the C-terminus, JH1 is a catalytically active tyrosine kinase (Feng et al. 1997), while the adjacent JH2 pseudokinase domain suppresses the basal kinase activity of the JH1 domain (Saharinen, Takaluoma, and Silvennoinen 2000, Saharinen and Silvennoinen 2002). Upon ligand binding, JAK2 undergoes a conformational change, which through a currently unknown mechanism prevents the inhibitory JH2 domian from interacting with JH1, and orientates the JAK2 proteins such that the activation loop can be phosphorylated by the adjacent JAK2. Once this transphosphorylation is complete, the activated JAKs then phosphorylate tyrosine residues on the cytoplasmic tails of the receptor, creating docking sites for SH2 domain-containing proteins such as STATs (Darnell, Kerr, and Stark 1994). It is thought that the JAK2 V617F mutation disrupts inhibition of JH1 by JH2, as the activation loop of JH1 becomes extended and is transphosphorylated by an adjacent JAK2 V617F kinase without any requirement for ligand binding (Lu et al. 2005). For this to occur, the JAK2 V617F proteins must be physically close to each other, therefore this mutant is not strictly constitutively active as the proteins still require the presence of the receptor (Lu et al. 2005).

If AMPK-mediated inhibition of STAT3 phosphorylation was dependent upon inhibition of JAK2 activation, then this would be expected to be abolished when JAK2 could no longer be inactivated. A769662 significantly stimulated AMPK activation in HEK-293 cells transfected with the active mutant JAK2 V617F or the empty plasmid control as measured by ACC Ser79 phosphorylation (Fig. 4.20A). Figure 4.20B demonstrated significant upregulation of JAK2 Y1007/1008 phosphorylation upon transfection with the active mutant, which was not reduced with AMPK activation. Moreover, AMPK activation failed to reduce the JAK2 V617F-induced phosphorylation of STAT3 and STAT5 (Fig. 4.20C and 4.20D). Unexpectedly, incubation with IL-6/sIL-6Rα did not stimulate STAT3 phosphorylation in HEK-293 cells (Fig. 4.20E); therefore while these data clearly indicated that suppression of JAK was required for the AMPK-mediated inhibition of STAT3 phosphorylation, it could not be demonstrated that this was the mechanism by which AMPK inhibited IL-6-stimulated STAT3 phosphorylation. Transfection of HeLa cells, which did respond to IL-6/sIL-6Rα, with the active

JAK2 mutant generated data which supported the observations made in HEK-293 cells. AMPK activation reduced IL-6-stimulated STAT3 phosphorylation in empty plasmid, mock and untransfected HeLa cells, but had no effect on basal or IL-6-stimulated STAT3 phosphorylation in JAK2 V617F mutant-transfected HeLa cells (Fig. 4.21). Interestingly, incubation with IL-6/sIL-6Rα in JAK2 V617F mutant-transfected cells further increased STAT3 phosphorylation, relative to the basal level (Fig. 4.21), thus indicating incomplete transfection efficiency. Taken together, these data suggest that AMPK does not inhibit STAT3 phosphorylation directly, and is likely to be dependent upon inhibition of JAK activity. Furthermore, these data support a very recent study by Nerstedt and co-workers, which reported an AICAR-mediated inhibition of JAK1 and JAK2 phosphorylation in HepG2 cells (Nerstedt et al. 2013). Conversely, IL-6-stimulated JAK1 phosphorylation was enhanced following siRNA-mediated knockdown of AMPK, further supporting the inhibitory role of AMPK in this pathway (Nerstedt et al. 2013). Finally, Kim and co-workers recently suggested that the mechanism by which long-term AMPK activation may suppress IL-6 signalling in the liver is via induction of the orphan nuclear receptor small heterodimer partner (SHP). They reported that the metformin-mediated induction of SHP caused a direct interaction between SHP and the DNA-binding domain of STAT3, thus blocking recruitment of STAT3 to target gene promoters, such as Socs3, thereby attenuating IL-6 signalling (Kim et al. 2012). It is possible that acute and sustained AMPK activation could differentially modulate the JAK/STAT pathway.

Overall, this current study has demonstrated for the first time in adipocytes that activation of AMPK suppresses IL-6-stimulated STAT3 phosphorylation, potentially via inhibition of JAK activity. Furthermore, this study has demonstrated for the first time that inhibition of mTOR also reduced IL-6-stimulated STAT3 phosphorylation via a mutually exclusive mechanism, possibly involving the phosphatase TC-PTP.

Chapter 5 - Functional effects of AMPK on inflammatory signalling

5.1 Introduction

5.1.1 Proinflammatory adipocytokines and obesity

Obesity is associated with the chronic, low-level inflammation of WAT. Briefly, adipocytes become hypertrophic and dysfunctional which can lead to the secretion of proinflammatory cytokines and chemokines, such as TNF-α, IL-1β, IL-6 and MCP-1. The induction of proinflammatory signalling pathways in addition to increased necrosis of adipocytes in obese WAT can result in the recruitment of macrophages. Upon migration into adipose tissue, macrophages undergo a shift in polarisation from an anti-inflammatory 'alternatively activated' M2 state, to a 'classically activated' proinflammatory M1 state; M1 macrophages are key producers of proinflammatory mediators in adipose tissue (Olefsky and Glass 2010). The variety of proinflammatory cytokines and chemokines secreted by both macrophages and adipocytes in obese WAT give rise to a complex proinflammatory profile, with the interplay between adipocytes and macrophages being central to the development of inflammation within the tissue. The chronic low-grade proinflammatory environment within obese adipose tissue has been reported to have a negative effect on whole body insulin sensitivity, with elevated levels of proinflammatory mediators in obese WAT associated with insulin resistance (Shoelson, Herrero, and Naaz 2007).

5.1.2 Consequences of AMPK-mediated inhibition of inflammation

In addition to inhibition of proinflammatory signalling pathway intermediates, AMPK activation has also been reported to influence cytokine production in a variety of cell types, including inhibition of TNF-α, IL-1β and IL-6 synthesis in macrophages (Yang et al. 2010, Sag et al. 2008, Jeong et al. 2009). AICAR-mediated AMPK activation was reported to stimulate an increase in adiponectin gene expression in human SCAT cultured *ex vivo* (Lihn et al. 2004). Furthermore, AMPK has been proposed to promote macrophage polarisation towards an anti-

inflammatory, M2 phenotype; a key study by Sag and co-workers utilised RNA interference and viruses expressing a constitutively active or dominant negative AMPK mutant in order to demonstrate that macrophages displayed an M1 phenotype and produced proinflammatory cytokines in the absence of AMPK, which was reversed when AMPK was constitutively active (Sag et al. 2008). It is well established that inflammation in obese adipose tissue is associated with insulin resistance (Guilherme et al. 2008, Schenk, Saberi, and Olefsky 2008), while AMPK activation has been suggested to improve insulin sensitivity in skeletal muscle and liver, with reduced AMPK activity or impaired AMPK activation being reported in skeletal muscle of obese, insulin resistant individuals (Bandyopadhyay et al. 2006, Sriwijitkamol et al. 2007). Furthermore, muscle-specific transgenic mice expressing an inactive form of the AMPKα2 catalytic subunit exhibited exacerbated HFD-induced insulin resistance compared to the wild-type control (Fujii et al. 2008). In adipocytes, however, AMPK has been reported to exert opposing effects, with Salt and co-workers demonstrating an inhibition of insulin-stimulated glucose uptake in 3T3-L1 adipocytes in response to AICAR (Salt, Connell, and Gould 2000). To our knowledge, there have been no reports elucidating the impact of AMPK activation on inflammation-mediated insulin resistance in adipocytes.

5.1.3 Aims

While it has been established in the current study that activation of AMPK in adipocytes inhibited phosphorylation and activation of several components of the NFκB, MAPK and JAK/STAT pathways in response to proinflammatory cytokines TNF-α, IL-1β and IL-6, it was of interest to examine the functional effects of AMPK activation on proinflammatory signalling. In the current study the effect of AMPK on cytokine and chemokine production in 3T3-L1 adipocytes and macrophages was assessed. Furthermore, the effect of individual proinflammatory cytokines or conditioned medium from activated macrophages on insulin-stimulated glucose uptake in 3T3-L1 adipocytes was determined. Finally, adipose tissue from *AMPKα1*$^{-/-}$ and litter-matched wild-type mice was examined to assess adipocyte cell size.

5.2 Results

5.2.1 Downstream effects of AMPK on the IL-6 signalling pathway

Suppressor of Cytokine Signalling-3 (SOCS3) is induced by IL-6 and acts as a negative regulator of the IL-6 signalling pathway, while another protein reported to be upregulated as a result of IL-6 signalling in many tissues is the transcription factor C/EBPβ, which plays a role in adipogenesis and immune functions; therefore it was of interest to investigate whether activation of AMPK affected expression of these downstream proteins. To examine whether AMPK altered IL-6-stimulated SOCS3 or C/EBPβ expression in 3T3-L1 adipocytes, cells were incubated with IL-6/sIL-6Rα in the presence or absence of A769662 following treatment with the proteasome inhibitor MG132. MG132 was utilised to reduce degradation of SOCS3 and C/EBPβ by the proteasome. The extent of SOCS3 or C/EBPβ protein expression was determined by western blotting analysis of 3T3-L1 adipocyte lysates. Incubation of 3T3-L1 adipocytes with IL-6/sIL-6Rα in the absence of A769662 caused a significant ($p < 0.01$) increase, compared to the basal level, in SOCS3 expression (Fig. 5.1A). Preincubation with A769662 had no effect on SOCS3 expression, relative to IL-6/sIL-6Rα treatment alone (Fig. 5.1A). Incubation of 3T3-L1 adipocytes with IL-6/sIL-6Rα did not significantly increase expression of C/EBPβ relative to the basal level (Fig. 5.1B). Similarly, preincubation with A769662 had no effect on C/EBPβ expression, relative to IL-6/sIL-6Rα treatment alone (Fig. 5.1B).

5.2.2 Effect of AMPK on cytokine-stimulated MCP-1 gene expression in 3T3-L1 adipocytes

To determine whether AMPK activation influenced the induction of MCP-1 gene expression by proinflammatory stimuli, RNA extracted from 3T3-L1 adipocytes incubated with TNF-α or IL-6/sIL-6Rα in the presence or absence of A769662 was reverse transcribed, and the extent of MCP-1 expression examined by semi-quantitative PCR using murine MCP-1 primers.

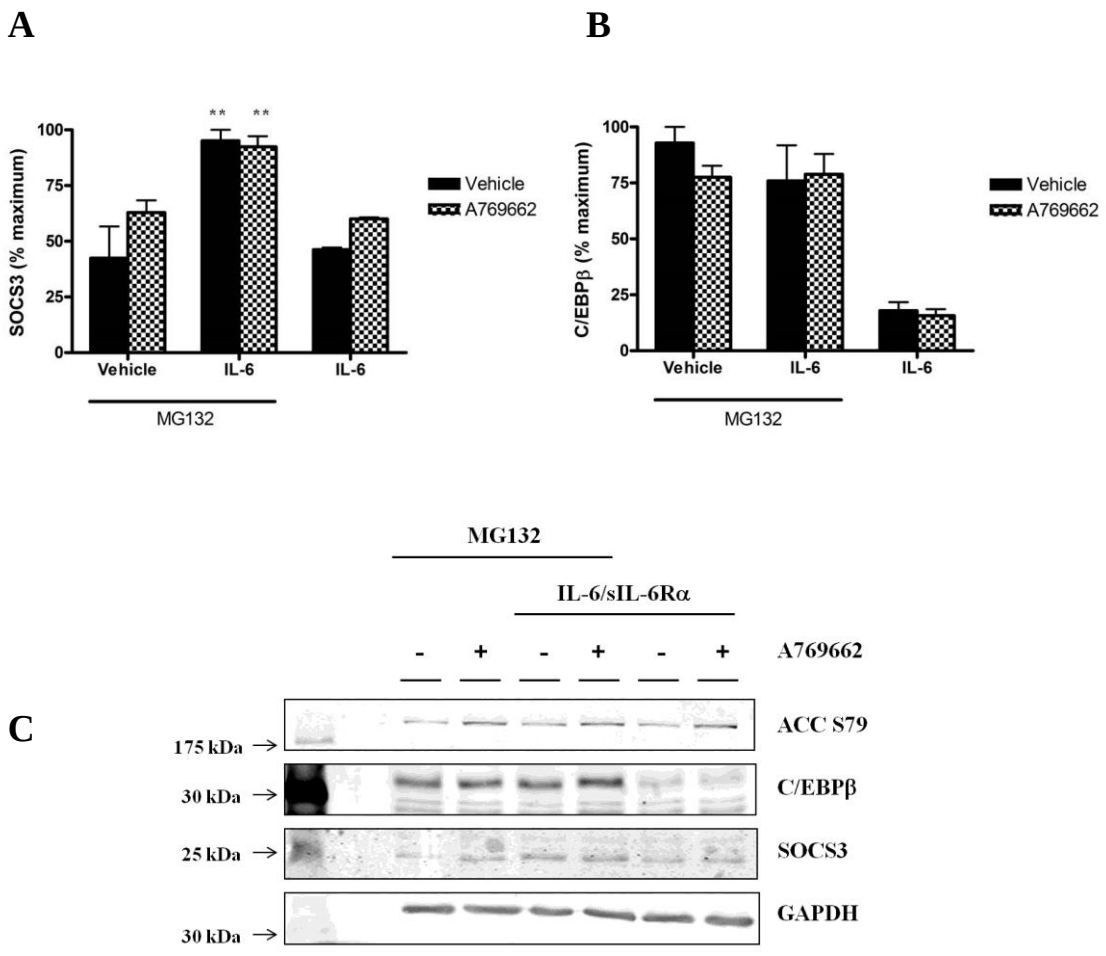

Figure 5-1: Effect of AMPK on IL-6-stimulated SOCS3 and C/EBPβ expression in 3T3-L1 adipocytes

*3T3-L1 adipocytes were incubated with IL-6/sIL-6Rα (5 ng/ml; 25 ng/ml) in the presence or absence of MG132 (6 μM) for 6 h following preincubation for 30 min in the presence or absence of A769662 (300 μM) and lysates prepared. Lysates were resolved by SDS-PAGE and subjected to immunoblotting with the antibodies indicated. (A) Quantification of SOCS3 expression relative to GAPDH was determined using densitometric analysis. Data shown represent the mean $\pm$ SEM % maximum SOCS3 expression of three independent experiments. **p < 0.01 (one-way ANOVA), increase in SOCS3 expression, relative to absence of IL-6. (B) Quantification of C/EBPβ expression relative to GAPDH was determined using densitometric analysis. Data shown represent the mean $\pm$ SEM % maximum C/EBPβ expression of three independent experiments. (C) Representative western blot.*

Incubation of 3T3-L1 adipocytes with TNF-α (6 h) in the absence of A769662 stimulated a significant ($p < 0.001$) increase compared to the basal level, in MCP-1 gene expression (Fig. 5.2A). Preincubation with A769662 caused a significant ($p < 0.01$) reduction in MCP-1 gene expression, compared to TNF-α treatment alone (Fig. 5.2A).

Incubation of 3T3-L1 adipocytes with IL-6/sIL-6Rα (6 h) in the absence of A769662 caused a significant ($p < 0.05$) increase compared to the basal level, in MCP-1 gene expression (Fig. 5.2C). MCP-1 gene expression was significantly ($p < 0.01$) reduced following preincubation with A769662, compared to IL-6/sIL-6Rα treatment alone (Fig. 5.2C).

5.2.3 Effect of AMPK on endogenous macrophage marker gene expression in murine adipose tissue

To examine the role of AMPK on the basal gene expression of markers of macrophage activation in adipose tissue, gonadal and subcutaneous adipose tissue was collected from female *AMPKα1*$^{-/-}$ and litter-matched wild-type sv129 mice. The extent of TNF-α and NOS2 (nitric oxide synthase 2) gene expression were assessed as markers of M1 macrophage activation and ARG1 (arginase 1), RELM-α (resistin like-α) and CHI313 (chitinase like lectin) gene expression were assessed as markers of M2 macrophage activation using quantitative PCR. Data is presented as fold change values ($2^{-\Delta\Delta CT}$) with expression relative to an endogenous control (TBP) and wild-type gonadal adipose. These data were generated and analysed by Dr Anna White (University of Glasgow). Subcutaneous or gonadal adipose tissue expression of TNF-α (Fig. 5.3A, 5.3B), NOS2 (Fig. 5.3C, 5.3D), ARG1 (Fig. 5.3E, 5.3F), RELM-α (Fig. 5.3G, 5.3H) and CHI313 (Fig. 5.3I, 5.3J) in *AMPKα1*$^{-/-}$ adipose tissue were not significantly altered compared to expression levels in wild-type adipose tissue.

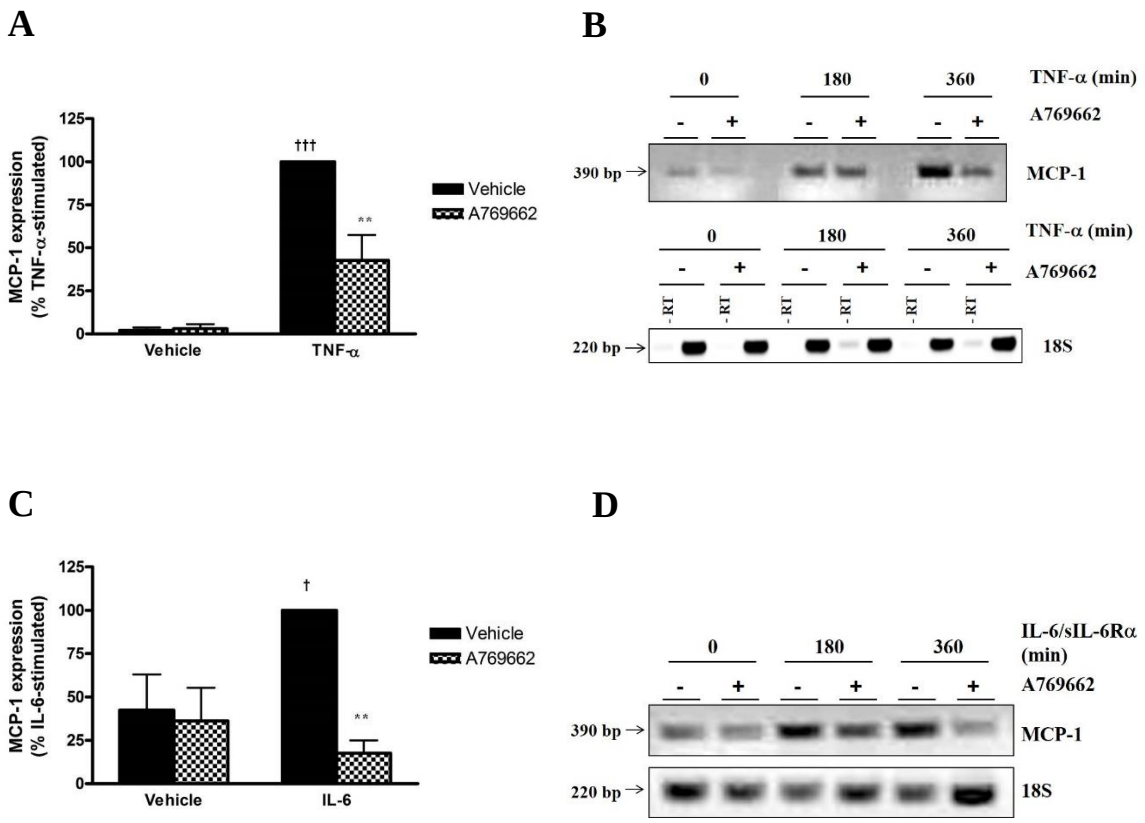

Figure 5-2: Effect of A769662 on TNF-α or IL-6-stimulated MCP-1 gene expression

3T3-L1 adipocytes were incubated with (A & B) TNF-α (10 ng/ml) or (C & D) IL-6/sIL-6Rα (5 ng/ml; 25 ng/ml) for 3 or 6 h following preincubation for 30 min in the presence or absence of A769662 (300 μM) and RNA prepared. RNA was reverse transcribed, with subsequent cDNA amplified by PCR using MCP-1 primers and resolved by agarose gel electrophoresis. (A & C) Quantification of MCP-1 expression was determined relative to 18S using densitometric analysis. (A) Data shown represent the mean ± SEM % 6h TNF-α-stimulated MCP-1 expression of three independent experiments. $^{\dagger\dagger\dagger}p < 0.001$ (one-way ANOVA), increase in MCP-1 expression, relative to vehicle. $^{**}p < 0.01$ (one-way ANOVA), reduction in MCP-1 expression, relative to the absence of A769662. (B) Representative agarose gel image. RT, reverse transcriptase. (C) Data shown represent the mean ± SEM % 6h IL-6-stimulated MCP-1 expression of four independent experiments. $^{\dagger}p < 0.05$ (one-way ANOVA), increase in MCP-1 expression, relative to vehicle. $^{**}p < 0.01$ (one-way ANOVA), reduction in MCP-1 expression, relative to the absence of A769662. (B) Representative agarose gel image.

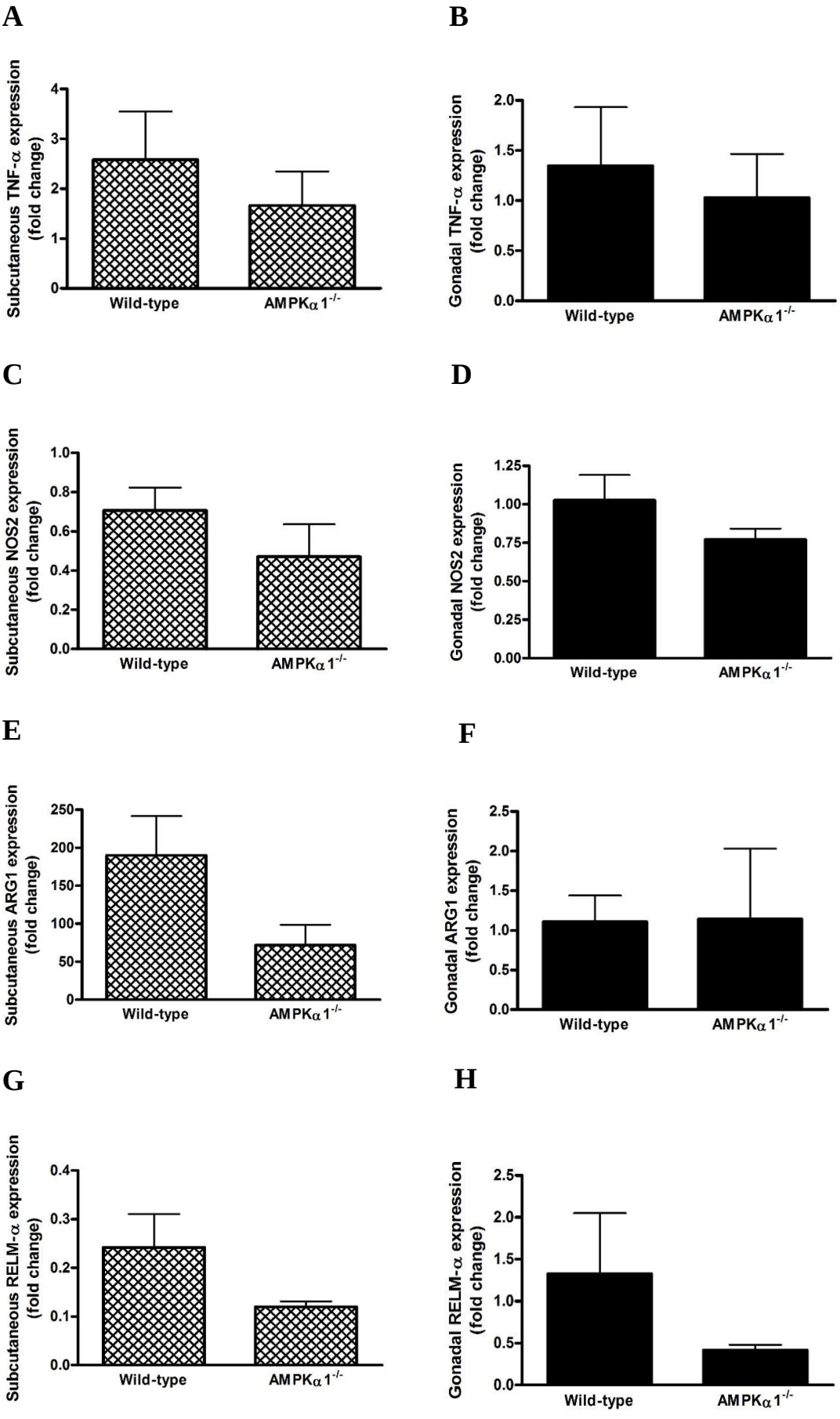
A
Subcutaneous TNF-α expression (fold change)
0
1
2
3
4
Wild-type
AMPKα1-/-
B
Gonadal TNF-α expression (fold change)
0.0
0.5
1.0
1.5
2.0
Wild-type
AMPKα1-/-
C
Subcutaneous NOS2 expression (fold change)
0.0
0.2
0.4
0.6
0.8
1.0
Wild-type
AMPKα1-/-
D
Gonadal NOS2 expression (fold change)
0.00
0.25
0.50
0.75
1.00
1.25
Wild-type
AMPKα1-/-
E
Subcutaneous ARG1 expression (fold change)
0
50
100
150
200
250
Wild-type
AMPKα1-/-
F
Gonadal ARG1 expression (fold change)
0.0
0.5
1.0
1.5
2.0
2.5
Wild-type
AMPKα1-/-
G
Subcutaneous RELM-α expression (fold change)
0.0
0.1
0.2
0.3
0.4
Wild-type
AMPKα1-/-
H
Gonadal RELM-α expression (fold change)
0.0
0.5
1.0
1.5
2.0
2.5
Wild-type
AMPKα1-/-

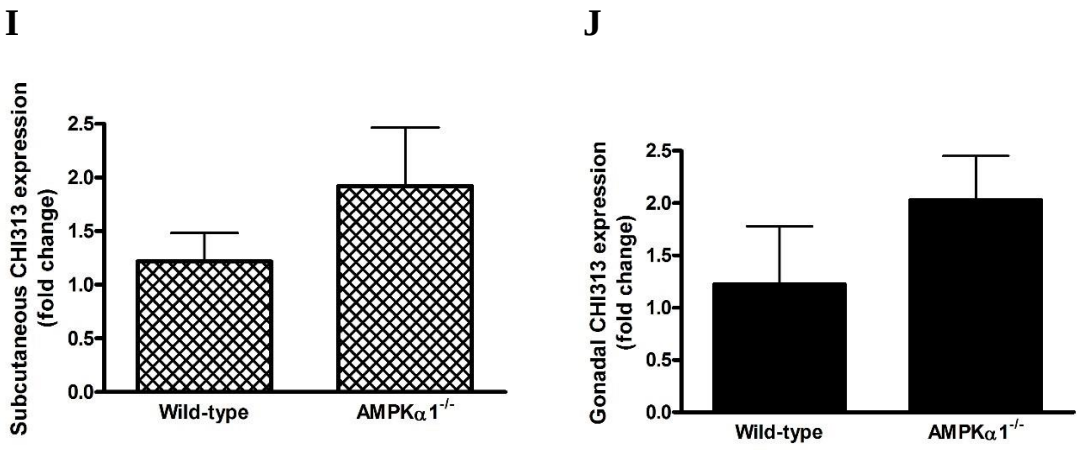

Figure 5-3: Effect of *AMPKα1$^{-/-}$* on basal macrophage marker gene expression in mouse adipose tissue

Adipose tissue was obtained from AMPKα1$^{-/-}$ and wild-type mice and RNA prepared. RNA was reverse transcribed, with subsequent cDNA amplified by qPCR using macrophage marker primers. Data shown represent the mean ± SEM fold change (A) TNF-α, (C) NOS2, (E) ARG1, (G) RELM-α, (I) CHI313 expression in subcutaneous adipose tissue of five wild-type and 3 AMPKα1$^{-/-}$ mice and (B) TNF-α, (D) NOS2, (F) ARG1, (H) RELM-α, (J) Chi313 expression in gonadal adipose tissue of five wild-type and three AMPKα1$^{-/-}$ mice. Macrophage marker expression was normalised to TBP and quantification determined relative to mean wild-type gonadal adipose. Data generated and analysed by Dr Anna White (University of Glasgow).

5.2.4 Effect of AMPK and proinflammatory cytokines on protein secretion

5.2.4.1 Adiponectin secretion in 3T3-L1 adipocytes

In order to investigate the effect of AMPK activation or proinflammatory cytokine stimulation on secretion of adiponectin, 3T3-L1 adipocytes were incubated with TNF-α or IL-6/sIL-6Rα in the presence or absence of A769662, and secretory proteins precipitated. The extent of adiponectin secretion was assessed by western blotting.

Incubation of 3T3-L1 adipocytes with A769662 caused a subtle, but significant ($p < 0.05$; two-tail t-test) increase, compared to the basal level, in adiponectin secretion (Fig. 5.4A). When analysed together with the entire data set (one-way ANOVA), this significance was lost (Fig. 5.4B). Incubation with TNF-α caused a subtle reduction in adiponectin secretion, compared to the basal level, which appeared to be increased following preincubation with A769662 ($p < 0.05$; two-tail t-test); however this did not reach significance when analysed using one-way ANOVA (Fig. 5.4B). Incubation with IL-6/sIL-6Rα did not alter adiponectin secretion (Fig. 5.4B).

5.2.4.2 Proinflammatory cytokine and chemokine production

This study has thus far demonstrated that AMPK activation in 3T3-L1 adipocytes ameliorated phosphorylation of cytokine-stimulated NFκB, MAPK and JAK/STAT signalling pathway intermediates, NFκB nuclear translocation and MCP-1 gene expression. It was of interest, therefore, to investigate the effect of A769662-mediated AMPK activation on the secretion of chemokines and cytokines. Concentrations of the chemokines IP-10 (CXCL10), KC (CXCL1), MCP-1 (CCL2), MIG (CXCL9), MIP-1α (CCL3) and the cytokines basic-FGF, GM-CSF, IFN-γ, IL-1α, IL-1β, IL-2, IL-4, IL-5, IL-6, IL-10, IL-12 (p40/p70), IL-13, IL-17, TNF-α and VEGF were assessed in 3T3-L1 CAR adipocytes infected with an empty vector or RAW 264.7 macrophages following proinflammatory stimulation using a murine cytokine/chemokine multiplex bead immunoassay and a Luminex® 100™ detection system (see 2.2.15).

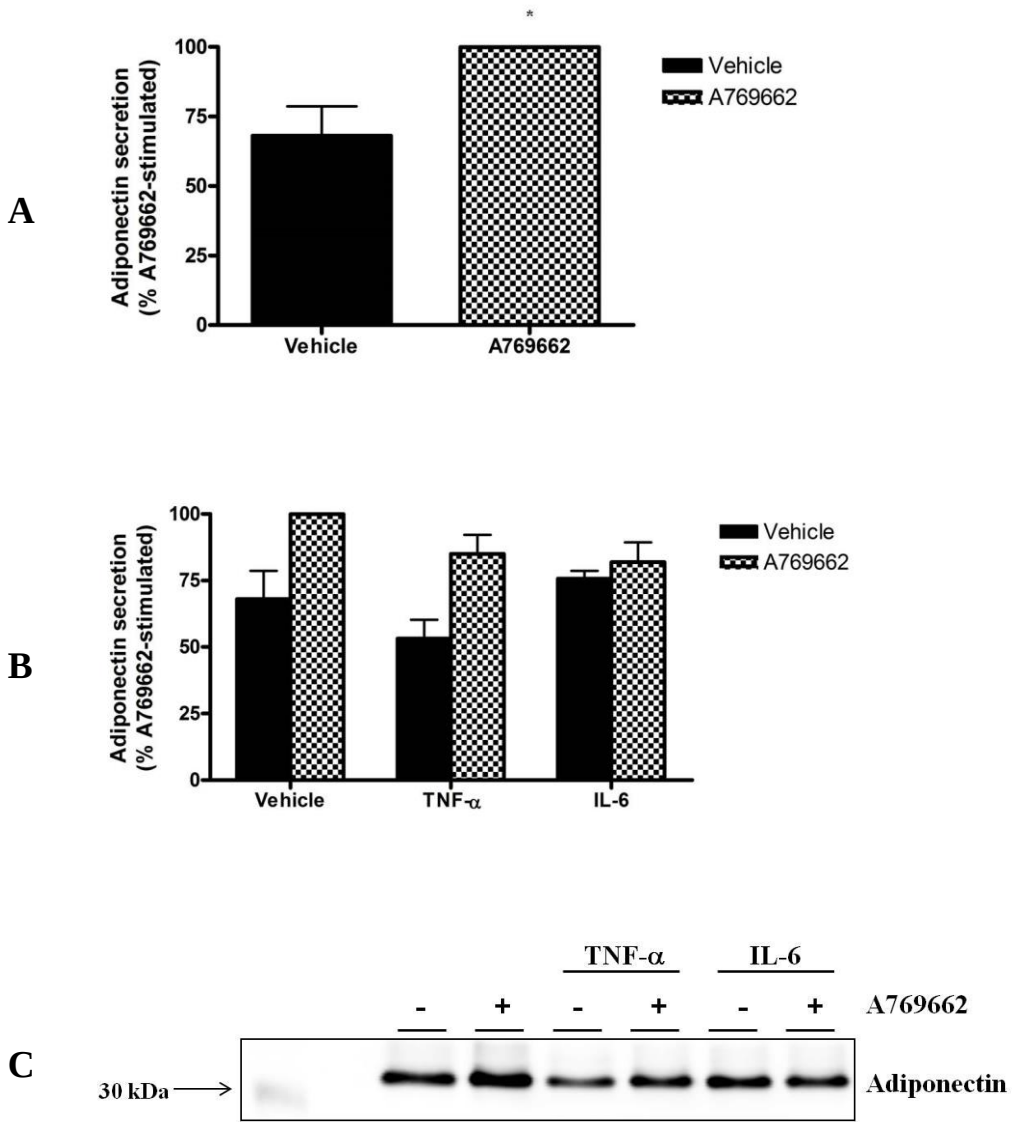

Figure 5-4: Effect of A769662, TNF-α or IL-6 on adiponectin secretion

*3T3-L1 adipocytes were incubated with IL-6/sIL-6Rα (5 ng/ml; 25 ng/ml) or TNF-α (10 ng/ml) for 6 h following preincubation for 30 min in the presence or absence of A769662 (300 μM) and secreted proteins precipitated from incubation media as described in section 2.2.16. Secreted proteins were resolved by SDS-PAGE and subjected to immunoblotting with anti-Acrp30. (A & B) Quantification of adiponectin secretion was determined using densitometric analysis. Data shown represent the mean ± SEM % A769662-stimulated adiponectin secretion of three independent experiments. *p < 0.05 (two-tail t-test), increase in adiponectin secretion, relative to absence of A769662. (C) Representative western blot.*

3T3-L1 adipocytes were incubated with IL-1β or IL-6/sIL-6Rα in the presence or absence of A769662 in order to determine the extent of cytokine/chemokine production. Analysis of cytokine/chemokine secretion showed that unstimulated or IL-6-stimulated 3T3-L1 CAR adipocytes did not produce measurable levels of any of the cytokine or chemokines listed above; however IP-10, KC and MCP-1 were found to be secreted at levels within the detection limits of the assay by 3T3-L1 adipocytes in response to IL-1β stimulation. IP-10 secretion was in the range of 52-398 pg/h/10^6 cells, KC secretion was in the range of 16-287 pg/h/10^6 cells and MCP-1 secretion was in the range of 16-30 pg/h/10^6 cells. IL-1β caused a significant ($p < 0.001$) increase in IP-10, KC and MCP-1 secretion in 3T3-L1 adipocytes, relative to the basal level (Fig. 5.5A, 5.5B and 5.5C, respectively). Preincubation with A769662 abolished secretion of IP-10, KC and MCP-1 ($p < 0.001$) (Fig. 5.5A, 5.5B and 5.5C, respectively). Furthermore, IL-1β and IL-6 were undetectable in the supernatant, indicating the stimuli were sufficiently washed away prior to the collection of the conditioned medium.

In order to determine the effect of AMPK on the extent of cytokine/chemokine production in activated macrophages, RAW 264.7 macrophages were incubated with LPS in the presence or absence of A769662. Analysis of cytokine/chemokine secretion showed that macrophages secreted measurable levels of IL-5 (152-520 pg/h/10 cm diameter dish), TNF-α (160-1916 pg/h/10 cm diameter dish), MCP-1 (602-2415 pg/h/10 cm diameter dish) and MIP-1α (3056-22124 pg/h/10 cm diameter dish). Levels of the other cytokines and chemokines detailed above were not detected within the limits of the assay. LPS caused a significant ($p < 0.001$) increase in IL-5, MCP-1 and MIP-1α secretion in macrophages, relative to the basal level (Fig. 5.6A, 5.6B and 5.6C, respectively). Preincubation with A769662 significantly ($p < 0.01$) reduced both IL-5 (60 ± 14.7 %) and MCP-1 (47 ± 17.1 %) secretion relative to LPS treatment alone (Fig. 5.6A and 5.6B, respectively). Preincubation with A769662 caused a subtle (33 ± 17.9 %) reduction in LPS-stimulated MIP-1α secretion; however this did not reach significance (Fig. 5.6C). LPS treatment induced a significant ($p < 0.001$) increase in TNF-α secretion relative to absence of LPS when analysed using a two-tail t-test; however this significance was lost upon one-way ANOVA analysis (Fig. 5.6D). Preincubation with A769662 did not significantly alter TNF-α secretion relative to absence of A769662 (Fig. 5.6D).

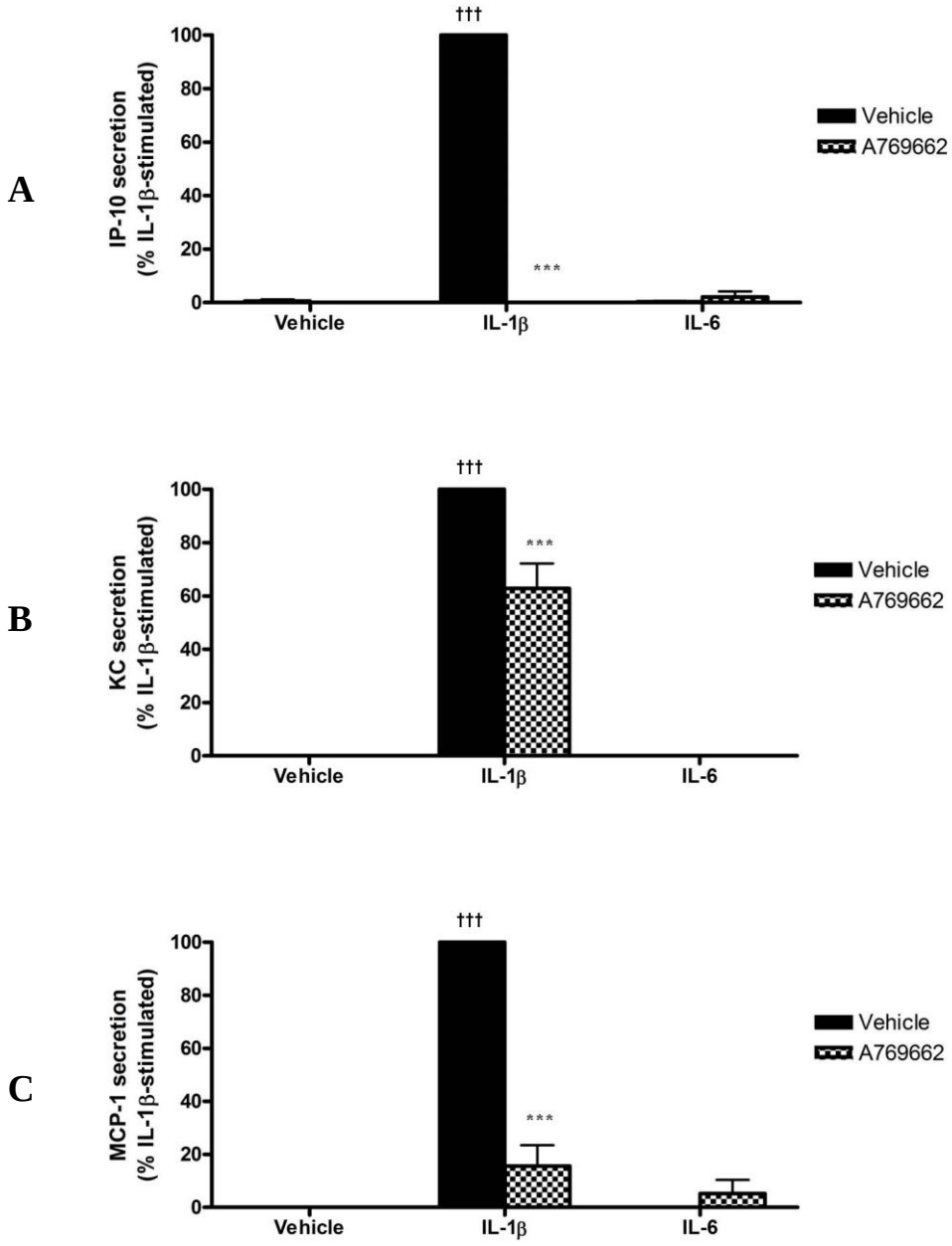

Figure 5-5: Effect of AMPK on 3T3-L1 adipocyte cytokine/chemokine secretion

*3T3-L1 CAR adipocytes were stimulated with IL-1β (10 ng/ml) or IL-6/sIL-6Rα (5 ng/ml; 25 ng/ml) for 6 h following preincubation for 30 min in the presence or absence of A769662 (300 μM). Thereafter, cells were thoroughly washed and incubated in SF-DMEM for 1 h and conditioned medium collected for chemokine analysis using a multiplex bead immunoassay and a Luminex® 100™ detection system. Data shown represent the mean $\pm$ SEM % IL-1β-stimulated (A) IP-10, (B) KC or (C) MCP-1 secretion of three independent experiments. †††$p < 0.001$ (one-way ANOVA), increase in secretion, relative to vehicle. ***$p < 0.001$ (one-way ANOVA), reduction in secretion, relative to absence of A769662.*

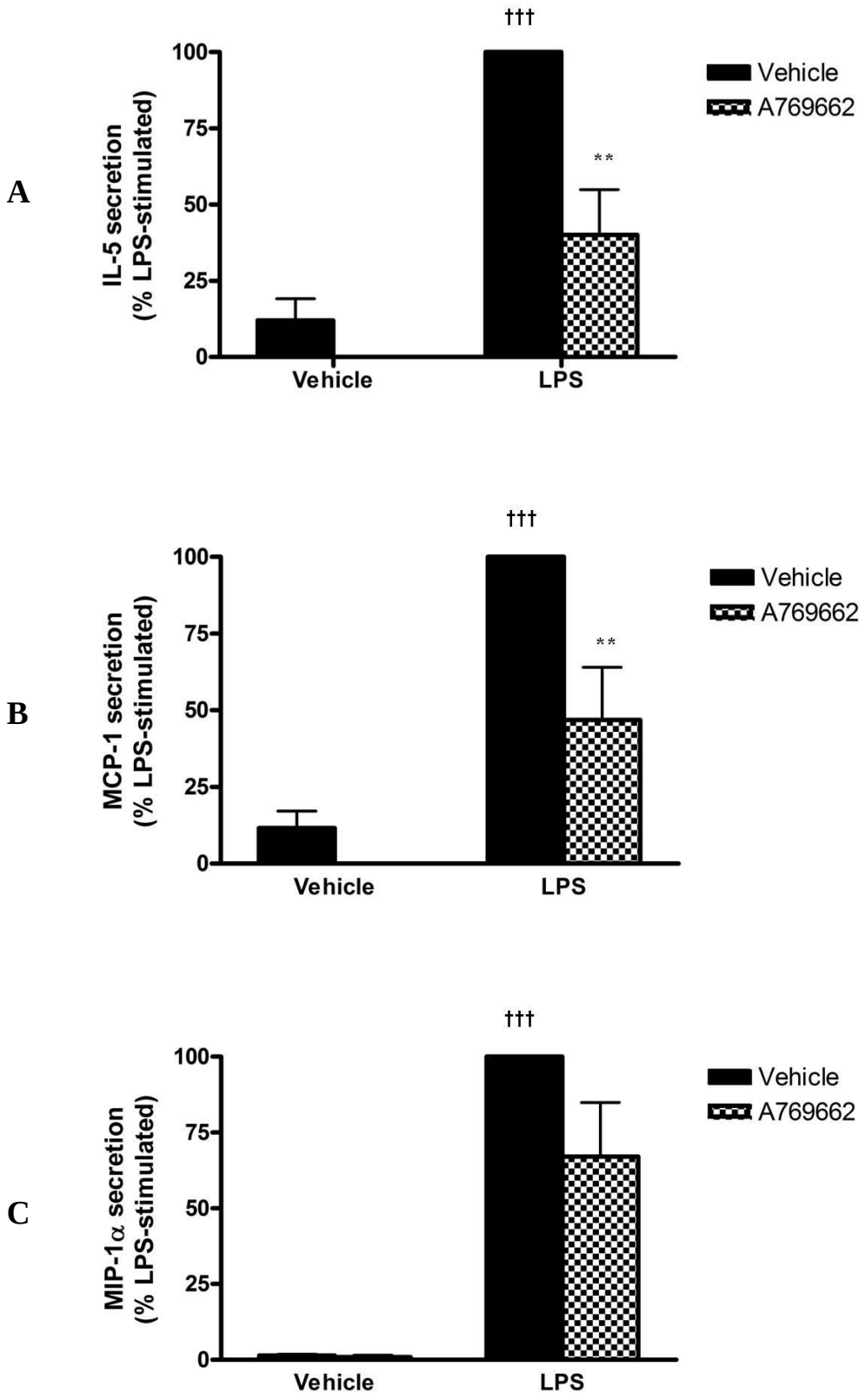

Figure 5-6: Effect of AMPK on macrophage cytokine/chemokine secretion *(continued overleaf)*

D

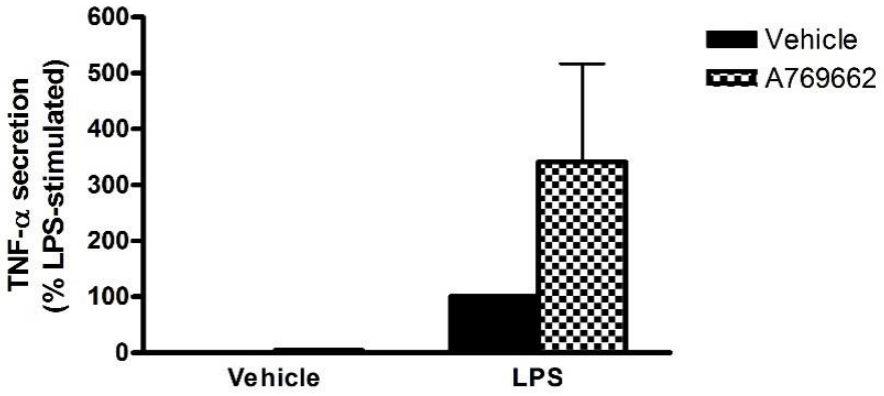

Figure 5-6: Effect of AMPK on macrophage cytokine/chemokine secretion

*RAW 264.7 macrophages were incubated with LPS (1 μg/ml) for 6 h following preincubation for 30 min in the presence or absence of A769662 (100 μM). Thereafter, cells were thoroughly washed and incubated in SF-RPMI for 1 h and conditioned medium collected for chemokine analysis using a multiplex bead immunoassay and a Luminex® 100™ detection system. Data shown represent the mean ± SEM % LPS-stimulated (A) IL-5, (B) MCP-1 or (C) MIP-1α secretion of four independent experiments. †††p < 0.001 (one-way ANOVA), increase in secretion, relative to vehicle. **p < 0.01 (one-way ANOVA), reduction in secretion, relative to absence of A769662. (D) Data shown represents the mean ± SEM % LPS-stimulated TNF-α secretion of three independent experiments.*

5.2.5 Effect of inflammation on 3T3-L1 adipocyte insulin sensitivity

5.2.5.1 Effect of cytokines on 3T3-L1 adipocyte glucose uptake

Proinflammatory cytokines and chemokines in adipose tissue have been proposed to play a key role in the development of obesity-associated insulin resistance. It was of interest, therefore, to investigate whether incubation with individual cytokines could suppress insulin-stimulated glucose transport in 3T3-L1 adipocytes. To determine whether individual cytokines reduce insulin sensitivity in adipocytes, 3T3-L1 adipocytes were stimulated with TNF-α, IL-1β or IL-6 for various durations. The extent of insulin-stimulated glucose uptake was assessed as a measure of incorporation of radiolabelled glucose.

In separate experiments, 3T3-L1 adipocytes were incubated with IL-6/sIL-6Rα for 1, 6, 24 or 72 h prior to insulin-stimulated glucose uptake being assessed. The raw data indicated that incubation with IL-6/sIL-6Rα did not alter insulin-stimulated glucose transport, compared to the vehicle control; however, basal glucose uptake was increased following 6, 24 and 72 h IL-6/sIL-6Rα incubation (Fig. 5.7C, 5.7E and 5.7G, respectively). Thus, analysis of the fold change in insulin-stimulated glucose uptake demonstrated that incubation with IL-6/sIL-6Rα caused a reduction in insulin-stimulated glucose uptake following 6 h (30 %), 24 h (88 %) and 72 h (50 %) treatment (Fig. 5.7D, 5.7F and 5.7H, respectively). A slight increase in insulin-stimulated glucose uptake was observed following incubation with IL-6/sIL-6Rα for 1h (Fig. 5.7B).

Similarly, 3T3-L1 adipocytes were incubated with IL-1β for 1 h or TNF-α for 1 or 6 h prior to insulin-stimulated glucose uptake being assessed. Analysis of the fold change in insulin-stimulated glucose uptake demonstrated that incubation with TNF-α caused a 50 % reduction in insulin-stimulated glucose uptake following 6 h treatment (Fig. 5.8D), and incubation with IL-1β caused a 48 % reduction in insulin-stimulated glucose uptake following 1 h treatment (Fig. 5.8F).

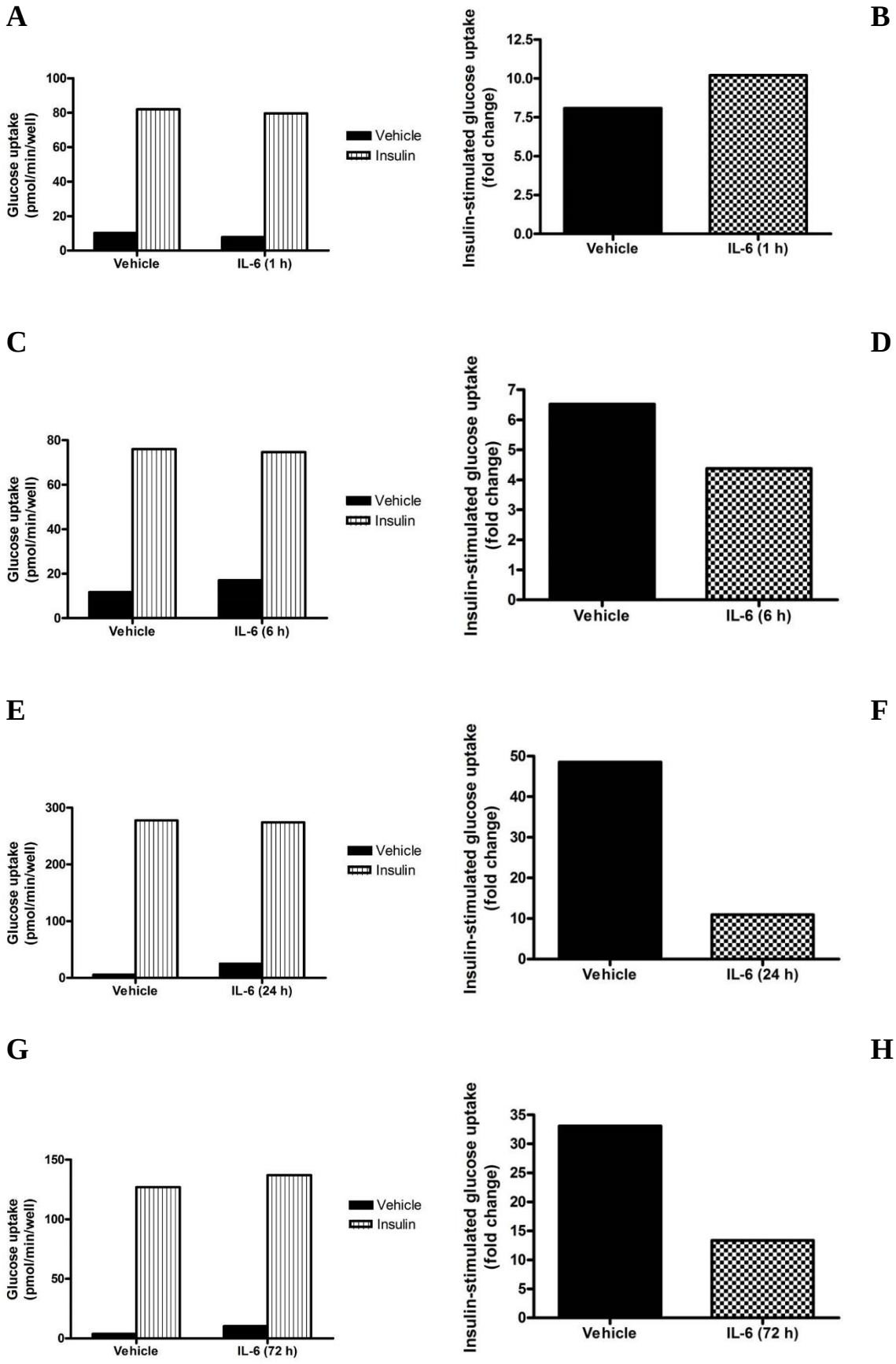

Figure 5-7: Effect of IL-6 on 3T3-L1 insulin-stimulated glucose uptake *(legend overleaf)*

Figure 5-7: Effect of IL-6 on 3T3-L1 insulin-stimulated glucose uptake

3T3-L1 adipocytes were incubated with IL-6/sIL-6Rα (5 ng/ml; 25 ng/ml) for various durations prior to stimulation with insulin (10 nM) for 15 min. Glucose transport was initiated by the addition of 2-[^{3}H]-deoxy-D-glucose, and terminated after 3 min. (A, C, E, G) Data shown represent 2-[^{3}H]-deoxy-D-glucose uptake (pmol/min/well) of single experiments conducted independently of each other. (B, D, F, H) Data shown represent the fold change in insulin stimulated glucose uptake relative to vehicle of single experiments conducted independently of each other.

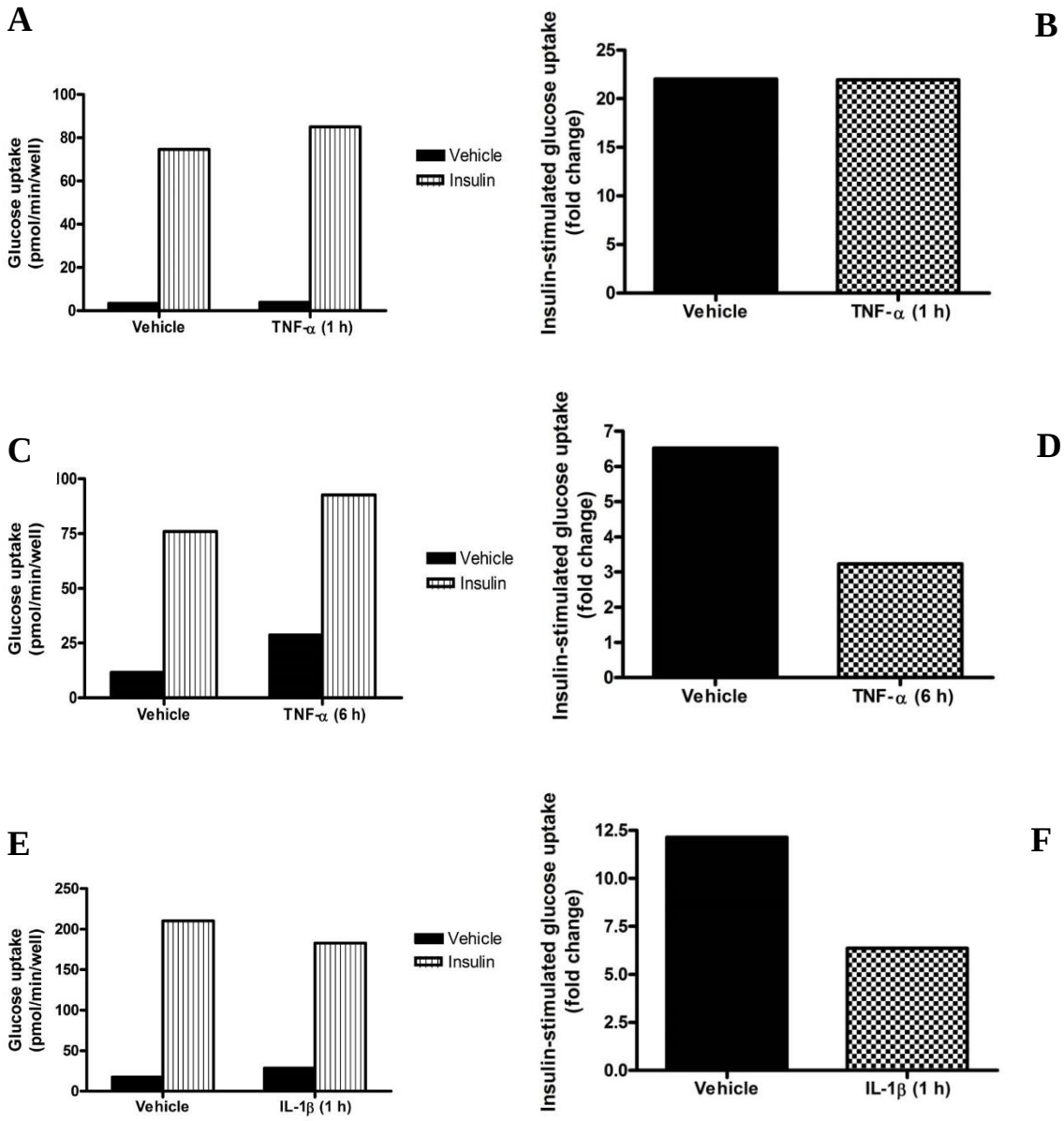

Figure 5-8: Effect of TNF-α or IL-1β on 3T3-L1 insulin-stimulated glucose uptake

3T3-L1 adipocytes were incubated with (A-D) TNF-α (10 ng/ml) or (E-F) IL-1β (10 ng/ml) for various durations prior to stimulation with insulin (10 nM) for 15 min. Glucose transport was initiated by the addition of 2-[^{3}H]-deoxy-D-glucose, and terminated after 3 min. (A), (C) and (E) Data shown represent 2-[^{3}H]-deoxy-D-glucose uptake (pmol/min/well) of single experiments conducted independently of each other. (B), (D) and (F) Data shown represent the fold change in insulin stimulated glucose uptake relative to vehicle of single experiments conducted independently of each other.

5.2.5.2 Effect of conditioned medium from activated macrophages on 3T3-L1 adipocyte glucose uptake

Interplay between adipocytes and macrophages in adipose tissue is key to the development of a sustained proinflammatory profile within the tissue; therefore it was of interest to investigate the effect of activated macrophage secretory products on adipocyte insulin sensitivity. Murine RAW 264.7 macrophages were stimulated with LPS to induce a shift in their polarity towards an M1 classically activated phenotype, and conditioned medium collected. 3T3-L1 adipocytes were incubated in this conditioned medium prior to glucose uptake being measured. 3T3-L1 adipocytes incubated in conditioned medium from macrophages stimulated for 6 h with LPS displayed a significant ($p < 0.05$) 55.2 $\pm$ 12.1 % reduction in insulin-stimulated glucose uptake, relative to incubation with conditioned medium from untreated macrophages, as determined by the fold change (Fig. 5.9). Similarly, incubation with conditioned medium collected from macrophages stimulated with LPS for 1 h caused a 29 $\pm$ 11.2 % reduction in 3T3-L1 adipocyte glucose uptake, relative to the basal level ($p = 0.06$; two-tail t-test) (Fig. 5.9).

In a similar, but separate, set of experiments, conditioned medium was collected from macrophages stimulated with LPS in the presence or absence of A769662. 3T3-L1 adipocytes were incubated in this conditioned medium and glucose uptake was measured to assess whether prior A769662-mediated AMPK activation in macrophages could rescue the LPS-induced reduction in glucose uptake observed in Figure 5.9. 3T3-L1 adipocytes incubated in conditioned medium from macrophages treated with A769662 alone exhibited a 44.3 $\pm$ 21 % ($p = 0.1$; two-tail t-test) increase in insulin-stimulated glucose uptake relative to incubation with conditioned medium from untreated macrophages (Fig. 5.10). While this did not reach significance with one-way ANOVA, it may indicate a tendency toward AMPK activation in macrophages improving adipocyte insulin sensitivity. In contrast to the set of experiments described in Figure 5.9, conditioned medium from macrophages stimulated with LPS did not significantly reduce adipocyte glucose uptake relative to the basal level. However, glucose uptake was significantly ($p < 0.05$) blunted in adipocytes incubated with conditioned medium from macrophages stimulated with LPS in the presence of A769662, relative to the absence of LPS (Fig. 5.10).

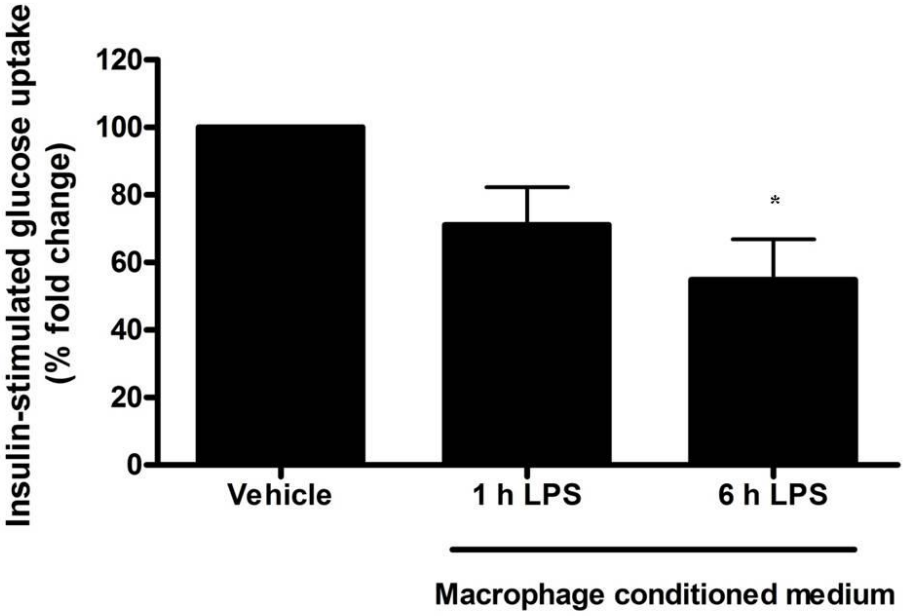

Figure 5-9: Effect of activated macrophage conditioned medium on 3T3-L1 insulin-stimulated glucose uptake

*RAW 264.7 macrophages were stimulated with LPS (1 μg/ml) for 1 or 6 h. Thereafter, cells were thoroughly washed and incubated in SF-RPMI for 1 h and conditioned medium collected. 3T3-L1 adipocytes were incubated with conditioned medium for 6 h prior to stimulation with insulin (10 nM) for 15 min. Glucose transport was initiated by the addition of 2-[^{3}H]-deoxy-D-glucose, and terminated after 3 min. Data shown represent the mean ± SEM % fold change in insulin stimulated 2-[^{3}H]-deoxy-D-glucose uptake relative to vehicle of three independent experiments. *p < 0.05 (one-way ANOVA), reduction in insulin-stimulated glucose uptake, relative to vehicle.*

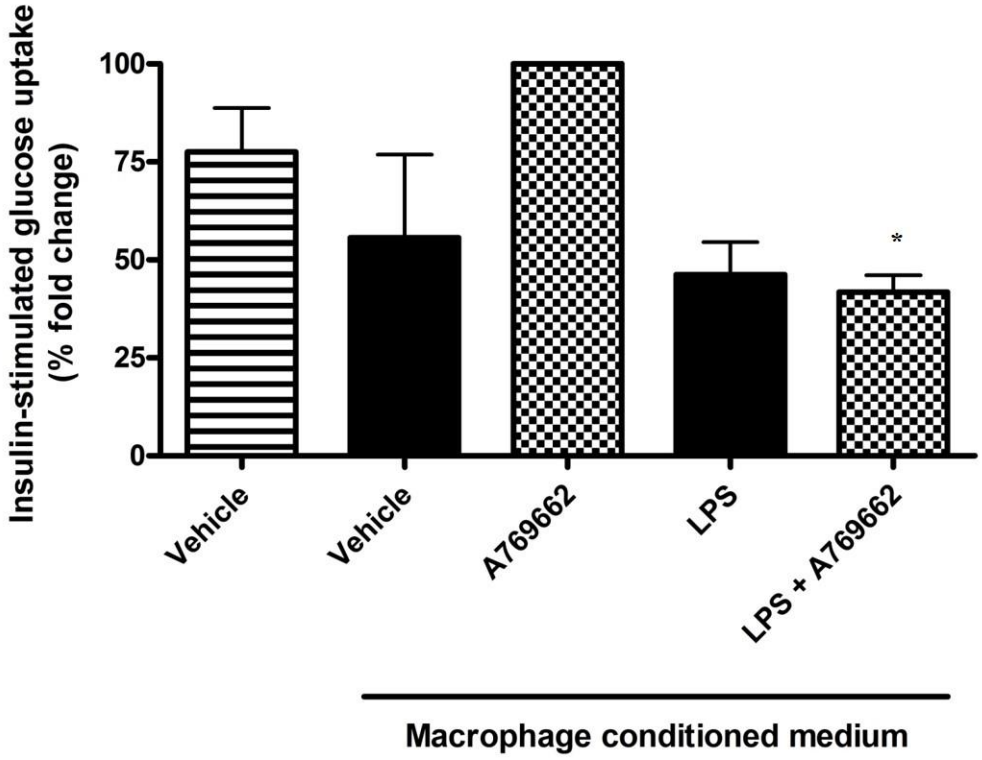

Figure 5-10: Effect of activated macrophage conditioned medium on 3T3-L1 insulin-stimulated glucose uptake

*RAW 264.7 macrophages were stimulated with LPS (1 μg/ml) for 6 h following preincubation for 30 min in the presence or absence of A769662 (100 μM). Thereafter, cells were thoroughly washed and incubated in SF-RPMI for 1 h and conditioned medium collected. 3T3-L1 adipocytes were incubated with conditioned medium for 6 h prior to stimulation with insulin (10 nM) for 15 min. Glucose transport was initiated by the addition of 2-[^{3}H]-deoxy-D-glucose, and terminated after 3 min. Data shown represent the mean ± SEM % fold change in insulin stimulated 2-[^{3}H]-deoxy-D-glucose uptake relative to vehicle of three independent experiments. *p < 0.05 (one-way ANOVA), reduction in insulin-stimulated glucose uptake, relative to absence of LPS.*

5.2.6 Effect of AMPK on adipocyte morphology and differentiation

5.2.6.1 Effect of A769662 on adipogenesis

Activation of AMPK by AICAR has been demonstrated to inhibit adipogenesis (Habinowski and Witters 2001) via a currently unknown mechanism, while it has also been reported that JAK2/STAT3 pathway activation is critical for adipogenesis to proceed (Wang, Zhou, et al. 2010). In order to investigate whether AMPK inhibited adipogenesis via regulation of STAT3, 3T3-L1 adipocytes were differentiated in the presence or absence of A769662 and lysates obtained at various intervals post-differentiation. The extent of ACC S79 and STAT3 Y705 phosphorylation, in addition to the expression of adipogenic markers: C/EBPβ, C/EBPδ, C/EBPα and PPARγ, was determined by western blotting analysis of 3T3-L1 adipocyte lysates.

Figure 5.11A demonstrates that expression of C/EBPβ is not increased, compared to undifferentiated fibroblasts, until day 8 post-differentiation, where it appears to be modestly reduced upon preincubation with A769662. C/EBPδ expression was not detected until day 4, and continued to be expressed until day 8 post-differentiation; however this appeared to be unaffected by preincubation with A769662 (Fig. 5.11A). Expression of C/EBPα could be observed from day 2 post-differentiation; preincubation with A769662 reduced C/EBPα expression at day 4 and day 6, but not day 8 (Fig. 5.11A). PPARγ expression was detected from day 4; however it remained unaffected by preincubation with A769662 (Fig. 5.11A). STAT3 Y705 phosphorylation was rapidly induced at 24 h post-differentiation and disappeared after 48 h; preincubation with A769662 clearly reduced STAT3 Y705 phosphorylation, relative to the absence of A769662 (Fig. 5.11A). In a separate experiment, the effect of A769662 on lipid accumulation in 3T3-L1 adipocytes during adipogenesis was examined by staining adipocytes with oil red O at various intervals post-differentiation. 3T3-L1 adipocytes differentiated in the presence of A769662 demonstrated a slightly reduced lipid accumulation at day 4 post differentiation, compared to the control cells (Fig. 5.11B). At day 8 post differentiation the control 3T3-L1 adipocytes displayed an abundance of lipid as detected by oil red O staining; by comparison, lipid accumulation was clearly

reduced in 3T3-L1 adipocytes differentiated in the presence of A769662 (Fig. 5.11B).

5.2.6.2 Effect of AMPKα1 on adipocyte cell size

In order to assess the consequences of a lack of AMPKα1 on adipocyte cell size, omental and subcutaneous adipose tissue were extracted from *AMPKα1*$^{-/-}$ and litter-matched wild-type mice and adipocyte cell size observed following H&E staining of the sectioned tissue. Adipocytes in omental adipose tissue from *AMPKα1*$^{-/-}$ mice appeared to be greatly reduced in size compared to omental adipocytes from wild-type adipose tissue (Fig. 5.12). A difference in size between adipocytes from *AMPKα1*$^{-/-}$ or wild-type subcutaneous adipose tissue was less clear; however there does appear to be a slight reduction in size in subcutaneous adipocytes from *AMPKα1*$^{-/-}$ mice compared to the wild-type (Fig. 5.12).

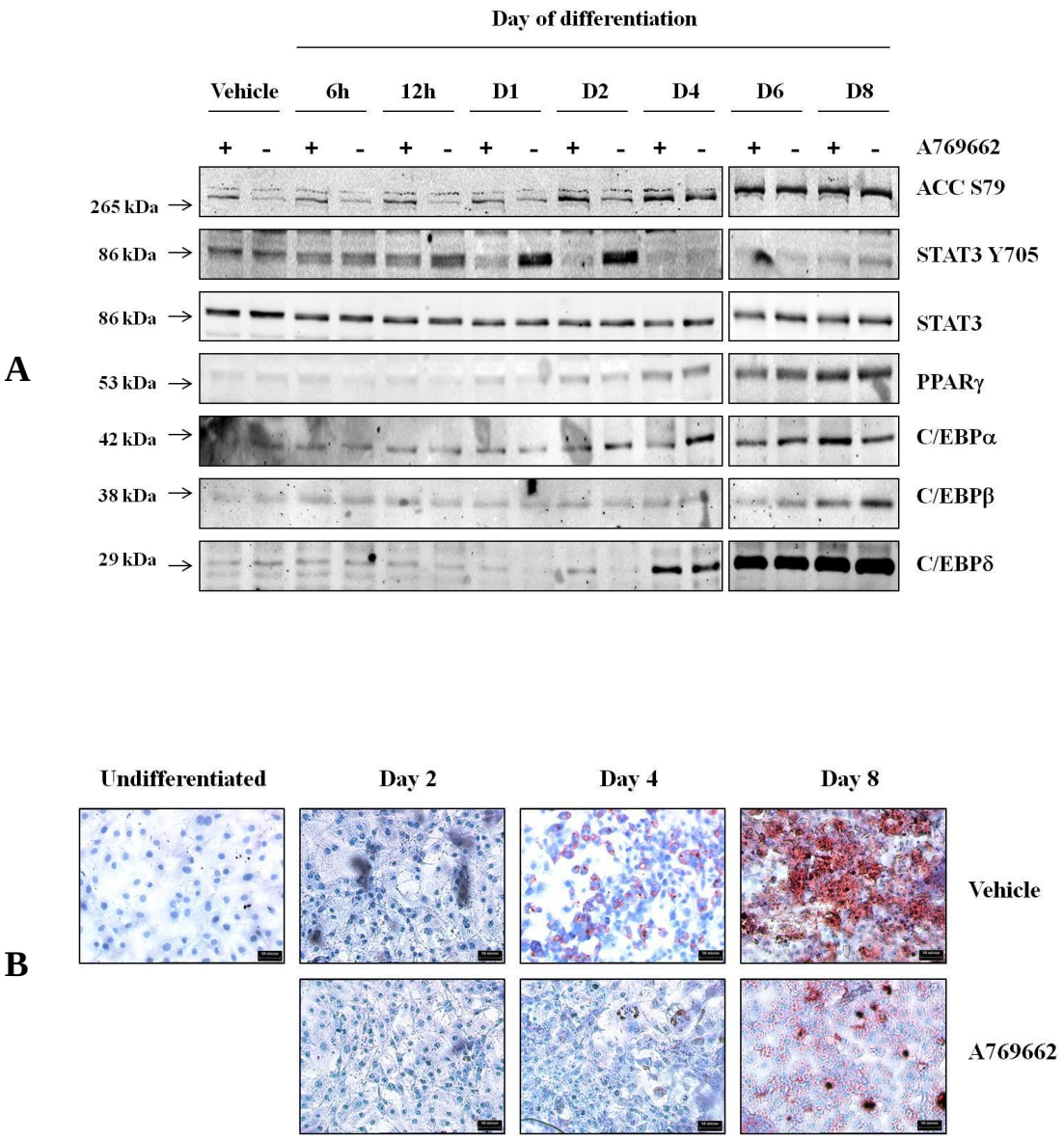

Figure 5-11: Effect of A769662 on adipogenesis

3T3-L1 adipocytes were differentiated (A) in the presence of troglitazone or (B) in the absence of troglitazone for various durations in the presence of A769662 (300 μM) or DMSO. (A) Lysates were prepared at various intervals post-differentiation and resolved by SDS-PAGE before being subjected to immunoblotting with the antibodies indicated. Western blot from a single experiment. (B) Cells were fixed and stained with oil red O at various intervals post differentiation. Representative microscope images from a single experiment. Scale bar = 50 μm.

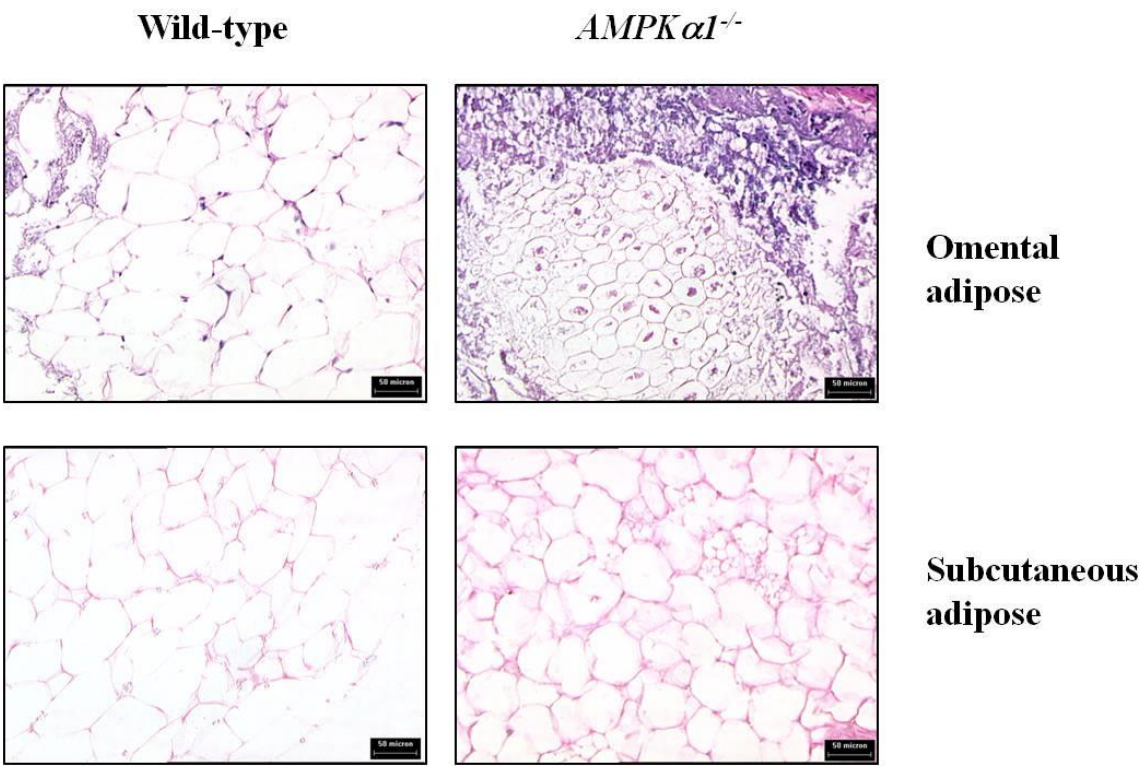

Figure 5-12: Effect of AMPKα1 on adipocyte cell size

Omental and subcutaneous adipose tissue harvested from AMPK$\alpha 1^{-/-}$ and litter-matched wild-type mice were embedded in paraffin and sections stained with haemotoxylin and eosin. Representative microscope images from a single experiment. Scale bar = 50 μm.

5.3 Discussion

The key findings of this chapter are that A769662 suppressed many downstream functional effects of cytokine-stimulated proinflammatory signalling pathways, including TNF-α and IL-6-stimulated MCP-1 gene expression, and IL-1β-stimulated MCP-1, KC and IP-10 secretion in 3T3-L1 adipocytes. Furthermore, A769662 reduced LPS-stimulated secretion of IL-5, MCP-1 and MIP-1α, but not TNF-α from macrophages. Preliminary data suggested that sustained, but not acute, IL-6 treatment may reduce insulin sensitivity in 3T3-L1 adipocytes, while acute stimulation with TNF-α or IL-1β may suppress insulin-stimulated glucose uptake. Secretory products from M1-activated macrophages rendered 3T3-L1 adipocytes insulin resistant, while conditioned medium from macrophages treated with A769662 alone appeared to enhance adipocyte glucose uptake; however it is unclear whether prior A769662-mediated AMPK activation in macrophages is sufficient to reduce secretion of proinflammatory mediators to the extent that 3T3-L1 insulin sensitivity is restored. Finally, mouse *AMPKα1*$^{-/-}$ gonadal and subcutaneous adipocytes appeared to be reduced in size compared to wild-type, while A769662 suppressed 3T3-L1 adipocyte differentiation and reduced early STAT3 phosphorylation which is thought to be crucial in the development of adipogenesis.

A key target of the IL-6-stimulated JAK/STAT pathway is SOCS3. SOCS3 is induced upon cytokine stimulation and functions as a negative regulator of the pathway via binding to phosphotyrosine residues on the intracellular domain of gp130 and inhibiting JAK activity (Kubo, Hanada, and Yoshimura 2003, Murray 2007). Both *in vitro* and *in vivo* studies have reported an increase in IL-6-induced SOCS3 expression in 3T3-L1 adipocytes (Fasshauer, Kralisch, et al. 2004, Lagathu et al. 2003) and in various tissues, including adipose (Carey et al. 2006, Shi et al. 2004). Elevated SOCS3 expression in adipocytes has been reported to be associated with a reduction in IRS expression and perturbed insulin signalling, leading to localised insulin resistance and impaired glucose tolerance (Shi et al. 2004, Shi, Cave, et al. 2006). Furthermore, skeletal muscle-specific *SOCS3*$^{-/-}$ mice were protected from HFD-induced insulin resistance due to enhanced phosphorylation of the insulin signalling pathway and elevated skeletal muscle glucose uptake (Jorgensen et al. 2013). It was of interest to investigate the effect of AMPK activation on

SOCS3 expression, which prior to beginning this study was previously unknown. 3T3-L1 adipocytes were incubated with the proteasome inhibitor MG132 to prevent degradation of the protein. Figure 5.1A demonstrated a significant increase in SOCS3 protein expression in response to IL-6 stimulation, which supports previous reports; however activation of AMPK had no effect on expression of SOCS3 (Fig. 5.1A). These data support a recent study which reported AICAR-mediated AMPK activation did not alter SOCS3 expression in HepG2 cells also following 6 h incubation (Nerstedt et al. 2013). In contrast, there is evidence for the AMPK-mediated reduction in SOCS3 production in the liver following acute (1 h) stimulation. Nerstedt and co-workers found that AICAR reduced IL-6-stimulated SOCS3 mRNA expression in mouse liver and HepG2 cells (Nerstedt et al. 2013), while Kim and co-workers reported that AMPK activation via metformin or constitutively active adenoviral infection suppressed IL-6-stimulated SOCS3 induction in rat primary hepatocytes (Kim et al. 2012). Conversely, inhibition of IL-6-induced SOCS3 expression was ablated upon downregulation of AMPK via adenovirus-mediated infection in hepatocytes (Kim et al. 2012). As these contrary findings were all observed in the liver or liver cells, it is possible that the effects of AMPK activation on SOCS3 induction could be cell or tissue-specific. Moreover, to our knowledge, these data are the first to demonstrate the effect of AMPK activation on SOCS3 induction in adipocytes.

Another protein upregulated as a result of IL-6 signalling is the transcription factor C/EBPβ (CCAAT/enhancer binding protein-β), which is involved in cellular differentiation and inflammatory responses (Lekstrom-Himes and Xanthopoulos 1998) and is activated via the ERK arm of the IL-6 signalling pathway (Hu et al. 2001). Figure 5.1B demonstrated that IL-6 or AMPK activation had no effect C/EBPβ protein expression in 3T3-L1 adipocytes; furthermore, A769662 had no effect on C/EBPβ expression during adipogenesis (Fig. 5.11A). These data are not surprising, given that C/EBPβ is induced via the Ras/Raf/ERK pathway, and Figure 4.3 showed no evidence of IL-6-stimulated ERK1/2 activation. There is conflicting evidence in the literature as to the effect of AMPK on C/EBPβ expression; AICAR was reported to elevate basal C/EBPβ expression in preadipocytes (Arai et al. 2007), while AICAR or constitutively active AMPK was reported to reduce ER stress-induced C/EBPβ expression in FAO hepatoma cells, which conversely was blocked following expression of a dominant-negative AMPK (Choudhury et al. 2011). It is

therefore possible that AMPK could exert differential effects on C/EBPβ expression depending on the cell type and stimuli.

AMPK activation has been widely reported to suppress the synthesis of proinflammatory cytokines including TNF-α, IL-1β and IL-6 in macrophages (Yang et al. 2010, Galic et al. 2011, Sag et al. 2008, Jeong et al. 2009); however, the effect of AMPK on the production of many other proinflammatory cytokines and chemokines, particularly in adipocytes, is currently poorly characterised. The two major families of chemokines are the C-C family, characterised by two adjacent cysteine residues near the amino terminus, and C-X-C family, whereby the amino terminal cysteine residues are separated by one amino acid (Ono et al. 2003). MCP-1 (CCL2) is a well-characterised chemokine produced in response to proinflammatory mediators, and stimulates the migration of monocytes to sites of inflammation where they then become macrophages (Ono et al. 2003). Furthermore, MCP-1 also stimulates chemotaxis and activation of T-cells; Wu and co-workers reported an increased infiltration of activated T-cells in adipose tissue from DIO mice (Wu et al. 2007), suggesting an accumulation of T-cells in obese adipose tissue may contribute to the immune dysfunction observed in obesity. In contrast, other groups have proposed inflammatory M1 activated macrophages to be central to the development of an inflammatory environment within the tissue (Galic et al. 2011, Weng and Schuppan 2013). In the current study, A769662 suppressed TNF-α or IL-6-stimulated MCP-1 gene expression in 3T3-L1 adipocytes (Fig. 5.2A and 5.2C, respectively). These data support similar observations reported in endothelial cells, where metformin or AICAR-mediated AMPK activation ameliorated TNF-α-stimulated MCP-1 expression (Hattori et al. 2006). Likewise, berberine has been reported to reduce elevated MCP-1 expression observed in obese *db/db* mice (Jeong et al. 2009). Moreover, secretion of MCP-1 was found to be elevated in 3T3-L1 adipocytes in response to IL-1β (Fig. 5.5C) and RAW 264.7 macrophages in response to LPS (Fig. 5.6B); this was significantly attenuated in both cell types following preincubation with A769662 (Fig. 5.5C and 5.6B). These data correlate with the suppression of cytokine-stimulated gene expression of MCP-1 observed in 3T3-L1 adipocytes (Fig. 5.2A), and are also consistent with a previous study in human endothelial cells conducted in this laboratory, which reported an inhibition of TNF-α-stimulated MCP-1 secretion by AICAR (Ewart, Kohlhaas, and Salt 2008). Similarly, an increase in serum MCP-1 was

reported in HFD-fed mice with hematopoietic deletion of AMPKβ1 (Galic et al. 2011), thus demonstrating the potential importance of AMPK in the suppression of MCP-1.

Secretion of several cytokines and chemokines from 3T3-L1 adipocytes or macrophages in response to proinflammatory mediatiors were analysed in the current study; however most were found to be at levels below the sensitivity of the assay. Interestingly, IL-6 failed to stimulate secretion of any of the chemokines or cytokines in the panel (IP-10 (CXCL10), KC (CXCL1), MCP-1 (CCL2), MIG (CCL9), MIP-1α (CCL3), FGF-basic, GM-CSF, IFN-γ, IL-1α, IL-1β, IL-2, IL-4, IL-5, IL-6, IL-10, IL-12 (p40/p70), IL-13, IL-17, TNF-α and VEGF). Given that IL-6 was demonstrated to induce MCP-1 gene expression (Fig. 5.2C), it is possible that incubation with IL-6 for 6 h may be sufficient to induce gene expression but not detectable protein production and secretion. The chemokines IP-10 and KC were found to be secreted from 3T3-L1 adipocytes in response to IL-1β stimulation, with levels markedly reduced following preincubation with A769662 (Fig. 5.5A and 5.5B, respectively). KC and IP-10 have not been as well characterized as MCP-1 in terms of the effect of AMPK; however these data support one recent study reporting a reduction in murine serum KC levels in response to resveratrol (Baron et al. 2014). As KC and IP-10 are members of the CXC chemokine family, they induce neutrophil chemotaxis (Ono et al. 2003). Neutrophils are generally recruited during the acute phase of inflammation, while macrophage infiltration of murine adipose tissue has not been observed until 8 weeks of HFD feeding (Strissel et al. 2007). Transient neutrophil infiltration which precedes macrophage infiltration has been reported in adipose tissue of HFD-fed mice (Elgazar-Carmon et al. 2008); in line with this, a clinical study demonstrated that circulating neutrophils are activated to a greater extent in morbidly obese subjects compared to lean individuals (Nijhuis et al. 2009). Considering neutrophils have a short life span and are primarily involved in acute inflammation, these studies imply that the chronic inflammatory profile associated with morbid obesity could be, in part, the result of a continuous activation of the innate immune system. The secretion of multiple chemokines from inflamed adipocytes demonstrates the complexity of the proinflammatory profile of adipose tissue, and the potential ability of A769662 to inhibit both macrophage recruitment via MCP-1, and neutrophil recruitment via KC and IP-10, indicates the pleiotropic nature of AMPK.

In addition to MCP-1, classically activated macrophages were found to secrete IL-5, MIP-1α and TNF-α (Fig. 5.6). IL-5 (interleukin-5) is predominantly produced by Th2 (T helper 2) cells and is involved in the differentiation of activated B cells and the maturation of eosinophils (Kouro and Takatsu 2009); thus it is a key factor in the development of allergic diseases which are characterised by inflammation. A769662-mediated AMPK activation significantly reduced IL-5 secretion from LPS-stimulated macrophages (Fig. 5.6A). To our knowledge, a link between AMPK and IL-5 has never been suggested, and the relevance of these data in terms of obesity-associated inflammation and insulin resistance is unknown; however it may suggest that AMPK activation could play a role in the suppression of the exaggerated immune response associated with allergy. Similarly to MCP-1, MIP-1α (macrophage inflammatory protein-1α) (CCL3) is a chemokine which induces synthesis of proinflammatory mediators and is a macrophage chemoattractant (Fahey et al. 1992). In the current study, activated macrophages exhibited an increase in MIP-1α secretion compared to an absence of LPS; however in contrast to MCP-1, preincubation with A769662 induced only a subtle reduction in MIP-1α secretion (Fig. 5.6C). Activated macrophages displayed an increase in TNF-α secretion relative to the basal level; however this did not reach significance using one-way ANOVA analysis (Fig. 5.6D). This is likely due to the high degree of variability across experimental replicates. Unexpectedly, preincubation with A769662 failed to reduce TNF-α secretion (Fig. 5.6D). These data are in direct contrast to the findings of several different groups: Sag and co-workers reported an inhibition of LPS-stimulated TNF-α secretion in macrophages expressing constitutively active AMPK, while conversely, expression of a dominant negative AMPK enhanced TNF-α secretion (Sag et al. 2008). Similarly, TNF-α secretion was reported to be elevated in macrophages deficient in AMPKβ1 (Galic et al. 2011). Furthermore, AICAR or berberine-mediated AMPK activation has been reported to suppress TNF-α expression in macrophages (Yang et al. 2010, Jeong et al. 2009). This intruiging result is most likely due to the high degree of variability across experimental replicates; however it is possible that A769662-mediated AMPK activation may not have any effect on TNF-α secretion from macrophages. Crucially, proinflammatory cytokine-induced transcription factors NFκB and AP-1 have been reported to regulate transcription of the chemokines IP-10 (Ohmori and Hamilton 1993), KC (Ohmori, Fukumoto, and Hamilton 1995), MCP-1 (Martin et al.

1997), MIP-1α (Grove and Plumb 1993) and the cytokines TNF-α (Shakhov et al. 1990) and IL-5 (Lee et al. 1995). Thus, with the exception of TNF-α, the finding that A769662 suppresses secretion of these proinflammatory proteins from 3T3-L1 adipocytes and RAW 264.7 macrophages correlates with the earlier findings in this study that A769662 inhibited MAPK and NFκB proinflammatory signalling and NFκB nuclear translocation (Fig. 3.2-3.7, 3.15-3.20).

To explore the importance of AMPK on the activation state of macrophages in adipose tissue, the basal gene transcription of markers associated with M1 and M2 activation states were assessed in subcutaneous and gonadal adipose tissue depots obtained from *AMPKα1*$^{-/-}$ and genetically matched wild-type mice. TNF-α and NOS2 (iNOS) are classical markers of M1 activation, while M2 macrophages are characterised by the expression of ARG1, RELM-α and CHI313. NOS2 is a proinflammatory gene induced by activation of MAPK/NFκB signalling pathways, and catalyses the production of NO and citrulline from arginine. The high levels of NO produced in response to inflammatory signalling pathways can react with the free radical superoxide, producing peroxynitrite, an oxidant which reacts with biological molecules (Pacher, Beckman, and Liaudet 2007). In contrast, the M2 marker ARG1 catalyses the hydrolysis of arginine, thus reducing its availability as a substrate for NOS (Pacher, Beckman, and Liaudet 2007). RELM-α and CHI313 mediate the Th2 cell-driven inflammatory response (Pesce et al. 2009, Elias et al. 2005). There was no clear difference in expression of M1 marker genes TNF-α (Fig. 5.3A, 5.3B) and NOS2 (Fig. 5.3C, 5.3D), or M2 marker genes ARG1 (Fig. 5.3E, 5.3F), RELM-α (Fig. 5.3G, 5.3H) and CHI313 (Fig. 5.3I, 5.3J) between *AMPKα1*$^{-/-}$ and wild-type in subcutaneous or gonadal adipose tissue, respectively. These data would suggest that there was no alteration in the M1/M2 ratio in adipose tissue in the presence or absence of AMPKα1. This is intriguing, as lysates prepared from the same samples yielded results suggesting an increase in basal inflammation existed within *AMPKα1*$^{-/-}$ tissue relative to wild-type, as demonstrated by elevated phosphorylation of JNK (Fig. 3.10A) and STAT3 (Fig. 4.7). Taken together, these data imply that as the macrophages within *AMPKα1*$^{-/-}$ adipose tissue do not appear to be predominantly polarised towards an M1 activation state, then the increased proinflammatory signalling observed may be coming from other cells within the tissue, such as adipocytes or possibly vascular cells. AMPK activation has been reported to promote the anti-inflammatory polarisation of macrophages to M2;

while conversely, *AMPKβ1*$^{-/-}$ mice have been reported to exhibit increased systemic inflammation and M1 macrophage infiltration in adipose tissue and liver (Galic et al. 2011, Weng and Schuppan 2013). While these reports, in contrast to the current study, indicate that loss of AMPK function drives the proinflammatory polarisation of macrophages, it is important to note that this was observed following HFD-feeding (Galic et al. 2011, Weng and Schuppan 2013). The *AMPKα1*$^{-/-}$ and wild-type mice analysed for M1 macrophage activation in the current study were fed a normal chow diet, therefore suggesting that while loss of AMPK alone may be sufficient to induce basal phosphorylation of proinflammatory mediators (Fig. 3.10A and Fig. 4.7), a shift in macrophage polarisation may require an additional inflammatory insult.

Lastly, the effect of AMPK activation, TNF-α or IL-6 stimulation on the secretion of the adipocytokine adiponectin was assessed via protein precipitation. It is well established that adiponectin can stimulate AMPK activation in liver and muscle both *in vitro* and *in vivo* (Yamauchi et al. 2002), and in rat primary adipocytes (Wu et al. 2003); however the effect of AMPK activation on adiponectin production is less clear. In the current study A769662 appeared to stimulate secretion of adiponectin in 3T3-L1 adipocytes compared to both the basal level and incubation with TNF-α, although it had no effect in the presence of IL-6 (Fig. 5.4). These data support a study by Lihn and co-workers, who reported an AICAR-mediated increase in adiponectin gene expression in human SCAT cultured *ex vivo* (Lihn et al. 2004). The opposite has also been reported, however; AICAR or metformin-mediated AMPK activation has been proposed to suppress adiponectin expression in 3T3-L1 adipocytes (Huypens, Quartier, et al. 2005). Furthermore, it has been suggested that proinflammatory cytokines may negatively regulate adiponectin production, which may explain the negative correlation of adiponectin plasma and mRNA levels with adiposity (Cnop et al. 2003). TNF-α has been reported to suppress adiponectin gene transcription (Maeda et al. 2001); however in this study only a very modest reduction in adiponectin secretion following TNF-α stimulation was observed; however preincubation with A769662 did appear to elevate adiponectin secretion compared to the absence of A769662 (Fig. 5.4). These data could indicate that while TNF-α alone did not have a substantial effect on adiponectin production in 3T3-L1 adipocytes, it did not ablate the A769662-mediated elevation of adiponectin secretion. Similarly, our observation that IL-6 did not alter

adiponectin secretion (Fig. 5.4) is in contrast to a study by Fasshauer and co-workers, which reported an inhibition of adiponectin gene expression and protein secretion in response to IL-6 in 3T3-L1 adipocytes (Fasshauer et al. 2003). In contrast to observations with TNF-α, however, the presence of IL-6 appeared to ablate any A769662-mediated increase in adiponectin secretion (Fig. 5.4); thus IL-6 may not directly reduce adiponectin secretion, but may preclude an increase by AMPK activation.

Taken together, these data demonstrate for the first time in adipocytes that A769662 suppresses cytokine-stimulated secretion of the chemokines MCP-1, IP-10 and KC, and gene expression of MCP-1. Furthermore, A769662 has been shown to reduce MCP-1, IL-5 and MIP-1α, but not TNF-α secretion from macrophages. These data further support previous observations made in this study, and provides further evidence in support of AMPK as an anti-inflammatory protein; in addition to inhibition of proinflammatory signalling pathway intermediates, it has also been demonstrated to suppress proinflammatory gene transcription and protein secretion.

Preliminary observations were made in this study regarding the effect of individual proinflammatory cytokines on insulin-stimulated glucose uptake in 3T3-L1 adipocytes. A consistent observation was that exposure of 3T3-L1 adipocytes to a proinflammatory stimulus caused an elevation in basal glucose uptake, without any concomitant increase in insulin-stimulated glucose uptake; therefore the data were analysed using the fold change in insulin-stimulated glucose uptake (Fig. 5.7 – 5.10). The increased basal glucose uptake was likely to be GLUT1-mediated, as reported by Lumeng and co-workers (Lumeng, Deyoung, and Saltiel 2007). Figure 5.7 demonstrated that acute (1 h) stimulation with IL-6 appeared to slightly increase the fold change insulin-stimulated glucose uptake, while this was clearly reduced upon chronic IL-6 exposure (Fig. 5.7D, 5.7F, 5.7H), with 24 h IL-6 causing the most pronounced inhibition (5.7F). These preliminary observations correlate with studies suggesting acute IL-6 exposure (as observed in muscle following exercise) has a positive effect on insulin sensitivity (Carey et al. 2006), while chronic IL-6 exposure (as reported in obesity) is associated with insulin resistance (Rotter, Nagaev, and Smith 2003). Furthermore, these observations would indicate that IL-6 is unlikely to perturb insulin signalling via inhibitory phosphorylation of

signalling pathway components, as this would promote a rapid inhibition of glucose uptake. It is more likely IL-6-mediated insulin resistance is the result of the negative regulation of longer term processes, such as the transcription of genes involved in the insulin signalling pathway. Indeed, these observations are supported by a study by Rotter and co-workers, who reported that acute IL-6 stimulation had no effect on phosphorylation of IRS-1 at Ser307 (Rotter, Nagaev, and Smith 2003); a site which if phosphorylated impairs tyrosine phosphorylation of IRS-1 and subsequent downstream signalling. Moreover, chronic (24 h) IL-6 stimulation has been reported to induce a marked reduction in gene expression of IRS-1 and GLUT4, with a concomitant inhibition of 3T3-L1 adipocyte insulin-stimulated glucose uptake independent of TNF-α (Rotter, Nagaev, and Smith 2003). In contrast, IL-6 has been reported to induce insulin resistance in the liver in an acute manner via the transient upregulation of SOCS3, which was proposed to be associated with inhibition of IRS-1 tyrosine phosphorylation, p85 binding and subsequent phosphorylation of PKB (Senn et al. 2003).

Further preliminary observations suggested that acute stimulation with cytokines which signal via the MAPK/NFκB pathways was sufficient to suppress insulin sensitivity in 3T3-L1 adipocytes, with IL-1β and TNF-α inducing a reduction in the fold change in insulin-stimulated glucose uptake after 1 h and 6 h, respectively (Fig. 5.8F and 5.8D). Unexpectedly, TNF-α stimulation appeared to have no effect on insulin-stimulated glucose uptake after 1 h (Fig. 5.8B); however these data are merely a preliminary observation. Several studies have suggested the mechanism by which TNF-α or IL-1β induce insulin resistance is via the inhibitory phopshorylation of components of the insulin signalling pathway, which would correlate with acute, rather than chronic, exposure of these cytokines inhibiting insulin-stimulated glucose uptake. TNF-α has been proposed to stimulate the inhibitory phosphorylation of IRS-1 Ser307 via JNK (Rotter, Nagaev, and Smith 2003, Aguirre et al. 2000, Hotamisligil et al. 1996) or IKKβ (Gao et al. 2002). Less is known about the mechanism by which IL-1β may acutely suppress insulin-stimulated glucose uptake in adipocytes; however it is likely to also occur via JNK/IKKβ-mediated inhibitory phosphorylation of IRS-1. Interestingly, chronic TNF-α stimulation has also been proposed to suppress IRS-1 and GLUT4 gene expression in 3T3-L1 adipocytes (Rotter, Nagaev, and Smith 2003), while chronic exposure to IL-1β in 3T3-L1 adipocytes has been reported to downregulate IRS-1

expression in an ERK-dependent manner (Jager et al. 2007). Taken together, TNF-α and IL-1β appear to acutely regulate insulin signalling via phosphorylation of key insulin signalling pathway components, and elicit longer term effects via inhibition of gene transcription.

When assessing the effects of chronic stimulation with an individual cytokine, it can be difficult to delineate whether a reduction in insulin sensitivity is due to that particular cytokine, or if it is the result of any number of other proinflammatory factors whose transcription has been induced by the cytokine in question. Moreover, when considering inflammation-mediated insulin resistance in obese adipose tissue, it is not likely to be mediated predominantly by a single cytokine; rather a combination of various proinflammatory factors secreted from macrophages as well as adipocytes. Indeed, while hypertrophic adipocytes do synthesise and secrete proinflammatory mediators, it is well established that the majority within adipose tissue originate from M1 activated macrophages. Furthermore, infiltration of macrophages into adipose tissue has been proposed to crucial to the development of obesity-related insulin resistance; mice deficient in factors related to macrophage recruitment such as MCP-1 or CCR2 (MCP-1 receptor) were reported to have reduced adipose tissue macrophage accumulation and were protected from HFD-induced insulin resistance (Kanda et al. 2006, Weisberg et al. 2006). TNF-α was originally considered to be the primary cytokine involved in the development of insulin resistance; obesity is associated with increased TNF-α, and a plethora of studies exist proposing its absence was sufficient to restore insulin sensitivity *in vitro* and *in vivo* (Hotamisligil, Shargill, and Spiegelman 1993, Uysal et al. 1997, Kern et al. 1995, Dandona et al. 1998). Interestingly, recent clinical studies targeting TNF-α individually with neutralising antibodies or chemical inhibitors proved unsuccessful in improving insulin sensitivity in humans (Ofei et al. 1996, Wascher et al. 2011, Ferraz-Amaro et al. 2011), thus indicating the clinical importance of proinflammatory cytokines other than TNF-α. Rather than examine the effect of individual cytokines, it would be more relevant to investigate the effect of M1 activated macrophage secretory products on adipocyte insulin sensitivity.

In this study, murine RAW 264.7 macrophages were exposed to LPS in order to promote a shift in polarisation towards M1, and therefore stimulate the secretion

of proinflammatory mediators. This conditioned medium was then applied to 3T3-L1 adipocytes to investigate the effect of macrophage secretory products on adipocyte insulin-stimulated glucose uptake utilising an indirect co-culture technique. Figure 5.9 demonstrated that macrophages stimulated for 6 h with LPS secreted proinflammatory factors which significantly reduced 3T3-L1 adipocyte insulin sensitivity upon exposure. These data suggest the existence of a paracrine interaction between macrophages and adipocytes. In a similar study, Lumeng and co-workers also reported a reduction in the fold change in insulin-stimulated glucose uptake in response to exposure of conditioned medium from LPS-activated macrophages (Lumeng, Deyoung, and Saltiel 2007). Furthermore, the group reported a reduction in IRS-1 protein expression and tyrosine phosphorylation, while no difference in IRS-1 Ser307 or JNK phosphorylation was observed following treatment with macrophage conditioned medium (Lumeng, Deyoung, and Saltiel 2007).

We hypothesised that activation of macrophage AMPK with A769662 would limit the secretion of LPS-stimulated proinflammatory mediators, and subsequently improve the reduced 3T3-L1 adipocyte insulin sensitivity observed in Figure 5.9. Interestingly, exposure of A769662-treated macrophage conditioned medium appeared to cause a subtle increase in 3T3-L1 glucose uptake, which was significantly ablated when macrophages had been exposed to LPS (Fig. 5.10). These data suggest that AMPK activation in macrophages may induce the production of anti-inflammatory, insulin-sensitising factors; however this may not be sufficient to restore the insulin resistance caused by the plethora of proinflammatory factors secreted by activated macrophages. Taken together with the data shown in Figure 5.6, which demonstrated that A769662 was able to suppress LPS-stimulated MCP-1, IL-5, and possibly MIP-1α, but not TNF-α, these data suggest it is possible that the elevated TNF-α secreted from these activated macrophages even in the presence of A769662 could explain the reduction in insulin-stimulated glucose uptake upon exposure of 3T3-L1 adipocytes to conditioned medium from these macrophages. This speculation would correlate well with other studies which have suggested TNF-α to be the key cytokine contributing to inflammation-associated insulin resistance *in vitro* (Hotamisligil, Shargill, and Spiegelman 1993, Nieto-Vazquez et al. 2008).

To our knowledge, no study has directly evaluated whether an AMPK-mediated reduction in inflammation corresponds to an improvement in adipocyte insulin sensitivity; however, a few studies have alluded to this possibility. Galic and co-workers reported that the hematopoietic deletion of AMPKβ1 in mice resulted in the infiltration of activated macrophages into liver and adipose tissue, and the subsequent development of hepatic insulin resistance (Galic et al. 2011). Furthermore, a clinical study proposed that the diminished AMPK activity in obese individuals was the cause of the increased adipose tissue inflammation and whole body insulin resistance observed (Gauthier et al. 2011). Taken together, this these data suggest both individual cytokines and M1 activated macrophage secretory products can induce insulin resistance in 3T3-L1 adipocytes; however A769662-mediated AMPK activation may not be sufficient to restore insulin sensitivity *in vitro* while macrophage TNF-α secretion remains elevated.

AMPK, adipocyte morphology and adipogenesis

Adipogenesis is an anabolic process, and is described in more detail in section 1.4.2. AMPK has been suggested to inhibit it in the MCE phase, with reduced expression of C/EBPβ (which is essential for initiation of the adipogenic transcriptional cascade), and subsequent inhibition of PPARγ, C/EBPα and late adipogenic markers (Habinowski and Witters 2001). The mechanism by which AMPK inhibits adipogenesis is currently unknown.

Separately, the JAK2-STAT3 pathway has been suggested to be important in the differentiation process, with several studies postulating that STAT phosphorylation in the MCE phase is essential for adipocyte differentiation (Stewart et al. 1999, Shang and Waters 2003). Indeed, selective pharmacological inhibitors, STAT3 siRNA and a dominant-negative STAT3 all inhibited adipogenesis in 3T3-L1 adipocytes (Wang, Zhou, et al. 2010). Taken together, it appears that AMPK inhibits adipocyte differentiation at the MCE, at a temporally similar manner to when STAT3 phosphorylation and activation is critical for differentiation to proceed. It was therefore of interest to investigate whether AMPK could inhibit adipogenesis via regulation of STAT3.

Figure 5.11A demonstrated that STAT3 was phosphorylated 24-48h post-differentiation; a finding which supports a study by Wang and co-workers

indicating STAT3 phosphorylation is rapidly and transiently elevated during adipogenesis (Wang, Zhou, et al. 2010). Basal ACC phosphorylation appeared increased from day 4 post-induction of differentiation (Fig. 5.11A), an observation also reported by Zhou and co-workers (Zhou, Wang, et al. 2009). This suggests that while AMPK activation during the MCE phase is detrimental to adipogenesis, it may be required during the later phase. Importantly, activation of AMPK with A769662 was found to inhibit this induction of STAT3 phosphorylation (Fig. 5.11A). It is unclear from these data whether differentiation was suppressed in response to AMPK activation, as despite a reduction in expression of the late adipogenic marker C/EBPα at day 4 post-differentiation, expression of C/EBPα and PPARγ was still maintained at day 8. It is likely that this could have been due to the presence of troglitazone, a PPARγ agonist, in the differentiation cocktail; this is not essential for differentiation but is often utilised to improve accumulation of lipid droplets within the cells. Indeed, Wang and co-workers reported progression of 3T3-L1 adipogenesis in the presence of troglitazone, despite pharmacological or RNAi-mediated inhibition of STAT3 (Wang, Zhou, et al. 2010). As troglitazone did not alter pharmacological downregulation of STAT3 activation, it was postulated that PPARγ may regulate adipogenesis downstream of STAT3 (Wang, Zhou, et al. 2010). Separately, 3T3-L1 adipocytes differentiated in the absence of troglitazone were incubated with and without A769662 prior to staining with Oil red O; observation of lipid accumulation via staining provided a clear indication of the progression of adipogenesis. Figure 5.11B demonstrated substantial lipid accumulation in vehicle 3T3-L1 adipocytes on day 8 post-differentiation as demonstrated by the presence of red staining, which was abolished with A769662-mediated AMPK activation. Taken together, these preliminary data showed for the first time that A769662 inhibited adipogenesis-induced STAT3 phosphorylation in 3T3-L1 adipocytes and suppressed the lipid accumulation characteristic of adipogenesis. The mechanism by which AMPK activation inhibits adipocyte differentiation may be via inhibition of STAT3 phosphorylation at the MCE phase of adipogenesis, however further investigation is required.

In order to evaluate whether AMPKα1 influenced adipocyte cell size, omental and subcutaneous adipose tissue from *AMPKα1$^{-/-}$* and genetically matched wild-type mice fed a chow diet were obtained. The size of the adipocytes appeared reduced in *AMPKα1$^{-/-}$* tissue relative to wild-type in both adipose depots, with a more

striking contrast observed in the omental adipose (Fig. 5.12). These observations support a study by Daval and co-workers, who reported smaller adipocytes in mice lacking AMPKα1 (Daval et al. 2005). On the other hand, an increase in adipocyte hypertrophy was reported in *AMPKα2$^{-/-}$* mice; however this occurred in response to HFD feeding (Villena et al. 2004). Moreover, AMPK activity in adipocytes is mainly represented by the α1 isoform (Daval et al. 2005). Smaller adipocytes in the absence of AMPKα1 could be attributed to an increase in lipolysis; furthermore, enhanced lipolysis would be reflected by an increase in serum FA, which can be proinflammatory (Shi, Kokoeva, et al. 2006). It could be speculated that the basal phosphorylation of proinflammatory cytokines JNK (Fig. 3.10A) and STAT3 (Fig. 4.7) in *AMPKα1$^{-/-}$* adipose tissue could be linked to an increase in serum FA, as Figure 5.3 suggests there to be no shift in macrophage polarisation to M1 in the *AMPKα1$^{-/-}$* adipose tissue.

Overall, this current work demonstrates for the first time in adipocytes that A769662 suppresses cytokine-stimulated chemokine expression and secretion, and suppresses IL-5, MCP-1 and MIP-1α, but not TNF-α secretion from activated macrophages. Furthermore, proinflammatory factors secreted from M1 activated macrophages suppress insulin-stimulated glucose uptake in adipocytes which could not be rescued by A769662, possibly due to the presence of TNF-α. Lastly, we observed no difference between M1/M2 activation state of macrophages in *AMPKα1$^{-/-}$* and wild-type adipose tissue, while *AMPKα1$^{-/-}$* is associated with comparatively small adipocytes.

Chapter 6 - Final Discussion

This study has demonstrated for the first time that AMPK activation in adipocytes is associated with inhibition of multiple distinct proinflammatory signalling pathways, and the subsequent inhibition of chemokine gene expression and chemokine and cytokine secretion. Furthermore, some of the mechanisms by which this occurs have also been characterised.

Work in this current study showed that the direct AMPK activator A769662 suppressed phosphorylation and activation of multiple proinflammatory signalling pathway intermediates in response to proinflammatory cytokine stimulation in 3T3-L1 adipocytes. As described (1.2.2.1), cytokines such as TNF-α and IL-1β simultaneously activate the NFκB pathway and MAPK cascade, regulating transcription of proinflammatory genes in the nucleus. In this study, AMPK activation suppressed phosphorylation of JNK, ERK1/2 and p38 MAPK, supporting similar findings by Jeong and co-workers in macrophages in response to berberine (Jeong et al. 2009). In addition, elevated JNK phosphorylation was reported in macrophages and endothelial cells of mice deficient in AMPKβ1 or AMPKα2, respectively (Galic et al. 2011, Dong et al. 2010). Furthermore, A769662 or adenoviral upregulation of a constitutively active AMPK mutant ablated nuclear translocation of the transcription factor NFκB; conversely, downregulation of AMPK activation suppressed the A769662-mediated inhibition of NFκB nuclear translocation. Thus, these data demonstrated that A769662 inhibited nuclear translocation in an AMPK-dependent manner. In line with this, AMPK activation ameliorated phosphorylation of upstream IκB and IKK. These data support previous findings that there was an increase in NFκB present in the nuclear fraction of endothelial cells deficient in AMPKα2 (Wang, Zhang, et al. 2010). Concomitantly, A769662 suppressed TNF-α-stimulated MCP-1 gene expression and IL-1β-stimulated secretion of chemokines MCP-1, IP-10 and KC from 3T3-L1 adipocytes; as these proteins are transcriptionally regulated by NFκB and/or AP-1, these data correlate with inhibition of NFκB nuclear translocation by AMPK. Furthermore, these data support previous reports that AMPK inhibits TNF-α-stimulated MCP-1 expression and secretion in endothelial cells (Ewart, Kohlhaas, and Salt 2008). Taken together, this study has demonstrated for the first time in adipocytes that

A769662-mediated AMPK activation simultaneously suppresses cytokine-stimulated phosphorylation of MAPKs and NFκB signalling pathway intermediates, and the downstream transcription and subsequent secretion of proinflammatory chemokines.

While AMPK has previously been reported to phosphorylate and activate eNOS (Morrow et al. 2003), results from the current study indicated that the mechanism by which AMPK produces its anti-inflammatory effects is likely to be independent of NO production. Thus, the molecular mechanism(s) by which AMPK elicits the inhibition of MAPK and NFκB signalling pathways remains to be determined, but occur at a site upstream of MAPK and IKK. A potential target of AMPK could be TAK1; as TNF-α and IL-1β engage different signalling pathways upstream of TAK1 activation, it is possible that the coordinated inhibition of JNK, p38 and IKK phosphorylation by AMPK in response to both TNF-α and IL-1β reflects targets common to both pathways. Several mechanisms have recently been proposed for the AMPK-mediated inhibition of NFκB signalling. Zhang and co-workers reported in cultured endothelial cells that constitutively active AMPK or long-term AICAR treatment phosphorylated the transcriptional co-activator p300, subsequently blocking acetylation of NFκB p65, and in turn inhibited TNF-α-stimulated NFκB DNA binding (Zhang et al. 2011). Similarly, it has been reported that AMPK may inhibit NFκB-mediated gene transcription via activation of the deacetylase SIRT1 which was demonstrated to deacetylate Lys310 of p65, stimulating Ser9-mediated methylation of Lys314/315 (Yang, Tajkhorshid, and Chen 2010). This leads to the polyubiquitination and subsequent proteasomal degradation of p65, thus ablating transcription of NFκB target genes. However, due to the rapid nature of AMPK-mediated inhibition of the NFκB pathway in 3T3-L1 adipocytes observed in the current study, it seems unlikely to be due to the suppression of p300 histone acetyltransferase activity. Lastly, another group reported that hyperphosphorylation of IKK by constitutively active AMPK blocked subsequent phosphorylation of IκB and p65, and in turn suppressed NFκB-mediated gene transcription in response to TNF-α I COS-7 cells (Bess et al. 2011). This is in direct contrast to the findings in the current study, whereby the rapid inhibition of IKK phosphorylation and subsequent downstream NFκB signalling further suggests TAK1 may be a potential target of AMPK in adipocytes to suppress downstream signalling.

The current study also investigated the effect of A769662-mediated AMPK activation on the IL-6 proinflammatory signalling pathway in adipocytes. A769662 suppressed IL-6-stimulated STAT3 phosphorylation and subsequent MCP-1 gene expression in 3T3-L1 adipocytes; in contrast, IL-6 did not appear to induce chemokine or cytokine secretion. This could indicate that while IL-6 stimulates chemokine gene expression, it is possible that secreted products were produced at too low a level to be observed. IL-6 was not found to stimulate ERK1/2 phosphorylation in these cells; consistent with this, no stimulation of C/EBPβ protein expression was observed. The mechanism by which AMPK inhibited IL-6-stimulated STAT3 phosphorylation was also investigated in this study. AMPK was not found to inhibit IL-6-stimulated STAT3 phosphorylation via the action of a phosphatase; however genetic manipulation of JAK2 in HEK-293 and HeLa cells suggested JAK may be a possible target for AMPK, as A769662-mediated inhibition of STAT3 phosphorylation was ablated following transfection with a constitutively active JAK2 mutant. Furthermore, this study demonstrated that pharmacological inhibition of mTORC1 and mTORC2 suppressed STAT3 phosphorylation in 3T3-L1 adipocytes, potentially via the action of the phosphatase TC-PTP. Prior to the beginning of the current study, the effect of AMPK on IL-6-stimulated STAT3 phosphorylation had, to our knowledge, never been reported in any cell type. During the course of this study, only a small number of groups have reported an AMPK-mediated reduction in IL-6-stimulated STAT3 phosphorylation (Nerstedt et al. 2010, Nerstedt et al. 2013, Kim et al. 2012); however these studies were all conducted in liver-derived cells. In contrast to adipocytes, and indeed the majority of cells, hepatocytes do not require the presence of a soluble IL-6 receptor as they possess membrane-bound IL-6 receptors. Trans-signalling, requiring the soluble IL-6 receptor, is proposed to be more proinflammatory than classical IL-6 signalling involving the membrane-bound receptor (Rose-John 2012); thus the consequences of IL-6 signalling in liver cells are likely to be different compared to adipocytes.

Collectively, these results demonstrate for the first time in adipocytes that A769662 inhibits IL-6-stimulated STAT3 phosphorylation independently of phosphatases and potentially via regulation of upstream JAK. Furthermore, mTOR inhibition suppresses STAT3 phosphorylation via a mutually exclusive mechanism, potentially mediated by TC-PTP. While IL-6 did not stimulate observable secretion

of proinflammatory mediators in this study, the upregulation of MCP-1 gene expression was suppressed by A769662, thereby indicating A769662-mediated AMPK activation inhibits a functional consequence of IL-6 signalling in 3T3-L1 adipocytes. The potential regulation of IL-6-stimulated JAK/STAT pathway is summarised below:

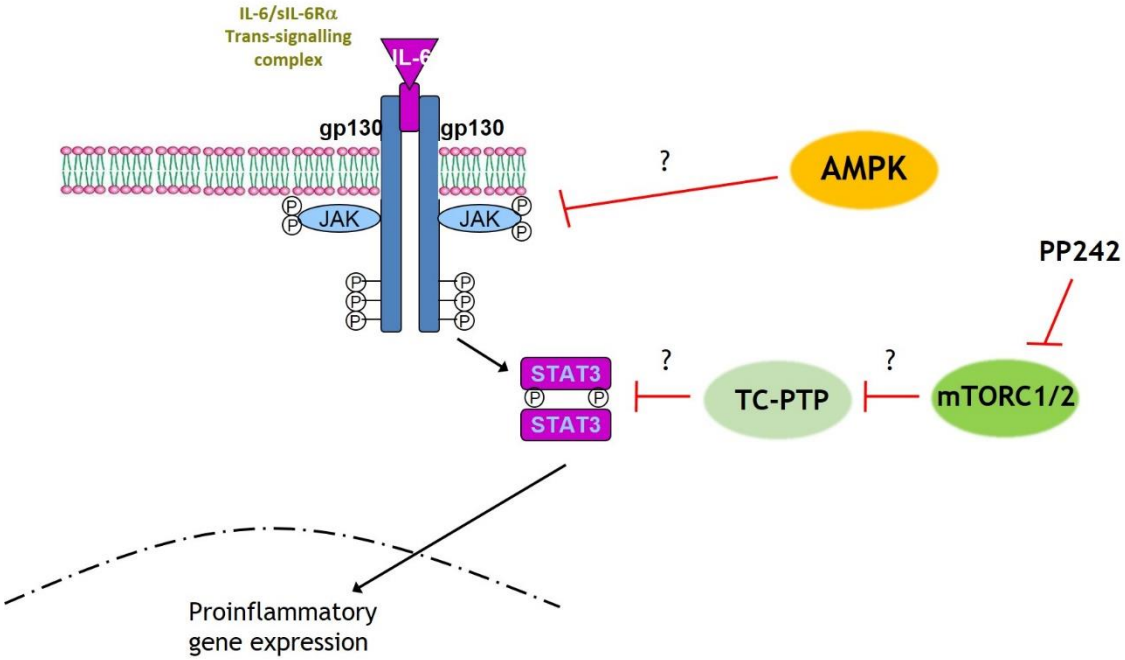

Figure 6-1: Potential regulation of IL-6-stimulated proinflammatory signalling by AMPK and mTOR in 3T3-L1 adipocytes

Macrophage recruitment and M1 activation in obese adipose tissue is critical for the development of a sustained proinflammatory environment, contributing to insulin resistance in metabolic tissues. In the current study A769662 suppressed secretion of MCP-1, MIP-1α and IL-5, but not TNF-α from activated RAW 264.7 macrophages; however the reduction in 3T3-L1 adipocyte glucose uptake following exposure to activated macrophage secreted products was not rescued upon prior AMPK activation in macrophages. This could be potentially due to the continued presence of TNF-α in the conditioned medium. Furthermore, preliminary data suggested that acute TNF-α or IL-1β and chronic IL-6 stimulation may ameliorate insulin-stimulated glucose uptake in 3T3-L1 adipocytes. Taken together, these data indicate that both individual cytokines and activated macrophage secreted

products suppress adipocyte insulin-stimulated glucose uptake; however, although A769662 inhibited secretion of several proinflammatory mediators from macrophages, the continued presence of TNF-α in the macrophage conditioned medium may have been sufficient to induce insulin resistance.

The basal proinflammatory profile of adipose tissue from *AMPKα1$^{-/-}$* mice was examined for the first time in this study. Basal phosphorylation of JNK and STAT3 was elevated in *AMPKα1$^{-/-}$* adipose tissue compared to wild-type. While this study provided evidence suggesting this may have been independent of alterations in macrophage M1/M2 ratio, FACS (fluorescence-activated cell sorting) analysis should be performed to fully address this. Overall, these results suggest that cells other than macrophages, such as adipocytes or endothelial cells, may have been the source of inflammation observed in *AMPKα1$^{-/-}$* adipose tissue. Alternatively, the smaller adipocytes observed in *AMPKα1$^{-/-}$* adipose tissue could be the result of an increase in lipolysis; thus the subsequent increase in serum FA could stimulate JNK and STAT3 phosphorylation in adipose tissue. As the mice are global AMPKα1 deficient, however, there is the potential for this to be a secondary, indirect effect due to the down-regulation of AMPKα1 in other tissues. Thus, there is an urgent need for the generation of animals with a tissue-specific AMPK ablation in order to truly characterise the role of AMPK in adipose.

AMPK has been reported to suppress NFκB and MAPK inflammatory signalling in cells that constitute adipose tissue, including endothelial cells and macrophages (Wang, Zhang, et al. 2010, Dong et al. 2010, Ewart, Kohlhaas, and Salt 2008, Jeong et al. 2009, Galic et al. 2011, Sag et al. 2008); however, the effect of AMPK activation on NFκB, MAPK and JAK/STAT signalling in adipocytes and the molecular mechanisms by which AMPK elicits its anti-inflammatory effects had never been examined. Overall, this study demonstrated for the first time that the AMPK activator A769662 inhibited multiple, distinct, proinflammatory signalling pathways in adipocytes, leading to the suppression of subsequent proinflammatory gene expression and chemokine secretion. Furthermore, *AMPKα1$^{-/-}$* mouse adipose tissue exhibited increased activation of proinflammatory signalling intermediates, despite no obvious alteration in the M1/M2 ratio as assessed by analysis of M1 and M2 marker mRNA. Finally, A769662 inhibited proinflammatory protein secretion from macrophages; however the ability of AMPK activation to rescue

inflammation-induced insulin resistance remains to be determined. Very few studies have investigated adipose tissue AMPK and inflammation; those that have found AMPK activation suppressed expression of proinflammatory cytokines in adipose tissue of obese *db/db* mice (Jeong et al. 2009) and TNF-α and IL-6 secretion from human SCAT cultured *ex vivo* (Lihn et al. 2008). Human *in vivo* studies revealed that AMPK expression and activity was lower in VAT compared with SCAT in morbidly obese individuals (Gauthier et al. 2011, Martínez-Agustin et al. 2010). Moreover, AMPK activity was further reduced in adipose tissue of insulin resistant volunteers compared with BMI (body mass index)-matched insulin sensitive controls (Gauthier et al. 2011, Martínez-Agustin et al. 2010). A schematic overview outlining the potential inhibition of adipose inflammation by AMPK is depicted below:

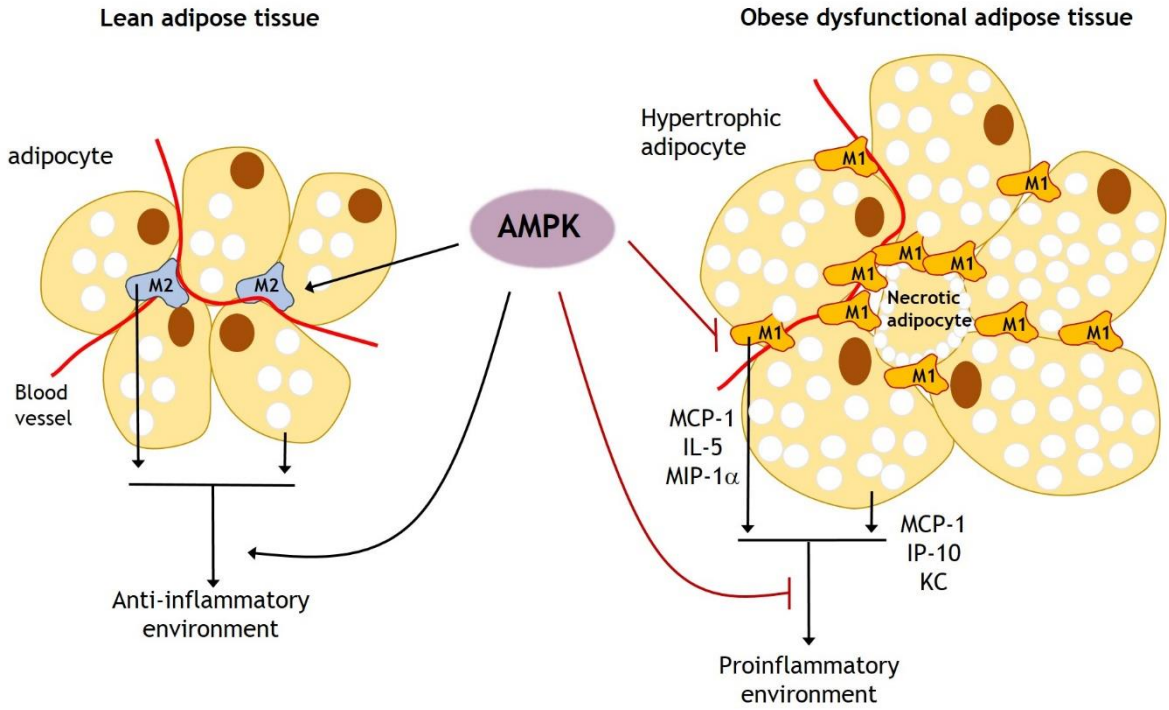

Figure 6-2: Regulation of adipose tissue inflammation by AMPK

This study suggests that activation of AMPK in adipocytes and macrophages may reduce the proinflammatory profile of adipose tissue which is associated with obesity and insulin resistance. The small number of studies examining AMPK activation in human adipose tissue have suggested that AMPK activation in adipose tissue could be both feasible and beneficial. Metformin is a widely-used anti-diabetic drug which promotes insulin-stimulated glucose uptake in muscle and

suppresses hepatic glucose output, while also lowering plasma TG; however the extent to which indirect AMPK activation by metformin underlies some of its effects, such as the ability to suppress hepatic glucose output (Foretz et al. 2010) is currently debated. Recent work in our laboratory has shown that metformin stimulated AMPK activity in SCAT of individuals with Type 2 diabetes in a randomised glycaemia-controlled cross-over study (Boyle et al. 2011). Furthermore, metformin was reported to reduce serum TNF-α in obese insulin resistant patients in a randomised clinical trial (Evia-Viscarra et al. 2012), therefore suggesting clinical anti-inflammatory effects of the drug. The thiazolidinedione class of anti-diabetic drugs, including rosiglitazone, also stimulate AMPK activation. Moreover, rosiglitazone was reported to suppress expression of proinflammatory genes in adipose tissue of patients with Type 2 diabetes (Kolak et al. 2007); however, as with metformin, the extent to which AMPK underlies their clinical action remains uncertain.

More recently, salicylate, the pharmacologically active breakdown product of aspirin and salsalate *in vivo*, has been reported to bind and allosterically activate β1-containing AMPK complexes in a similar manner to A769662 (Hawley et al. 2012). Salicylate has been shown to stimulate hepatocyte ACC phosphorylation and FA oxidation *in vitro* and fat utilisation *in vivo* in an AMPK-dependent manner (Hawley et al. 2012). Moreover, salicylates have also been reported to improve the proinflammatory profile and glucose tolerance in patients with Type 2 diabetes (Hundal et al. 2002). Salicylate has long been proposed to exert its anti-inflammatory actions via inhibition of NFκB activation (Kopp and Ghosh 1994, Kiss et al. 2004); thus findings in the current study suggest that salicylate may suppress NFκB activation via AMPK, although this has yet to be directly investigated.

The widespread use of metformin, thiazolidinediones and salicylate suggests that AMPK-activating drugs could be relatively safe for the long-term management of chronic inflammatory conditions. As the activators salicylate and A769662 selectively target β1-containing AMPK complexes, this indicates that it may be feasible to design AMPK activators that are targeted to specific tissues by exploiting tissue-specific variation of subunit isoforms. Furthermore, the different γ subunit isoforms within the AMPK complexes have been shown to influence sensitivity to AMP (Cheung et al. 2000), and therefore may be differentially

sensitive to pharmacological AMPK activators. Using known compositions of AMPK complexes as a starting point, it could be possible to screen for selective activators which have an anti-inflammatory effect in adipocytes or macrophages. Important considerations when developing an AMPK activator to target inflammation would be firstly, that it should elicit anti-inflammatory effects without inducing hypoglycaemia which would not necessarily be desirable for all patients. Secondly, the drug should not cross the blood-brain barrier, considering that CaMMKβ-mediated AMPK activation in the hypothalamus is a key mechanism by which ghrelin stimulates appetite and feeding responses (Kola and Korbonits 2009).

Activating AMPK in adipose tissue macrophages in particular could represent an effective way in which obesity-related inflammation and subsequent insulin resistance could be ameliorated. As discussed (1.2.3), while hypertrophic adipocytes release proinflammatory cytokines and chemokines, they do so to a far lesser degree than activated macrophages. Furthermore, while macrophages are recruited to adipose tissue and M1-activated in response to chemokines and cytokines secreted from adipocytes, they have also been proposed to be recruited and activated by increased FA and necrotic adipocytes. Thus, while activating AMPK in adipocytes would be beneficial in terms of suppressing adipocyte production of proinflammatory mediators, it could potentially be insufficient to ablate macrophage recruitment and M1 activation. Importantly, directly activating AMPK in adipocytes has been reported to inhibit insulin-stimulated glucose uptake (Salt, Connell, and Gould 2000). As described (1.1.2), glucose enters adipocytes in the fed state and is stored as TG. Therefore inhibition of glucose uptake into adipocytes subsequently suppresses FA and TG synthesis which is an energy-consuming process. It could therefore be reasoned that AMPK activation inhibits insulin-stimulated glucose uptake in adipocytes in order to reduce the ATP-dependent synthesis of FA and TG, and moreover allow glucose to be utilised as an energy source by tissues other than adipose, which could simply use the TG stored in adipocytes. Thus, while direct AMPK activation in adipocytes could reduce inflammation, it would also inhibit insulin-stimulated glucose uptake. In contrast, if AMPK could be selectively activated in adipose tissue macrophages, this would promote their polarisation towards an M2 anti-inflammatory phenotype, ameliorating secretion of proinflammatory cytokines;

thus AMPK activation in adipose tissue macrophages could potentially overcome cytokine-induced insulin resistance.

A significant limitation in this study is that adipocytes are relatively genetically intractable, thus there is a marked difficulty associated with using standard molecular biology techniques such as siRNA or adenoviruses to up- or down-regulate AMPK in terminally differentiated adipocytes. In the current study, attempts to elucidate the effects of adenovirus-mediated up- or down-regulation of AMPK in whole cell lysates were unsuccessful; however, the inhibition of NFκB nuclear translocation was demonstrated to be AMPK-dependent using Ad.α1CA and Ad.α1DN adenoviruses. In addition, siRNA-mediated knockdown of AMPK in HUVECs demonstrated that inhibition of STAT3 phosphorylation was AMPK dependent. Moreover, analysis of adipose tissue from AMPKα1-deficient mice provided evidence supporting a role for AMPK in the regulation of inflammatory signalling. The 3T3-L1 preadipocyte cell line is a model system for investigating adipocyte biology and differentiation, as upon induction of differentiation they accumulate the biochemical and morphological characteristics of adipocytes. One limitation of using cultured adipocytes is that they do not represent adipocytes from a specific type of depot, thus it is not possible to extrapolate findings to SCAT or VAT *in vivo*. As discussed (1.1.1) different fat depots are associated with differential metabolic risk. VAT has been widely proposed to be particularly pathogenic as it exhibits enhanced lipolysis and endocrine activity. Indeed, VAT is more strongly associated with an increased risk of the metabolic syndrome and cardiovascular disease (Fox et al. 2007). The current study provides evidence in adipose tissue suggesting that the basal proinflammatory profile of both visceral and subcutaneous depots may be altered in *AMPKα1*$^{-/-}$ mice.

Published studies of AMPK function in adipose tissue tend to be based on isolated rodent adipocytes or cells that have been differentiated to adipocytes *in vitro*, and also rely on less-specific methods of transiently activating or inhibiting AMPK. Similarly, *in vivo* data generated using animals which are genetically deficient in one isoform of AMPK have alluded to potential actions of AMPK in adipose tissue; however as discussed above, there is an urgent need for the development of animals in which AMPK is specifically deleted in adipocytes to confirm the role of AMPK in adipose.

Future work

Currently the mechanism by which AMPK activation in 3T3-L1 adipocytes inhibits TNF-α/IL-1β-stimulated proinflammatory signalling remains to be elucidated. As previously discussed, TAK1 is the point at which TNF-α and IL-1β signalling pathways converge; furthermore TAK1 is an upstream kinase of IKK, and MAPKs JNK and p38. Thus, the potential regulation of TAK1 activation by AMPK could be investigated by immunoblotting with phospho-specific TAK1 antibodies. If TAK1 phosphorylation appears to be regulated by AMPK, *in vitro* kinase assays with TAK1 immunoprecipitates could also be performed to assess whether it is a direct target of AMPK. The association of MAPKs with scaffolding proteins has been proposed to underlie the specificity of MAPK activation and action (Brown and Sacks 2009), thus the potential for AMPK activation to alter MAPK association with scaffolds could be investigated in immunoprecipitates under basal and stimulated conditions. The AMPK-mediated activation of a phosphatase could potentially inhibit phosphorylation of TNF-α/IL-1β pathway intermediates, thus it would be of interest to assess whether AMPK-mediated inhibition of phosphorylation could be reversed by preincubation with the general phosphatase inhibitor vanadate.

Results from the current study suggest that mTOR may suppress IL-6-stimulated STAT3 phosphorylation via TC-PTP and potentially independently of AMPK activation. This should be further explored using cells lacking components of the mTOR complex to establish whether this is altered by prior AMPK activation. Results from this study also suggested that the inhibition of STAT3 phosphorylation by AMPK may be mediated via JAK. Once potential target protein(s) (such as JAK) that underlie the AMPK-mediated anti-inflammatory effects have been identified, *in vitro* kinase assays of purified proteins to establish whether they are bona fide AMPK substrates and peptide arrays to identify potential phosphorylation sites targeted by AMPK could be undertaken. Site-specific antibodies and mass spectrometry could also be used to investigate AMPK-regulated phosphorylation *in vivo*, and mutants to establish the consequences on activity.

To further investigate whether AMPK activation can overcome cytokine-induced insulin resistance, western blotting to determine expression and phosphorylation of insulin signalling pathway intermediates including IRS1, IRS2 and PKB in lysates

obtained from 3T3-L1 adipocytes incubated with TNF-α, IL-1β, IL-6 or activated macrophage conditioned medium, and AMPK activators in the presence and absence of insulin. Furthermore, the effect of AMPK on the migration of macrophages towards 3T3-L1 conditioned medium could be assessed in a Boyden chamber.

Finally, as preliminary results from this study showed AMPK activation ameliorated STAT3 phosphorylation and lipid accumulation during 3T3-L1 adipogenesis, it would be interesting to establish whether inhibition of STAT3 phosphorylation during the early phase of adipocyte differentiation is the mechanism by which AMPK suppresses adipogenesis. 3T3-L1 preadipocytes could be infected with adenovirus expressing a constitutively active mutant STAT3 or JAK2 prior to treatment with an AMPK activator and induction of differentiation to assess whether AMPK-mediated inhibition of adipogenesis is STAT3-mediated.

Adipose tissue inflammation contributes to insulin resistance and the development of Type 2 diabetes. Thus, elucidation of the molecular mechanisms by which AMPK may inhibit inflammatory pathways in adipocytes could uncover novel potential therapeutic targets, which could lead to the development of novel therapies for treating Type 2 diabetes.

List of References

Abu-Elheiga, L., M. M. Matzuk, P. Kordari, W. Oh, T. Shaikenov, Z. Gu, and S. J. Wakil. 2005. "Mutant mice lacking acetyl-CoA carboxylase 1 are embryonically lethal." *Proc Natl Acad Sci U S A* no. 102 (34):12011-6. doi: 10.1073/pnas.0505714102.

Aguirre, V., T. Uchida, L. Yenush, R. Davis, and M. F. White. 2000. "The c-Jun NH(2)-terminal kinase promotes insulin resistance during association with insulin receptor substrate-1 and phosphorylation of Ser(307)." *J Biol Chem* no. 275 (12):9047-54.

Ahmadian, M., M. J. Abbott, T. Tang, C. S. Hudak, Y. Kim, M. Bruss, M. K. Hellerstein, H. Y. Lee, V. T. Samuel, G. I. Shulman, Y. Wang, R. E. Duncan, C. Kang, and H. S. Sul. 2011. "Desnutrin/ATGL is regulated by AMPK and is required for a brown adipose phenotype." *Cell Metab* no. 13 (6):739-48. doi: 10.1016/j.cmet.2011.05.002.

Alessi, D. R., S. R. James, C. P. Downes, A. B. Holmes, P. R. Gaffney, C. B. Reese, and P. Cohen. 1997. "Characterization of a 3-phosphoinositide-dependent protein kinase which phosphorylates and activates protein kinase Balpha." *Curr Biol* no. 7 (4):261-9.

Amar, J., J. Fauvel, L. Drouet, J. B. Ruidavets, B. Perret, B. Chamontin, H. Boccalon, and J. Ferrieres. 2006. "Interleukin 6 is associated with subclinical atherosclerosis: a link with soluble intercellular adhesion molecule 1." *J Hypertens* no. 24 (6):1083-8. doi: 10.1097/01.hjh.0000226198.44181.0c.

Anderson, K. A., R. L. Means, Q. H. Huang, B. E. Kemp, E. G. Goldstein, M. A. Selbert, A. M. Edelman, R. T. Fremeau, and A. R. Means. 1998. "Components of a calmodulin-dependent protein kinase cascade. Molecular cloning, functional characterization and cellular localization of Ca2+/calmodulin-dependent protein kinase kinase beta." *J Biol Chem* no. 273 (48):31880-9.

Andersson, C. X., V. R. Sopasakis, E. Wallerstedt, and U. Smith. 2007. "Insulin antagonizes interleukin-6 signaling and is anti-inflammatory in 3T3-L1 adipocytes." *J Biol Chem* no. 282 (13):9430-5. doi: 10.1074/jbc.M609980200.

Anthonsen, M. W., L. Rönnstrand, C. Wernstedt, E. Degerman, and C. Holm. 1998. "Identification of novel phosphorylation sites in hormone-sensitive lipase that are phosphorylated in response to isoproterenol and govern activation properties in vitro." *J Biol Chem* no. 273 (1):215-21.

Anthony, N. M., M. P. Gaidhu, and R. B. Ceddia. 2009. "Regulation of visceral and subcutaneous adipocyte lipolysis by acute AICAR-induced AMPK activation." *Obesity (Silver Spring)* no. 17 (7):1312-7. doi: 10.1038/oby.2008.645.

Arad, M., C. E. Seidman, and J. G. Seidman. 2007. "AMP-activated protein kinase in the heart: role during health and disease." *Circ Res* no. 100 (4):474-88. doi: 10.1161/01.RES.0000258446.23525.37.

Arai, N., H. Masuzaki, T. Tanaka, T. Ishii, S. Yasue, N. Kobayashi, T. Tomita, M. Noguchi, T. Kusakabe, J. Fujikura, K. Ebihara, M. Hirata, K. Hosoda, T. Hayashi, H. Sawai, Y. Minokoshi, and K. Nakao. 2007. "Ceramide and adenosine 5'-monophosphate-activated protein kinase are two novel regulators of 11beta-hydroxysteroid dehydrogenase type 1 expression and activity in cultured preadipocytes." *Endocrinology* no. 148 (11):5268-77. doi: 10.1210/en.2007-0349.

Araki, E., M. A. Lipes, M. E. Patti, J. C. Brüning, B. Haag, R. S. Johnson, and C. R. Kahn. 1994. "Alternative pathway of insulin signalling in mice with targeted disruption of the IRS-1 gene." *Nature* no. 372 (6502):186-90. doi: 10.1038/372186a0.

Arita, Y., S. Kihara, N. Ouchi, M. Takahashi, K. Maeda, J. Miyagawa, K. Hotta, I. Shimomura, T. Nakamura, K. Miyaoka, H. Kuriyama, M. Nishida, S. Yamashita, K. Okubo, K. Matsubara, M. Muraguchi, Y. Ohmoto, T. Funahashi, and Y. Matsuzawa. 1999. "Paradoxical decrease of an adipose-specific protein, adiponectin, in obesity." *Biochem Biophys Res Commun* no. 257 (1):79-83.

Arkan, M. C., A. L. Hevener, F. R. Greten, S. Maeda, Z. W. Li, J. M. Long, A. Wynshaw-Boris, G. Poli, J. Olefsky, and M. Karin. 2005. "IKK-beta links inflammation to obesity-induced insulin resistance." *Nat Med* no. 11 (2):191-8. doi: 10.1038/nm1185.

Arner, P. 2005. "Human fat cell lipolysis: biochemistry, regulation and clinical role." *Best Pract Res Clin Endocrinol Metab* no. 19 (4):471-82. doi: 10.1016/j.beem.2005.07.004.

Assifi, M. M., G. Suchankova, S. Constant, M. Prentki, A. K. Saha, and N. B. Ruderman. 2005. "AMP-activated protein kinase and coordination of hepatic fatty acid metabolism of starved/carbohydrate-refed rats." *Am J Physiol Endocrinol Metab* no. 289 (5):E794-800. doi: 10.1152/ajpendo.00144.2005.

Bai, A., M. Yong, A. G. Ma, Y. Ma, C. R. Weiss, Q. Guan, C. N. Bernstein, and Z. Peng. 2010. "Novel anti-inflammatory action of 5-aminoimidazole-4-carboxamide ribonucleoside with protective effect in dextran sulfate sodium-induced acute and chronic colitis." *J Pharmacol Exp Ther* no. 333 (3):717-25. doi: 10.1124/jpet.109.164954.

Bain, J., L. Plater, M. Elliott, N. Shpiro, C. J. Hastie, H. McLauchlan, I. Klevernic, J. S. Arthur, D. R. Alessi, and P. Cohen. 2007. "The selectivity of protein kinase inhibitors: a further update." *Biochem J* no. 408 (3):297-315. doi: 10.1042/BJ20070797.

Bandyopadhyay, G. K., J. G. Yu, J. Ofrecio, and J. M. Olefsky. 2006. "Increased malonyl-CoA levels in muscle from obese and type 2 diabetic subjects lead to decreased fatty acid oxidation and increased lipogenesis; thiazolidinedione treatment reverses these defects." *Diabetes* no. 55 (8):2277-85. doi: 10.2337/db06-0062.

Baron, S., T. Bedarida, C. H. Cottart, F. Vibert, E. Vessieres, A. Ayer, D. Henrion, B. Hommeril, J. L. Paul, G. Renault, B. Saubamea, J. L. Beaudeux, V. Procaccio, and V. Nivet-Antoine. 2014. "Dual effects of resveratrol on arterial damage induced by insulin resistance in aged mice." *J Gerontol A Biol Sci Med Sci* no. 69 (3):260-9. doi: 10.1093/gerona/glt081.

Bastard, J. P., M. Maachi, J. T. Van Nhieu, C. Jardel, E. Bruckert, A. Grimaldi, J. J. Robert, J. Capeau, and B. Hainque. 2002. "Adipose tissue IL-6 content correlates with resistance to insulin activation of glucose uptake both in vivo and in vitro." *J Clin Endocrinol Metab* no. 87 (5):2084-9. doi: 10.1210/jcem.87.5.8450.

Bateman, A. 1997. "The structure of a domain common to archaebacteria and the homocystinuria disease protein." *Trends Biochem Sci* no. 22 (1):12-3.

Beg, Z. H., J. A. Stonik, and H. B. Brewer. 1978. "3-Hydroxy-3-methylglutaryl coenzyme A reductase: regulation of enzymatic activity by phosphorylation and dephosphorylation." *Proc Natl Acad Sci U S A* no. 75 (8):3678-82.

Bess, E., B. Fisslthaler, T. Frömel, and I. Fleming. 2011. "Nitric oxide-induced activation of the AMP-activated protein kinase α2 subunit attenuates IκB

kinase activity and inflammatory responses in endothelial cells." *PLoS One* no. 6 (6):e20848. doi: 10.1371/journal.pone.0020848.

Bianchi, K., and P. Meier. 2009. "A tangled web of ubiquitin chains: breaking news in TNF-R1 signaling." *Mol Cell* no. 36 (5):736-42. doi: 10.1016/j.molcel.2009.11.029.

Boyle, J. G., P. J. Logan, G. C. Jones, M. Small, N. Sattar, J. M. Connell, S. J. Cleland, and I. P. Salt. 2011. "AMP-activated protein kinase is activated in adipose tissue of individuals with type 2 diabetes treated with metformin: a randomised glycaemia-controlled crossover study." *Diabetologia* no. 54 (7):1799-809. doi: 10.1007/s00125-011-2126-4.

Bradford, M. M. 1976. "A rapid and sensitive method for the quantitation of microgram quantities of protein utilizing the principle of protein-dye binding." *Anal Biochem* no. 72:248-54.

Brandt, C., A. H. Jakobsen, H. Adser, J. Olesen, N. Iversen, J. M. Kristensen, P. Hojman, J. F. Wojtaszewski, J. Hidalgo, and H. Pilegaard. 2012. "IL-6 regulates exercise and training-induced adaptations in subcutaneous adipose tissue in mice." *Acta Physiol (Oxf)* no. 205 (2):224-35. doi: 10.1111/j.1748-1716.2011.02373.x.

Brandt, C., and B. K. Pedersen. 2010. "The role of exercise-induced myokines in muscle homeostasis and the defense against chronic diseases." *J Biomed Biotechnol* no. 2010:520258. doi: 10.1155/2010/520258.

Brazil, D. P., Z. Z. Yang, and B. A. Hemmings. 2004. "Advances in protein kinase B signalling: AKTion on multiple fronts." *Trends Biochem Sci* no. 29 (5):233-42. doi: 10.1016/j.tibs.2004.03.006.

Brikos, C., R. Wait, S. Begum, L. A. O'Neill, and J. Saklatvala. 2007. "Mass spectrometric analysis of the endogenous type I interleukin-1 (IL-1) receptor signaling complex formed after IL-1 binding identifies IL-1RAcP, MyD88, and IRAK-4 as the stable components." *Mol Cell Proteomics* no. 6 (9):1551-9. doi: 10.1074/mcp.M600455-MCP200.

Bromberg, J. F., M. H. Wrzeszczynska, G. Devgan, Y. Zhao, R. G. Pestell, C. Albanese, and J. E. Darnell. 1999. "Stat3 as an oncogene." *Cell* no. 98 (3):295-303.

Brown, M. D., and D. B. Sacks. 2009. "Protein scaffolds in MAP kinase signalling." *Cell Signal* no. 21 (4):462-9. doi: 10.1016/j.cellsig.2008.11.013.

Brunmair, B., K. Staniek, F. Gras, N. Scharf, A. Althaym, R. Clara, M. Roden, E. Gnaiger, H. Nohl, W. Waldhäusl, and C. Fürnsinn. 2004. "Thiazolidinediones, like metformin, inhibit respiratory complex I: a common mechanism contributing to their antidiabetic actions?" *Diabetes* no. 53 (4):1052-9.

Bruun, J. M., A. S. Lihn, S. B. Pedersen, and B. Richelsen. 2005. "Monocyte chemoattractant protein-1 release is higher in visceral than subcutaneous human adipose tissue (AT): implication of macrophages resident in the AT." *J Clin Endocrinol Metab* no. 90 (4):2282-9. doi: 10.1210/jc.2004-1696.

Buhl, E. S., N. Jessen, O. Schmitz, S. B. Pedersen, O. Pedersen, G. D. Holman, and S. Lund. 2001. "Chronic treatment with 5-aminoimidazole-4-carboxamide-1-beta-D-ribofuranoside increases insulin-stimulated glucose uptake and GLUT4 translocation in rat skeletal muscles in a fiber type-specific manner." *Diabetes* no. 50 (1):12-7.

Bultot, L., B. Guigas, A. Von Wilamowitz-Moellendorff, L. Maisin, D. Vertommen, N. Hussain, M. Beullens, J. J. Guinovart, M. Foretz, B. Viollet, K. Sakamoto, L. Hue, and M. H. Rider. 2012. "AMP-activated protein kinase phosphorylates and inactivates liver glycogen synthase." *Biochem J* no. 443 (1):193-203. doi: 10.1042/BJ20112026.

Burks, D. J., S. Pons, H. Towery, J. Smith-Hall, M. G. Myers, L. Yenush, and M. F. White. 1997. "Heterologous pleckstrin homology domains do not couple IRS-1 to the insulin receptor." *J Biol Chem* no. 272 (44):27716-21.

Buss, H., A. Dörrie, M. L. Schmitz, E. Hoffmann, K. Resch, and M. Kracht. 2004. "Constitutive and interleukin-1-inducible phosphorylation of p65 NF-{kappa}B at serine 536 is mediated by multiple protein kinases including I{kappa}B kinase (IKK)-{alpha}, IKK{beta}, IKK{epsilon}, TRAF family member-associated (TANK)-binding kinase 1 (TBK1), and an unknown kinase and couples p65 to TATA-binding protein-associated factor II31-mediated interleukin-8 transcription." *J Biol Chem* no. 279 (53):55633-43. doi: 10.1074/jbc.M409825200.

Cacicedo, J. M., N. Yagihashi, J. F. Keaney, N. B. Ruderman, and Y. Ido. 2004. "AMPK inhibits fatty acid-induced increases in NF-kappaB transactivation in cultured human umbilical vein endothelial cells." *Biochem Biophys Res Commun* no. 324 (4):1204-9. doi: 10.1016/j.bbrc.2004.09.177.

Caligiuri, A., C. Bertolani, C. T. Guerra, S. Aleffi, S. Galastri, M. Trappoliere, F. Vizzutti, S. Gelmini, G. Laffi, M. Pinzani, and F. Marra. 2008. "Adenosine monophosphate-activated protein kinase modulates the activated phenotype of hepatic stellate cells." *Hepatology* no. 47 (2):668-76. doi: 10.1002/hep.21995.

Calleja, V., D. Alcor, M. Laguerre, J. Park, B. Vojnovic, B. A. Hemmings, J. Downward, P. J. Parker, and B. Larijani. 2007. "Intramolecular and intermolecular interactions of protein kinase B define its activation in vivo." *PLoS Biol* no. 5 (4):e95. doi: 10.1371/journal.pbio.0050095.

Cao, Z., W. J. Henzel, and X. Gao. 1996. "IRAK: a kinase associated with the interleukin-1 receptor." *Science* no. 271 (5252):1128-31.

Cao, Z., J. Xiong, M. Takeuchi, T. Kurama, and D. V. Goeddel. 1996. "TRAF6 is a signal transducer for interleukin-1." *Nature* no. 383 (6599):443-6. doi: 10.1038/383443a0.

Carey, A. L., G. R. Steinberg, S. L. Macaulay, W. G. Thomas, A. G. Holmes, G. Ramm, O. Prelovsek, C. Hohnen-Behrens, M. J. Watt, D. E. James, B. E. Kemp, B. K. Pedersen, and M. A. Febbraio. 2006. "Interleukin-6 increases insulin-stimulated glucose disposal in humans and glucose uptake and fatty acid oxidation in vitro via AMP-activated protein kinase." *Diabetes* no. 55 (10):2688-97. doi: 10.2337/db05-1404.

Carling, D., and D. G. Hardie. 1989. "The substrate and sequence specificity of the AMP-activated protein kinase. Phosphorylation of glycogen synthase and phosphorylase kinase." *Biochim Biophys Acta* no. 1012 (1):81-6.

Carling, D., C. Thornton, A. Woods, and M. J. Sanders. 2012. "AMP-activated protein kinase: new regulation, new roles?" *Biochem J* no. 445 (1):11-27. doi: 10.1042/BJ20120546.

Carling, D., V. A. Zammit, and D. G. Hardie. 1987. "A common bicyclic protein kinase cascade inactivates the regulatory enzymes of fatty acid and cholesterol biosynthesis." *FEBS Lett* no. 223 (2):217-22.

Caton, P. W., J. Kieswich, M. M. Yaqoob, M. J. Holness, and M. C. Sugden. 2011. "Metformin opposes impaired AMPK and SIRT1 function and deleterious changes in core clock protein expression in white adipose tissue of genetically-obese db/db mice." *Diabetes Obes Metab* no. 13 (12):1097-104. doi: 10.1111/j.1463-1326.2011.01466.x.

Cederberg, A., L. M. Grønning, B. Ahrén, K. Taskén, P. Carlsson, and S. Enerbäck. 2001. "FOXC2 is a winged helix gene that counteracts obesity, hypertriglyceridemia, and diet-induced insulin resistance." *Cell* no. 106 (5):563-73.

Chen, L., S. S. Sung, M. L. Yip, H. R. Lawrence, Y. Ren, W. C. Guida, S. M. Sebti, N. J. Lawrence, and J. Wu. 2006. "Discovery of a novel shp2 protein tyrosine phosphatase inhibitor." *Mol Pharmacol* no. 70 (2):562-70. doi: 10.1124/mol.106.025536.

Chen, W., T. Ma, X. N. Shen, X. F. Xia, G. D. Xu, X. L. Bai, and T. B. Liang. 2012. "Macrophage-induced tumor angiogenesis is regulated by the TSC2-mTOR pathway." *Cancer Res* no. 72 (6):1363-72. doi: 10.1158/0008-5472.CAN-11-2684.

Chen, Y., R. Wen, S. Yang, J. Schuman, E. E. Zhang, T. Yi, G. S. Feng, and D. Wang. 2003. "Identification of Shp-2 as a Stat5A phosphatase." *J Biol Chem* no. 278 (19):16520-7. doi: 10.1074/jbc.M210572200.

Cheung, P. C., I. P. Salt, S. P. Davies, D. G. Hardie, and D. Carling. 2000. "Characterization of AMP-activated protein kinase gamma-subunit isoforms and their role in AMP binding." *Biochem J* no. 346 Pt 3:659-69.

Choudhury, M., I. Qadri, S. M. Rahman, J. Schroeder-Gloeckler, R. C. Janssen, and J. E. Friedman. 2011. "C/EBPβ is AMP kinase sensitive and up-regulates PEPCK in response to ER stress in hepatoma cells." *Mol Cell Endocrinol* no. 331 (1):102-8. doi: 10.1016/j.mce.2010.08.014.

Chung, J., E. Uchida, T. C. Grammer, and J. Blenis. 1997. "STAT3 serine phosphorylation by ERK-dependent and -independent pathways negatively modulates its tyrosine phosphorylation." *Mol Cell Biol* no. 17 (11):6508-16.

Cinti, S., G. Mitchell, G. Barbatelli, I. Murano, E. Ceresi, E. Faloia, S. Wang, M. Fortier, A. S. Greenberg, and M. S. Obin. 2005. "Adipocyte death defines macrophage localization and function in adipose tissue of obese mice and humans." *J Lipid Res* no. 46 (11):2347-55. doi: 10.1194/jlr.M500294-JLR200.

Clarke, M., M. A. Ewart, L. C. Santy, R. Prekeris, and G. W. Gould. 2006. "ACRP30 is secreted from 3T3-L1 adipocytes via a Rab11-dependent pathway." *Biochem Biophys Res Commun* no. 342 (4):1361-7. doi: 10.1016/j.bbrc.2006.02.102.

Cnop, M., P. J. Havel, K. M. Utzschneider, D. B. Carr, M. K. Sinha, E. J. Boyko, B. M. Retzlaff, R. H. Knopp, J. D. Brunzell, and S. E. Kahn. 2003. "Relationship of adiponectin to body fat distribution, insulin sensitivity and plasma lipoproteins: evidence for independent roles of age and sex." *Diabetologia* no. 46 (4):459-69. doi: 10.1007/s00125-003-1074-z.

Coffer, P., C. Lutticken, A. van Puijenbroek, M. Klop-de Jonge, F. Horn, and W. Kruijer. 1995. "Transcriptional regulation of the junB promoter: analysis of STAT-mediated signal transduction." *Oncogene* no. 10 (5):985-94.

Coleman, R. A., and D. P. Lee. 2004. "Enzymes of triacylglycerol synthesis and their regulation." *Prog Lipid Res* no. 43 (2):134-76.

Collins, S., W. Cao, and J. Robidoux. 2004. "Learning new tricks from old dogs: beta-adrenergic receptors teach new lessons on firing up adipose tissue metabolism." *Mol Endocrinol* no. 18 (9):2123-31. doi: 10.1210/me.2004-0193.

Cool, B., B. Zinker, W. Chiou, L. Kifle, N. Cao, M. Perham, R. Dickinson, A. Adler, G. Gagne, R. Iyengar, G. Zhao, K. Marsh, P. Kym, P. Jung, H. S. Camp, and E. Frevert. 2006. "Identification and characterization of a small molecule AMPK activator that treats key components of type 2 diabetes and the metabolic syndrome." *Cell Metab* no. 3 (6):403-16. doi: 10.1016/j.cmet.2006.05.005.

Coppari, R., and C. Bjørbæk. 2012. "Leptin revisited: its mechanism of action and potential for treating diabetes." *Nat Rev Drug Discov* no. 11 (9):692-708. doi: 10.1038/nrd3757.

Corton, J. M., J. G. Gillespie, S. A. Hawley, and D. G. Hardie. 1995. "5-aminoimidazole-4-carboxamide ribonucleoside. A specific method for activating AMP-activated protein kinase in intact cells?" *Eur J Biochem* no. 229 (2):558-65.

Crute, B. E., K. Seefeld, J. Gamble, B. E. Kemp, and L. A. Witters. 1998. "Functional domains of the alpha1 catalytic subunit of the AMP-activated protein kinase." *J Biol Chem* no. 273 (52):35347-54.

Currie, R. A., K. S. Walker, A. Gray, M. Deak, A. Casamayor, C. P. Downes, P. Cohen, D. R. Alessi, and J. Lucocq. 1999. "Role of phosphatidylinositol 3,4,5-trisphosphate in regulating the activity and localization of 3-phosphoinositide-dependent protein kinase-1." *Biochem J* no. 337 (Pt 3):575-83.

Czech, M. P., and S. Corvera. 1999. "Signaling mechanisms that regulate glucose transport." *J Biol Chem* no. 274 (4):1865-8.

Dadson, K., H. Chasiotis, S. Wannaiampikul, R. Tungtrongchitr, A. Xu, and G. Sweeney. 2014. "Adiponectin Mediated APPL1-AMPK Signaling Induces Cell Migration, MMP Activation, and Collagen Remodeling in Cardiac Fibroblasts." *J Cell Biochem* no. 115 (4):785-93. doi: 10.1002/jcb.24722.

Dandona, P., R. Weinstock, K. Thusu, E. Abdel-Rahman, A. Aljada, and T. Wadden. 1998. "Tumor necrosis factor-alpha in sera of obese patients: fall with weight loss." *J Clin Endocrinol Metab* no. 83 (8):2907-10. doi: 10.1210/jcem.83.8.5026.

Darnell, J. E., I. M. Kerr, and G. R. Stark. 1994. "Jak-STAT pathways and transcriptional activation in response to IFNs and other extracellular signaling proteins." *Science* no. 264 (5164):1415-21.

Daval, M., F. Diot-Dupuy, R. Bazin, I. Hainault, B. Viollet, S. Vaulont, E. Hajduch, P. Ferré, and F. Foufelle. 2005. "Anti-lipolytic action of AMP-activated protein kinase in rodent adipocytes." *J Biol Chem* no. 280 (26):25250-7. doi: 10.1074/jbc.M414222200.

Davies, S. P., N. R. Helps, P. T. Cohen, and D. G. Hardie. 1995. "5'-AMP inhibits dephosphorylation, as well as promoting phosphorylation, of the AMP-activated protein kinase. Studies using bacterially expressed human protein phosphatase-2C alpha and native bovine protein phosphatase-2AC." *FEBS Lett* no. 377 (3):421-5. doi: 10.1016/0014-5793(95)01368-7.

de Luca, C., and J. M. Olefsky. 2008. "Inflammation and insulin resistance." *FEBS Lett* no. 582 (1):97-105. doi: 10.1016/j.febslet.2007.11.057.

Derecka, M., A. Gornicka, S. B. Koralov, K. Szczepanek, M. Morgan, V. Raje, J. Sisler, Q. Zhang, D. Otero, J. Cichy, K. Rajewsky, K. Shimoda, V. Poli, B. Strobl, S. Pellegrini, T. E. Harris, P. Seale, A. P. Russell, A. J. McAinch, P. E. O'Brien, S. R. Keller, C. M. Croniger, T. Kordula, and A. C. Larner. 2012. "Tyk2 and Stat3 regulate brown adipose tissue differentiation and obesity." *Cell Metab* no. 16 (6):814-24. doi: 10.1016/j.cmet.2012.11.005.

DiDonato, J. A., M. Hayakawa, D. M. Rothwarf, E. Zandi, and M. Karin. 1997. "A cytokine-responsive IkappaB kinase that activates the transcription factor NF-kappaB." *Nature* no. 388 (6642):548-54. doi: 10.1038/41493.

Dobrian, A. D., E. V. Galkina, Q. Ma, M. Hatcher, S. M. Aye, M. J. Butcher, K. Ma, B. A. Haynes, M. H. Kaplan, and J. L. Nadler. 2013. "STAT4 deficiency reduces obesity-induced insulin resistance and adipose tissue inflammation." *Diabetes* no. 62 (12):4109-21. doi: 10.2337/db12-1275.

Dong, Y., M. Zhang, B. Liang, Z. Xie, Z. Zhao, S. Asfa, H. C. Choi, and M. H. Zou. 2010. "Reduction of AMP-activated protein kinase alpha2 increases endoplasmic reticulum stress and atherosclerosis in vivo." *Circulation* no. 121 (6):792-803. doi: 10.1161/CIRCULATIONAHA.109.900928.

Ducommun, S., R. J. Ford, L. Bultot, M. Deak, L. Bertrand, B. E. Kemp, G. R. Steinberg, and K. Sakamoto. 2014. "Enhanced activation of cellular AMPK by dual small molecule treatment: AICAR and A769662." *Am J Physiol Endocrinol Metab*. doi: 10.1152/ajpendo.00672.2013.

Dzamko, N., B. J. van Denderen, A. L. Hevener, S. B. Jørgensen, J. Honeyman, S. Galic, Z. P. Chen, M. J. Watt, D. J. Campbell, G. R. Steinberg, and B. E. Kemp. 2010. "AMPK beta1 deletion reduces appetite, preventing obesity and hepatic insulin resistance." *J Biol Chem* no. 285 (1):115-22. doi: 10.1074/jbc.M109.056762.

Elgazar-Carmon, V., A. Rudich, N. Hadad, and R. Levy. 2008. "Neutrophils transiently infiltrate intra-abdominal fat early in the course of high-fat feeding." *J Lipid Res* no. 49 (9):1894-903. doi: 10.1194/jlr.M800132-JLR200.

Elias, J. A., R. J. Homer, Q. Hamid, and C. G. Lee. 2005. "Chitinases and chitinase-like proteins in T(H)2 inflammation and asthma." *J Allergy Clin Immunol* no. 116 (3):497-500. doi: 10.1016/j.jaci.2005.06.028.

Evia-Viscarra, M. L., E. R. Rodea-Montero, E. Apolinar-Jiménez, N. Muñoz-Noriega, L. M. García-Morales, C. Leaños-Pérez, M. Figueroa-Barrón, D. Sánchez-Fierros, and J. G. Reyes-García. 2012. "The effects of metformin on inflammatory mediators in obese adolescents with insulin resistance: controlled randomized clinical trial." *J Pediatr Endocrinol Metab* no. 25 (1-2):41-9.

Ewart, M. A., C. F. Kohlhaas, and I. P. Salt. 2008. "Inhibition of tumor necrosis factor alpha-stimulated monocyte adhesion to human aortic endothelial cells by AMP-activated protein kinase." *Arterioscler Thromb Vasc Biol* no. 28 (12):2255-7. doi: 10.1161/ATVBAHA.108.175919.

Fahey, T. J., K. J. Tracey, P. Tekamp-Olson, L. S. Cousens, W. G. Jones, G. T. Shires, A. Cerami, and B. Sherry. 1992. "Macrophage inflammatory protein 1 modulates macrophage function." *J Immunol* no. 148 (9):2764-9.

Fasshauer, M., J. Klein, S. Kralisch, M. Klier, U. Lossner, M. Bluher, and R. Paschke. 2004. "Monocyte chemoattractant protein 1 expression is stimulated by growth hormone and interleukin-6 in 3T3-L1 adipocytes." *Biochem Biophys Res Commun* no. 317 (2):598-604. doi: 10.1016/j.bbrc.2004.03.090.

Fasshauer, M., S. Kralisch, M. Klier, U. Lossner, M. Bluher, J. Klein, and R. Paschke. 2003. "Adiponectin gene expression and secretion is inhibited by interleukin-6 in 3T3-L1 adipocytes." *Biochem Biophys Res Commun* no. 301 (4):1045-50.

Fasshauer, M., S. Kralisch, M. Klier, U. Lossner, M. Bluher, J. Klein, and R. Paschke. 2004. "Insulin resistance-inducing cytokines differentially regulate SOCS mRNA expression via growth factor- and Jak/Stat-signaling pathways in 3T3-L1 adipocytes." *J Endocrinol* no. 181 (1):129-38.

Fazakerley, D. J., G. D. Holman, A. Marley, D. E. James, J. Stöckli, and A. C. Coster. 2010. "Kinetic evidence for unique regulation of GLUT4 trafficking by insulin and AMP-activated protein kinase activators in L6 myotubes." *J Biol Chem* no. 285 (3):1653-60. doi: 10.1074/jbc.M109.051185.

Feldman, M. E., B. Apsel, A. Uotila, R. Loewith, Z. A. Knight, D. Ruggero, and K. M. Shokat. 2009. "Active-site inhibitors of mTOR target rapamycin-resistant outputs of mTORC1 and mTORC2." *PLoS Biol* no. 7 (2):e38. doi: 10.1371/journal.pbio.1000038.

Feng, J., B. A. Witthuhn, T. Matsuda, F. Kohlhuber, I. M. Kerr, and J. N. Ihle. 1997. "Activation of Jak2 catalytic activity requires phosphorylation of Y1007 in the kinase activation loop." *Mol Cell Biol* no. 17 (5):2497-501.

Feng, Z., W. Hu, E. de Stanchina, A. K. Teresky, S. Jin, S. Lowe, and A. J. Levine. 2007. "The regulation of AMPK beta1, TSC2, and PTEN expression by p53: stress, cell and tissue specificity, and the role of these gene products in modulating the IGF-1-AKT-mTOR pathways." *Cancer Res* no. 67 (7):3043-53. doi: 10.1158/0008-5472.CAN-06-4149.

Ferraz-Amaro, I., M. Arce-Franco, J. Muñiz, J. López-Fernández, V. Hernández-Hernández, A. Franco, J. Quevedo, J. Martínez-Martín, and F. Díaz-González. 2011. "Systemic blockade of TNF-α does not improve insulin resistance in humans." *Horm Metab Res* no. 43 (11):801-8. doi: 10.1055/s-0031-1287783.

Feuerer, M., L. Herrero, D. Cipolletta, A. Naaz, J. Wong, A. Nayer, J. Lee, A. B. Goldfine, C. Benoist, S. Shoelson, and D. Mathis. 2009. "Lean, but not obese, fat is enriched for a unique population of regulatory T cells that affect metabolic parameters." *Nat Med* no. 15 (8):930-9. doi: 10.1038/nm.2002.

Fink, S. L., and B. T. Cookson. 2005. "Apoptosis, pyroptosis, and necrosis: mechanistic description of dead and dying eukaryotic cells." *Infect Immun* no. 73 (4):1907-16. doi: 10.1128/IAI.73.4.1907-1916.2005.

Fischer, M., K. Timper, T. Radimerski, K. Dembinski, D. M. Frey, H. Zulewski, U. Keller, B. Müller, M. Christ-Crain, and J. Grisouard. 2010. "Metformin induces glucose uptake in human preadipocyte-derived adipocytes from various fat depots." *Diabetes Obes Metab* no. 12 (4):356-9. doi: 10.1111/j.1463-1326.2009.01169.x.

Foretz, M., S. Hébrard, J. Leclerc, E. Zarrinpashneh, M. Soty, G. Mithieux, K. Sakamoto, F. Andreelli, and B. Viollet. 2010. "Metformin inhibits hepatic gluconeogenesis in mice independently of the LKB1/AMPK pathway via a decrease in hepatic energy state." *J Clin Invest* no. 120 (7):2355-69. doi: 10.1172/JCI40671.

Fox, C. S., J. M. Massaro, U. Hoffmann, K. M. Pou, P. Maurovich-Horvat, C. Y. Liu, R. S. Vasan, J. M. Murabito, J. B. Meigs, L. A. Cupples, R. B. D'Agostino, and C. J. O'Donnell. 2007. "Abdominal visceral and subcutaneous adipose tissue compartments: association with metabolic risk factors in the Framingham Heart Study." *Circulation* no. 116 (1):39-48. doi: 10.1161/CIRCULATIONAHA.106.675355.

Fredrikson, G., H. Tornqvist, and P. Belfrage. 1986. "Hormone-sensitive lipase and monoacylglycerol lipase are both required for complete degradation of adipocyte triacylglycerol." *Biochim Biophys Acta* no. 876 (2):288-93.

Fried, S. K., D. A. Bunkin, and A. S. Greenberg. 1998. "Omental and subcutaneous adipose tissues of obese subjects release interleukin-6: depot difference and regulation by glucocorticoid." *J Clin Endocrinol Metab* no. 83 (3):847-50. doi: 10.1210/jcem.83.3.4660.

Frühbeck, G. 2006. "Intracellular signalling pathways activated by leptin." *Biochem J* no. 393 (Pt 1):7-20. doi: 10.1042/BJ20051578.

Fujii, N., R. C. Ho, Y. Manabe, N. Jessen, T. Toyoda, W. L. Holland, S. A. Summers, M. F. Hirshman, and L. J. Goodyear. 2008. "Ablation of AMP-activated protein kinase alpha2 activity exacerbates insulin resistance induced by high-fat feeding of mice." *Diabetes* no. 57 (11):2958-66. doi: 10.2337/db07-1187.

Fujisaka, S., I. Usui, A. Bukhari, M. Ikutani, T. Oya, Y. Kanatani, K. Tsuneyama, Y. Nagai, K. Takatsu, M. Urakaze, M. Kobayashi, and K. Tobe. 2009. "Regulatory mechanisms for adipose tissue M1 and M2 macrophages in diet-induced obese mice." *Diabetes* no. 58 (11):2574-82. doi: 10.2337/db08-1475.

Fukada, T., M. Hibi, Y. Yamanaka, M. Takahashi-Tezuka, Y. Fujitani, T. Yamaguchi, K. Nakajima, and T. Hirano. 1996. "Two signals are necessary for cell proliferation induced by a cytokine receptor gp130: involvement of STAT3 in anti-apoptosis." *Immunity* no. 5 (5):449-60.

Fukushima, A., K. Loh, S. Galic, B. Fam, B. Shields, F. Wiede, M. L. Tremblay, M. J. Watt, S. Andrikopoulos, and T. Tiganis. 2010. "T-cell protein tyrosine phosphatase attenuates STAT3 and insulin signaling in the liver to regulate gluconeogenesis." *Diabetes* no. 59 (8):1906-14. doi: 10.2337/db09-1365.

Gaidhu, M. P., S. Fediuc, N. M. Anthony, M. So, M. Mirpourian, R. L. Perry, and R. B. Ceddia. 2009. "Prolonged AICAR-induced AMP-kinase activation promotes energy dissipation in white adipocytes: novel mechanisms integrating HSL and ATGL." *J Lipid Res* no. 50 (4):704-15. doi: 10.1194/jlr.M800480-JLR200.

Gaidhu, M. P., S. Fediuc, and R. B. Ceddia. 2006. "5-Aminoimidazole-4-carboxamide-1-beta-D-ribofuranoside-induced AMP-activated protein kinase phosphorylation inhibits basal and insulin-stimulated glucose uptake, lipid synthesis, and fatty acid oxidation in isolated rat adipocytes." *J Biol Chem* no. 281 (36):25956-64. doi: 10.1074/jbc.M602992200.

Gaidhu, M. P., A. Frontini, S. Hung, K. Pistor, S. Cinti, and R. B. Ceddia. 2011. "Chronic AMP-kinase activation with AICAR reduces adiposity by remodeling adipocyte metabolism and increasing leptin sensitivity." *J Lipid Res* no. 52 (9):1702-11. doi: 10.1194/jlr.M015354.

Gaidhu, M. P., R. L. Perry, F. Noor, and R. B. Ceddia. 2010. "Disruption of AMPKalpha1 signaling prevents AICAR-induced inhibition of AS160/TBC1D4 phosphorylation and glucose uptake in primary rat adipocytes." *Mol Endocrinol* no. 24 (7):1434-40. doi: 10.1210/me.2009-0502.

Galic, S., M. D. Fullerton, J. D. Schertzer, S. Sikkema, K. Marcinko, C. R. Walkley, D. Izon, J. Honeyman, Z. P. Chen, B. J. van Denderen, B. E. Kemp, and G. R. Steinberg. 2011. "Hematopoietic AMPK β1 reduces mouse adipose tissue macrophage inflammation and insulin resistance in obesity." *J Clin Invest* no. 121 (12):4903-15. doi: 10.1172/JCI58577.

Gao, Z., D. Hwang, F. Bataille, M. Lefevre, D. York, M. J. Quon, and J. Ye. 2002. "Serine phosphorylation of insulin receptor substrate 1 by inhibitor kappa B kinase complex." *J Biol Chem* no. 277 (50):48115-21. doi: 10.1074/jbc.M209459200.

Gao, Z., X. Zhang, A. Zuberi, D. Hwang, M. J. Quon, M. Lefevre, and J. Ye. 2004. "Inhibition of insulin sensitivity by free fatty acids requires activation of multiple serine kinases in 3T3-L1 adipocytes." *Mol Endocrinol* no. 18 (8):2024-34. doi: 10.1210/me.2003-0383.

Gauthier, M. S., H. Miyoshi, S. C. Souza, J. M. Cacicedo, A. K. Saha, A. S. Greenberg, and N. B. Ruderman. 2008. "AMP-activated protein kinase is activated as a consequence of lipolysis in the adipocyte: potential mechanism and physiological relevance." *J Biol Chem* no. 283 (24):16514-24. doi: 10.1074/jbc.M708177200.

Gauthier, M. S., E. L. O'Brien, S. Bigornia, M. Mott, J. M. Cacicedo, X. J. Xu, N. Gokce, C. Apovian, and N. Ruderman. 2011. "Decreased AMP-activated protein kinase activity is associated with increased inflammation in visceral adipose tissue and with whole-body insulin resistance in morbidly obese humans." *Biochem Biophys Res Commun* no. 404 (1):382-7. doi: 10.1016/j.bbrc.2010.11.127.

Geerling, J. J., M. R. Boon, G. C. van der Zon, S. A. van den Berg, A. M. van den Hoek, M. Lombès, H. M. Princen, L. M. Havekes, P. C. Rensen, and B. Guigas. 2013. "Metformin lowers plasma triglycerides by promoting VLDL-

triglyceride clearance by brown adipose tissue in mice." *Diabetes*. doi: 10.2337/db13-0194.

Gerhartz, C., B. Heesel, J. Sasse, U. Hemmann, C. Landgraf, J. Schneider-Mergener, F. Horn, P. C. Heinrich, and L. Graeve. 1996. "Differential activation of acute phase response factor/STAT3 and STAT1 via the cytoplasmic domain of the interleukin 6 signal transducer gp130. I. Definition of a novel phosphotyrosine motif mediating STAT1 activation." *J Biol Chem* no. 271 (22):12991-8.

Gibbs, E. M., G. E. Lienhard, and G. W. Gould. 1988. "Insulin-induced translocation of glucose transporters to the plasma membrane precedes full stimulation of hexose transport." *Biochemistry* no. 27 (18):6681-5.

Giri, S., N. Nath, B. Smith, B. Viollet, A. K. Singh, and I. Singh. 2004. "5-aminoimidazole-4-carboxamide-1-beta-4-ribofuranoside inhibits proinflammatory response in glial cells: a possible role of AMP-activated protein kinase." *J Neurosci* no. 24 (2):479-87. doi: 10.1523/JNEUROSCI.4288-03.2004.

Giri, S., R. Rattan, E. Haq, M. Khan, R. Yasmin, J. S. Won, L. Key, A. K. Singh, and I. Singh. 2006. "AICAR inhibits adipocyte differentiation in 3T3L1 and restores metabolic alterations in diet-induced obesity mice model." *Nutr Metab (Lond)* no. 3:31. doi: 10.1186/1743-7075-3-31.

Glass, C. K., and J. M. Olefsky. 2012. "Inflammation and lipid signaling in the etiology of insulin resistance." *Cell Metab* no. 15 (5):635-45. doi: 10.1016/j.cmet.2012.04.001.

Goncharova, E. A., D. A. Goncharov, G. Damera, O. Tliba, Y. Amrani, R. A. Panettieri, and V. P. Krymskaya. 2009. "Signal transducer and activator of transcription 3 is required for abnormal proliferation and survival of TSC2-deficient cells: relevance to pulmonary lymphangioleiomyomatosis." *Mol Pharmacol* no. 76 (4):766-77. doi: 10.1124/mol.109.057042.

Gonzalez-Gay, M. A., J. M. De Matias, C. Gonzalez-Juanatey, C. Garcia-Porrua, A. Sanchez-Andrade, J. Martin, and J. Llorca. 2006. "Anti-tumor necrosis factor-alpha blockade improves insulin resistance in patients with rheumatoid arthritis." *Clin Exp Rheumatol* no. 24 (1):83-6.

Gowans, G. J., S. A. Hawley, F. A. Ross, and D. G. Hardie. 2013. "AMP is a true physiological regulator of AMP-activated protein kinase by both allosteric activation and enhancing net phosphorylation." *Cell Metab* no. 18 (4):556-66. doi: 10.1016/j.cmet.2013.08.019.

Green, C. J., M. Pedersen, B. K. Pedersen, and C. Scheele. 2011. "Elevated NF-κB activation is conserved in human myocytes cultured from obese type 2 diabetic patients and attenuated by AMP-activated protein kinase." *Diabetes* no. 60 (11):2810-9. doi: 10.2337/db11-0263.

Green, E. D., M. Maffei, V. V. Braden, R. Proenca, U. DeSilva, Y. Zhang, S. C. Chua, R. L. Leibel, J. Weissenbach, and J. M. Friedman. 1995. "The human obese (OB) gene: RNA expression pattern and mapping on the physical, cytogenetic, and genetic maps of chromosome 7." *Genome Res* no. 5 (1):5-12.

Grimaldi, C., F. Chiarini, G. Tabellini, F. Ricci, P. L. Tazzari, M. Battistelli, E. Falcieri, R. Bortul, F. Melchionda, I. Iacobucci, P. Pagliaro, G. Martinelli, A. Pession, J. T. Barata, J. A. McCubrey, and A. M. Martelli. 2012. "AMP-dependent kinase/mammalian target of rapamycin complex 1 signaling in T-cell acute lymphoblastic leukemia: therapeutic implications." *Leukemia* no. 26 (1):91-100. doi: 10.1038/leu.2011.269.

Grove, M., and M. Plumb. 1993. "C/EBP, NF-kappa B, and c-Ets family members and transcriptional regulation of the cell-specific and inducible macrophage

inflammatory protein 1 alpha immediate-early gene." *Mol Cell Biol* no. 13 (9):5276-89.

Guilherme, A., J. V. Virbasius, V. Puri, and M. P. Czech. 2008. "Adipocyte dysfunctions linking obesity to insulin resistance and type 2 diabetes." *Nat Rev Mol Cell Biol* no. 9 (5):367-77. doi: 10.1038/nrm2391.

Gustafson, B. 2010. "Adipose tissue, inflammation and atherosclerosis." *J Atheroscler Thromb* no. 17 (4):332-41.

Gwinn, D. M., D. B. Shackelford, D. F. Egan, M. M. Mihaylova, A. Mery, D. S. Vasquez, B. E. Turk, and R. J. Shaw. 2008. "AMPK phosphorylation of raptor mediates a metabolic checkpoint." *Mol Cell* no. 30 (2):214-26. doi: 10.1016/j.molcel.2008.03.003.

Ha, J., J. K. Lee, K. S. Kim, L. A. Witters, and K. H. Kim. 1996. "Cloning of human acetyl-CoA carboxylase-beta and its unique features." *Proc Natl Acad Sci U S A* no. 93 (21):11466-70.

Habinowski, S. A., and L. A. Witters. 2001. "The effects of AICAR on adipocyte differentiation of 3T3-L1 cells." *Biochem Biophys Res Commun* no. 286 (5):852-6. doi: 10.1006/bbrc.2001.5484.

Handy, J. A., N. K. Saxena, P. Fu, S. Lin, J. E. Mells, N. A. Gupta, and F. A. Anania. 2010. "Adiponectin activation of AMPK disrupts leptin-mediated hepatic fibrosis via suppressors of cytokine signaling (SOCS-3)." *J Cell Biochem* no. 110 (5):1195-207. doi: 10.1002/jcb.22634.

Haq, S. E., A. Clerk, and P. H. Sugden. 1998. "Activation of mitogen-activated protein kinases (p38-MAPKs, SAPKs/JNKs and ERKs) by adenosine in the perfused rat heart." *FEBS Lett* no. 434 (3):305-8.

Hardie, D. G. 2004. "The AMP-activated protein kinase pathway--new players upstream and downstream." *J Cell Sci* no. 117 (Pt 23):5479-87. doi: 10.1242/jcs.01540.

Hardie, D. G. 2008. "AMPK: a key regulator of energy balance in the single cell and the whole organism." *Int J Obes (Lond)* no. 32 Suppl 4:S7-12. doi: 10.1038/ijo.2008.116.

Hardie, D. G., F. A. Ross, and S. A. Hawley. 2012a. "AMP-activated protein kinase: a target for drugs both ancient and modern." *Chem Biol* no. 19 (10):1222-36. doi: 10.1016/j.chembiol.2012.08.019.

Hardie, D. G., F. A. Ross, and S. A. Hawley. 2012b. "AMPK: a nutrient and energy sensor that maintains energy homeostasis." *Nat Rev Mol Cell Biol* no. 13 (4):251-62. doi: 10.1038/nrm3311.

Hardie, D. G., J. W. Scott, D. A. Pan, and E. R. Hudson. 2003. "Management of cellular energy by the AMP-activated protein kinase system." *FEBS Lett* no. 546 (1):113-20.

Hattori, Y., Y. Nakano, S. Hattori, A. Tomizawa, K. Inukai, and K. Kasai. 2008. "High molecular weight adiponectin activates AMPK and suppresses cytokine-induced NF-kappaB activation in vascular endothelial cells." *FEBS Lett* no. 582 (12):1719-24. doi: 10.1016/j.febslet.2008.04.037.

Hattori, Y., K. Suzuki, S. Hattori, and K. Kasai. 2006. "Metformin inhibits cytokine-induced nuclear factor kappaB activation via AMP-activated protein kinase activation in vascular endothelial cells." *Hypertension* no. 47 (6):1183-8. doi: 10.1161/01.HYP.0000221429.94591.72.

Hawley, S. A., J. Boudeau, J. L. Reid, K. J. Mustard, L. Udd, T. P. Mäkelä, D. R. Alessi, and D. G. Hardie. 2003. "Complexes between the LKB1 tumor suppressor, STRAD alpha/beta and MO25 alpha/beta are upstream kinases in the AMP-activated protein kinase cascade." *J Biol* no. 2 (4):28. doi: 10.1186/1475-4924-2-28.

Hawley, S. A., M. Davison, A. Woods, S. P. Davies, R. K. Beri, D. Carling, and D. G. Hardie. 1996. "Characterization of the AMP-activated protein kinase kinase from rat liver and identification of threonine 172 as the major site at which it phosphorylates AMP-activated protein kinase." *J Biol Chem* no. 271 (44):27879-87.

Hawley, S. A., M. D. Fullerton, F. A. Ross, J. D. Schertzer, C. Chevtzoff, K. J. Walker, M. W. Peggie, D. Zibrova, K. A. Green, K. J. Mustard, B. E. Kemp, K. Sakamoto, G. R. Steinberg, and D. G. Hardie. 2012. "The ancient drug salicylate directly activates AMP-activated protein kinase." *Science* no. 336 (6083):918-22. doi: 10.1126/science.1215327.

Hawley, S. A., D. A. Pan, K. J. Mustard, L. Ross, J. Bain, A. M. Edelman, B. G. Frenguelli, and D. G. Hardie. 2005. "Calmodulin-dependent protein kinase kinase-beta is an alternative upstream kinase for AMP-activated protein kinase." *Cell Metab* no. 2 (1):9-19. doi: 10.1016/j.cmet.2005.05.009.

Hawley, S. A., F. A. Ross, C. Chevtzoff, K. A. Green, A. Evans, S. Fogarty, M. C. Towler, L. J. Brown, O. A. Ogunbayo, A. M. Evans, and D. G. Hardie. 2010. "Use of cells expressing gamma subunit variants to identify diverse mechanisms of AMPK activation." *Cell Metab* no. 11 (6):554-65. doi: 10.1016/j.cmet.2010.04.001.

Hawley, S. A., M. A. Selbert, E. G. Goldstein, A. M. Edelman, D. Carling, and D. G. Hardie. 1995. "5'-AMP activates the AMP-activated protein kinase cascade, and Ca2+/calmodulin activates the calmodulin-dependent protein kinase I cascade, via three independent mechanisms." *J Biol Chem* no. 270 (45):27186-91.

Heinrich, P. C., I. Behrmann, G. Müller-Newen, F. Schaper, and L. Graeve. 1998. "Interleukin-6-type cytokine signalling through the gp130/Jak/STAT pathway." *Biochem J* no. 334 (Pt 2):297-314.

Hellgren, G., K. Albertsson-Wikland, H. Billig, L. M. Carlsson, and B. Carlsson. 2001. "Growth hormone receptor interaction with Jak proteins differs between tissues." *J Interferon Cytokine Res* no. 21 (2):75-83. doi: 10.1089/107999001750069935.

Hermiston, M. L., J. Zikherman, and J. W. Zhu. 2009. "CD45, CD148, and Lyp/Pep: critical phosphatases regulating Src family kinase signaling networks in immune cells." *Immunol Rev* no. 228 (1):288-311. doi: 10.1111/j.1600-065X.2008.00752.x.

Holm, C., T. Osterlund, H. Laurell, and J. A. Contreras. 2000. "Molecular mechanisms regulating hormone-sensitive lipase and lipolysis." *Annu Rev Nutr* no. 20:365-93. doi: 10.1146/annurev.nutr.20.1.365.

Holmes, B. F., E. J. Kurth-Kraczek, and W. W. Winder. 1999. "Chronic activation of 5'-AMP-activated protein kinase increases GLUT-4, hexokinase, and glycogen in muscle." *J Appl Physiol (1985)* no. 87 (5):1990-5.

Hoppe, S., H. Bierhoff, I. Cado, A. Weber, M. Tiebe, I. Grummt, and R. Voit. 2009. "AMP-activated protein kinase adapts rRNA synthesis to cellular energy supply." *Proc Natl Acad Sci U S A* no. 106 (42):17781-6. doi: 10.1073/pnas.0909873106.

Hotamisligil, G. S., P. Peraldi, A. Budavari, R. Ellis, M. F. White, and B. M. Spiegelman. 1996. "IRS-1-mediated inhibition of insulin receptor tyrosine kinase activity in TNF-alpha- and obesity-induced insulin resistance." *Science* no. 271 (5249):665-8.

Hotamisligil, G. S., N. S. Shargill, and B. M. Spiegelman. 1993. "Adipose expression of tumor necrosis factor-alpha: direct role in obesity-linked insulin resistance." *Science* no. 259 (5091):87-91.

Hotta, K., T. Funahashi, N. L. Bodkin, H. K. Ortmeyer, Y. Arita, B. C. Hansen, and Y. Matsuzawa. 2001. "Circulating concentrations of the adipocyte protein adiponectin are decreased in parallel with reduced insulin sensitivity during the progression to type 2 diabetes in rhesus monkeys." *Diabetes* no. 50 (5):1126-33.

Hresko, R. C., and M. Mueckler. 2005. "mTOR.RICTOR is the Ser473 kinase for Akt/protein kinase B in 3T3-L1 adipocytes." *J Biol Chem* no. 280 (49):40406-16. doi: 10.1074/jbc.M508361200.

Hsu, P. P., S. A. Kang, J. Rameseder, Y. Zhang, K. A. Ottina, D. Lim, T. R. Peterson, Y. Choi, N. S. Gray, M. B. Yaffe, J. A. Marto, and D. M. Sabatini. 2011. "The mTOR-regulated phosphoproteome reveals a mechanism of mTORC1-mediated inhibition of growth factor signaling." *Science* no. 332 (6035):1317-22. doi: 10.1126/science.1199498.

Hu, J., S. K. Roy, P. S. Shapiro, S. R. Rodig, S. P. Reddy, L. C. Platanias, R. D. Schreiber, and D. V. Kalvakolanu. 2001. "ERK1 and ERK2 activate CCAAAT/enhancer-binding protein-beta-dependent gene transcription in response to interferon-gamma." *J Biol Chem* no. 276 (1):287-97. doi: 10.1074/jbc.M004885200.

Huang, N. L., S. H. Chiang, C. H. Hsueh, Y. J. Liang, Y. J. Chen, and L. P. Lai. 2009. "Metformin inhibits TNF-alpha-induced IkappaB kinase phosphorylation, IkappaB-alpha degradation and IL-6 production in endothelial cells through PI3K-dependent AMPK phosphorylation." *Int J Cardiol* no. 134 (2):169-75. doi: 10.1016/j.ijcard.2008.04.010.

Hudson, E. R., D. A. Pan, J. James, J. M. Lucocq, S. A. Hawley, K. A. Green, O. Baba, T. Terashima, and D. G. Hardie. 2003. "A novel domain in AMP-activated protein kinase causes glycogen storage bodies similar to those seen in hereditary cardiac arrhythmias." *Curr Biol* no. 13 (10):861-6.

Hundal, R. S., K. F. Petersen, A. B. Mayerson, P. S. Randhawa, S. Inzucchi, S. E. Shoelson, and G. I. Shulman. 2002. "Mechanism by which high-dose aspirin improves glucose metabolism in type 2 diabetes." *J Clin Invest* no. 109 (10):1321-6. doi: 10.1172/JCI14955.

Hunter, R. W., J. T. Treebak, J. F. Wojtaszewski, and K. Sakamoto. 2011. "Molecular mechanism by which AMP-activated protein kinase activation promotes glycogen accumulation in muscle." *Diabetes* no. 60 (3):766-74. doi: 10.2337/db10-1148.

Hurley, R. L., K. A. Anderson, J. M. Franzone, B. E. Kemp, A. R. Means, and L. A. Witters. 2005. "The Ca2+/calmodulin-dependent protein kinase kinases are AMP-activated protein kinase kinases." *J Biol Chem* no. 280 (32):29060-6. doi: 10.1074/jbc.M503824200.

Hutchinson, D. S., E. Chernogubova, O. S. Dallner, B. Cannon, and T. Bengtsson. 2005. "Beta-adrenoceptors, but not alpha-adrenoceptors, stimulate AMP-activated protein kinase in brown adipocytes independently of uncoupling protein-1." *Diabetologia* no. 48 (11):2386-95. doi: 10.1007/s00125-005-1936-7.

Huypens, P., K. Moens, H. Heimberg, Z. Ling, D. Pipeleers, and M. Van de Casteele. 2005. "Adiponectin-mediated stimulation of AMP-activated protein kinase (AMPK) in pancreatic beta cells." *Life Sci* no. 77 (11):1273-82. doi: 10.1016/j.lfs.2005.03.008.

Huypens, P., E. Quartier, D. Pipeleers, and M. Van de Casteele. 2005. "Metformin reduces adiponectin protein expression and release in 3T3-L1 adipocytes involving activation of AMP activated protein kinase." *Eur J Pharmacol* no. 518 (2-3):90-5. doi: 10.1016/j.ejphar.2005.06.016.

Ibarra-Sánchez, M. J., J. Wagner, M. T. Ong, C. Lampron, and M. L. Tremblay. 2001. "Murine embryonic fibroblasts lacking TC-PTP display delayed G1 phase through defective NF-kappaB activation." *Oncogene* no. 20 (34):4728-39. doi: 10.1038/sj.onc.1204648.

Imamura, K., T. Ogura, A. Kishimoto, M. Kaminishi, and H. Esumi. 2001. "Cell cycle regulation via p53 phosphorylation by a 5'-AMP activated protein kinase activator, 5-aminoimidazole- 4-carboxamide-1-beta-D-ribofuranoside, in a human hepatocellular carcinoma cell line." *Biochem Biophys Res Commun* no. 287 (2):562-7. doi: 10.1006/bbrc.2001.5627.

Inoki, K., H. Ouyang, T. Zhu, C. Lindvall, Y. Wang, X. Zhang, Q. Yang, C. Bennett, Y. Harada, K. Stankunas, C. Y. Wang, X. He, O. A. MacDougald, M. You, B. O. Williams, and K. L. Guan. 2006. "TSC2 integrates Wnt and energy signals via a coordinated phosphorylation by AMPK and GSK3 to regulate cell growth." *Cell* no. 126 (5):955-68. doi: 10.1016/j.cell.2006.06.055.

Inoki, K., T. Zhu, and K. L. Guan. 2003. "TSC2 mediates cellular energy response to control cell growth and survival." *Cell* no. 115 (5):577-90.

Israël, A. 2010. "The IKK complex, a central regulator of NF-kappaB activation." *Cold Spring Harb Perspect Biol* no. 2 (3):a000158. doi: 10.1101/cshperspect.a000158.

Jacquet, S., E. Zarrinpashneh, A. Chavey, A. Ginion, I. Leclerc, B. Viollet, G. A. Rutter, L. Bertrand, and M. S. Marber. 2007. "The relationship between p38 mitogen-activated protein kinase and AMP-activated protein kinase during myocardial ischemia." *Cardiovasc Res* no. 76 (3):465-72. doi: 10.1016/j.cardiores.2007.08.001.

Jager, J., T. Grémeaux, M. Cormont, Y. Le Marchand-Brustel, and J. F. Tanti. 2007. "Interleukin-1beta-induced insulin resistance in adipocytes through down-regulation of insulin receptor substrate-1 expression." *Endocrinology* no. 148 (1):241-51. doi: 10.1210/en.2006-0692.

James, C., V. Ugo, J. P. Le Couédic, J. Staerk, F. Delhommeau, C. Lacout, L. Garçon, H. Raslova, R. Berger, A. Bennaceur-Griscelli, J. L. Villeval, S. N. Constantinescu, N. Casadevall, and W. Vainchenker. 2005. "A unique clonal JAK2 mutation leading to constitutive signalling causes polycythaemia vera." *Nature* no. 434 (7037):1144-8. doi: 10.1038/nature03546.

Jayakumar, A. R., K. S. Panickar, C.R Murthy, and M. D. Norenberg. 2006. "Oxidative stress and mitogen-activated protein kinase phosphorylation mediate ammonia-induced cell swelling and glutamate uptake inhibition in cultured astrocytes." *J Neurosci* no. 26 (18):4774-84. doi: 10.1523/JNEUROSCI.0120-06.2006.

Jeong, H. W., K. C. Hsu, J. W. Lee, M. Ham, J. Y. Huh, H. J. Shin, W. S. Kim, and J. B. Kim. 2009. "Berberine suppresses proinflammatory responses through AMPK activation in macrophages." *Am J Physiol Endocrinol Metab* no. 296 (4):E955-64. doi: 10.1152/ajpendo.90599.2008.

Jonsdottir, I. H., P. Schjerling, K. Ostrowski, S. Asp, E. A. Richter, and B. K. Pedersen. 2000. "Muscle contractions induce interleukin-6 mRNA production in rat skeletal muscles." *J Physiol* no. 528 Pt 1:157-63.

Jorgensen, S. B., H. M. O'Neill, L. Sylow, J. Honeyman, K. A. Hewitt, R. Palanivel, M. D. Fullerton, L. Öberg, A. Balendran, S. Galic, C. van der Poel, I. A. Trounce, G. S. Lynch, J. D. Schertzer, and G. R. Steinberg. 2013. "Deletion of skeletal muscle SOCS3 prevents insulin resistance in obesity." *Diabetes* no. 62 (1):56-64. doi: 10.2337/db12-0443.

Kahn, B. B., T. Alquier, D. Carling, and D. G. Hardie. 2005. "AMP-activated protein kinase: ancient energy gauge provides clues to modern understanding of metabolism." *Cell Metab* no. 1 (1):15-25. doi: 10.1016/j.cmet.2004.12.003.

Kanda, H., S. Tateya, Y. Tamori, K. Kotani, K. Hiasa, R. Kitazawa, S. Kitazawa, H. Miyachi, S. Maeda, K. Egashira, and M. Kasuga. 2006. "MCP-1 contributes to macrophage infiltration into adipose tissue, insulin resistance, and hepatic steatosis in obesity." *J Clin Invest* no. 116 (6):1494-505. doi: 10.1172/JCI26498.

Kaptein, A., V. Paillard, and M. Saunders. 1996. "Dominant negative stat3 mutant inhibits interleukin-6-induced Jak-STAT signal transduction." *J Biol Chem* no. 271 (11):5961-4.

Karin, M., and E. Gallagher. 2009. "TNFR signaling: ubiquitin-conjugated TRAFfic signals control stop-and-go for MAPK signaling complexes." *Immunol Rev* no. 228 (1):225-40. doi: 10.1111/j.1600-065X.2008.00755.x.

Kelleher, Z. T., A. Matsumoto, J. S. Stamler, and H. E. Marshall. 2007. "NOS2 regulation of NF-kappaB by S-nitrosylation of p65." *J Biol Chem* no. 282 (42):30667-72. doi: 10.1074/jbc.M705929200.

Kelly, M., C. Keller, P. R. Avilucea, P. Keller, Z. Luo, X. Xiang, M. Giralt, J. Hidalgo, A. K. Saha, B. K. Pedersen, and N. B. Ruderman. 2004. "AMPK activity is diminished in tissues of IL-6 knockout mice: the effect of exercise." *Biochem Biophys Res Commun* no. 320 (2):449-54. doi: 10.1016/j.bbrc.2004.05.188.

Kemp, B. E. 2004. "Bateman domains and adenosine derivatives form a binding contract." *J Clin Invest* no. 113 (2):182-4. doi: 10.1172/JCI20846.

Kern, P. A., S. Ranganathan, C. Li, L. Wood, and G. Ranganathan. 2001. "Adipose tissue tumor necrosis factor and interleukin-6 expression in human obesity and insulin resistance." *Am J Physiol Endocrinol Metab* no. 280 (5):E745-51.

Kern, P. A., M. Saghizadeh, J. M. Ong, R. J. Bosch, R. Deem, and R. B. Simsolo. 1995. "The expression of tumor necrosis factor in human adipose tissue. Regulation by obesity, weight loss, and relationship to lipoprotein lipase." *J Clin Invest* no. 95 (5):2111-9. doi: 10.1172/JCI117899.

Kim, H., and H. Baumann. 1999. "Dual signaling role of the protein tyrosine phosphatase SHP-2 in regulating expression of acute-phase plasma proteins by interleukin-6 cytokine receptors in hepatic cells." *Mol Cell Biol* no. 19 (8):5326-38.

Kim, H. Y., E. J. Park, E. H. Joe, and I. Jou. 2003. "Curcumin suppresses Janus kinase-STAT inflammatory signaling through activation of Src homology 2 domain-containing tyrosine phosphatase 2 in brain microglia." *J Immunol* no. 171 (11):6072-9.

Kim, J., M. Kundu, B. Viollet, and K. L. Guan. 2011. "AMPK and mTOR regulate autophagy through direct phosphorylation of Ulk1." *Nat Cell Biol* no. 13 (2):132-41. doi: 10.1038/ncb2152.

Kim, T., J. Davis, A. J. Zhang, X. He, and S. T. Mathews. 2009. "Curcumin activates AMPK and suppresses gluconeogenic gene expression in hepatoma cells." *Biochem Biophys Res Commun* no. 388 (2):377-82. doi: 10.1016/j.bbrc.2009.08.018.

Kim, Y. D., Y. H. Kim, Y. M. Cho, D. K. Kim, S. W. Ahn, J. M. Lee, D. Chanda, M. Shong, C. H. Lee, and H. S. Choi. 2012. "Metformin ameliorates IL-6-induced hepatic insulin resistance via induction of orphan nuclear receptor small heterodimer partner (SHP) in mouse models." *Diabetologia* no. 55 (5):1482-94. doi: 10.1007/s00125-012-2494-4.

Kim, Y. D., K. G. Park, Y. S. Lee, Y. Y. Park, D. K. Kim, B. Nedumaran, W. G. Jang, W. J. Cho, J. Ha, I. K. Lee, C. H. Lee, and H. S. Choi. 2008. "Metformin inhibits hepatic gluconeogenesis through AMP-activated protein kinase-dependent regulation of the orphan nuclear receptor SHP." *Diabetes* no. 57 (2):306-14. doi: 10.2337/db07-0381.

Kimura, N., C. Tokunaga, S. Dalal, C. Richardson, K. Yoshino, K. Hara, B. E. Kemp, L. A. Witters, O. Mimura, and K. Yonezawa. 2003. "A possible linkage between AMP-activated protein kinase (AMPK) and mammalian target of rapamycin (mTOR) signalling pathway." *Genes Cells* no. 8 (1):65-79.

Kintscher, U., M. Hartge, K. Hess, A. Foryst-Ludwig, M. Clemenz, M. Wabitsch, P. Fischer-Posovszky, T. F. Barth, D. Dragun, T. Skurk, H. Hauner, M. Blüher, T. Unger, A. M. Wolf, U. Knippschild, V. Hombach, and N. Marx. 2008. "T-lymphocyte infiltration in visceral adipose tissue: a primary event in adipose tissue inflammation and the development of obesity-mediated insulin resistance." *Arterioscler Thromb Vasc Biol* no. 28 (7):1304-10. doi: 10.1161/ATVBAHA.108.165100.

Kiss, K., J. Kiss, E. Rudolf, M. Cervinka, and J. Szeberényi. 2004. "Sodium salicylate inhibits NF-kappaB and induces apoptosis in PC12 cells." *J Biochem Biophys Methods* no. 61 (1-2):229-40. doi: 10.1016/j.jbbm.2004.06.003.

Klover, P. J., A. H. Clementi, and R. A. Mooney. 2005. "Interleukin-6 depletion selectively improves hepatic insulin action in obesity." *Endocrinology* no. 146 (8):3417-27. doi: 10.1210/en.2004-1468.

Klover, P. J., T. A. Zimmers, L. G. Koniaris, and R. A. Mooney. 2003. "Chronic exposure to interleukin-6 causes hepatic insulin resistance in mice." *Diabetes* no. 52 (11):2784-9.

Knudsen, N. H., and C. H. Lee. 2013. "STAT4: an initiator of meta-inflammation in adipose tissue?" *Diabetes* no. 62 (12):4002-3. doi: 10.2337/db13-1416.

Koh, H. J., M. F. Hirshman, H. He, Y. Li, Y. Manabe, J. A. Balschi, and L. J. Goodyear. 2007. "Adrenaline is a critical mediator of acute exercise-induced AMP-activated protein kinase activation in adipocytes." *Biochem J* no. 403 (3):473-81. doi: 10.1042/BJ20061479.

Koistinen, H. A., D. Galuska, A. V. Chibalin, J. Yang, J. R. Zierath, G. D. Holman, and H. Wallberg-Henriksson. 2003. "5-amino-imidazole carboxamide riboside increases glucose transport and cell-surface GLUT4 content in skeletal muscle from subjects with type 2 diabetes." *Diabetes* no. 52 (5):1066-72.

Kola, B., and M. Korbonits. 2009. "Shedding light on the intricate puzzle of ghrelin's effects on appetite regulation." *J Endocrinol* no. 202 (2):191-8. doi: 10.1677/JOE-09-0056.

Kolak, M., H. Yki-Järvinen, K. Kannisto, M. Tiikkainen, A. Hamsten, P. Eriksson, and R. M. Fisher. 2007. "Effects of chronic rosiglitazone therapy on gene expression in human adipose tissue in vivo in patients with type 2 diabetes." *J Clin Endocrinol Metab* no. 92 (2):720-4. doi: 10.1210/jc.2006-1465.

Kopp, E., and S. Ghosh. 1994. "Inhibition of NF-kappa B by sodium salicylate and aspirin." *Science* no. 265 (5174):956-9.

Kouro, T., and K. Takatsu. 2009. "IL-5- and eosinophil-mediated inflammation: from discovery to therapy." *Int Immunol* no. 21 (12):1303-9. doi: 10.1093/intimm/dxp102.

Kraegen, E. W., and G. J. Cooney. 2008. "Free fatty acids and skeletal muscle insulin resistance." *Curr Opin Lipidol* no. 19 (3):235-41. doi: 10.1097/01.mol.0000319118.44995.9a.

Kraegen, E. W., G. J. Cooney, J. Ye, and A. L. Thompson. 2001. "Triglycerides, fatty acids and insulin resistance--hyperinsulinemia." *Exp Clin Endocrinol Diabetes* no. 109 (4):S516-26.

Krinninger, P., C. Brunner, P. A. Ruiz, E. Schneider, N. Marx, A. Foryst-Ludwig, U. Kintscher, D. Haller, H. Laumen, and H. Hauner. 2011. "Role of the adipocyte-specific NF-κB activity in the regulation of IP-10 and T cell

migration." *Am J Physiol Endocrinol Metab* no. 300 (2):E304-11. doi: 10.1152/ajpendo.00143.2010.

Kubo, M., T. Hanada, and A. Yoshimura. 2003. "Suppressors of cytokine signaling and immunity." *Nat Immunol* no. 4 (12):1169-76. doi: 10.1038/ni1012.

Kubota, N., Y. Terauchi, T. Kubota, H. Kumagai, S. Itoh, H. Satoh, W. Yano, H. Ogata, K. Tokuyama, I. Takamoto, T. Mineyama, M. Ishikawa, M. Moroi, K. Sugi, T. Yamauchi, K. Ueki, K. Tobe, T. Noda, R. Nagai, and T. Kadowaki. 2006. "Pioglitazone ameliorates insulin resistance and diabetes by both adiponectin-dependent and -independent pathways." *J Biol Chem* no. 281 (13):8748-55. doi: 10.1074/jbc.M505649200.

Kuo, C. L., F. M. Ho, M. Y. Chang, E. Prakash, and W. W. Lin. 2008. "Inhibition of lipopolysaccharide-induced inducible nitric oxide synthase and cyclooxygenase-2 gene expression by 5-aminoimidazole-4-carboxamide riboside is independent of AMP-activated protein kinase." *J Cell Biochem* no. 103 (3):931-40. doi: 10.1002/jcb.21466.

Kwiatkowski, D. J., H. Zhang, J. L. Bandura, K. M. Heiberger, M. Glogauer, N. el-Hashemite, and H. Onda. 2002. "A mouse model of TSC1 reveals sex-dependent lethality from liver hemangiomas, and up-regulation of p70S6 kinase activity in Tsc1 null cells." *Hum Mol Genet* no. 11 (5):525-34.

Kyriakis, J. M., and J. Avruch. 2012. "Mammalian MAPK signal transduction pathways activated by stress and inflammation: a 10-year update." *Physiol Rev* no. 92 (2):689-737. doi: 10.1152/physrev.00028.2011.

Lagathu, C., J. P. Bastard, M. Auclair, M. Maachi, J. Capeau, and M. Caron. 2003. "Chronic interleukin-6 (IL-6) treatment increased IL-6 secretion and induced insulin resistance in adipocyte: prevention by rosiglitazone." *Biochem Biophys Res Commun* no. 311 (2):372-9.

Lagathu, C., L. Yvan-Charvet, J. P. Bastard, M. Maachi, A. Quignard-Boulangé, J. Capeau, and M. Caron. 2006. "Long-term treatment with interleukin-1beta induces insulin resistance in murine and human adipocytes." *Diabetologia* no. 49 (9):2162-73. doi: 10.1007/s00125-006-0335-z.

Lam, M. H., B. J. Michell, M. T. Fodero-Tavoletti, B. E. Kemp, N. K. Tonks, and T. Tiganis. 2001. "Cellular stress regulates the nucleocytoplasmic distribution of the protein-tyrosine phosphatase TCPTP." *J Biol Chem* no. 276 (40):37700-7. doi: 10.1074/jbc.M105128200.

Larsen, C. M., M. Faulenbach, A. Vaag, J. A. Ehses, M. Y. Donath, and T. Mandrup-Poulsen. 2009. "Sustained effects of interleukin-1 receptor antagonist treatment in type 2 diabetes." *Diabetes Care* no. 32 (9):1663-8. doi: 10.2337/dc09-0533.

Larsen, C. M., M. Faulenbach, A. Vaag, A. Vølund, J. A. Ehses, B. Seifert, T. Mandrup-Poulsen, and M. Y. Donath. 2007. "Interleukin-1-receptor antagonist in type 2 diabetes mellitus." *N Engl J Med* no. 356 (15):1517-26. doi: 10.1056/NEJMoa065213.

Lee, C. W., L. L. Wong, E. Y. Tse, H. F. Liu, V. Y. Leong, J. M. Lee, D. G. Hardie, I. O. Ng, and Y. P. Ching. 2012. "AMPK promotes p53 acetylation via phosphorylation and inactivation of SIRT1 in liver cancer cells." *Cancer Res* no. 72 (17):4394-404. doi: 10.1158/0008-5472.CAN-12-0429.

Lee, H. J., E. S. Masuda, N. Arai, K. Arai, and T. Yokota. 1995. "Definition of cis-regulatory elements of the mouse interleukin-5 gene promoter. Involvement of nuclear factor of activated T cell-related factors in interleukin-5 expression." *J Biol Chem* no. 270 (29):17541-50.

Lee, J. M., S. R. Kim, S. J. Yoo, O. K. Hong, H. S. Son, and S. A. Chang. 2009. "The relationship between adipokines, metabolic parameters and insulin

resistance in patients with metabolic syndrome and type 2 diabetes." *J Int Med Res* no. 37 (6):1803-12.

Lee, J., and P. F. Pilch. 1994. "The insulin receptor: structure, function, and signaling." *Am J Physiol* no. 266 (2 Pt 1):C319-34.

Lehmann, J. M., L. B. Moore, T. A. Smith-Oliver, W. O. Wilkison, T. M. Willson, and S. A. Kliewer. 1995. "An antidiabetic thiazolidinedione is a high affinity ligand for peroxisome proliferator-activated receptor gamma (PPAR gamma)." *J Biol Chem* no. 270 (22):12953-6.

Lekstrom-Himes, J., and K. G. Xanthopoulos. 1998. "Biological role of the CCAAT/enhancer-binding protein family of transcription factors." *J Biol Chem* no. 273 (44):28545-8.

Li, J., E. J. Miller, J. Ninomiya-Tsuji, R. R. Russell, and L. H. Young. 2005. "AMP-activated protein kinase activates p38 mitogen-activated protein kinase by increasing recruitment of p38 MAPK to TAB1 in the ischemic heart." *Circ Res* no. 97 (9):872-9. doi: 10.1161/01.RES.0000187458.77026.10.

Lihn, A. S., N. Jessen, S. B. Pedersen, S. Lund, and B. Richelsen. 2004. "AICAR stimulates adiponectin and inhibits cytokines in adipose tissue." *Biochem Biophys Res Commun* no. 316 (3):853-8. doi: 10.1016/j.bbrc.2004.02.139.

Lihn, A. S., S. B. Pedersen, S. Lund, and B. Richelsen. 2008. "The anti-diabetic AMPK activator AICAR reduces IL-6 and IL-8 in human adipose tissue and skeletal muscle cells." *Mol Cell Endocrinol* no. 292 (1-2):36-41. doi: 10.1016/j.mce.2008.06.004.

Lin, C. C., H. H. Yeh, W. L. Huang, J. J. Yan, W. W. Lai, W. P. Su, H. H. Chen, and W. C. Su. 2013. "Metformin enhances cisplatin cytotoxicity by suppressing signal transducer and activator of transcription-3 activity independently of the liver kinase B1-AMP-activated protein kinase pathway." *Am J Respir Cell Mol Biol* no. 49 (2):241-50. doi: 10.1165/rcmb.2012-0244OC.

Lin, J., C. Handschin, and B. M. Spiegelman. 2005. "Metabolic control through the PGC-1 family of transcription coactivators." *Cell Metab* no. 1 (6):361-70. doi: 10.1016/j.cmet.2005.05.004.

Liu, Q., M. S. Gauthier, L. Sun, N. Ruderman, and H. Lodish. 2010. "Activation of AMP-activated protein kinase signaling pathway by adiponectin and insulin in mouse adipocytes: requirement of acyl-CoA synthetases FATP1 and Acsl1 and association with an elevation in AMP/ATP ratio." *FASEB J* no. 24 (11):4229-39. doi: 10.1096/fj.10-159723.

Lizcano, J. M., O. Göransson, R. Toth, M. Deak, N. A. Morrice, J. Boudeau, S. A. Hawley, L. Udd, T. P. Mäkelä, D. G. Hardie, and D. R. Alessi. 2004. "LKB1 is a master kinase that activates 13 kinases of the AMPK subfamily, including MARK/PAR-1." *EMBO J* no. 23 (4):833-43. doi: 10.1038/sj.emboj.7600110.

Lochhead, P. A., I. P. Salt, K. S. Walker, D. G. Hardie, and C. Sutherland. 2000. "5-aminoimidazole-4-carboxamide riboside mimics the effects of insulin on the expression of the 2 key gluconeogenic genes PEPCK and glucose-6-phosphatase." *Diabetes* no. 49 (6):896-903.

Loh, K., A. Fukushima, X. Zhang, S. Galic, D. Briggs, P. J. Enriori, S. Simonds, F. Wiede, A. Reichenbach, C. Hauser, N. A. Sims, K. K. Bence, S. Zhang, Z. Y. Zhang, B. B. Kahn, B. G. Neel, Z. B. Andrews, M. A. Cowley, and T. Tiganis. 2011. "Elevated hypothalamic TCPTP in obesity contributes to cellular leptin resistance." *Cell Metab* no. 14 (5):684-99. doi: 10.1016/j.cmet.2011.09.011.

Londos, C., D. L. Brasaemle, C. J. Schultz, J. P. Segrest, and A. R. Kimmel. 1999. "Perilipins, ADRP, and other proteins that associate with intracellular neutral lipid droplets in animal cells." *Semin Cell Dev Biol* no. 10 (1):51-8. doi: 10.1006/scdb.1998.0275.

Longnus, S. L., R. B. Wambolt, H. L. Parsons, R. W. Brownsey, and M. F. Allard. 2003. "5-Aminoimidazole-4-carboxamide 1-beta -D-ribofuranoside (AICAR) stimulates myocardial glycogenolysis by allosteric mechanisms." *Am J Physiol Regul Integr Comp Physiol* no. 284 (4):R936-44. doi: 10.1152/ajpregu.00319.2002.

Lovren, F., Y. Pan, A. Quan, P. E. Szmitko, K. K. Singh, P. C. Shukla, M. Gupta, L. Chan, M. Al-Omran, H. Teoh, and S. Verma. 2010. "Adiponectin primes human monocytes into alternative anti-inflammatory M2 macrophages." *Am J Physiol Heart Circ Physiol* no. 299 (3):H656-63. doi: 10.1152/ajpheart.00115.2010.

Lu, X., R. Levine, W. Tong, G. Wernig, Y. Pikman, S. Zarnegar, D. G. Gilliland, and H. Lodish. 2005. "Expression of a homodimeric type I cytokine receptor is required for JAK2V617F-mediated transformation." *Proc Natl Acad Sci U S A* no. 102 (52):18962-7. doi: 10.1073/pnas.0509714102.

Lumeng, C. N., J. L. Bodzin, and A. R. Saltiel. 2007. "Obesity induces a phenotypic switch in adipose tissue macrophage polarization." *J Clin Invest* no. 117 (1):175-84. doi: 10.1172/JCI29881.

Lumeng, C. N., S. M. Deyoung, J. L. Bodzin, and A. R. Saltiel. 2007. "Increased inflammatory properties of adipose tissue macrophages recruited during diet-induced obesity." *Diabetes* no. 56 (1):16-23. doi: 10.2337/db06-1076.

Lumeng, C. N., S. M. Deyoung, and A. R. Saltiel. 2007. "Macrophages block insulin action in adipocytes by altering expression of signaling and glucose transport proteins." *Am J Physiol Endocrinol Metab* no. 292 (1):E166-74. doi: 10.1152/ajpendo.00284.2006.

Luo, B., G. J. Parker, R. C. Cooksey, Y. Soesanto, M. Evans, D. Jones, and D. A. McClain. 2007. "Chronic hexosamine flux stimulates fatty acid oxidation by activating AMP-activated protein kinase in adipocytes." *J Biol Chem* no. 282 (10):7172-80. doi: 10.1074/jbc.M607362200.

Lönnqvist, F., L. Nordfors, M. Jansson, A. Thörne, M. Schalling, and P. Arner. 1997. "Leptin secretion from adipose tissue in women. Relationship to plasma levels and gene expression." *J Clin Invest* no. 99 (10):2398-404. doi: 10.1172/JCI119422.

MacDougald, O. A., and M. D. Lane. 1995. "Transcriptional regulation of gene expression during adipocyte differentiation." *Annu Rev Biochem* no. 64:345-73. doi: 10.1146/annurev.bi.64.070195.002021.

Maeda, N., M. Takahashi, T. Funahashi, S. Kihara, H. Nishizawa, K. Kishida, H. Nagaretani, M. Matsuda, R. Komuro, N. Ouchi, H. Kuriyama, K. Hotta, T. Nakamura, I. Shimomura, and Y. Matsuzawa. 2001. "PPARgamma ligands increase expression and plasma concentrations of adiponectin, an adipose-derived protein." *Diabetes* no. 50 (9):2094-9.

Marsin, A. S., L. Bertrand, M. H. Rider, J. Deprez, C. Beauloye, M. F. Vincent, G. Van den Berghe, D. Carling, and L. Hue. 2000. "Phosphorylation and activation of heart PFK-2 by AMPK has a role in the stimulation of glycolysis during ischaemia." *Curr Biol* no. 10 (20):1247-55.

Martin, T., P. M. Cardarelli, G. C. Parry, K. A. Felts, and R. R. Cobb. 1997. "Cytokine induction of monocyte chemoattractant protein-1 gene expression in human endothelial cells depends on the cooperative action of NF-kappa B and AP-1." *Eur J Immunol* no. 27 (5):1091-7. doi: 10.1002/eji.1830270508.

Martínez-Agustin, O., J. J. Hernández-Morante, E. Martínez-Plata, F. Sánchez de Medina, and M. Garaulet. 2010. "Differences in AMPK expression between subcutaneous and visceral adipose tissue in morbid obesity." *Regul Pept* no. 163 (1-3):31-6. doi: 10.1016/j.regpep.2010.04.008.

McBride, A., S. Ghilagaber, A. Nikolaev, and D. G. Hardie. 2009. "The glycogen-binding domain on the AMPK beta subunit allows the kinase to act as a glycogen sensor." *Cell Metab* no. 9 (1):23-34. doi: 10.1016/j.cmet.2008.11.008.

McGarry, J. D. 1995. "The mitochondrial carnitine palmitoyltransferase system: its broadening role in fuel homoeostasis and new insights into its molecular features." *Biochem Soc Trans* no. 23 (2):321-4.

Meier, C. A., E. Bobbioni, C. Gabay, F. Assimacopoulos-Jeannet, A. Golay, and J. M. Dayer. 2002. "IL-1 receptor antagonist serum levels are increased in human obesity: a possible link to the resistance to leptin?" *J Clin Endocrinol Metab* no. 87 (3):1184-8. doi: 10.1210/jcem.87.3.8351.

Meloni, L., M. Ruscazio, R. Versace, Q. Mela, and A. Cherchi. 1988. "Unusual pericardial cyst location. Value of two-dimensional echocardiography in diagnosis." *J Ultrasound Med* no. 7 (9):519-22.

Mercurio, F., H. Zhu, B. W. Murray, A. Shevchenko, B. L. Bennett, J. Li, D. B. Young, M. Barbosa, M. Mann, A. Manning, and A. Rao. 1997. "IKK-1 and IKK-2: cytokine-activated IkappaB kinases essential for NF-kappaB activation." *Science* no. 278 (5339):860-6.

Merrill, G. F., E. J. Kurth, D. G. Hardie, and W. W. Winder. 1997. "AICA riboside increases AMP-activated protein kinase, fatty acid oxidation, and glucose uptake in rat muscle." *Am J Physiol* no. 273 (6 Pt 1):E1107-12.

Milburn, C. C., J. Boudeau, M. Deak, D. R. Alessi, and D. M. van Aalten. 2004. "Crystal structure of MO25 alpha in complex with the C terminus of the pseudo kinase STE20-related adaptor." *Nat Struct Mol Biol* no. 11 (2):193-200. doi: 10.1038/nsmb716.

Milocco, L. H., J. A. Haslam, J. Rosen, and H. M. Seidel. 1999. "Design of conditionally active STATs: insights into STAT activation and gene regulatory function." *Mol Cell Biol* no. 19 (4):2913-20.

Minokoshi, Y., T. Alquier, N. Furukawa, Y. B. Kim, A. Lee, B. Xue, J. Mu, F. Foufelle, P. Ferré, M. J. Birnbaum, B. J. Stuck, and B. B. Kahn. 2004. "AMP-kinase regulates food intake by responding to hormonal and nutrient signals in the hypothalamus." *Nature* no. 428 (6982):569-74. doi: 10.1038/nature02440.

Minokoshi, Y., Y. B. Kim, O. D. Peroni, L. G. Fryer, C. Müller, D. Carling, and B. B. Kahn. 2002. "Leptin stimulates fatty-acid oxidation by activating AMP-activated protein kinase." *Nature* no. 415 (6869):339-43. doi: 10.1038/415339a.

Mohamed-Ali, V., S. Goodrick, A. Rawesh, D. R. Katz, J. M. Miles, J. S. Yudkin, S. Klein, and S. W. Coppack. 1997. "Subcutaneous adipose tissue releases interleukin-6, but not tumor necrosis factor-alpha, in vivo." *J Clin Endocrinol Metab* no. 82 (12):4196-200. doi: 10.1210/jcem.82.12.4450.

Moldoveanu, A. I., R. J. Shephard, and P. N. Shek. 2000. "Exercise elevates plasma levels but not gene expression of IL-1beta, IL-6, and TNF-alpha in blood mononuclear cells." *J Appl Physiol (1985)* no. 89 (4):1499-504.

Morrow, V. A., F. Foufelle, J. M. Connell, J. R. Petrie, G. W. Gould, and I. P. Salt. 2003. "Direct activation of AMP-activated protein kinase stimulates nitric-oxide synthesis in human aortic endothelial cells." *J Biol Chem* no. 278 (34):31629-39. doi: 10.1074/jbc.M212831200.

Moschen, A. R., C. Molnar, B. Enrich, S. Geiger, C. F. Ebenbichler, and H. Tilg. 2011. "Adipose and liver expression of interleukin (IL)-1 family members in morbid obesity and effects of weight loss." *Mol Med* no. 17 (7-8):840-5. doi: 10.2119/molmed.2010.00108.

Mulligan, J. D., A. A. Gonzalez, A. M. Stewart, H. V. Carey, and K. W. Saupe. 2007. "Upregulation of AMPK during cold exposure occurs via distinct mechanisms in brown and white adipose tissue of the mouse." *J Physiol* no. 580 (Pt. 2):677-84. doi: 10.1113/jphysiol.2007.128652.

Munday, M. R., D. G. Campbell, D. Carling, and D. G. Hardie. 1988. "Identification by amino acid sequencing of three major regulatory phosphorylation sites on rat acetyl-CoA carboxylase." *Eur J Biochem* no. 175 (2):331-8.

Muoio, D. M., G. L. Dohm, F. T. Fiedorek, E. B. Tapscott, R. A. Coleman, and G. L. Dohn. 1997. "Leptin directly alters lipid partitioning in skeletal muscle." *Diabetes* no. 46 (8):1360-3.

Murray, P. J. 2007. "The JAK-STAT signaling pathway: input and output integration." *J Immunol* no. 178 (5):2623-9.

Muslin, A. J. 2008. "MAPK signalling in cardiovascular health and disease: molecular mechanisms and therapeutic targets." *Clin Sci (Lond)* no. 115 (7):203-18. doi: 10.1042/CS20070430.

Neel, B. G., and N. K. Tonks. 1997. "Protein tyrosine phosphatases in signal transduction." *Curr Opin Cell Biol* no. 9 (2):193-204.

Nerstedt, A., E. Cansby, M. Amrutkar, U. Smith, and M. Mahlapuu. 2013. "Pharmacological activation of AMPK suppresses inflammatory response evoked by IL-6 signalling in mouse liver and in human hepatocytes." *Mol Cell Endocrinol* no. 375 (1-2):68-78. doi: 10.1016/j.mce.2013.05.013.

Nerstedt, A., A. Johansson, C. X. Andersson, E. Cansby, U. Smith, and M. Mahlapuu. 2010. "AMP-activated protein kinase inhibits IL-6-stimulated inflammatory response in human liver cells by suppressing phosphorylation of signal transducer and activator of transcription 3 (STAT3)." *Diabetologia* no. 53 (11):2406-16. doi: 10.1007/s00125-010-1856-z.

Nieto-Vazquez, I., S. Fernández-Veledo, D. K. Krämer, R. Vila-Bedmar, L. Garcia-Guerra, and M. Lorenzo. 2008. "Insulin resistance associated to obesity: the link TNF-alpha." *Arch Physiol Biochem* no. 114 (3):183-94. doi: 10.1080/13813450802181047.

Nijhuis, J., S. S. Rensen, Y. Slaats, F. M. van Dielen, W. A. Buurman, and J. W. Greve. 2009. "Neutrophil activation in morbid obesity, chronic activation of acute inflammation." *Obesity (Silver Spring)* no. 17 (11):2014-8. doi: 10.1038/oby.2009.113.

Nishimoto, N. 2006. "Interleukin-6 in rheumatoid arthritis." *Curr Opin Rheumatol* no. 18 (3):277-81. doi: 10.1097/01.bor.0000218949.19860.d1.

Nishimura, S., I. Manabe, M. Nagasaki, K. Eto, H. Yamashita, M. Ohsugi, M. Otsu, K. Hara, K. Ueki, S. Sugiura, K. Yoshimura, T. Kadowaki, and R. Nagai. 2009. "CD8+ effector T cells contribute to macrophage recruitment and adipose tissue inflammation in obesity." *Nat Med* no. 15 (8):914-20. doi: 10.1038/nm.1964.

O'Neill, L. A. 2008. "The interleukin-1 receptor/Toll-like receptor superfamily: 10 years of progress." *Immunol Rev* no. 226:10-8. doi: 10.1111/j.1600-065X.2008.00701.x.

Odegaard, J. I., R. R. Ricardo-Gonzalez, M. H. Goforth, C. R. Morel, V. Subramanian, L. Mukundan, A. Red Eagle, D. Vats, F. Brombacher, A. W. Ferrante, and A. Chawla. 2007. "Macrophage-specific PPARgamma controls alternative activation and improves insulin resistance." *Nature* no. 447 (7148):1116-20. doi: 10.1038/nature05894.

Ofei, F., S. Hurel, J. Newkirk, M. Sopwith, and R. Taylor. 1996. "Effects of an engineered human anti-TNF-alpha antibody (CDP571) on insulin sensitivity and glycemic control in patients with NIDDM." *Diabetes* no. 45 (7):881-5.

Ohmori, Y., S. Fukumoto, and T. A. Hamilton. 1995. "Two structurally distinct kappa B sequence motifs cooperatively control LPS-induced KC gene transcription in mouse macrophages." *J Immunol* no. 155 (7):3593-600.

Ohmori, Y., and T. A. Hamilton. 1993. "Cooperative interaction between interferon (IFN) stimulus response element and kappa B sequence motifs controls IFN gamma- and lipopolysaccharide-stimulated transcription from the murine IP-10 promoter." *J Biol Chem* no. 268 (9):6677-88.

Ohtani, T., K. Ishihara, T. Atsumi, K. Nishida, Y. Kaneko, T. Miyata, S. Itoh, M. Narimatsu, H. Maeda, T. Fukada, M. Itoh, H. Okano, M. Hibi, and T. Hirano. 2000. "Dissection of signaling cascades through gp130 in vivo: reciprocal roles for STAT3- and SHP2-mediated signals in immune responses." *Immunity* no. 12 (1):95-105.

Ojuka, E. O., L. A. Nolte, and J. O. Holloszy. 2000. "Increased expression of GLUT-4 and hexokinase in rat epitrochlearis muscles exposed to AICAR in vitro." *J Appl Physiol (1985)* no. 88 (3):1072-5.

Olefsky, J. M., and C. K. Glass. 2010. "Macrophages, inflammation, and insulin resistance." *Annu Rev Physiol* no. 72:219-46. doi: 10.1146/annurev-physiol-021909-135846.

Onda, H., P. B. Crino, H. Zhang, R. D. Murphey, L. Rastelli, B. E. Gould Rothberg, and D. J. Kwiatkowski. 2002. "Tsc2 null murine neuroepithelial cells are a model for human tuber giant cells, and show activation of an mTOR pathway." *Mol Cell Neurosci* no. 21 (4):561-74.

Ono, S. J., T. Nakamura, D. Miyazaki, M. Ohbayashi, M. Dawson, and M. Toda. 2003. "Chemokines: roles in leukocyte development, trafficking, and effector function." *J Allergy Clin Immunol* no. 111 (6):1185-99; quiz 1200.

Orci, L., W. S. Cook, M. Ravazzola, M. Y. Wang, B. H. Park, R. Montesano, and R. H. Unger. 2004. "Rapid transformation of white adipocytes into fat-oxidizing machines." *Proc Natl Acad Sci U S A* no. 101 (7):2058-63. doi: 10.1073/pnas.0308258100.

Ouchi, N., and K. Walsh. 2007. "Adiponectin as an anti-inflammatory factor." *Clin Chim Acta* no. 380 (1-2):24-30. doi: 10.1016/j.cca.2007.01.026.

Pacher, P., J. S. Beckman, and L. Liaudet. 2007. "Nitric oxide and peroxynitrite in health and disease." *Physiol Rev* no. 87 (1):315-424. doi: 10.1152/physrev.00029.2006.

Park, H., V. K. Kaushik, S. Constant, M. Prentki, E. Przybytkowski, N. B. Ruderman, and A. K. Saha. 2002. "Coordinate regulation of malonyl-CoA decarboxylase, sn-glycerol-3-phosphate acyltransferase, and acetyl-CoA carboxylase by AMP-activated protein kinase in rat tissues in response to exercise." *J Biol Chem* no. 277 (36):32571-7. doi: 10.1074/jbc.M201692200.

Peairs, A., A. Radjavi, S. Davis, L. Li, A. Ahmed, S. Giri, and C. M. Reilly. 2009. "Activation of AMPK inhibits inflammation in MRL/lpr mouse mesangial cells." *Clin Exp Immunol* no. 156 (3):542-51. doi: 10.1111/j.1365-2249.2009.03924.x.

Pesce, J. T., T. R. Ramalingam, M. S. Wilson, M. M. Mentink-Kane, R. W. Thompson, A. W. Cheever, J. F. Urban, and T. A. Wynn. 2009. "Retnla (relmalpha/fizz1) suppresses helminth-induced Th2-type immunity." *PLoS Pathog* no. 5 (4):e1000393. doi: 10.1371/journal.ppat.1000393.

Petrovic, N., T. B. Walden, I. G. Shabalina, J. A. Timmons, B. Cannon, and J. Nedergaard. 2010. "Chronic peroxisome proliferator-activated receptor gamma (PPARgamma) activation of epididymally derived white adipocyte cultures reveals a population of thermogenically competent, UCP1-containing adipocytes molecularly distinct from classic brown adipocytes." *J Biol Chem* no. 285 (10):7153-64. doi: 10.1074/jbc.M109.053942.

Peyton, K. J., X. M. Liu, Y. Yu, B. Yates, and W. Durante. 2012. "Activation of AMP-activated protein kinase inhibits the proliferation of human endothelial cells." *J Pharmacol Exp Ther* no. 342 (3):827-34. doi: 10.1124/jpet.112.194712.

Plotnikov, A., E. Zehorai, S. Procaccia, and R. Seger. 2011. "The MAPK cascades: signaling components, nuclear roles and mechanisms of nuclear translocation." *Biochim Biophys Acta* no. 1813 (9):1619-33. doi: 10.1016/j.bbamcr.2010.12.012.

Polekhina, G., A. Gupta, B. J. Michell, B. van Denderen, S. Murthy, S. C. Feil, I. G. Jennings, D. J. Campbell, L. A. Witters, M. W. Parker, B. E. Kemp, and D. Stapleton. 2003. "AMPK beta subunit targets metabolic stress sensing to glycogen." *Curr Biol* no. 13 (10):867-71.

Pradhan, A. D., J. E. Manson, N. Rifai, J. E. Buring, and P. M. Ridker. 2001. "C-reactive protein, interleukin 6, and risk of developing type 2 diabetes mellitus." *JAMA* no. 286 (3):327-34.

Prasad, R., S. Giri, N. Nath, I. Singh, and A. K. Singh. 2006. "5-aminoimidazole-4-carboxamide-1-beta-4-ribofuranoside attenuates experimental autoimmune encephalomyelitis via modulation of endothelial-monocyte interaction." *J Neurosci Res* no. 84 (3):614-25. doi: 10.1002/jnr.20953.

Pulinilkunnil, T., H. He, D. Kong, K. Asakura, O. D. Peroni, A. Lee, and B. B. Kahn. 2011. "Adrenergic regulation of AMP-activated protein kinase in brown adipose tissue in vivo." *J Biol Chem* no. 286 (11):8798-809. doi: 10.1074/jbc.M111.218719.

Reihill, J. A., M. A. Ewart, and I. P. Salt. 2011. "The role of AMP-activated protein kinase in the functional effects of vascular endothelial growth factor-A and -B in human aortic endothelial cells." *Vasc Cell* no. 3:9. doi: 10.1186/2045-824X-3-9.

Riccioni, T., C. Cirielli, X. Wang, A. Passaniti, and M. C. Capogrossi. 1998. "Adenovirus-mediated wild-type p53 overexpression inhibits endothelial cell differentiation in vitro and angiogenesis in vivo." *Gene Ther* no. 5 (6):747-54. doi: 10.1038/sj.gt.3300681.

Ridker, P. M., C. H. Hennekens, J. E. Buring, and N. Rifai. 2000. "C-reactive protein and other markers of inflammation in the prediction of cardiovascular disease in women." *N Engl J Med* no. 342 (12):836-43. doi: 10.1056/NEJM200003233421202.

Ridker, P. M., N. Rifai, M. J. Stampfer, and C. H. Hennekens. 2000. "Plasma concentration of interleukin-6 and the risk of future myocardial infarction among apparently healthy men." *Circulation* no. 101 (15):1767-72.

Rose, B. A., T. Force, and Y. Wang. 2010. "Mitogen-activated protein kinase signaling in the heart: angels versus demons in a heart-breaking tale." *Physiol Rev* no. 90 (4):1507-46. doi: 10.1152/physrev.00054.2009.

Rose-John, S. 2012. "IL-6 trans-signaling via the soluble IL-6 receptor: importance for the pro-inflammatory activities of IL-6." *Int J Biol Sci* no. 8 (9):1237-47. doi: 10.7150/ijbs.4989.

Rosen, E. D., C. J. Walkey, P. Puigserver, and B. M. Spiegelman. 2000. "Transcriptional regulation of adipogenesis." *Genes Dev* no. 14 (11):1293-307.

Rosenwald, M., A. Perdikari, T. Rülicke, and C. Wolfrum. 2013. "Bi-directional interconversion of brite and white adipocytes." *Nat Cell Biol* no. 15 (6):659-67. doi: 10.1038/ncb2740.

Ross, S. A., X. Song, M. W. Burney, Y. Kasai, and D. J. Orlicky. 2003. "Efficient adenovirus transduction of 3T3-L1 adipocytes stably expressing coxsackie-adenovirus receptor." *Biochem Biophys Res Commun* no. 302 (2):354-8.

Rotter, V., I. Nagaev, and U. Smith. 2003. "Interleukin-6 (IL-6) induces insulin resistance in 3T3-L1 adipocytes and is, like IL-8 and tumor necrosis factor-alpha, overexpressed in human fat cells from insulin-resistant subjects." *J Biol Chem* no. 278 (46):45777-84. doi: 10.1074/jbc.M301977200.

Rouillé, Y., S. J. Duguay, K. Lund, M. Furuta, Q. Gong, G. Lipkind, A. A. Oliva, S. J. Chan, and D. F. Steiner. 1995. "Proteolytic processing mechanisms in the biosynthesis of neuroendocrine peptides: the subtilisin-like proprotein convertases." *Front Neuroendocrinol* no. 16 (4):322-61. doi: 10.1006/frne.1995.1012.

Ruderman, N. B., C. Keller, A. M. Richard, A. K. Saha, Z. Luo, X. Xiang, M. Giralt, V. B. Ritov, E. V. Menshikova, D. E. Kelley, J. Hidalgo, B. K. Pedersen, and M. Kelly. 2006. "Interleukin-6 regulation of AMP-activated protein kinase. Potential role in the systemic response to exercise and prevention of the metabolic syndrome." *Diabetes* no. 55 Suppl 2:S48-54. doi: 10.2337/diabetes.

Ruderman, N. B., H. Park, V. K. Kaushik, D. Dean, S. Constant, M. Prentki, and A. K. Saha. 2003. "AMPK as a metabolic switch in rat muscle, liver and adipose tissue after exercise." *Acta Physiol Scand* no. 178 (4):435-42. doi: 10.1046/j.1365-201X.2003.01164.x.

Saberi, M., N. B. Woods, C. de Luca, S. Schenk, J. C. Lu, G. Bandyopadhyay, I. M. Verma, and J. M. Olefsky. 2009. "Hematopoietic cell-specific deletion of toll-like receptor 4 ameliorates hepatic and adipose tissue insulin resistance in high-fat-fed mice." *Cell Metab* no. 10 (5):419-29. doi: 10.1016/j.cmet.2009.09.006.

Sag, D., D. Carling, R. D. Stout, and J. Suttles. 2008. "Adenosine 5'-monophosphate-activated protein kinase promotes macrophage polarization to an anti-inflammatory functional phenotype." *J Immunol* no. 181 (12):8633-41.

Saharinen, P., and O. Silvennoinen. 2002. "The pseudokinase domain is required for suppression of basal activity of Jak2 and Jak3 tyrosine kinases and for cytokine-inducible activation of signal transduction." *J Biol Chem* no. 277 (49):47954-63. doi: 10.1074/jbc.M205156200.

Saharinen, P., K. Takaluoma, and O. Silvennoinen. 2000. "Regulation of the Jak2 tyrosine kinase by its pseudokinase domain." *Mol Cell Biol* no. 20 (10):3387-95.

Sakamoto, K., O. Göransson, D. G. Hardie, and D. R. Alessi. 2004. "Activity of LKB1 and AMPK-related kinases in skeletal muscle: effects of contraction, phenformin, and AICAR." *Am J Physiol Endocrinol Metab* no. 287 (2):E310-7. doi: 10.1152/ajpendo.00074.2004.

Sakamoto, K., and G. D. Holman. 2008. "Emerging role for AS160/TBC1D4 and TBC1D1 in the regulation of GLUT4 traffic." *Am J Physiol Endocrinol Metab* no. 295 (1):E29-37. doi: 10.1152/ajpendo.90331.2008.

Sakaue, H., A. Nishizawa, W. Ogawa, K. Teshigawara, T. Mori, Y. Takashima, T. Noda, and M. Kasuga. 2003. "Requirement for 3-phosphoinositide-kependent dinase-1 (PDK-1) in insulin-induced glucose uptake in immortalized brown adipocytes." *J Biol Chem* no. 278 (40):38870-4. doi: 10.1074/jbc.M306151200.

Sakoda, H., T. Ogihara, M. Anai, M. Fujishiro, H. Ono, Y. Onishi, H. Katagiri, M. Abe, Y. Fukushima, N. Shojima, K. Inukai, M. Kikuchi, Y. Oka, and T. Asano. 2002. "Activation of AMPK is essential for AICAR-induced glucose uptake by skeletal muscle but not adipocytes." *Am J Physiol Endocrinol Metab* no. 282 (6):E1239-44. doi: 10.1152/ajpendo.00455.2001.

Sakurai, H., H. Chiba, H. Miyoshi, T. Sugita, and W. Toriumi. 1999. "IkappaB kinases phosphorylate NF-kappaB p65 subunit on serine 536 in the transactivation domain." *J Biol Chem* no. 274 (43):30353-6.

Sakurai, H., S. Suzuki, N. Kawasaki, H. Nakano, T. Okazaki, A. Chino, T. Doi, and I. Saiki. 2003. "Tumor necrosis factor-alpha-induced IKK phosphorylation of NF-kappaB p65 on serine 536 is mediated through the TRAF2, TRAF5, and TAK1 signaling pathway." *J Biol Chem* no. 278 (38):36916-23. doi: 10.1074/jbc.M301598200.

Salt, I. P., J. M. Connell, and G. W. Gould. 2000. "5-aminoimidazole-4-carboxamide ribonucleoside (AICAR) inhibits insulin-stimulated glucose transport in 3T3-L1 adipocytes." *Diabetes* no. 49 (10):1649-56.

Saltiel, A. R., and C. R. Kahn. 2001. "Insulin signalling and the regulation of glucose and lipid metabolism." *Nature* no. 414 (6865):799-806. doi: 10.1038/414799a.

Sanders, M. J., Z. S. Ali, B. D. Hegarty, R. Heath, M. A. Snowden, and D. Carling. 2007. "Defining the mechanism of activation of AMP-activated protein kinase by the small molecule A-769662, a member of the thienopyridone family." *J Biol Chem* no. 282 (45):32539-48. doi: 10.1074/jbc.M706543200.

Sano, H., S. Kane, E. Sano, C. P. Mîinea, J. M. Asara, W. S. Lane, C. W. Garner, and G. E. Lienhard. 2003. "Insulin-stimulated phosphorylation of a Rab GTPase-activating protein regulates GLUT4 translocation." *J Biol Chem* no. 278 (17):14599-602. doi: 10.1074/jbc.C300063200.

Sarbassov, D. D., D. A. Guertin, S. M. Ali, and D. M. Sabatini. 2005. "Phosphorylation and regulation of Akt/PKB by the rictor-mTOR complex." *Science* no. 307 (5712):1098-101. doi: 10.1126/science.1106148.

Schenk, S., M. Saberi, and J. M. Olefsky. 2008. "Insulin sensitivity: modulation by nutrients and inflammation." *J Clin Invest* no. 118 (9):2992-3002. doi: 10.1172/JCI34260.

Schultz, O., F. Oberhauser, J. Saech, A. Rubbert-Roth, M. Hahn, W. Krone, and M. Laudes. 2010. "Effects of inhibition of interleukin-6 signalling on insulin sensitivity and lipoprotein (a) levels in human subjects with rheumatoid diseases." *PLoS One* no. 5 (12):e14328. doi: 10.1371/journal.pone.0014328.

Schulz, E., J. Dopheide, S. Schuhmacher, S. R. Thomas, K. Chen, A. Daiber, P. Wenzel, T. Münzel, and J. F. Keaney. 2008. "Suppression of the JNK pathway by induction of a metabolic stress response prevents vascular injury and dysfunction." *Circulation* no. 118 (13):1347-57. doi: 10.1161/CIRCULATIONAHA.108.784298.

Scott, J. W., S. A. Hawley, K. A. Green, M. Anis, G. Stewart, G. A. Scullion, D. G. Norman, and D. G. Hardie. 2004. "CBS domains form energy-sensing modules whose binding of adenosine ligands is disrupted by disease mutations." *J Clin Invest* no. 113 (2):274-84. doi: 10.1172/JCI19874.

Scott, J. W., B. J. van Denderen, S. B. Jorgensen, J. E. Honeyman, G. R. Steinberg, J. S. Oakhill, T. J. Iseli, A. Koay, P. R. Gooley, D. Stapleton, and B. E. Kemp. 2008. "Thienopyridone drugs are selective activators of AMP-activated protein kinase beta1-containing complexes." *Chem Biol* no. 15 (11):1220-30. doi: 10.1016/j.chembiol.2008.10.005.

Seale, P., B. Bjork, W. Yang, S. Kajimura, S. Chin, S. Kuang, A. Scimè, S. Devarakonda, H. M. Conroe, H. Erdjument-Bromage, P. Tempst, M. A. Rudnicki, D. R. Beier, and B. M. Spiegelman. 2008. "PRDM16 controls a brown fat/skeletal muscle switch." *Nature* no. 454 (7207):961-7. doi: 10.1038/nature07182.

Seale, P., H. M. Conroe, J. Estall, S. Kajimura, A. Frontini, J. Ishibashi, P. Cohen, S. Cinti, and B. M. Spiegelman. 2011. "Prdm16 determines the thermogenic

program of subcutaneous white adipose tissue in mice." *J Clin Invest* no. 121 (1):96-105. doi: 10.1172/JCI44271.

Senn, J. J. 2006. "Toll-like receptor-2 is essential for the development of palmitate-induced insulin resistance in myotubes." *J Biol Chem* no. 281 (37):26865-75. doi: 10.1074/jbc.M513304200.

Senn, J. J., P. J. Klover, I. A. Nowak, and R. A. Mooney. 2002. "Interleukin-6 induces cellular insulin resistance in hepatocytes." *Diabetes* no. 51 (12):3391-9.

Senn, J. J., P. J. Klover, I. A. Nowak, T. A. Zimmers, L. G. Koniaris, R. W. Furlanetto, and R. A. Mooney. 2003. "Suppressor of cytokine signaling-3 (SOCS-3), a potential mediator of interleukin-6-dependent insulin resistance in hepatocytes." *J Biol Chem* no. 278 (16):13740-6. doi: 10.1074/jbc.M210689200.

Serrano-Marco, L., R. Rodríguez-Calvo, I. El Kochairi, X. Palomer, L. Michalik, W. Wahli, and M. Vázquez-Carrera. 2011. "Activation of peroxisome proliferator-activated receptor-β/-δ (PPAR-β/-δ) ameliorates insulin signaling and reduces SOCS3 levels by inhibiting STAT3 in interleukin-6-stimulated adipocytes." *Diabetes* no. 60 (7):1990-9. doi: 10.2337/db10-0704.

Shakhov, A. N., M. A. Collart, P. Vassalli, S. A. Nedospasov, and C. V. Jongeneel. 1990. "Kappa B-type enhancers are involved in lipopolysaccharide-mediated transcriptional activation of the tumor necrosis factor alpha gene in primary macrophages." *J Exp Med* no. 171 (1):35-47.

Shakur, Y., L. S. Holst, T. R. Landstrom, M. Movsesian, E. Degerman, and V. Manganiello. 2001. "Regulation and function of the cyclic nucleotide phosphodiesterase (PDE3) gene family." *Prog Nucleic Acid Res Mol Biol* no. 66:241-77.

Shang, C. A., and M. J. Waters. 2003. "Constitutively active signal transducer and activator of transcription 5 can replace the requirement for growth hormone in adipogenesis of 3T3-F442A preadipocytes." *Mol Endocrinol* no. 17 (12):2494-508. doi: 10.1210/me.2003-0139.

Shaw, R. J., M. Kosmatka, N. Bardeesy, R. L. Hurley, L. A. Witters, R. A. DePinho, and L. C. Cantley. 2004. "The tumor suppressor LKB1 kinase directly activates AMP-activated kinase and regulates apoptosis in response to energy stress." *Proc Natl Acad Sci U S A* no. 101 (10):3329-35. doi: 10.1073/pnas.0308061100.

Shaw, R. J., K. A. Lamia, D. Vasquez, S. H. Koo, N. Bardeesy, R. A. Depinho, M. Montminy, and L. C. Cantley. 2005. "The kinase LKB1 mediates glucose homeostasis in liver and therapeutic effects of metformin." *Science* no. 310 (5754):1642-6. doi: 10.1126/science.1120781.

Shi, H., B. Cave, K. Inouye, C. Bjørbaek, and J. S. Flier. 2006. "Overexpression of suppressor of cytokine signaling 3 in adipose tissue causes local but not systemic insulin resistance." *Diabetes* no. 55 (3):699-707.

Shi, H., M. V. Kokoeva, K. Inouye, I. Tzameli, H. Yin, and J. S. Flier. 2006. "TLR4 links innate immunity and fatty acid-induced insulin resistance." *J Clin Invest* no. 116 (11):3015-25. doi: 10.1172/JCI28898.

Shi, H., I. Tzameli, C. Bjørbaek, and J. S. Flier. 2004. "Suppressor of cytokine signaling 3 is a physiological regulator of adipocyte insulin signaling." *J Biol Chem* no. 279 (33):34733-40. doi: 10.1074/jbc.M403886200.

Shoelson, S. E., L. Herrero, and A. Naaz. 2007. "Obesity, inflammation, and insulin resistance." *Gastroenterology* no. 132 (6):2169-80. doi: 10.1053/j.gastro.2007.03.059.

Shuai, K., and B. Liu. 2003. "Regulation of JAK-STAT signalling in the immune system." *Nat Rev Immunol* no. 3 (11):900-11. doi: 10.1038/nri1226.

Shuai, K., A. Ziemiecki, A. F. Wilks, A. G. Harpur, H. B. Sadowski, M. Z. Gilman, and J. E. Darnell. 1993. "Polypeptide signalling to the nucleus through tyrosine phosphorylation of Jak and Stat proteins." *Nature* no. 366 (6455):580-3. doi: 10.1038/366580a0.

Simoncic, P. D., A. Lee-Loy, D. L. Barber, M. L. Tremblay, and C. J. McGlade. 2002. "The T cell protein tyrosine phosphatase is a negative regulator of janus family kinases 1 and 3." *Curr Biol* no. 12 (6):446-53.

Solinas, G., C. Vilcu, J. G. Neels, G. K. Bandyopadhyay, J. L. Luo, W. Naugler, S. Grivennikov, A. Wynshaw-Boris, M. Scadeng, J. M. Olefsky, and M. Karin. 2007. "JNK1 in hematopoietically derived cells contributes to diet-induced inflammation and insulin resistance without affecting obesity." *Cell Metab* no. 6 (5):386-97. doi: 10.1016/j.cmet.2007.09.011.

Sopasakis, V. R., M. Sandqvist, B. Gustafson, A. Hammarstedt, M. Schmelz, X. Yang, P. A. Jansson, and U. Smith. 2004. "High local concentrations and effects on differentiation implicate interleukin-6 as a paracrine regulator." *Obes Res* no. 12 (3):454-60. doi: 10.1038/oby.2004.51.

Sponarova, J., K. J. Mustard, O. Horakova, P. Flachs, M. Rossmeisl, P. Brauner, K. Bardova, M. Thomason-Hughes, R. Braunerova, P. Janovska, D. G. Hardie, and J. Kopecky. 2005. "Involvement of AMP-activated protein kinase in fat depot-specific metabolic changes during starvation." *FEBS Lett* no. 579 (27):6105-10. doi: 10.1016/j.febslet.2005.09.078.

Sriwijitkamol, A., D. K. Coletta, E. Wajcberg, G. B. Balbontin, S. M. Reyna, J. Barrientes, P. A. Eagan, C. P. Jenkinson, E. Cersosimo, R. A. DeFronzo, K. Sakamoto, and N. Musi. 2007. "Effect of acute exercise on AMPK signaling in skeletal muscle of subjects with type 2 diabetes: a time-course and dose-response study." *Diabetes* no. 56 (3):836-48. doi: 10.2337/db06-1119.

Stahl, N., T. J. Farruggella, T. G. Boulton, Z. Zhong, J. E. Darnell, and G. D. Yancopoulos. 1995. "Choice of STATs and other substrates specified by modular tyrosine-based motifs in cytokine receptors." *Science* no. 267 (5202):1349-53.

Steinberg, G. R., B. J. Michell, B. J. van Denderen, M. J. Watt, A. L. Carey, B. C. Fam, S. Andrikopoulos, J. Proietto, C. Z. Görgün, D. Carling, G. S. Hotamisligil, M. A. Febbraio, T. W. Kay, and B. E. Kemp. 2006. "Tumor necrosis factor alpha-induced skeletal muscle insulin resistance involves suppression of AMP-kinase signaling." *Cell Metab* no. 4 (6):465-74. doi: 10.1016/j.cmet.2006.11.005.

Steinberg, G. R., H. M. O'Neill, N. L. Dzamko, S. Galic, T. Naim, R. Koopman, S. B. Jørgensen, J. Honeyman, K. Hewitt, Z. P. Chen, J. D. Schertzer, J. W. Scott, F. Koentgen, G. S. Lynch, M. J. Watt, B. J. van Denderen, D. J. Campbell, and B. E. Kemp. 2010. "Whole body deletion of AMP-activated protein kinase {beta}2 reduces muscle AMPK activity and exercise capacity." *J Biol Chem* no. 285 (48):37198-209. doi: 10.1074/jbc.M110.102434.

Steinberg, G. R., J. W. Rush, and D. J. Dyck. 2003. "AMPK expression and phosphorylation are increased in rodent muscle after chronic leptin treatment." *Am J Physiol Endocrinol Metab* no. 284 (3):E648-54. doi: 10.1152/ajpendo.00318.2002.

Stewart, W. C., R. F. Morrison, S. L. Young, and J. M. Stephens. 1999. "Regulation of signal transducers and activators of transcription (STATs) by effectors of adipogenesis: coordinate regulation of STATs 1, 5A, and 5B with peroxisome proliferator-activated receptor-gamma and C/AAAT enhancer binding protein-alpha." *Biochim Biophys Acta* no. 1452 (2):188-96.

Strissel, K. J., Z. Stancheva, H. Miyoshi, J. W. Perfield, J. DeFuria, Z. Jick, A. S. Greenberg, and M. S. Obin. 2007. "Adipocyte death, adipose tissue remodeling, and obesity complications." *Diabetes* no. 56 (12):2910-8. doi: 10.2337/db07-0767.

Suganami, T., K. Tanimoto-Koyama, J. Nishida, M. Itoh, X. Yuan, S. Mizuarai, H. Kotani, S. Yamaoka, K. Miyake, S. Aoe, Y. Kamei, and Y. Ogawa. 2007. "Role of the Toll-like receptor 4/NF-kappaB pathway in saturated fatty acid-induced inflammatory changes in the interaction between adipocytes and macrophages." *Arterioscler Thromb Vasc Biol* no. 27 (1):84-91. doi: 10.1161/01.ATV.0000251608.09329.9a.

Sullivan, J. E., K. J. Brocklehurst, A. E. Marley, F. Carey, D. Carling, and R. K. Beri. 1994. "Inhibition of lipolysis and lipogenesis in isolated rat adipocytes with AICAR, a cell-permeable activator of AMP-activated protein kinase." *FEBS Lett* no. 353 (1):33-6.

Sztalryd, C., G. Xu, H. Dorward, J. T. Tansey, J. A. Contreras, A. R. Kimmel, and C. Londos. 2003. "Perilipin A is essential for the translocation of hormone-sensitive lipase during lipolytic activation." *J Cell Biol* no. 161 (6):1093-103. doi: 10.1083/jcb.200210169.

Tanaka, T., K. Nakatani, K. Morioka, H. Urakawa, N. Maruyama, N. Kitagawa, A. Katsuki, R. Araki-Sasaki, Y. Hori, E. C. Gabazza, Y. Yano, H. Wada, T. Nobori, Y. Sumida, and Y. Adachi. 2003. "Nitric oxide stimulates glucose transport through insulin-independent GLUT4 translocation in 3T3-L1 adipocytes." *Eur J Endocrinol* no. 149 (1):61-7.

Tang, X. X., H. Chen, S. Yu, L. Zhang, M. J. Caplan, and H. C. Chan. 2010. "Lymphocytes accelerate epithelial tight junction assembly: role of AMP-activated protein kinase (AMPK)." *PLoS One* no. 5 (8):e12343. doi: 10.1371/journal.pone.0012343.

Thornton, C., M. A. Snowden, and D. Carling. 1998. "Identification of a novel AMP-activated protein kinase beta subunit isoform that is highly expressed in skeletal muscle." *J Biol Chem* no. 273 (20):12443-50.

Timmers, S., P. Schrauwen, and J. de Vogel. 2008. "Muscular diacylglycerol metabolism and insulin resistance." *Physiol Behav* no. 94 (2):242-51. doi: 10.1016/j.physbeh.2007.12.002.

Tong, L. 2005. "Acetyl-coenzyme A carboxylase: crucial metabolic enzyme and attractive target for drug discovery." *Cell Mol Life Sci* no. 62 (16):1784-803. doi: 10.1007/s00018-005-5121-4.

Tonks, N. K., and B. G. Neel. 2001. "Combinatorial control of the specificity of protein tyrosine phosphatases." *Curr Opin Cell Biol* no. 13 (2):182-95.

Ullrich, A., and J. Schlessinger. 1990. "Signal transduction by receptors with tyrosine kinase activity." *Cell* no. 61 (2):203-12.

Uysal, K. T., S. M. Wiesbrock, M. W. Marino, and G. S. Hotamisligil. 1997. "Protection from obesity-induced insulin resistance in mice lacking TNF-alpha function." *Nature* no. 389 (6651):610-4. doi: 10.1038/39335.

Vandanmagsar, B., Y. H. Youm, A. Ravussin, J. E. Galgani, K. Stadler, R. L. Mynatt, E. Ravussin, J. M. Stephens, and V. D. Dixit. 2011. "The NLRP3 inflammasome instigates obesity-induced inflammation and insulin resistance." *Nat Med* no. 17 (2):179-88. doi: 10.1038/nm.2279.

Vanhaesebroeck, B., S. J. Leevers, G. Panayotou, and M. D. Waterfield. 1997. "Phosphoinositide 3-kinases: a conserved family of signal transducers." *Trends Biochem Sci* no. 22 (7):267-72.

Verhoeven, A. J., A. Woods, C. H. Brennan, S. A. Hawley, D. G. Hardie, J. Scott, R. K. Beri, and D. Carling. 1995. "The AMP-activated protein kinase gene is

highly expressed in rat skeletal muscle. Alternative splicing and tissue distribution of the mRNA." *Eur J Biochem* no. 228 (2):236-43.

Vila-Bedmar, R., M. Lorenzo, and S. Fernández-Veledo. 2010. "Adenosine 5'-monophosphate-activated protein kinase-mammalian target of rapamycin cross talk regulates brown adipocyte differentiation." *Endocrinology* no. 151 (3):980-92. doi: 10.1210/en.2009-0810.

Villena, J. A., B. Viollet, F. Andreelli, A. Kahn, S. Vaulont, and H. S. Sul. 2004. "Induced adiposity and adipocyte hypertrophy in mice lacking the AMP-activated protein kinase-alpha2 subunit." *Diabetes* no. 53 (9):2242-9.

Vincent, M. F., P. J. Marangos, H. E. Gruber, and G. Van den Berghe. 1991. "Inhibition by AICA riboside of gluconeogenesis in isolated rat hepatocytes." *Diabetes* no. 40 (10):1259-66.

Vingtdeux, V., P. Chandakkar, H. Zhao, P. Davies, and P. Marambaud. 2011. "Small-molecule activators of AMP-activated protein kinase (AMPK), RSVA314 and RSVA405, inhibit adipogenesis." *Mol Med* no. 17 (9-10):1022-30. doi: 10.2119/molmed.2011.00163.

Vitali, A., I. Murano, M. C. Zingaretti, A. Frontini, D. Ricquier, and S. Cinti. 2012. "The adipose organ of obesity-prone C57BL/6J mice is composed of mixed white and brown adipocytes." *J Lipid Res* no. 53 (4):619-29. doi: 10.1194/jlr.M018846.

Vucetic, M., V. Otasevic, A. Korac, A. Stancic, A. Jankovic, M. Markelic, I. Golic, K. Velickovic, B. Buzadzic, and B. Korac. 2011. "Interscapular brown adipose tissue metabolic reprogramming during cold acclimation: Interplay of HIF-1α and AMPKα." *Biochim Biophys Acta* no. 1810 (12):1252-61. doi: 10.1016/j.bbagen.2011.09.007.

Wakahara, R., H. Kunimoto, K. Tanino, H. Kojima, A. Inoue, H. Shintaku, and K. Nakajima. 2012. "Phospho-Ser727 of STAT3 regulates STAT3 activity by enhancing dephosphorylation of phospho-Tyr705 largely through TC45." *Genes Cells* no. 17 (2):132-45. doi: 10.1111/j.1365-2443.2011.01575.x.

Wakil, S. J. 1989. "Fatty acid synthase, a proficient multifunctional enzyme." *Biochemistry* no. 28 (11):4523-30.

Wakil, S. J., J. K. Stoops, and V. C. Joshi. 1983. "Fatty acid synthesis and its regulation." *Annu Rev Biochem* no. 52:537-79. doi: 10.1146/annurev.bi.52.070183.002541.

Walczak, H. 2011. "TNF and ubiquitin at the crossroads of gene activation, cell death, inflammation, and cancer." *Immunol Rev* no. 244 (1):9-28. doi: 10.1111/j.1600-065X.2011.01066.x.

Wan, Z., I. Ritchie, M. S. Beaudoin, L. Castellani, C. B. Chan, and D. C. Wright. 2012. "IL-6 indirectly modulates the induction of glyceroneogenic enzymes in adipose tissue during exercise." *PLoS One* no. 7 (7):e41719. doi: 10.1371/journal.pone.0041719.

Wang, D., Y. Zhou, W. Lei, K. Zhang, J. Shi, Y. Hu, G. Shu, and J. Song. 2010. "Signal transducer and activator of transcription 3 (STAT3) regulates adipocyte differentiation via peroxisome-proliferator-activated receptor gamma (PPARgamma)." *Biol Cell* no. 102 (1):1-12. doi: 10.1042/BC20090070.

Wang, M. Y., L. Orci, M. Ravazzola, and R. H. Unger. 2005. "Fat storage in adipocytes requires inactivation of leptin's paracrine activity: implications for treatment of human obesity." *Proc Natl Acad Sci U S A* no. 102 (50):18011-6. doi: 10.1073/pnas.0509001102.

Wang, Q. A., C. Tao, R. K. Gupta, and P. E. Scherer. 2013. "Tracking adipogenesis during white adipose tissue development, expansion and regeneration." *Nat Med* no. 19 (10):1338-44. doi: 10.1038/nm.3324.

Wang, S., M. Zhang, B. Liang, J. Xu, Z. Xie, C. Liu, B. Viollet, D. Yan, and M. H. Zou. 2010. "AMPKalpha2 deletion causes aberrant expression and activation of NAD(P)H oxidase and consequent endothelial dysfunction in vivo: role of 26S proteasomes." *Circ Res* no. 106 (6):1117-28. doi: 10.1161/CIRCRESAHA.109.212530.

Ward, C. W., and M. C. Lawrence. 2009. "Ligand-induced activation of the insulin receptor: a multi-step process involving structural changes in both the ligand and the receptor." *Bioessays* no. 31 (4):422-34. doi: 10.1002/bies.200800210.

Wascher, T. C., J. H. Lindeman, H. Sourij, T. Kooistra, G. Pacini, and M. Roden. 2011. "Chronic TNF-α neutralization does not improve insulin resistance or endothelial function in "healthy" men with metabolic syndrome." *Mol Med* no. 17 (3-4):189-93. doi: 10.2119/molmed.2010.00221.

Watkins, P. A. 1997. "Fatty acid activation." *Prog Lipid Res* no. 36 (1):55-83.

Watt, M. J., A. G. Holmes, S. K. Pinnamaneni, A. P. Garnham, G. R. Steinberg, B. E. Kemp, and M. A. Febbraio. 2006. "Regulation of HSL serine phosphorylation in skeletal muscle and adipose tissue." *Am J Physiol Endocrinol Metab* no. 290 (3):E500-8. doi: 10.1152/ajpendo.00361.2005.

Weber, A., P. Wasiliew, and M. Kracht. 2010. "Interleukin-1 (IL-1) pathway." *Sci Signal* no. 3 (105):cm1. doi: 10.1126/scisignal.3105cm1.

Weber, J. D., and D. H. Gutmann. 2012. "Deconvoluting mTOR biology." *Cell Cycle* no. 11 (2):236-48. doi: 10.4161/cc.11.2.19022.

Weichhart, T., G. Costantino, M. Poglitsch, M. Rosner, M. Zeyda, K. M. Stuhlmeier, T. Kolbe, T. M. Stulnig, W. H. Hörl, M. Hengstschläger, M. Müller, and M. D. Säemann. 2008. "The TSC-mTOR signaling pathway regulates the innate inflammatory response." *Immunity* no. 29 (4):565-77. doi: 10.1016/j.immuni.2008.08.012.

Weisberg, S. P., D. Hunter, R. Huber, J. Lemieux, S. Slaymaker, K. Vaddi, I. Charo, R. L. Leibel, and A. W. Ferrante. 2006. "CCR2 modulates inflammatory and metabolic effects of high-fat feeding." *J Clin Invest* no. 116 (1):115-24. doi: 10.1172/JCI24335.

Weisberg, S. P., D. McCann, M. Desai, M. Rosenbaum, R. L. Leibel, and A. W. Ferrante. 2003. "Obesity is associated with macrophage accumulation in adipose tissue." *J Clin Invest* no. 112 (12):1796-808. doi: 10.1172/JCI19246.

Wen, Z., Z. Zhong, and J. E. Darnell. 1995. "Maximal activation of transcription by Stat1 and Stat3 requires both tyrosine and serine phosphorylation." *Cell* no. 82 (2):241-50.

Weng, S. Y., and D. Schuppan. 2013. "AMPK regulates macrophage polarization in adipose tissue inflammation and NASH." *J Hepatol* no. 58 (3):619-21. doi: 10.1016/j.jhep.2012.09.031.

Wieser, V., A. R. Moschen, and H. Tilg. 2013. "Inflammation, cytokines and insulin resistance: a clinical perspective." *Arch Immunol Ther Exp (Warsz)* no. 61 (2):119-25. doi: 10.1007/s00005-012-0210-1.

Winder, W. W., B. F. Holmes, D. S. Rubink, E. B. Jensen, M. Chen, and J. O. Holloszy. 2000. "Activation of AMP-activated protein kinase increases mitochondrial enzymes in skeletal muscle." *J Appl Physiol (1985)* no. 88 (6):2219-26.

Withers, D. J., J. S. Gutierrez, H. Towery, D. J. Burks, J. M. Ren, S. Previs, Y. Zhang, D. Bernal, S. Pons, G. I. Shulman, S. Bonner-Weir, and M. F. White. 1998. "Disruption of IRS-2 causes type 2 diabetes in mice." *Nature* no. 391 (6670):900-4. doi: 10.1038/36116.

Wolff, N. C., S. Vega-Rubin-de-Celis, X. J. Xie, D. H. Castrillon, W. Kabbani, and J. Brugarolas. 2011. "Cell-type-dependent regulation of mTORC1 by REDD1

and the tumor suppressors TSC1/TSC2 and LKB1 in response to hypoxia." *Mol Cell Biol* no. 31 (9):1870-84. doi: 10.1128/MCB.01393-10.

Woods, A., D. Azzout-Marniche, M. Foretz, S. C. Stein, P. Lemarchand, P. Ferré, F. Foufelle, and D. Carling. 2000. "Characterization of the role of AMP-activated protein kinase in the regulation of glucose-activated gene expression using constitutively active and dominant negative forms of the kinase." *Mol Cell Biol* no. 20 (18):6704-11.

Woods, A., K. Dickerson, R. Heath, S. P. Hong, M. Momcilovic, S. R. Johnstone, M. Carlson, and D. Carling. 2005. "Ca2+/calmodulin-dependent protein kinase kinase-beta acts upstream of AMP-activated protein kinase in mammalian cells." *Cell Metab* no. 2 (1):21-33. doi: 10.1016/j.cmet.2005.06.005.

Woods, A., S. R. Johnstone, K. Dickerson, F. C. Leiper, L. G. Fryer, D. Neumann, U. Schlattner, T. Wallimann, M. Carlson, and D. Carling. 2003. "LKB1 is the upstream kinase in the AMP-activated protein kinase cascade." *Curr Biol* no. 13 (22):2004-8.

Woods, A., M. R. Munday, J. Scott, X. Yang, M. Carlson, and D. Carling. 1994. "Yeast SNF1 is functionally related to mammalian AMP-activated protein kinase and regulates acetyl-CoA carboxylase in vivo." *J Biol Chem* no. 269 (30):19509-15.

Woods, A., I. Salt, J. Scott, D. G. Hardie, and D. Carling. 1996. "The alpha1 and alpha2 isoforms of the AMP-activated protein kinase have similar activities in rat liver but exhibit differences in substrate specificity in vitro." *FEBS Lett* no. 397 (2-3):347-51.

Wu, H., S. Ghosh, X. D. Perrard, L. Feng, G. E. Garcia, J. L. Perrard, J. F. Sweeney, L. E. Peterson, L. Chan, C. W. Smith, and C. M. Ballantyne. 2007. "T-cell accumulation and regulated on activation, normal T cell expressed and secreted upregulation in adipose tissue in obesity." *Circulation* no. 115 (8):1029-38. doi: 10.1161/CIRCULATIONAHA.106.638379.

Wu, J., P. Cohen, and B. M. Spiegelman. 2013. "Adaptive thermogenesis in adipocytes: is beige the new brown?" *Genes Dev* no. 27 (3):234-50. doi: 10.1101/gad.211649.112.

Wu, X., H. Motoshima, K. Mahadev, T. J. Stalker, R. Scalia, and B. J. Goldstein. 2003. "Involvement of AMP-activated protein kinase in glucose uptake stimulated by the globular domain of adiponectin in primary rat adipocytes." *Diabetes* no. 52 (6):1355-63.

Wu, X., Q. Yan, Z. Zhang, G. Du, and X. Wan. 2012. "Acrp30 inhibits leptin-induced metastasis by downregulating the JAK/STAT3 pathway via AMPK activation in aggressive SPEC-2 endometrial cancer cells." *Oncol Rep* no. 27 (5):1488-96. doi: 10.3892/or.2012.1670.

Xi, X., J. Han, and J. Z. Zhang. 2001. "Stimulation of glucose transport by AMP-activated protein kinase via activation of p38 mitogen-activated protein kinase." *J Biol Chem* no. 276 (44):41029-34. doi: 10.1074/jbc.M102824200.

Xiao, B., R. Heath, P. Saiu, F. C. Leiper, P. Leone, C. Jing, P. A. Walker, L. Haire, J. F. Eccleston, C. T. Davis, S. R. Martin, D. Carling, and S. J. Gamblin. 2007. "Structural basis for AMP binding to mammalian AMP-activated protein kinase." *Nature* no. 449 (7161):496-500. doi: 10.1038/nature06161.

Xiao, K., J. Jiang, C. Guan, C. Dong, G. Wang, L. Bai, J. Sun, C. Hu, and C. Bai. 2013. "Curcumin induces autophagy via activating the AMPK signaling pathway in lung adenocarcinoma cells." *J Pharmacol Sci* no. 123 (2):102-9.

Xu, D., and C. K. Qu. 2008. "Protein tyrosine phosphatases in the JAK/STAT pathway." *Front Biosci* no. 13:4925-32.

Yamamoto, T., Y. Sekine, K. Kashima, A. Kubota, N. Sato, N. Aoki, and T. Matsuda. 2002. "The nuclear isoform of protein-tyrosine phosphatase TC-PTP

regulates interleukin-6-mediated signaling pathway through STAT3 dephosphorylation." *Biochem Biophys Res Commun* no. 297 (4):811-7.

Yamaoka, S., G. Courtois, C. Bessia, S. T. Whiteside, R. Weil, F. Agou, H. E. Kirk, R. J. Kay, and A. Israël. 1998. "Complementation cloning of NEMO, a component of the IkappaB kinase complex essential for NF-kappaB activation." *Cell* no. 93 (7):1231-40.

Yamauchi, T., J. Kamon, Y. Minokoshi, Y. Ito, H. Waki, S. Uchida, S. Yamashita, M. Noda, S. Kita, K. Ueki, K. Eto, Y. Akanuma, P. Froguel, F. Foufelle, P. Ferre, D. Carling, S. Kimura, R. Nagai, B. B. Kahn, and T. Kadowaki. 2002. "Adiponectin stimulates glucose utilization and fatty-acid oxidation by activating AMP-activated protein kinase." *Nat Med* no. 8 (11):1288-95. doi: 10.1038/nm788.

Yamazaki, K., J. Gohda, A. Kanayama, Y. Miyamoto, H. Sakurai, M. Yamamoto, S. Akira, H. Hayashi, B. Su, and J. Inoue. 2009. "Two mechanistically and temporally distinct NF-kappaB activation pathways in IL-1 signaling." *Sci Signal* no. 2 (93):ra66. doi: 10.1126/scisignal.2000387.

Yang, X. D., E. Tajkhorshid, and L. F. Chen. 2010. "Functional interplay between acetylation and methylation of the RelA subunit of NF-kappaB." *Mol Cell Biol* no. 30 (9):2170-80. doi: 10.1128/MCB.01343-09.

Yang, Z., B. B. Kahn, H. Shi, and B. Z. Xue. 2010. "Macrophage alpha1 AMP-activated protein kinase (alpha1AMPK) antagonizes fatty acid-induced inflammation through SIRT1." *J Biol Chem* no. 285 (25):19051-9. doi: 10.1074/jbc.M110.123620.

Yin, W., J. Mu, and M. J. Birnbaum. 2003. "Role of AMP-activated protein kinase in cyclic AMP-dependent lipolysis In 3T3-L1 adipocytes." *J Biol Chem* no. 278 (44):43074-80. doi: 10.1074/jbc.M308484200.

Yokogami, K., S. Wakisaka, J. Avruch, and S. A. Reeves. 2000. "Serine phosphorylation and maximal activation of STAT3 during CNTF signaling is mediated by the rapamycin target mTOR." *Curr Biol* no. 10 (1):47-50.

You, M., D. H. Yu, and G. S. Feng. 1999. "Shp-2 tyrosine phosphatase functions as a negative regulator of the interferon-stimulated Jak/STAT pathway." *Mol Cell Biol* no. 19 (3):2416-24.

Yu, C., Y. Chen, G. W. Cline, D. Zhang, H. Zong, Y. Wang, R. Bergeron, J. K. Kim, S. W. Cushman, G. J. Cooney, B. Atcheson, M. F. White, E. W. Kraegen, and G. I. Shulman. 2002. "Mechanism by which fatty acids inhibit insulin activation of insulin receptor substrate-1 (IRS-1)-associated phosphatidylinositol 3-kinase activity in muscle." *J Biol Chem* no. 277 (52):50230-6. doi: 10.1074/jbc.M200958200.

Yu, C. L., and S. J. Burakoff. 1997. "Involvement of proteasomes in regulating Jak-STAT pathways upon interleukin-2 stimulation." *J Biol Chem* no. 272 (22):14017-20.

Yu, S., G. Shen, T. O. Khor, J. H. Kim, and A. N. Kong. 2008. "Curcumin inhibits Akt/mammalian target of rapamycin signaling through protein phosphatase-dependent mechanism." *Mol Cancer Ther* no. 7 (9):2609-20. doi: 10.1158/1535-7163.MCT-07-2400.

Yuan, M., N. Konstantopoulos, J. Lee, L. Hansen, Z. W. Li, M. Karin, and S. E. Shoelson. 2001. "Reversal of obesity- and diet-induced insulin resistance with salicylates or targeted disruption of Ikkbeta." *Science* no. 293 (5535):1673-7. doi: 10.1126/science.1061620.

Yuen, D. Y., R. M. Dwyer, V. B. Matthews, L. Zhang, B. G. Drew, B. Neill, B. A. Kingwell, M. G. Clark, S. Rattigan, and M. A. Febbraio. 2009. "Interleukin-6 attenuates insulin-mediated increases in endothelial cell signaling but augments skeletal muscle insulin action via differential effects on tumor

necrosis factor-alpha expression." *Diabetes* no. 58 (5):1086-95. doi: 10.2337/db08-0775.

Zabel, U., and P. A. Baeuerle. 1990. "Purified human I kappa B can rapidly dissociate the complex of the NF-kappa B transcription factor with its cognate DNA." *Cell* no. 61 (2):255-65.

Zakut-Houri, R., B. Bienz-Tadmor, D. Givol, and M. Oren. 1985. "Human p53 cellular tumor antigen: cDNA sequence and expression in COS cells." *EMBO J* no. 4 (5):1251-5.

Zhang, D., M. Sun, D. Samols, and I. Kushner. 1996. "STAT3 participates in transcriptional activation of the C-reactive protein gene by interleukin-6." *J Biol Chem* no. 271 (16):9503-9.

Zhang, H., G. Cicchetti, H. Onda, H. B. Koon, K. Asrican, N. Bajraszewski, F. Vazquez, C. L. Carpenter, and D. J. Kwiatkowski. 2003. "Loss of Tsc1/Tsc2 activates mTOR and disrupts PI3K-Akt signaling through downregulation of PDGFR." *J Clin Invest* no. 112 (8):1223-33. doi: 10.1172/JCI17222.

Zhang, S., L. Chen, Y. Luo, A. Gunawan, D. S. Lawrence, and Z. Y. Zhang. 2009. "Acquisition of a potent and selective TC-PTP inhibitor via a stepwise fluorophore-tagged combinatorial synthesis and screening strategy." *J Am Chem Soc* no. 131 (36):13072-9. doi: 10.1021/ja903733z.

Zhang, Y., J. Qiu, X. Wang, and M. Xia. 2011. "AMP-activated protein kinase suppresses endothelial cell inflammation through phosphorylation of transcriptional coactivator p300." *Arterioscler Thromb Vasc Biol* no. 31 (12):2897-908. doi: 10.1161/ATVBAHA.111.237453.

Zhang, Z., S. F. Lowry, L. Guarente, and B. Haimovich. 2010. "Roles of SIRT1 in the acute and restorative phases following induction of inflammation." *J Biol Chem* no. 285 (53):41391-401. doi: 10.1074/jbc.M110.174482.

Zhao, X., J. W. Zmijewski, E. Lorne, G. Liu, Y. J. Park, Y. Tsuruta, and E. Abraham. 2008. "Activation of AMPK attenuates neutrophil proinflammatory activity and decreases the severity of acute lung injury." *Am J Physiol Lung Cell Mol Physiol* no. 295 (3):L497-504. doi: 10.1152/ajplung.90210.2008.

Zhou, G., R. Myers, Y. Li, Y. Chen, X. Shen, J. Fenyk-Melody, M. Wu, J. Ventre, T. Doebber, N. Fujii, N. Musi, M. F. Hirshman, L. J. Goodyear, and D. E. Moller. 2001. "Role of AMP-activated protein kinase in mechanism of metformin action." *J Clin Invest* no. 108 (8):1167-74. doi: 10.1172/JCI13505.

Zhou, L., S. S. Deepa, J. C. Etzler, J. Ryu, X. Mao, Q. Fang, D. D. Liu, J. M. Torres, W. Jia, J. D. Lechleiter, F. Liu, and L. Q. Dong. 2009. "Adiponectin activates AMP-activated protein kinase in muscle cells via APPL1/LKB1-dependent and phospholipase C/Ca2+/Ca2+/calmodulin-dependent protein kinase kinase-dependent pathways." *J Biol Chem* no. 284 (33):22426-35. doi: 10.1074/jbc.M109.028357.

Zhou, Y., D. Wang, Q. Zhu, X. Gao, S. Yang, A. Xu, and D. Wu. 2009. "Inhibitory effects of A-769662, a novel activator of AMP-activated protein kinase, on 3T3-L1 adipogenesis." *Biol Pharm Bull* no. 32 (6):993-8.

Zigman, J. M., and J. K. Elmquist. 2003. "Minireview: From anorexia to obesity--the yin and yang of body weight control." *Endocrinology* no. 144 (9):3749-56. doi: 10.1210/en.2003-0241.